Terumasa Komuro

Atlas of Interstitial Cells of Cajal in the Gastrointestinal Tract

Springer

Atlas of Interstitial Cells of Cajal in the Gastrointestinal Tract

Terumasa Komuro

Atlas of Interstitial Cells of Cajal in the Gastrointestinal Tract

Springer

Prof. Terumasa Komuro
Faculty of Human Sciences
Waseda University
Tokorozawa, Saitama
Japan

ISBN 978-94-007-2916-2 e-ISBN 978-94-007-2917-9
DOI 10.1007/978-94-007-2917-9
Springer Dordrecht Heidelberg London New York

Library of Congress Control Number: 2012930013

Foreword

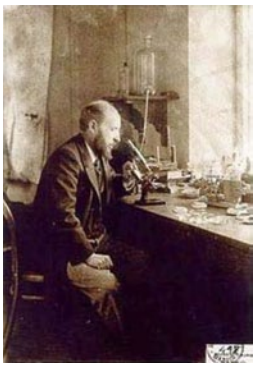

It has been more than 100 years since the cells, now known as interstitial cells of Cajal (ICC), were described by the Spanish neuroanatomist, Santiago Ramón y Cajal. Much of what we have learned about these cells has developed from hypotheses based on extensive morphological observations, first using classical histochemical staining techniques, then electron-microscopy, and currently immunohistochemistry. More recently, a second population of interstitial cells has come under investigation: the so-called 'fibroblast-like' cells that occupy most of the same anatomical niches as ICC in gastrointestinal (GI) muscles, but they are a discrete population of cells, with a different phenotype and identifying biomarkers, and with different physiological functions. While touching on the latter type of interstitial cell, Professor Terumasa Komuro concentrates his efforts in this monograph on the various classes of ICC, showing distributions through the GI tract, cellular ultrastructure, and relationships of ICC to other cell-types of the *tunica muscularis*. What emerges is a beautiful and lasting montage of the morphological complexities of the ICC of the GI tract.

Professor Komuro starts his tour of ICC with historical images comparing the cells drawn by Cajal and Taxi from sections stained by histochemical methods with modern immunohistochemical images. The shapes of cell somas and complex branching patterns of processes leave no doubt that the cells described by Cajal were the ICC now of front row interest to neurogastroenterologists. In a section on electron microscopy, he demonstrates the major ultrastructural features of ICC in various tissues of the gut, and in other chapters shows very clear images of specific classes of ICC using immunofluorescence. Then he steps diligently through the GI tract, organ-by-organ, providing a panorama of his vast collection of images. By showing projections from whole mounts and cross sections and by the extensive use of stereo images, the reader will develop a sophisticated impression of the vast distribution of ICC, the differences between classes of ICC, the networks they form, and their close associations with motor neurons. One sees that ICC are not a single type of cell, but a family of cells or a continuum of cellular phenotypes tailored to specific functions. Important unanswered questions in the ICC field will also occur to the reader when examining these images, such as: (i) what is the utility of such varied cell morphology? and (ii) what drives the development of ICC in specific niches within the gut wall?

A striking feature of ICC, noted often by historical anatomists and by current practitioners, is their very close association with the varicosities (or nerve terminals) of motor neurons. In immunofluorescence images this is evidenced by chains of varicosities decorating lengths of intramuscular ICC (ICC-CM and ICC-LM in the terminology used by Professor Komuro), and by < 20 nm contacts observed frequently between ICC and varicosities containing secretory vesicles in electron micrographs. Cajal thought ICC were a type of primitive neuron positioned at the terminus of autonomic neurons and possibly involved in neural transduction. Contemporary developmental studies have shown these cells are not neurons, but instead are of mesenchymal origin. However, the frequent proximity of varicosities to ICC and the observation that ICC form gap junctions with surrounding smooth muscle cells led to revival of the concept that ICC are innervated by motor neurons and involved in neurotransmission. Physiological studies, using mutants lacking most ICC, have demonstrated that intramuscular ICC are involved in the transduction of motor signals from the enteric nervous system. Professor Komuro has pointed out that smooth muscle cells can also make close contacts with varicosities of motor neurons, and thus motor innervation in the gut is likely to be of a parallel nature.

The complex network of cells found between the circular and longitudinal muscle layers and running around myenteric ganglia (ICC-MP) in the stomach, small bowel and colon and along the submucosal surface of the colon have a pacemaker role in GI motility. Professor Komuro uses stereo imaging very effectively to illustrate the baskets formed by ICC-MP around myenteric ganglia. Loss of ICC-MP, as documented in a variety of motility disorders, leads to loss of or inappropriate propagation of electrical slow waves, which time the phasic contractions of the gut. Such a result can lead to poor emptying of the stomach and poor propulsion in the small intestine and colon. For example, many cases of slow transit constipation in human patients are characterized by loss of ICC. The morphology detailed by Professor Komuro provides a basis for pacemaker activity and regenerative propagation of slow waves: (i) gap junctions between ICC to form a continuous network of cells, and (ii) gap junctions with smooth muscle cells through which slow waves can depolarize and activate smooth muscle cells in stereotypic motility patterns.

There are mysteries remaining about the ICC of the GI tract, and many are apparent from the images in this monograph. For example, an extensive network of ICC lies along the serosal surface of the colon (ICC-SS). At the present time nothing is known about the function of these cells. Additionally, while it is known that pacemaker activity is generated at the submucosal surface in the colon, few investigators have considered the extent of the ICC-SMP and depth of penetration of this network into the submucosa as documented in the images provided by Professor Komuro. ICC-SP extend away from the muscularis and actually surround ganglia of the submucous plexus. We know little about this population of cells. Perhaps they serve as a means of motor communication between the submucous ganglia and the *tunica muscularis*.

It is my belief that the breathtaking images provided in this monograph will be greatly enjoyed by readers for many years, and they will provide essential didactic materials for students of histology and neurogastroenterology. Professor Komuro has done the field a great service with his diligence as an investigator and marvelous craftsmanship as a morphologist!

Department of Physiology and Cell Biology,
Foundation Professor of the University
of Nevada, Reno

Kenton M. Sanders, Ph.D.

Preface

The objective of this Atlas is to introduce the structure and distributions of interstitial cells of Cajal (ICC) to researchers, clinicians and students of biomedical fields who are interested in the motility of the gastrointestinal (GI) tract and the regulatory mechanism of the smooth muscle in general. Recent development of ICC studies have broadened the research horizon from only the GI tract to other hollow organs with smooth muscle coats outside GI tract, and the presence or absence of ICC and their functional states in these organs are often discussed in the context of a variety of diseases.

However, there have been difficulties to understand whole morphological characteristics of ICC by conventional histological sections or ultrathin sections because of their peculiar shape, the presence of long slender processes projecting from the cell bodies similar to neurons. This is a reason why earlier histologists misunderstood ICC as neurons. Another reason for the difficulty is the presence of ICC subtypes that show different distributions and different ultrastructural features depending on the levels of the GI tract. Therefore, a detailed morphological guide for ICC in each organ of the GI tract is necessary for starting to understand ICC

A stable morphological foundation is essential for understanding the function of tissues and organs and for interpreting their changes in disease.

For this Atlas, I assembled many images of whole-mount stretch preparations stained with immunohistochemistry. Such preparations are among the most useful to reveal the whole shape of ICC in a similar way to the silver impregnation method for nerves used in traditional histology. Stereo-micrographs reconstructed from confocal microscopic images of ICC are especially helpful for understanding their three-dimensional (3D) structures *in situ* to readers who are unfamiliar with the morphology of GI tract in general and ICC in particular. Electron micrographs contained in this book reveal a more precise character of ICC as a peculiar cell type and provide clues for discussing their functional aspects. The approaches presented here effectively display the whole characteristics of ICC. Some functional aspects of ICC are described in the relevant sections and a miminal number of literature citations are listed.

I still remember the strong impression I got when I read the paper on ICC and his pacemaker hypothesis by Lars Thuneberg (1982), since I had also published a small paper on ICC in the extension of the studies of the enteric nervous system at almost the same time. My work was based simply on my cytological interest using modern ultrastructural observations of ICC trying to get an answer to a long-standing puzzle of whether ICC are neurons or glial cells or connective tissue cells. This great shock made me determined

to examine Thuneberg's hypothesis rather skeptically. However, I gradually accumulated evidence to support his idea.

As described above, modern ICC research has developed as the study of the regulatory system of the smooth muscle movement of the muscle coat, mainly focusing on peristalsis. However, the recent demonstration of ICC associated with the submucosal plexus (ICC-SP) suggests that ICC are also involved in mucosal functions, such as secretion and absorption, which are more fundamental and peculiar to each level of GI tract. This may also give useful hints to the approach and interpretation of the study of the visceral organs outside of the GI tract.

I would like to thank Professor Yasuo Uehara, the Chairman of the Anatomy Department in Ehime, Japan, who stimulated active, independent research projects by all members of the department, including my ICC studies at that time. Further progress in my studies of ICC ensued in my laboratory in Waseda University with the cooperation of several PhD students and research associates. I feel proud that except for a few of my own pictures, all of the figures contained in this Atlas have been obtained by these young collaborators in this small laboratory. I am grateful for their stimulation and for their generosity in allowing me to use their valuable figures. I am deeply indebted to Dr Peter Baluk for his reading the manuscript and correction of English. I also acknowledge valuable advice on the technical terms by Dr Menachem Hanani and Professor Hikaru Suzuki. It is my good luck to have good friends and good competitors in carrying out my work for a long time. Above all, the international ICC-meeting truly stimulating. I would like to express my appreciation to the main members of the meeting. In particular, I am cordially grateful to Professor Kenton Sanders for writing a marvelous Foreword for this Atlas. Finally, I cannot miss expressing my appreciation to my wife Yoko, who has continued to make daily lunch boxes for more than 30 years to let her husband work in the laboratory!

Contents

Introduction 1

1.1 What are ICC?

1.1.1 First Description of ICC by Cajal

Santiago Ramon y Cajal, who contributed to the establishment of the neuron theory and was awarded the Nobel Prize for Medicine and Physiology in 1906, regarded the demonstration of the histological basis of autonomic innervation and how nerves transmit signals to effector tissues as a major challenge. He described a fine cellular network that he designated as "*cellules interstitielles*" or "*neurones sympathiques interstitiels*" in association with the terminal arborization of the autonomic nerves of intestines, glands, and blood vessels stained with methylene blue or the Golgi method [1, 2]. Cajal considered these cells as primitive nerve cells that mediate nerve impulses from the terminal portions of the sympathetic nerves to the smooth muscle cells, because at that time these staining methods were believed to be specific to the nerves. Since then, interstitial cells of Cajal (ICC), as referred to by later microscopists, have been a subject of a historical debate in respect of their cytological nature. ICC were regarded by different microscopists as neurons or Schwann cells or connective tissue cells or smooth muscle cells [3–5]. With the development of electron microscopy, the ultrastructural identification of ICC was attempted by several investigators [4, 6, 7], but the cytological definition and the developmental origin of ICC remained unsettled.

1.1.2 Pacemaker Hypothesis

A breakthrough in ICC research was triggered by the novel hypothesis proposed by Thuneberg [8], suggesting that ICC act as pacemaker cells and that they conduct impulses in the gut musculature in an analogous fashion to that in the heart. This hypothesis greatly stimulated both morphological and physiological studies of ICC. Subsequently, various cells in different regions of the digestive tract from a variety of species were described by many authors by a variety of methods [9–11]. However, again, it was uncertain whether different cytological features of these cells represented different profiles of the same cell type, morphological variations of the same cell type, or a mixture of different cell types. Part of the reason for the confusion was the lack of a truly specific staining method for ICC, and the difficulty of correlating ultrastructural observations with the traditional histological descriptions by silver-impregnations and methylene blue staining. Therefore, to establish an unambiguous set of cytological criteria, it was essential that the whole shape of a given cell type and its relation to nerve and muscle cells should correspond closely to that originally described by Cajal.

1.1.3 Finding of c-Kit in ICC

The discovery of a significant role of c-*kit* in the maturation of ICC and the finding that ICC cor-

T. Komuro, *Atlas of Interstitial Cells of Cajal in the Gastrointestinal Tract,*
DOI 10.1007/978-94-007-2917-9_1, © Springer Science+Business Media B.V. 2012

respond to the cells expressing c-Kit receptor tyrosine kinase was a major advance. Abnormal development of ICC was demonstrated in studies using experimental blockade of c-Kit [12, 13]. Then immunohistochemical staining for c-Kit became accepted as a useful marker of ICC at the light microscopic level.

Studies using combinations of c-Kit immunostaining, the zinc iodide-osmium tetroxide (ZIO) method, which shares many staining properties with methylene blue staining and the Golgi method, and ultrastructural observations, contributed to bridging the gap between the old histological descriptions and more recent findings on ICC [14, 15].

1.1.4 Definition and Developmental Origin

As described above, c-Kit-immunostaining proved to depict exactly the same features of the cells as demonstrated by methylene-blue or Golgi methods originally used for the detection of ICC. Therefore, ICC are defined here as c-Kit immunoreactive cells showing bipolar or multipolar shape within the gastrointestinal tract. Meanwhile, studies using chick-quail chimeras [16] and studies using transplants of intestinal segments of the mouse embryo [17] demonstrated that all classes of ICC share a common embryological origin from mesenchymal cells. Developmental studies also showed that ICC in the myenteric plexus originate from the same mesenchymal progenitor cells expressing c-Kit as smooth muscle cells of the longitudinal muscle layer [18, 19].

1.1.5 Distribution of ICC

The presence of ICC has been reported in a wide variety of species, including the frog, lizard, turkey, and many mammals including opossum, bat, rabbit, hedgehog, pig, horse, and conventional experimental animals such as the mouse, rat, guinea-pig and dog, and also in the monkey and human. In the human, ICC have been found throughout the digestive tract from the esophagus to the inner sphincter region of the anus.

1.1.6 Functional Role

Soon after the proposal of the pacemaker hypothesis [8], physiological studies started to provide evidence for a pacemaker function of ICC associated with the myenteric plexus (ICC-MP) and for their generation of slow waves [20, 21]. After the discovery that the c-Kit receptor is essential for the normal development of ICC [12, 13], further strong evidence for such a pacemaker function came from the demonstration of the loss of pacemaker activity of mice with a genetic defect in c-Kit [22, 23]. Eventually, direct recording of the pacemaker activity and slow waves were made from ICC-MP in the stomach of guinea-pig [24].

A pacemaker function was also reported for the ICC associated with the submuscular plexus (ICC-SMP) of the colon in the dog [25–27], human [28], and rat [29].

On the other hand, an intermediary role in the neuromuscular transmission was suggested by morphological studies that certain types of ICC were closely apposed to nerve terminals and formed numerous gap junctions with neighboring smooth muscle cells at different levels of the gastrointestinal tract in many species [30]. Indeed, cytochemical and physiological studies [31, 32] supported that idea that ICC of the circular (ICC-CM) and the deep muscular plexus in the small intestine (ICC-DMP) had a functional significance in both inhibitory and excitatory neurotransmission in the smooth muscles in the GI tract.

In addition, mechanosensitive functions has also been suggested for ICC. Arrays of intramuscular vagal nerves innervating smooth muscles and ICC-CM are believed to be intramuscular mechanoreceptors [33, 34]. A role as stretch receptors was also proposed for ICC located in the subserosal layer (ICC-SS) in the guinea-pig colon to detect the circumferential expansion and swelling of the colon caused by active absorption of water and electrolytes [35]. However, in general, further convincing evidence is required to demonstrate mechanosensitive functions of ICC.

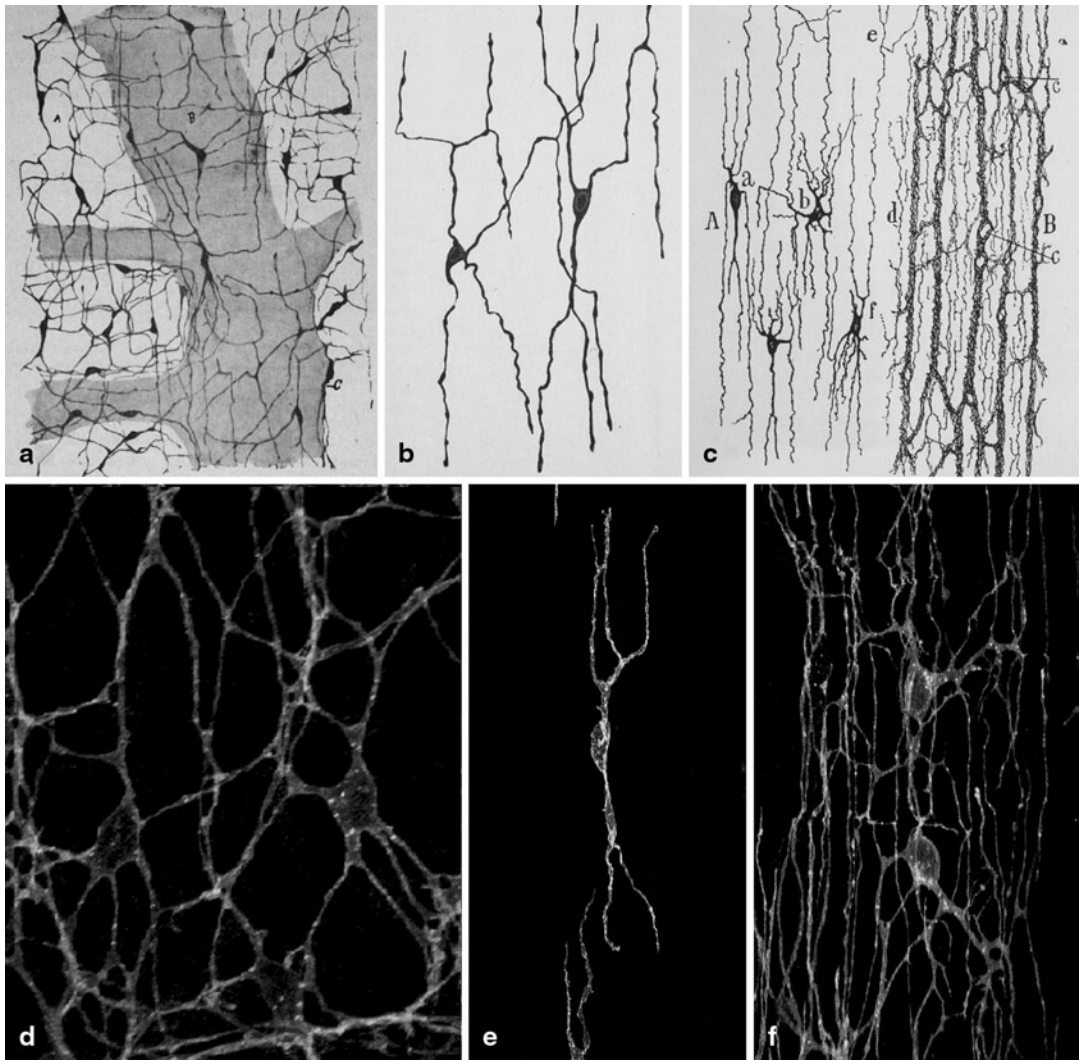

Fig. 1.1 Drawings by Cajal and ICC depicted by modern method. **a** A drawing by Cajal of ICC-MP in the rabbit intestine stained with methylene blue. (Reproduced from Cajal [2], Fig. 572). **b** A drawing by Cajal of ICC-CM in the rabbit stained with methylene blue. (Reproduced from Cajal [2], Fig. 573). **c** A drawing by Cajal of ICC-DMP in the guinea-pig small intestine stained with Golgi method. (Reproduced from Cajal [2], Fig. 575). **d** ICC-MP of the guinea-pig small intestine stained with c-Kit immunohistochemistry. **e** ICC-CM of the guinea-pig small intestine stained with c-Kit immunohistochemistry. **f** ICC-DMP of the guinea-pig small intestine stained with c-Kit-immunohistochemistry. (Note, close similarity of the whole shape and branching patterns of their processes between the pairs of **a** and **d**, **b** and **e**, and **c** and **f**, respectively).

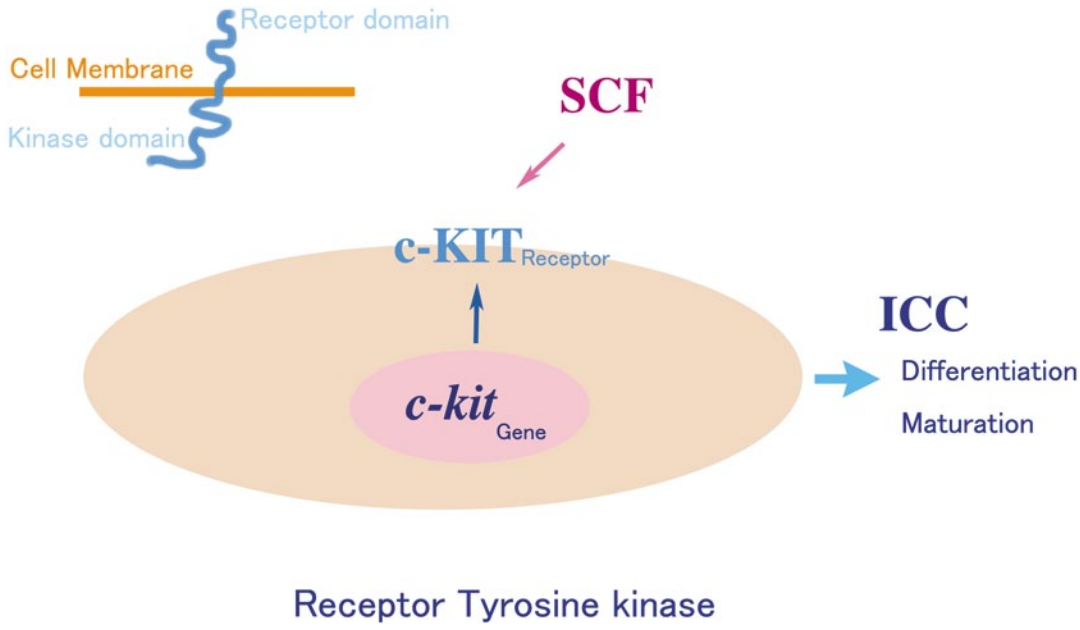

Fig. 1.2 Schematic illustration of c-Kit. c-Kit is a receptor tyrosine kinase that is encoded by the proto-oncogene (*c-kit*) and its ligand is stem cell factor (*SCF*). c-Kit consists of an extracellular domain, a transmembrane domain and an intracellular tyrosine kinase domain. Antibodies against a part of the extracelluar domain can be used immunohistochemistry for labelling ICC. Accumulated evidence indicates that ICC depend on SCF signaling via c-Kit for their development, proliferation and maintenance of function.

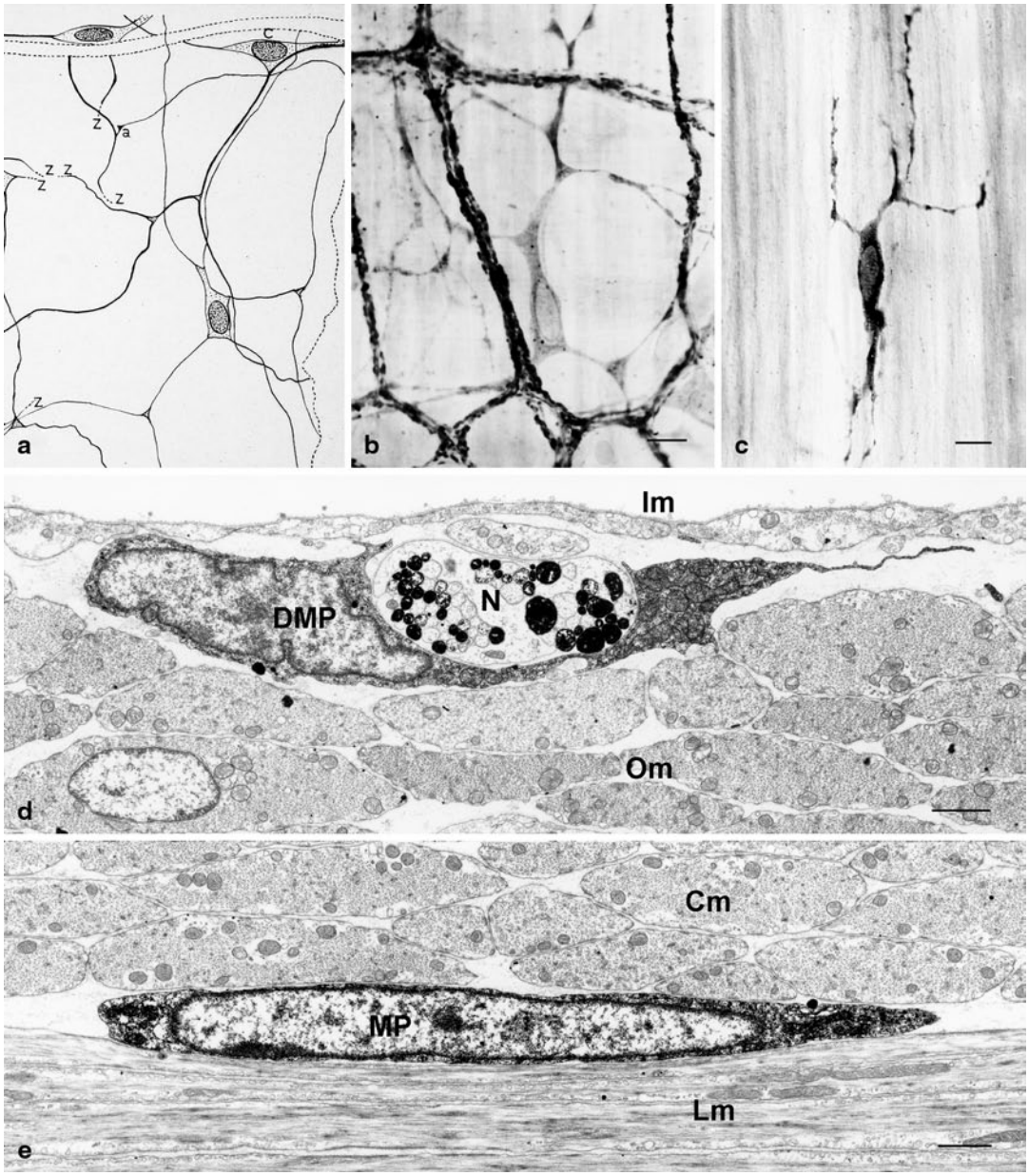

Fig. 1.3 ICC depicted by traditional staining methods. **a** Drawing of ICC-MP by Taxi in the guinea-pig intestine stained with the Bielschowsky-Gross method. Note close similarity of the cell shape with those of Fig. 1.1a, d. (Reproduced with permission from Taxi [4], Fig. 43). **b** ICC-MP of the guinea-pig small intestine stained by the zinc-iodide tetroxide (ZIO) method, which shows a very similar appearance to the cell in a. ×650. *Bar* 10 μm. (Reproduced from Komuro and Zhou [14] with permission of the publisher). **c** ICC-CM of the guinea-pig small intestine stained by ZIO method, which shows close similarity to those of Fig. 1.1b, e. ×600. *Bar* 10 μm. (Reproduced from Komuro et al. [15] with permission of the publisher). **d** Electron micrograph showing ICC-DMP (*DMP*) densely stained by ZIO method located between the inner (*Im*) and outer (*Om*) circular muscle layers of the guinea-pig small intestine. Many mitochondria can be noticed in the cytoplasm. Nerve bundles (*N*) containing ZIO-positive fibres are observed in the cytoplasmic indentation of the ICC-DMP. ×10,000. *Bar* 1 μm. **e** Electron micrograph showing ICC-MP (*MP*) densely stained by ZIO method located between the inner circular (*Cm*) and outer longitudinal (*Lm*) muscle layers of the guinea-pig small intestine. ×9000. *Bar* 1 μm.

Here, it is worth noting that ICC and neurons share staining affinity in several histological methods including the Bielschowsky-Gross method and ZIO method as well as the supravital methylene blue staining and Golgi method used for their original demonstration of ICC. These features have been one of the main reasons for difficulty in understanding true nature of ICC. The reason why ICC and neurons share similar staining affinity has not been fully clarified.

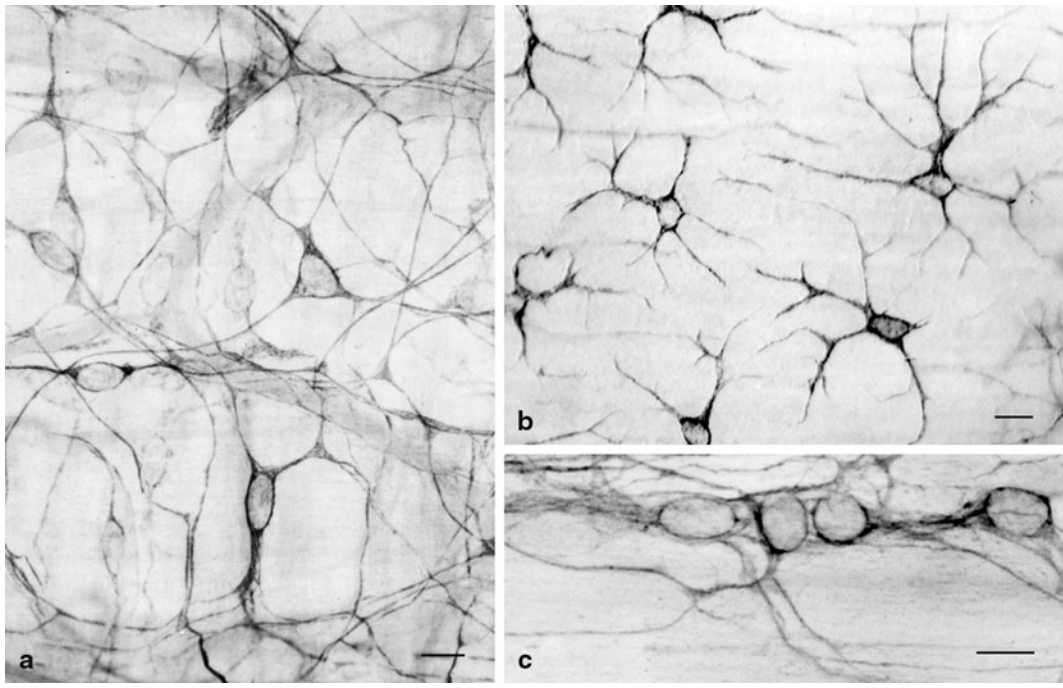

Fig. 1.4 ICC demonstrated by immunohistochemistry for vimentin. **a** ICC-MP of the guinea-pig small intestine. The ICC in his picture also show close similarity in shape to Fig. 1.1a, d and Fig. 1.2a, b. ×650. *Bar* 10 μm. (Modified from Komuro et al. [74]). **b** ICC-SS of the guinea-pig colon. ×600 *Bar* 10 μm. (See section on Colon). **c** ICC-DMP of the guinea-pig small intestine. ×900. *Bar* 10 μm. (See section on small intestine).

Vimentin filaments are commonly found in ICC and seem to function as cytoskeletal elements for supporting well-developed long slender processes, in a similar way in which neurotubules and neurofilaments support long processes of the neurons. Thus vimentin staining can be used as a substitute for c-Kit staining in a similar manner to using neurotubule staining to depict neurons.

1.2 Structure of the Gastrointestinal Tract

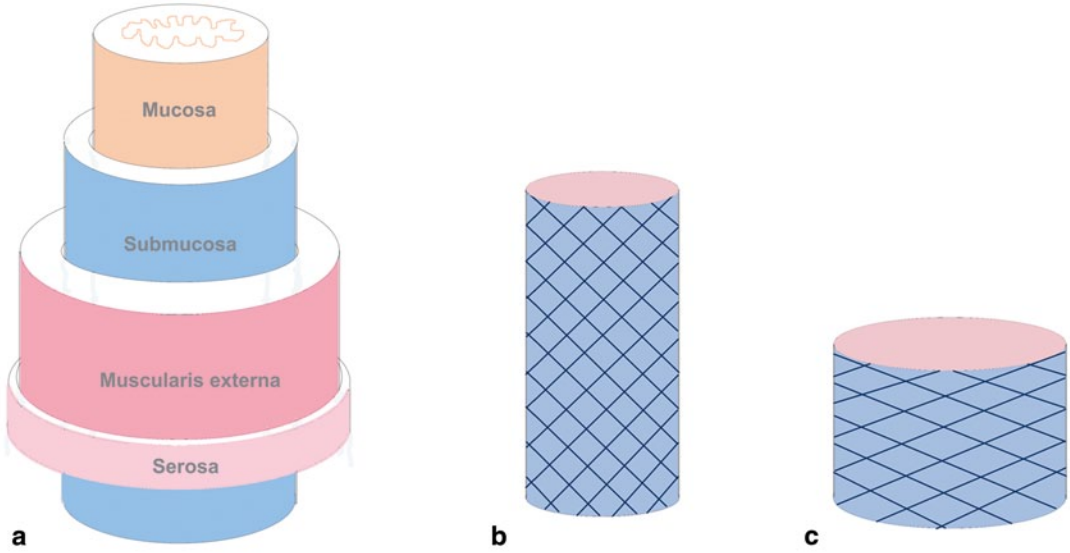

Fig. 1.5 General organization of the gastrointestinal wall. The wall of the alimentary tract is made up of four layers from the inside to outer surfaces: the mucosa, the submucosa, the tunica muscularis and the serosa (**a**). The innermost of these layers, the mucosa is responsible for the main role peculiar to each segment of the GI tract, such as secretion or digestion or absorption. In most parts of the GI tract, the tunica muscularis is composed of two layers of smooth muscle cells—a circumferentially oriented inner layer and a longitudinally oriented outer layer. The myenteric plexus located between two muscle layers coordinates their peristaltic contractions to move the luminal contents along the GI tract. Between the mucosa and muscle layers, the submucosa acts as a skeleton of the hollow organ to connect the mucosa with tunica muscularis and transmit the contractile power of the muscle to the mucosa. This results in the movement of the whole organ, reminiscent of the relationship between skeletal bones and body muscles. The diagonal arrangement of collagen bundles in the submucosa (**b c**, see below) is essential for the flexibility of the gut skeleton in allowing the deformation of the gastrointestinal tract during peristaltic movements.

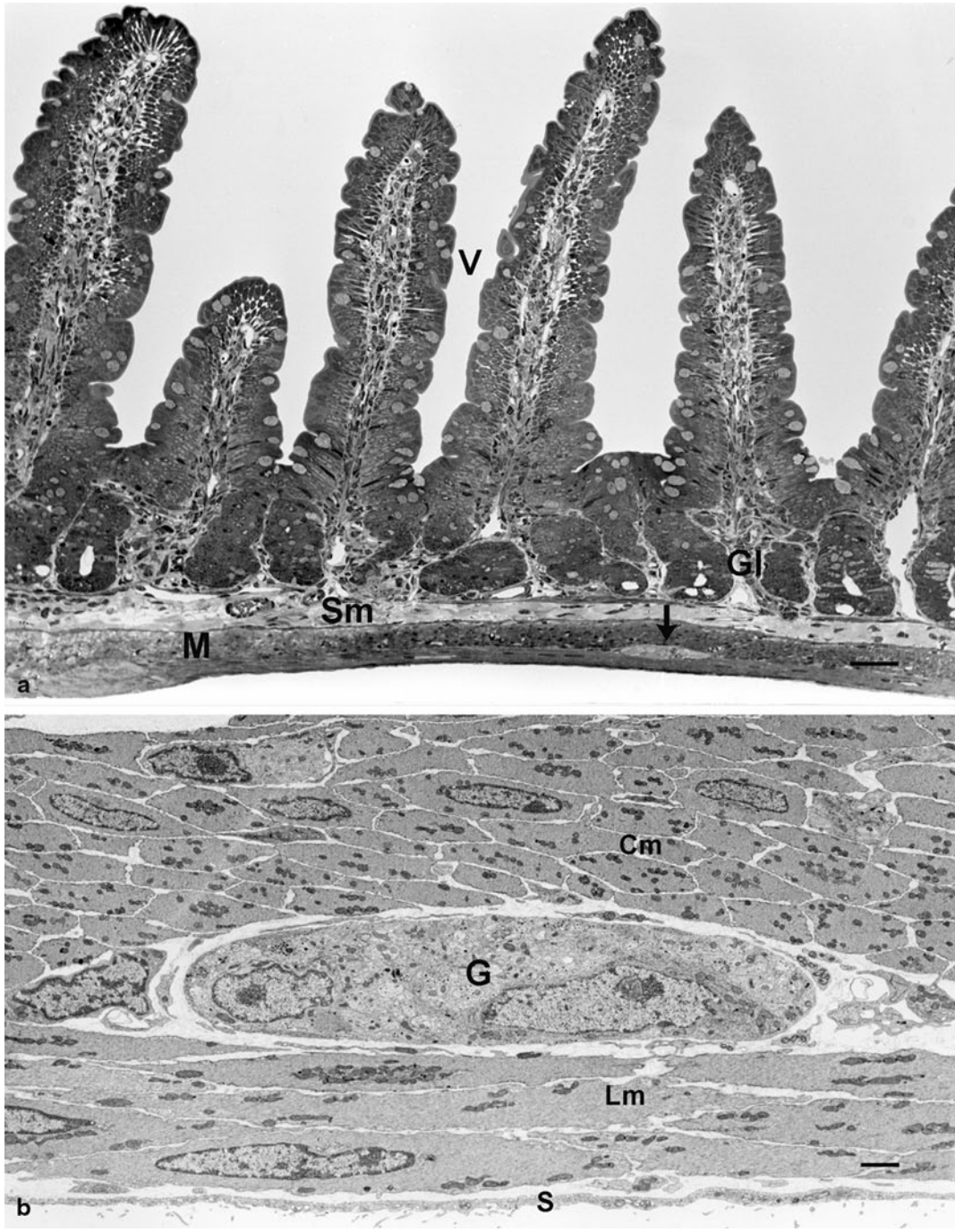

Fig. 1.6 A sectioned profile of the gut wall. **a** A longitudinal section of the rat small intestine stained with toluidine blue. The mucosa including villi (*V*) and glands (*Gl*) are separated by the pale-staining layer of the submucosa (*Sm*) from the tunica muscularis or external muscle layer (*M*). Myenteric ganglia (*arrow*) are located between two muscle layers. ×180. *Bar* 50 μm. (Reproduced from Komuro and Hashimoto [77] with permission of the publisher). **b** An electron micrograph showing the tunica muscularis consisting of the inner circular (*Cm*) and the outer longitudinal (*Lm*) muscle layers of the mouse intestine. A myenteric ganglion (*G*) is observed between two muscle layers. Mesothelium of the serosa (*S*) is observed at the outermost layer of the intestinal wall. ×7000. *Bar* 1 μm. (Reproduced from Hanani et al. [36] with permission of the publisher).

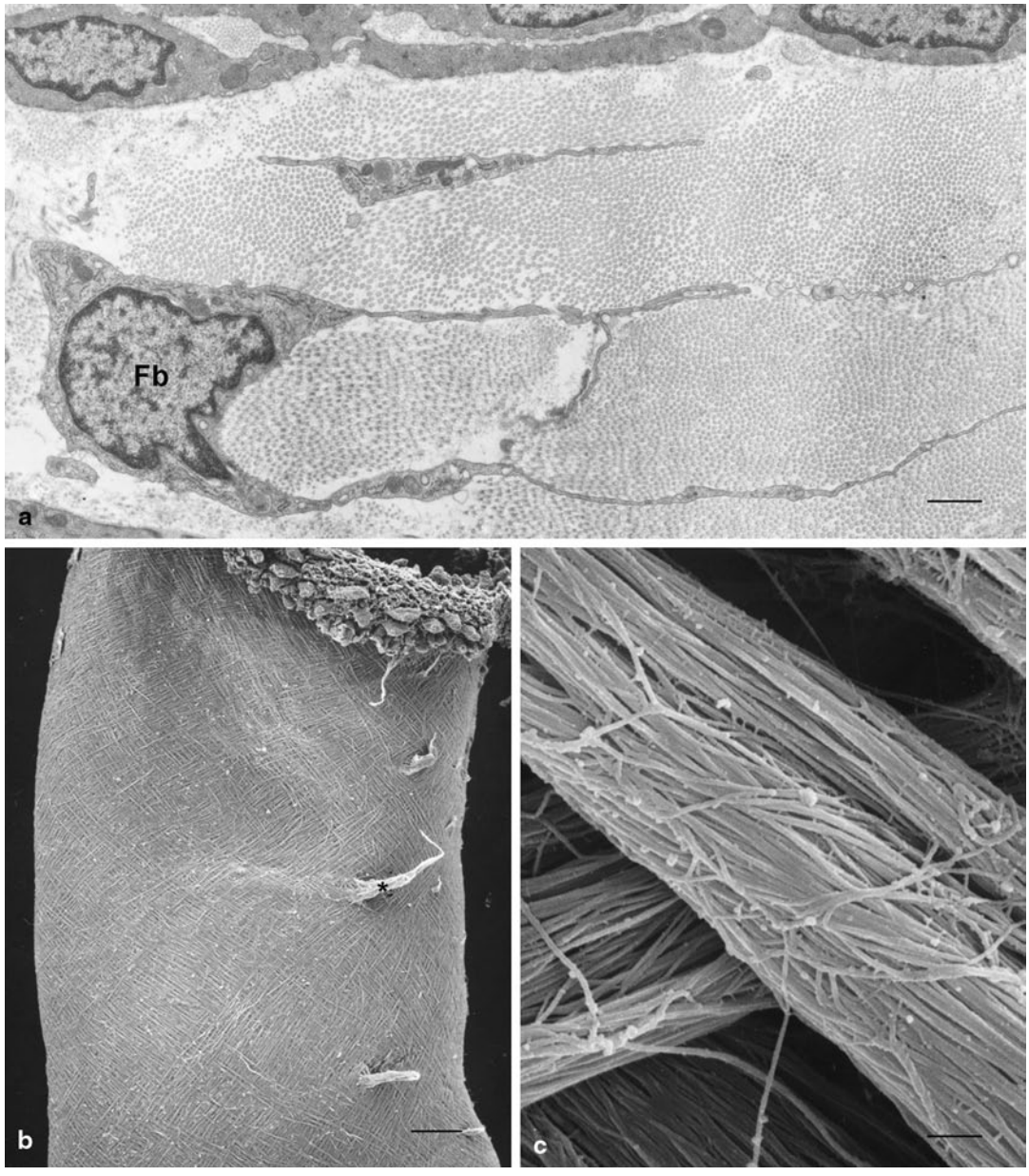

Fig. 1.7 Ultrastructural demonstration of the framework of the submucosa. **a** Transmission electron micrograph showing the submucosa of the rat intestine composed of layered, abundant collagen fibrils. The thin processes of a fibroblast (*Fb*) are located between layered collagen fibrils. ×9000. *Bar* 1 µm. (Reproduced from Komuro and Hashimoto [77] with permission of the publisher). **b** Scanning electron micrograph showing collagenous framework of the submucosa of the rat small intestine. The collagen fibres are arranged in two sets of interweaving helices. Cord-like structures are traces of blood vessels (*). ×45. *Bar* 200 µm. (Figure 1.3b, c: Reproduced from Komuro [78] with permission of the publisher). **c** Higher magnification of the collagen fibers composed of densely packed collagen fibrils. ×9200. *Bar* 1 µm.

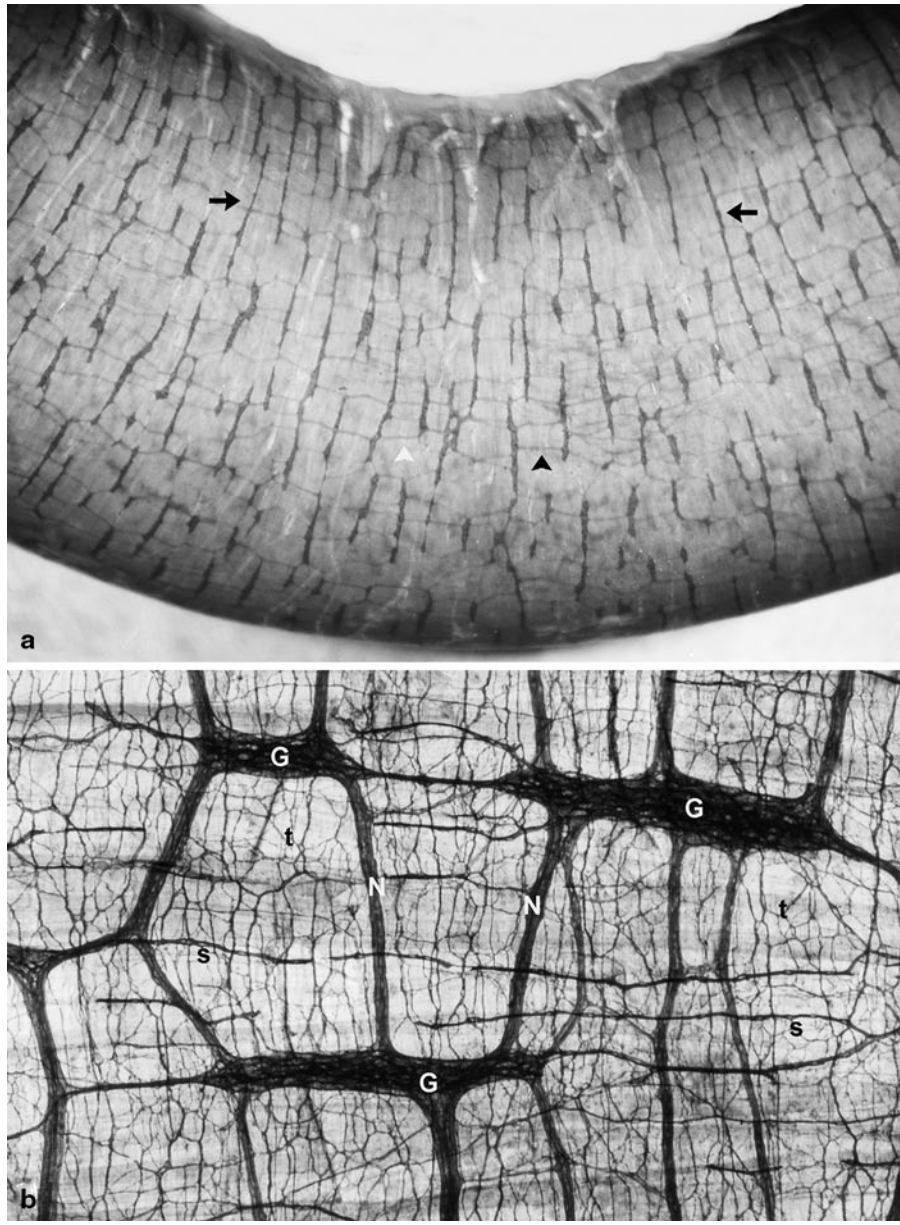

Fig. 1.8 Myenteric plexus. **a** Surface view of the whole tube of the guinea-pig small intestine stained by NADH histochemistry. A rectangular pattern of the myenteric plexus can be seen through the longitudinal muscle layer and the serous membrane. The plexus consists of elongated ganglia (*arrows*) mainly orientated along the axis of the circular muscle connected by nerve strands (*arrow heads*) running perpendicularly. The pattern of the myenteric plexus is different depending on the level of the digestive tract and shows features specific for each region. ×15. *Bar* 400 μm. **b** Whole-mount stretch preparation of the guinea-pig small intestine stained with ZIO method. The primary network of the myenteric plexus consists of ganglion strands (*G*) and connecting nerve strands (*N*). Fine nerve bundles of the secondary (*s*) and tertiary network (*t*) are clearly observed among the primary framework. ×150. *Bar* 40 μm.

The myenteric plexus is distributed throughout the GI tract and plays a central role in regulating the motor activity of the gastrointestinal tract. Accumulated evidence shows that ICC-MP associated with the myenteric plexus act as the primary pacemaker cells both in the stomach and small intestine and as secondary pacemaker cells in the colon. Thus, the specific features of the myenteric plexus in each organ are key in the movement of the external muscle layer.

Table 1.1 Abbreviations of subtypes of ICC in the GI tract

ICC	Location	Synonym
ICC-MP	Associated with myenteric plexus	ICC-AP Thuneberg [9] IC-MY Sanders [52]
ICC-DMP	Associated with deep muscular plexus of the small intestine	IC-DMP Sanders [52]
ICC-SMP	Associated with submuscular plexus of the colon	IC-SM Sanders [52]
ICC-SM	Located at submucosal border of the circular muscle in the antrum	IC-SM Sanders [52]
ICC-CM	Located within the circular muscle layer	IC-IM Sanders [52]
ICC-LM	Located within the longitudinal muscle layer	IC-IM Sanders [52]
ICC-IM	General term for ICC within the muscle layer	IC-IM Sanders [52]
ICC-SS	Located in the subserous connective tissue space	
ICC-SP	Associated with submucosal plexus	

1.3 Nomenclature of ICC

The terminology adopted in this Atlas is a minor modification of that used in Hanani et al. [36] and Komuro [37]. It is based on the Thuneberg's invention [8] of classifying ICC depending on the tissue layer with which they are associated, and follows the modern practice of avoiding attribution of the individual name of discoverer of cells and tissues, and the addition of new subtypes.

Three principles are set in this terminology. First, ICC is used as an abbreviation for Interstitial Cells of Cajal to make clear their nature, since the abbreviation IC has also been used in the literature but represents interstitial cells in general and only has a neutral meaning regarding connective tissue cells. Second, where a nerve plexus is associated with the ICC, the initial letters of the plexus are added to ICC with a hyphen, for example, DMP for the deep muscular plexus, or MP for the myenteric plexus. Third, where the nerve plexus has no particular name, hyphenated abbreviations of the tissue layer are added to ICC, e.g. ICC-CM in the circular muscle layer and ICC-SM in the submucosal layer. ICC-IM is also adopted as a general term for ICC within a muscle coat (Table 1.1) (Fig. 1.9).

ICC-SM and ICC-SMP are found at the submucosal border of the circular muscle layer of the gastric pylorus and the colon, respectively. ICC-DMP are observed in association with the deep muscular plexus located between the inner thin and outer main layers of the circular muscles in the small intestine. ICC-MP are seen in association with the myenteric plexus located between the circular and longitudinal muscle layers throughout the gastrointestinal tract except the proximal part of the stomach. ICC-CM and ICC-LM are distributed within the circular and longitudinal muscle layers, respectively. ICC-SS are found in the subserosal connective tissue space.

ICC-SP associated with the submucosal plexus are not included in this illustration. To date, ICC-SP have been only found in the gastric corpus, proximal colon and caecum in the guinea-pig.

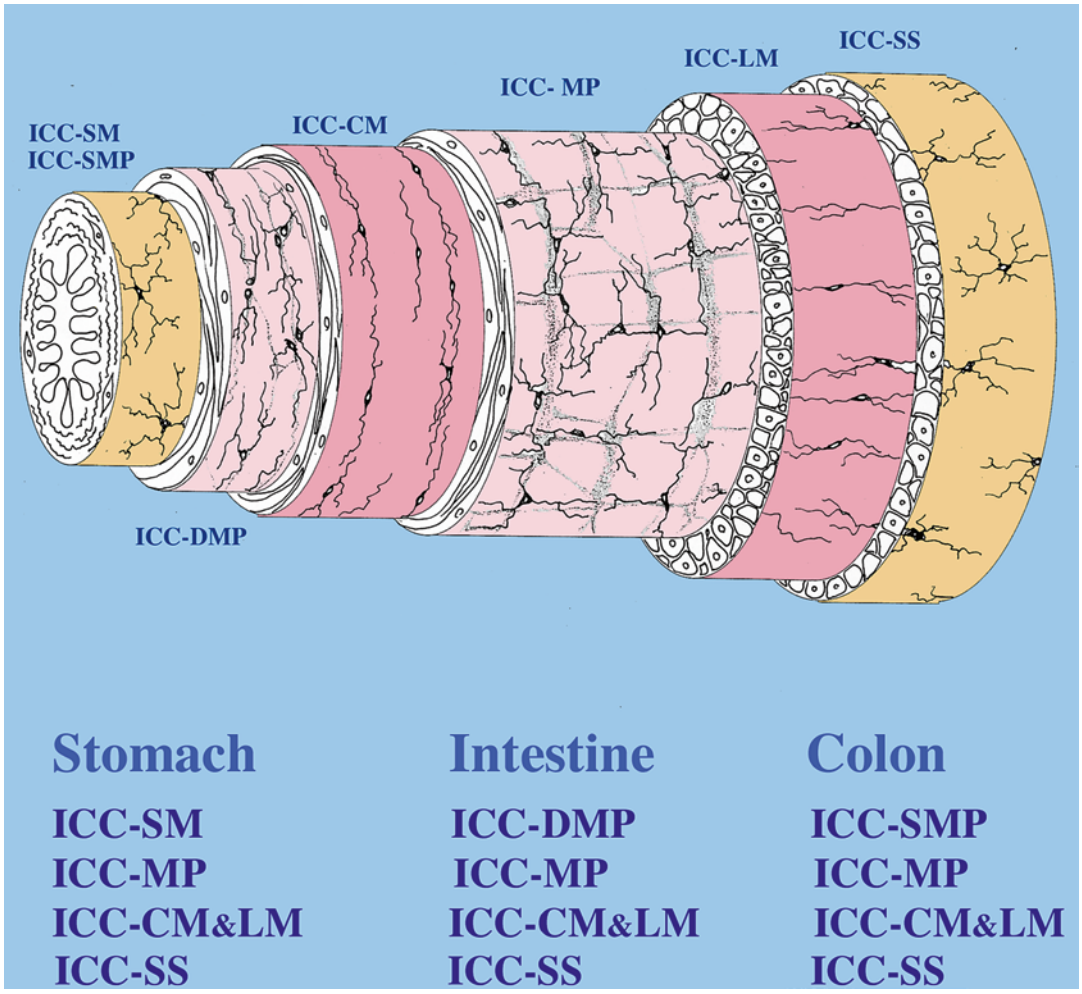

Fig. 1.9 Schematic demonstration of ICC found in the different tissue layers in different regions of the GI tract. (Modified from Hanani et al. [36]).

1.4 Shape and Size of ICC

The cell shape of ICC appears to be determined by several factors, including the presence or absence of a nerve plexus, their relationships to those plexuses and the frequency of connections between ICC themselves.

ICC-IM located within the muscle layers are mainly bipolar cells oriented parallel with the axis of surrounding smooth muscle cells. The secondary and tertiary processes are generally not well developed.

On the other hand, some of ICC-IM show a multipolar shape with three to five primary processes while they maintaining their longer cell axis among the muscle cells. These cells are found in the circular muscle layer of the guinea-pig small intestine and in the colon. ICC-DMP of the small intestine, which are regarded as a special type of ICC-CM, can take a variety of forms depending on the sites of their associated nerve bundles. At straight portions of the nerves, they show slim spindle shapes with long bipolar processes, while at the intersections the cells project three to five processes along the nerve bundles.

In contrast, ICC-MP located in the meshes of the primary network of the myenteric plexus do not show a clear cell axis but project several processes in multiple directions. Similar multipolar cells with no obvious cell axes are found in the subserosal layer of the guinea-pig proximal colon.

Footnote Morphological features of ICC illustrated in this Atlas were mainly demonstrated by immunohistochemistry using whole-mount stretch preparation. Specimens were pre-incubated in 4% Block Ace solution for 20 min and then incubated with a rat monoclonal antibody against mouse CD117 (c-Kit) to label ICC and with a rabbit antibody against human protein gene product (PGP) 9.5 to label nerve components. Then specimens were incubated with a fluorescein isothiocyanate (FITC)-conjugated secondary antibody and a Cy^{TM}3-conjugated secondary antibody. Specimens were observed with a confocal laser scanning microscope (Leica TCS SP2; Leica Microsystems, Wetzlar, Germany).

Specimens (jejunum) from the guinea-pigs (weighing 300 ~ 400 g) fixed slightly distended condition measure about 2 cm in the circumference. In these intestines, an approximate estimation indicate, that at least 40 smooth muscle cells are needed to encircle the whole tube if they contact each other tip to tip. Similar estimates indicate that more than 100 ICC-CM and about 80 ICC-DMP are needed to cover the whole circumference of the intestine. Such estimates suggest that role of ICC as intermediate cells in the neural transmission to the smooth muscles may be effective in the lateral direction but not in the axial direction of the circular muscle.

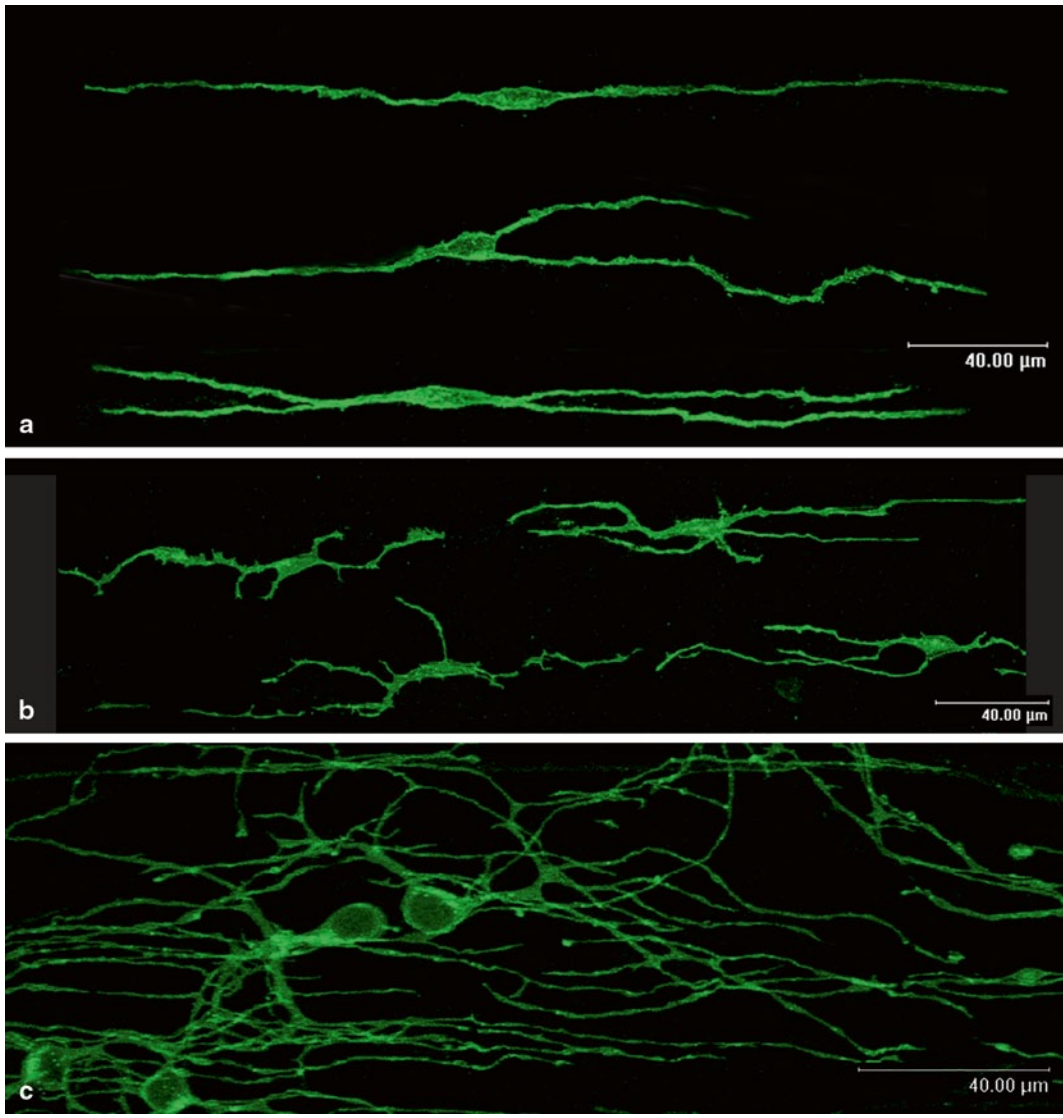

Fig. 1.10 ICC within the muscle layer. **a** Bipolar cells found within the circular muscle layer (ICC-CM) in the guinea-pig stomach. Simple bipolar cell with only primary processes projecting to the opposite directions (*top of the figure*) are frequently observed in the fundus, and cells with secondary branches in both ends (*bottom of the figure*) are numerous in the antrum. These types of cells are observed in almost every muscle layer in the GI tract, but the cell size differs depending on the organ or region. For example, their cell lengths measure around 200 µm in the guinea-pig gastric fundus and more than 300 µm in the guinea-pig caecum. *Bar* 40 µm. **b** Multipolar cells found in the circular muscle layer (ICC-CM) in the guinea-pig small intestine. They project 3~5 primary processes while they maintain their longer cell axis aligned with that of the muscle layer (*horizontal direction*). They are slightly shorter than the bipolar cells and their length measures around 180 µm in the small intestine and around 120 µm in the colon, though the small intestine contains long bipolar cells around 350 µm long. *Bar* 40 µm. **c** Multipolar cells associated with the deep muscular plexus (ICC-DMP) of the guinea-pig small intestine. Their secondary and tertiary processes are well developed and are mainly arranged in parallel with the axis of the muscle layer (*horizontal direction*). The processes of ICC-DMP often span lengths of 300 µm and they are aligned with the axis of the circular muscle cell. *Bar* 40 µm.

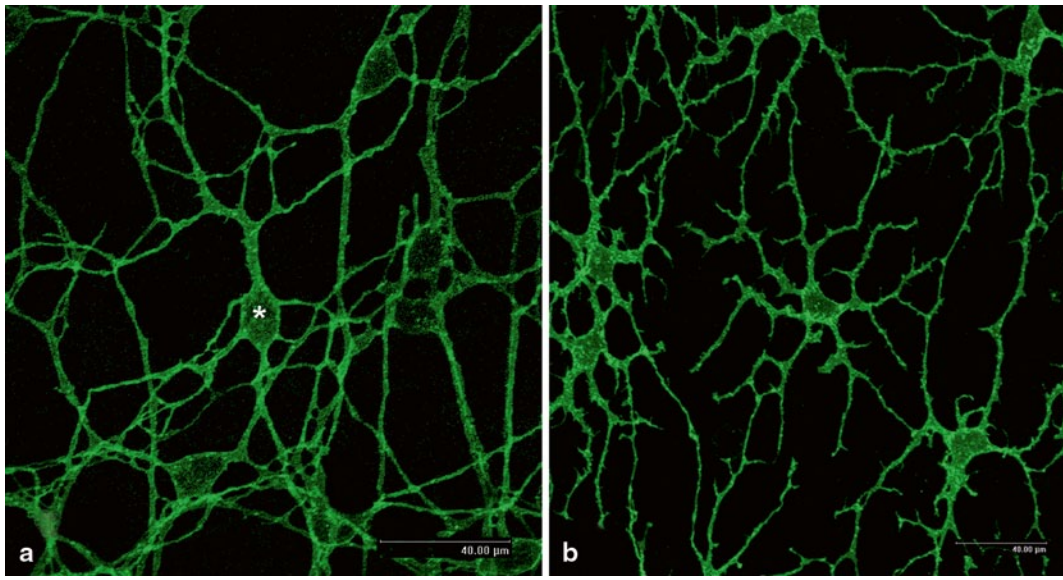

Fig. 1.11 ICC forming their own network. **a** Multipolar cells associated with the myenteric plexus (ICC-MP) of the guinea-pig small intestine. These cells form a net on the framework of the primary nerve plexus located between two muscle layers and thus ICC-MP (*) do not show a clear cell axis. They usually have three to five primary processes that branch off repeatedly to form secondary, tertiary and further branches. The cell processes of these cells measure around 100 µm in one direction from the base of the cell body to the tip. *Bar* 40 µm. (Modified from Hanani et al. [36]). **b** Multipolar cells found in the subserosal layer (ICC-SS) of the guinea-pig proximal colon. These cells are distributed in the connective tissue space beneath the serosal mesothelium without firm connection with any structures and thus do not show clear cell axis. Spiny processes along the long processes are one of the different features from ICC-MP described above. The cell processes also measure around 100 µm in one direction from the base to the tip. (Reproduced from Aranishi et al. [35] with permission of the publisher). *Bar* 40 µm.

Here, it is worth noting that ICC-MP and ICC-SS send their processes into the different tissue layers and form cellular networks in three-dimensions. These features will be described in a later chapter with stereo-micrographs (see section on colon).

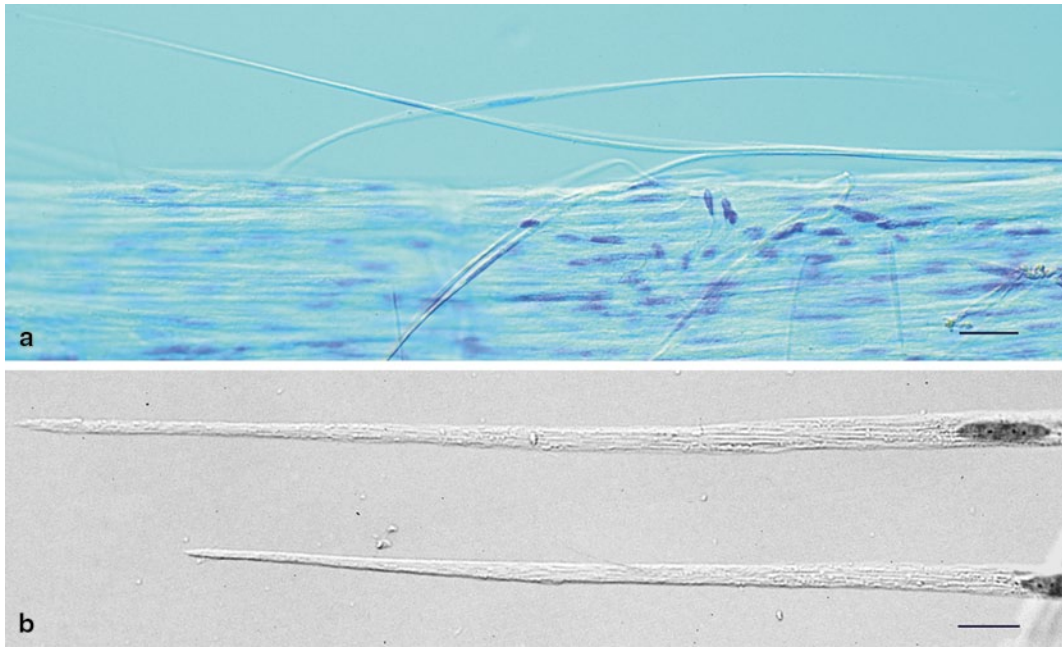

Fig. 1.12 Smooth muscle cells. **a** Images with Nomarski optics of the smooth muscle cells of the guinea-pig small intestine which are isolated under a dissection microscope and stained with toluidine blue. *Bar* 50 µm. **b** Higher magnification of the smooth muscle cells in the same preparation as a. These cells measure about 500 ~ 600 µm in length. *Bar* 20 µm.

Part I
Distribution and Arrangement of ICC in the GI Tract

ICC have different distribution patterns and morphological features depending on their anatomical locations, and are classified into several subtypes on this basis. The structural arrangement of ICC appears to reflect their physiological tasks and thus provides a clue for a critical understanding of the motility of the GI tract. Specific distribution of ICC in the stomach, small intestine, duodenum, colon, caecum and in the ileocaecal junction are described. ICC found in the submucosal layer are separately described.

Stomach

2

The stomach is unique in that ICC have a different distribution in proximal and distal regions of the same organ. ICC-CM and ICC-LM are densely distributed throughout the thick circular and longitudinal muscle layers of the cardia, fundus and of the proximal half of the corpus in the mouse, rat and guinea-pig. In contrast, ICC-MP are completely lacking from the space between the circular and longitudinal muscle layers in these regions. ICC-MP emerge in the mid-corpus and become well-developed in the distal region of the corpus with a thin muscle coat, while both ICC-CM and ICC-LM decrease in number in this region.

ICC-MP are particularly dense in the pyloric antrum, though the distribution of ICC-CM and ICC-LM appear similar to those in the distal corpus. Another characteristic feature of the pylorus is the presence of ICC-SM at the submucosal border of the circular muscle layer, despite lack of a nerve plexus in this region corresponding to either the DMP of the small intestine or the SMP of the colon. ICC-SM are observed in a confined area directly adjacent to the pyloric sphincter and are not found in the rest of the stomach in the mouse, rat, guinea-pig, dogs and in the human.

T. Komuro, *Atlas of Interstitial Cells of Cajal in the Gastrointestinal Tract,*
DOI 10.1007/978-94-007-2917-9_2, © Springer Science+Business Media B.V. 2012

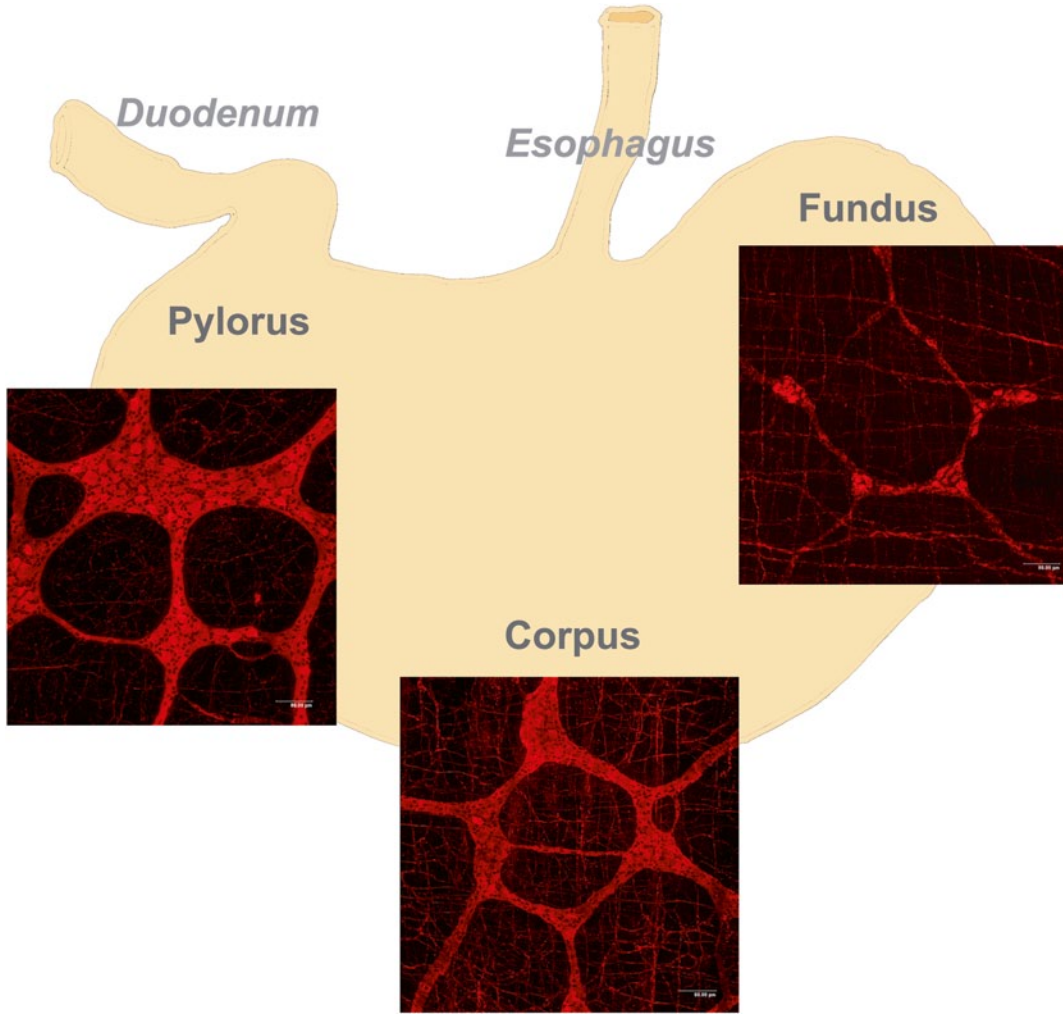

Fig. 2.1 An illustration showing different patterns of the myenteric plexus peculiar to the regions in the guinea-pig stomach stained with PGP9.5 immunohistochemistry Whole-mount stretch preparation of the fundus shows the loose network of the myenteric plexus characterized by small ganglia and thin connecting nerve strands. The corpus shows the myenteric plexus consisting of slightly larger sized ganglia and thicker connecting nerve strands in comparison of those of the fundus. Fine nerve fibres in both circular (*horizontal direction*) and longitudinal (*perpendicular direction*) muscle layers are also seen. The pyloric antrum shows the myenteric plexus composed of large ganglia and thick nerve strands. (Courtesy of Dr Kunisawa, Waseda University).

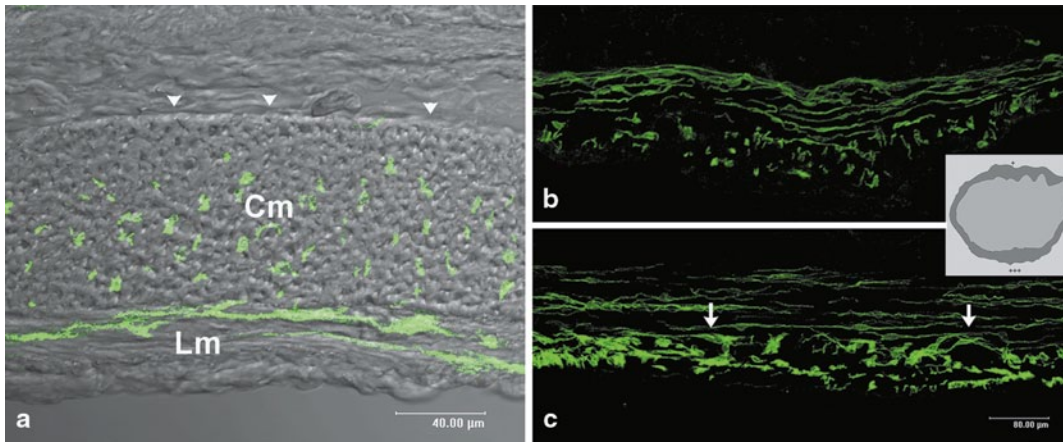

Fig. 2.2 Sectioned profiles of the guinea-pig stomach. **a** A longitudinal section of the corpus observed with Nomarski optics merged with c-Kit immunoreactive ICC (*green*). *Note*, green dots (ICC-CM) are mainly located within roughly the basal three quarters of the circular muscle layer (*Cm*) excluding one quarter from the submucosal surface (*arrow heads*). This tendency is also observed in the cardia, fundus, corpus and the proximal portion of the antrum. Elongated c-Kit immunoreactive deposits representing ICC-LM are also seen in the longitudinal muscle layer (*Lm*). *Bar* 40 µm. **b, c** Transverse sections of the lesser and greater curvatures of the pyloric antrum of the guinea-pig stomach, respectively. c-Kit immunoreactivity representing ICC-MP is stronger in the greater curvature (*bottom*) than the lesser curvature (*top*) (*arrows* in **c**). *Bar* 80 µm. (Courtesy of Dr Kunisawa, Waseda University).

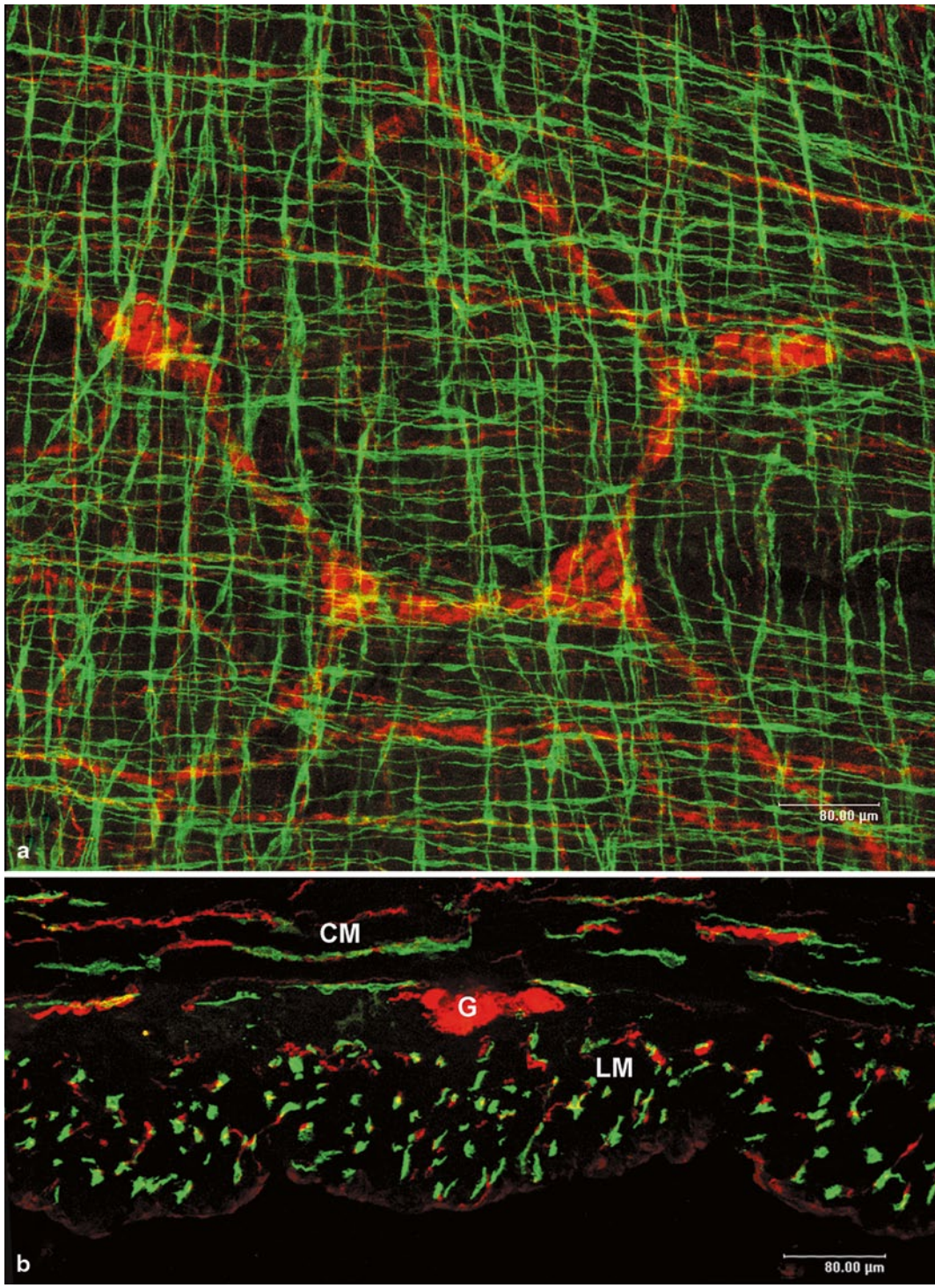

Fig. 2.3 Confocal images of the guinea-pig fundus stained with c-Kit (*green*)/PGP9.5 (*red*) immunohistochemistry. **a** Whole-mount stretch preparation showing the lattice structures composed of horizontal ICC-CM and perpendicular ICC-LM over the loose network of the myenteric plexus, because of lack of ICC-MP in this region. *Bar* 80 µm. **b** A transverse section of the fundus. Bipolar shape of ICC-CM (*CM*) and cross-sectioned dots of ICC-LM (*LM*) are densely observed within the circular and longitudinal muscle layers, respectively. Between these two layers, however, ICC-MP are not observed around the myenteric ganglion (*G*). *Bar* 80 µm. (Courtesy of Dr Kunisawa, Waseda University).

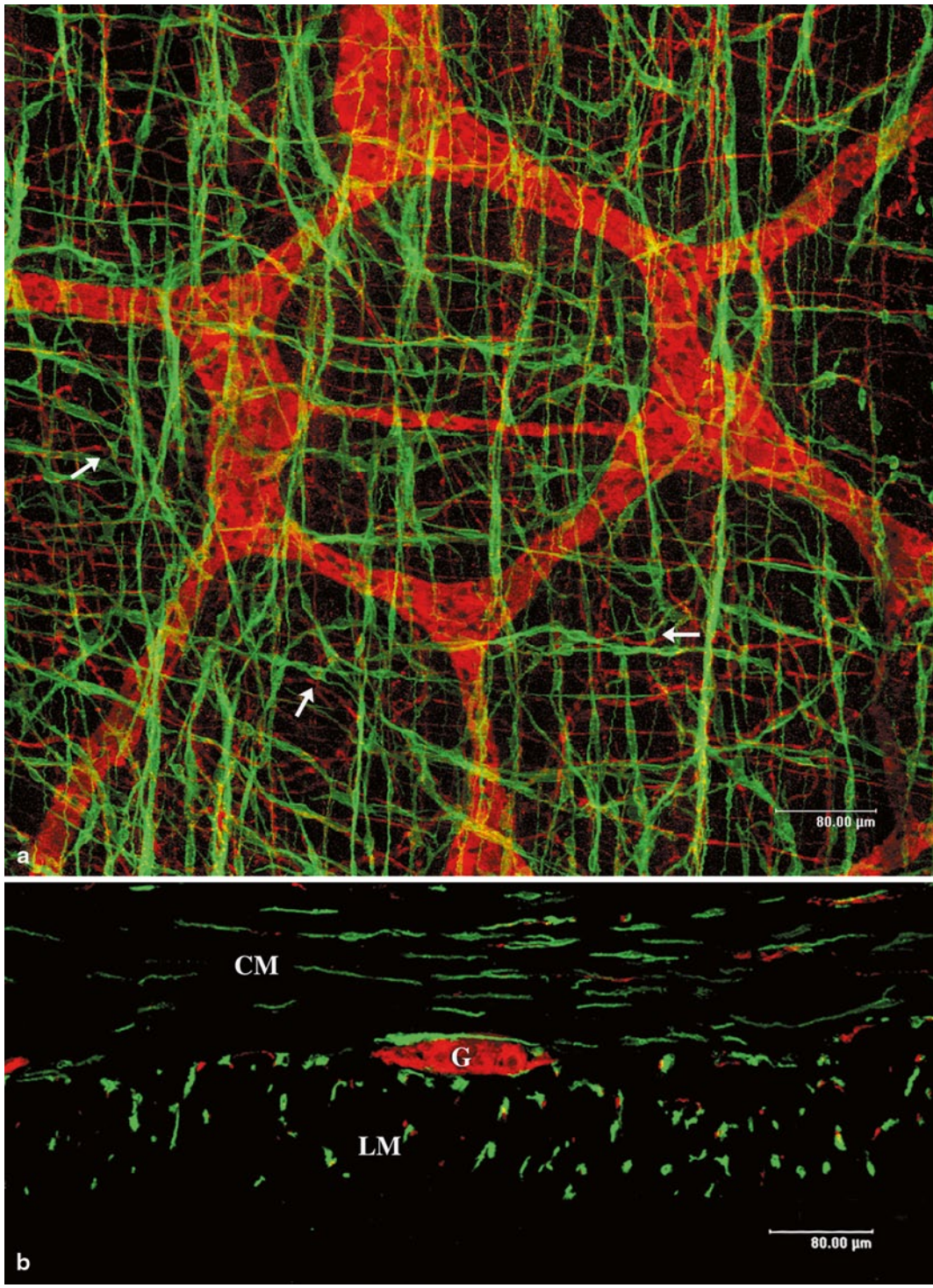

Fig. 2.4 Confocal images of the guinea-pig corpus stained with c-Kit (*green*)/PGP9.5 (*red*) immunohistochemistry. **a** Whole-mount stretch preparation of corpus showing the lattice structures composed of ICC-CM and ICC-LM similar to those of the fundus, into which, however, are a few regions of intervention by multipolar cells of ICC-MP emerging from the mid portion of the corpus (*arrows*). *Bar* 80 µm. **b** A transverse section of the corpus showing a few c-Kit immunoreactive deposits representing ICC-MP around the myenteric ganglion (*G*). ICC-CM (*CM*) and ICC-LM (*LM*) are also observed in the circular and longitudinal muscle layers, respectively. *Bar* 80 µm. (Courtesy of Dr Kunisawa, Waseda University).

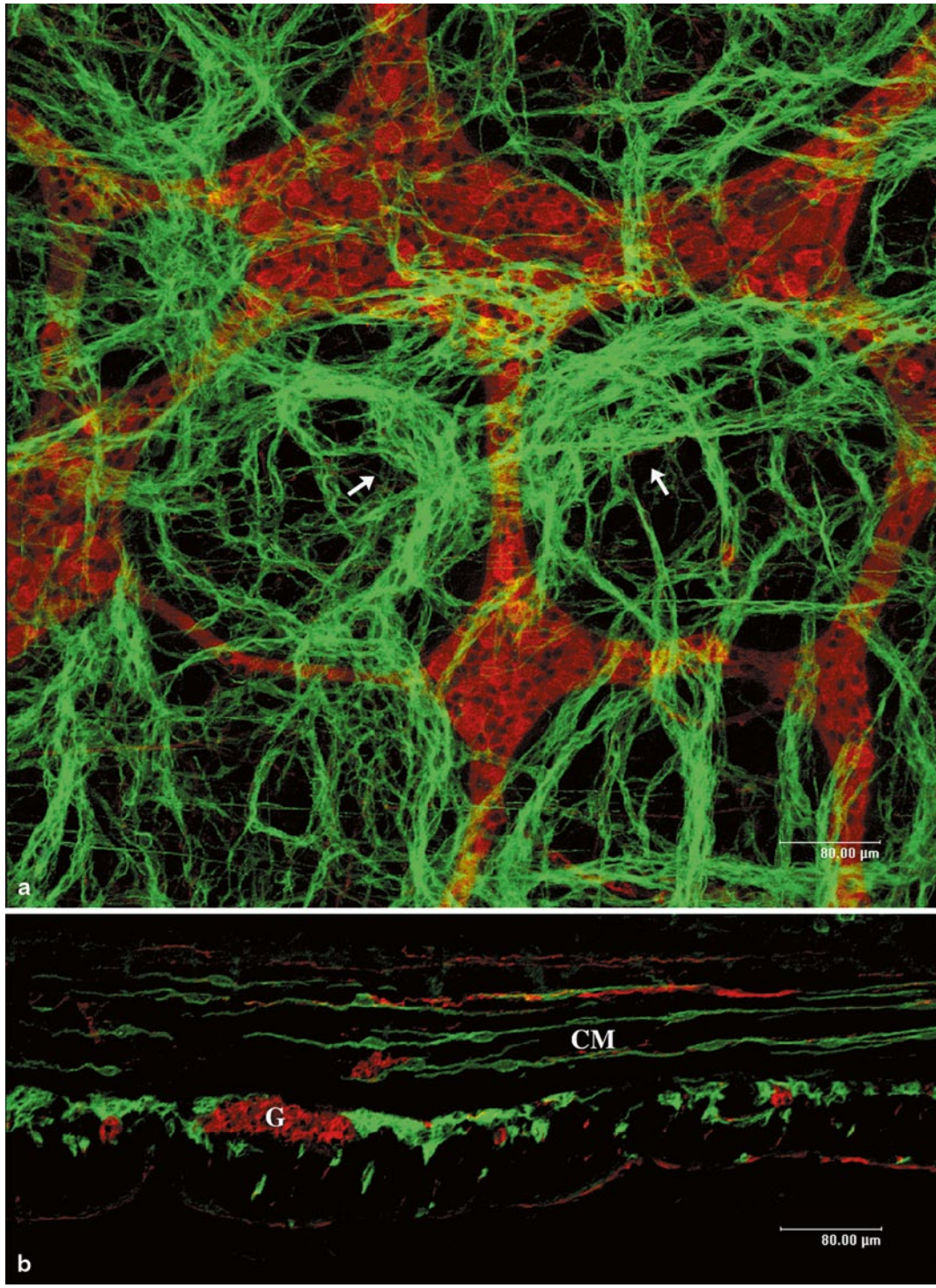

Fig. 2.5 Confocal images of the guinea-pig pyloric antrum stained with c-Kit (*green*)/PGP9.5 (*red*) immunohistochemistry. **a** ICC-MP are abundant around the nerve plexus in forms of bundles or in clusters (*arrows*). They do not make clear basket formations surrounding ganglia as in the small intestine (see below). *Bar* 80 µm. **b** A transverse section of the pyloric antrum showing strong c-Kit immunoreactive deposits in the myenteric region representing a rich distribution of ICC-MP around the ganglion (*G*). Bipolar shape of ICC-CM (*CM*) are also clearly seen in the circular muscle layer. *Bar* 80 µm. (Courtesy of Dr Kunisawa, Waseda University).

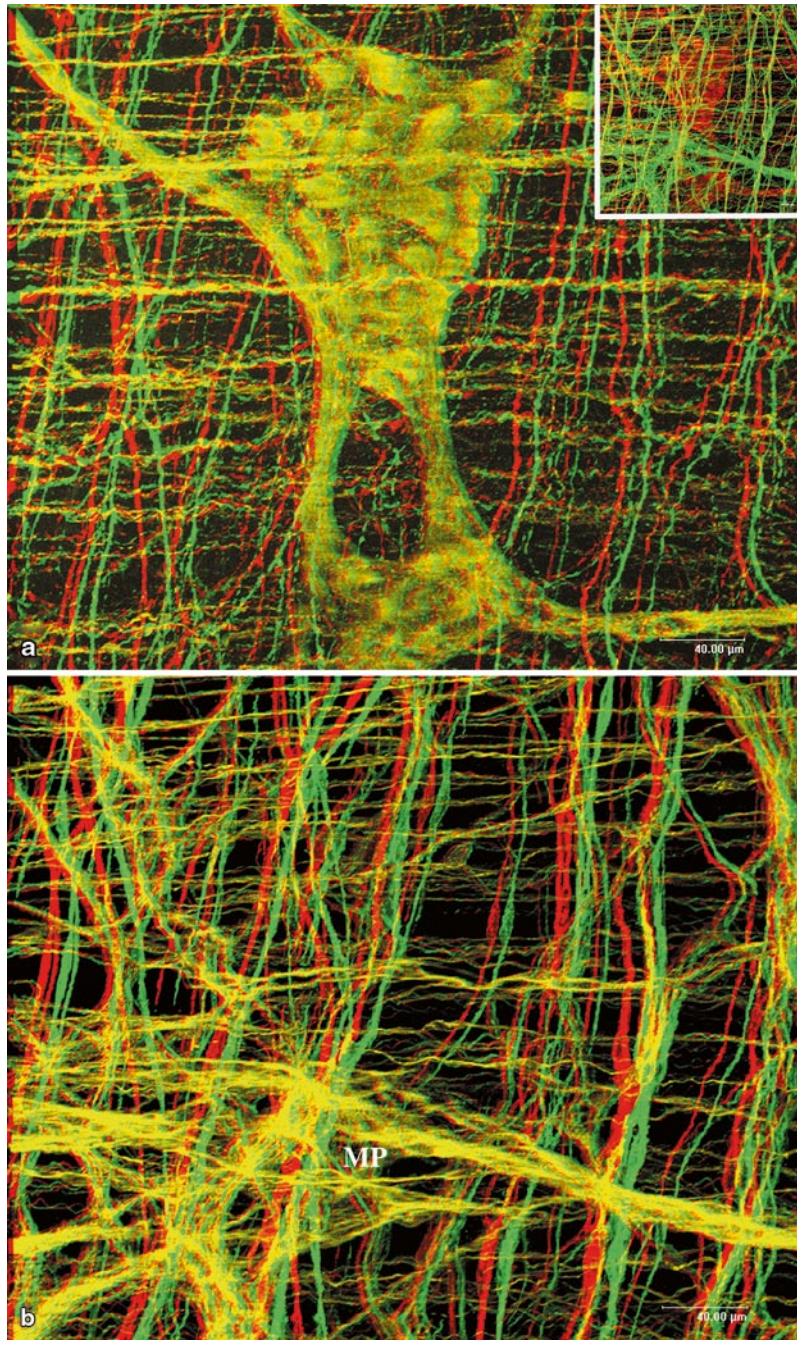

Fig. 2.6 Three-dimensional (3D) reconstruction of the nerve and ICC in the guinea-pig antrum confirming the existence of irregular clusters of ICC-MP. **a** Stereo-micrograph of the nerve plexus in the guinea-pig pyloric antrum, showing the myenteric ganglia sandwiched by nerve fibres in the circular and longitudinal muscle layers, running in horizontal and perpendicular directions, respectively (view with *red/green* stereoscopic glasses). *Bar* 40 µm. *Inset* Image merged with **a** and **b** to show spatial relationship of the nerves and ICC. **b** Stereo-micrograph of ICC associated with the nerves in **a** Bundles of ICC-MP (*MP*) show uneven distribution around the ganglia. These structures appear to represent their arrangement *in situ* and are not caused by preparation artifact, since they are located between the both circular and longitudinal muscle layers in which nerve fibres show regular arrangement seen in **a** (view with *red/green* stereoscopic glasses). *Bar* 40 µm. (Courtesy of Dr Kunisawa, Waseda University).

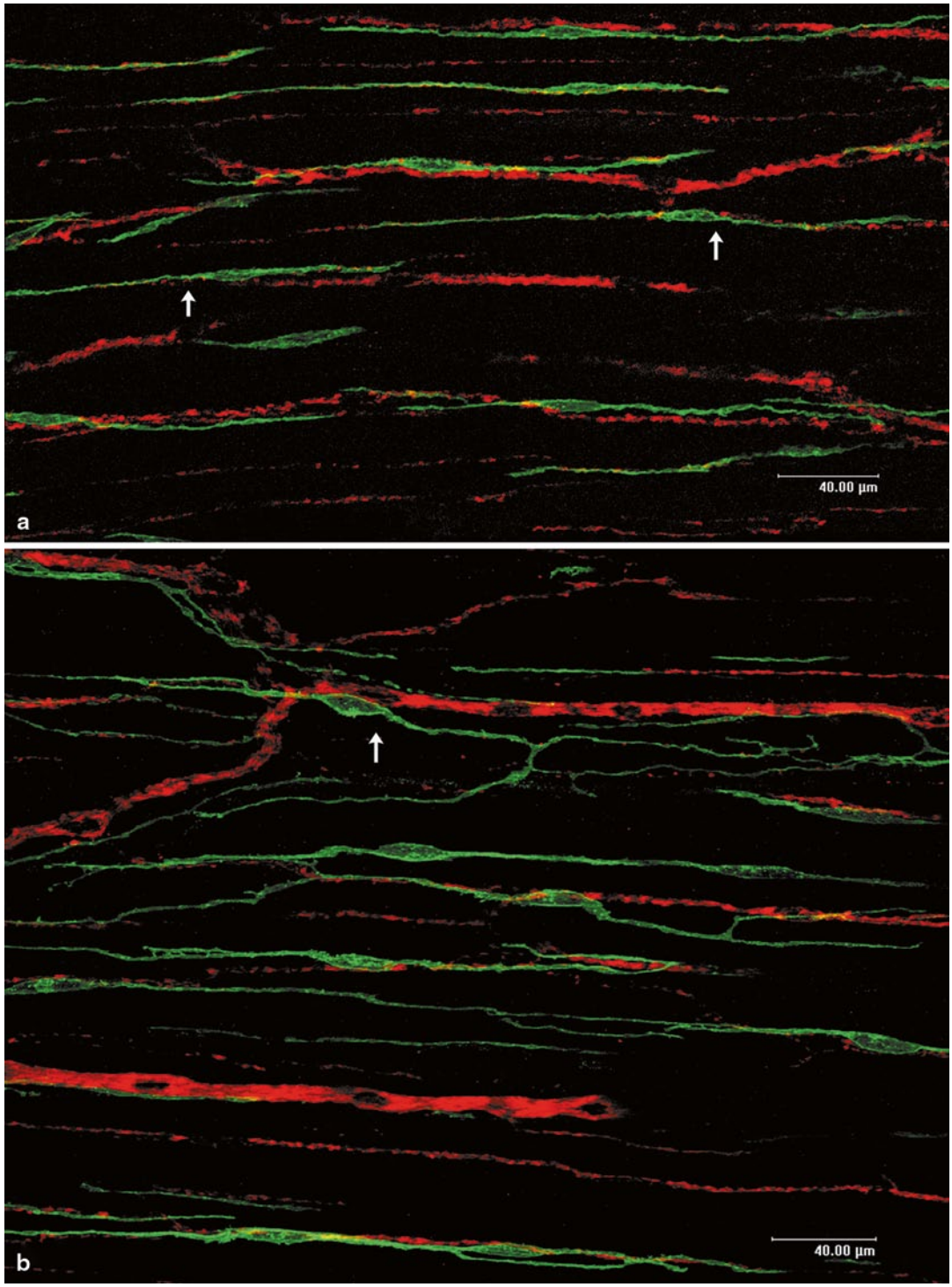

Fig. 2.7 ICC in the circular muscle layer of the guinea-pig stomach. **a** Simple bipolar shape of ICC-CM closely associated with the nerves in the fundus (*arrows*). *Bar* 40 µm. **b** ICC-CM (*arrow*) with branching processes associated with the nerves in the pyloric antrum. *Note*, ICC-CM in this region have long secondary branches. *Bar* 40 µm. (Courtesy of Dr Kunisawa, Waseda University).

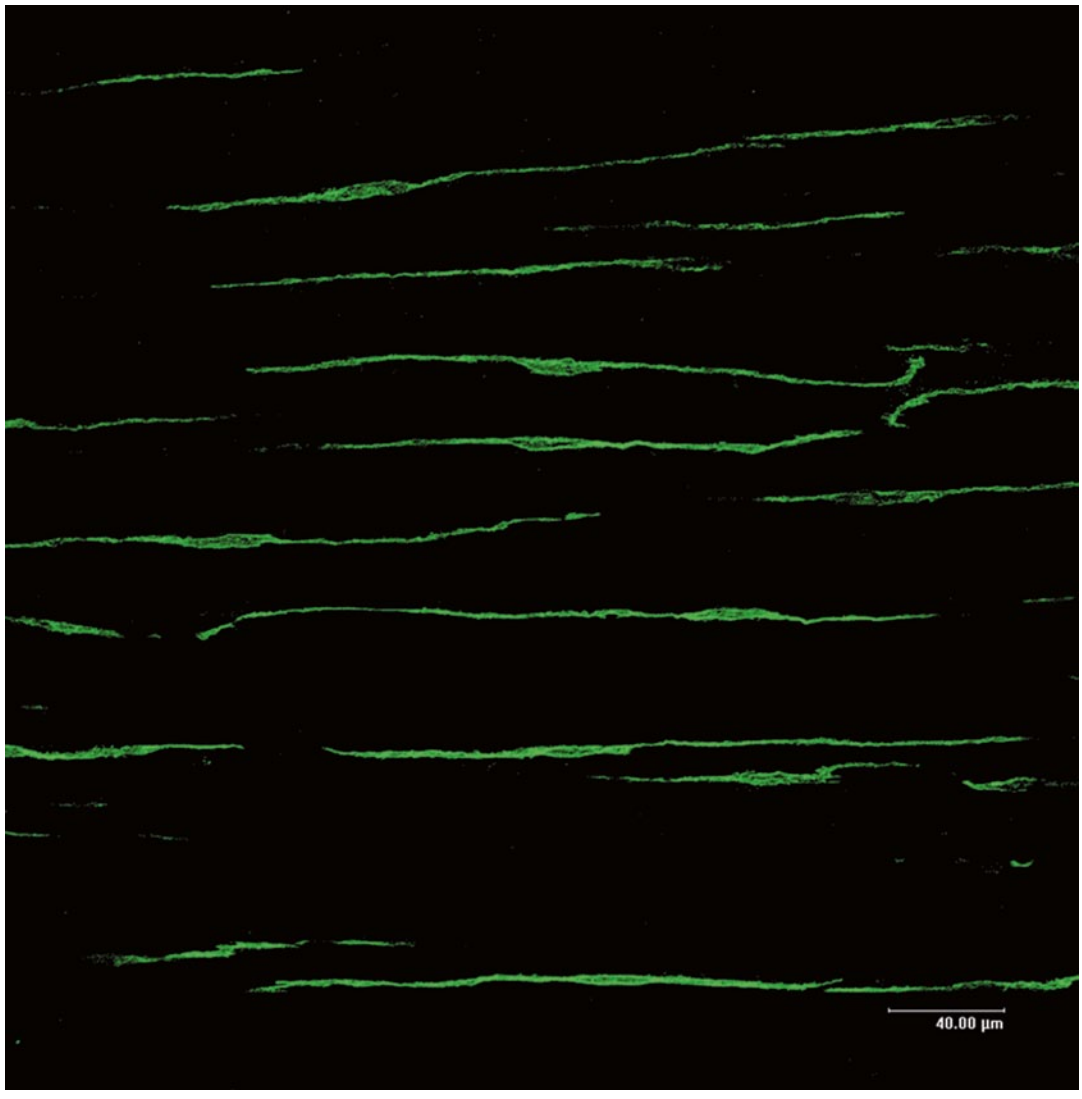

Fig. 2.8 Typical bipolar shape of ICC-CM in the guinea-pig fundus. All ICC-CM in this observation field have a simple bipolar shape and they are rather loosely arranged with wide gaps. These cells measure 200–240 µm in length. *Bar* 40 µm. (Courtesy of Dr Kunisawa, Waseda University).

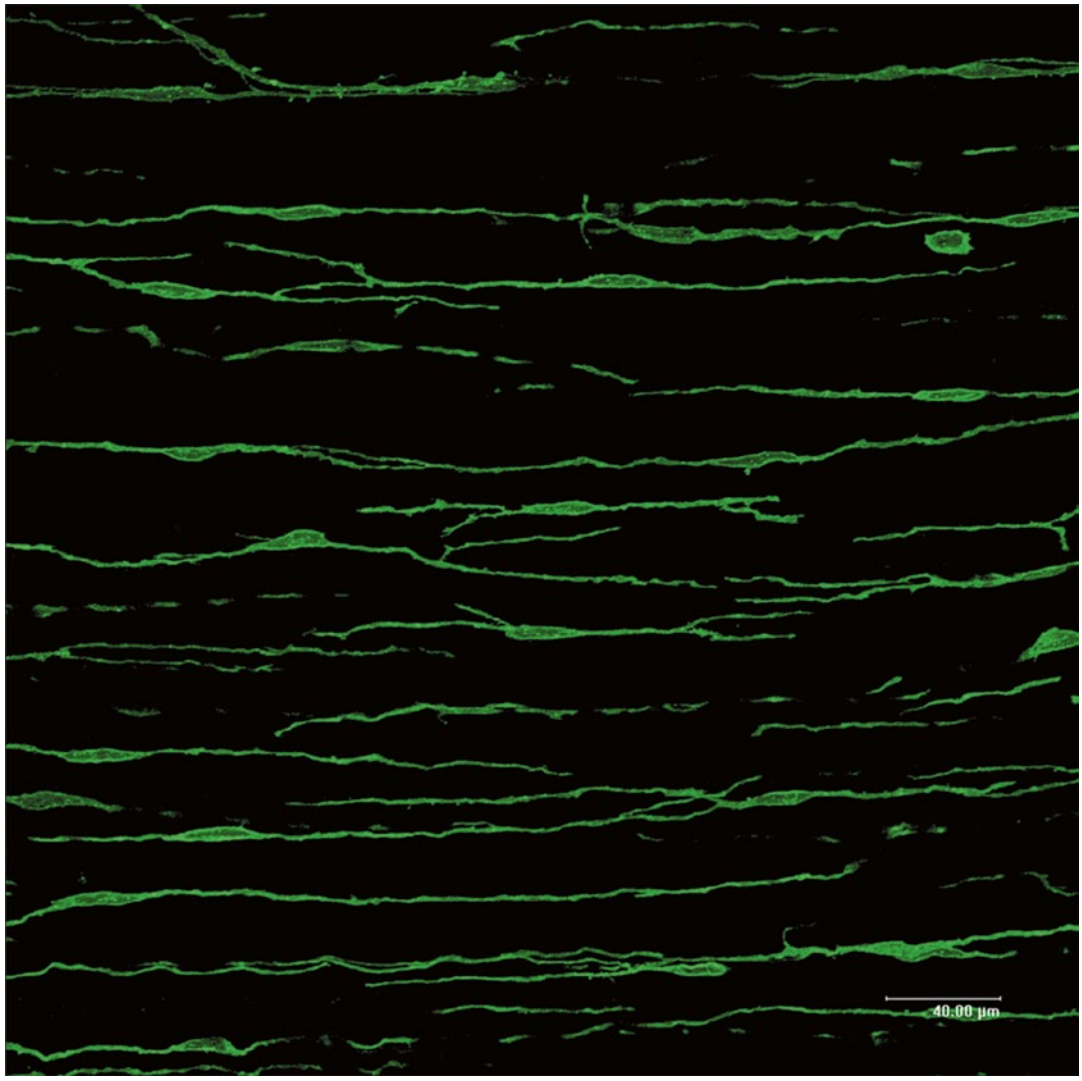

Fig. 2.9 ICC-CM in the guinea-pig corpus. ICC-CM of the corpus show secondary branches and are more closely arranged than the fundus. These cells measure 250–280 µm in length. *Bar* 40 µm. (Courtesy of Dr Kunisawa, Waseda University).

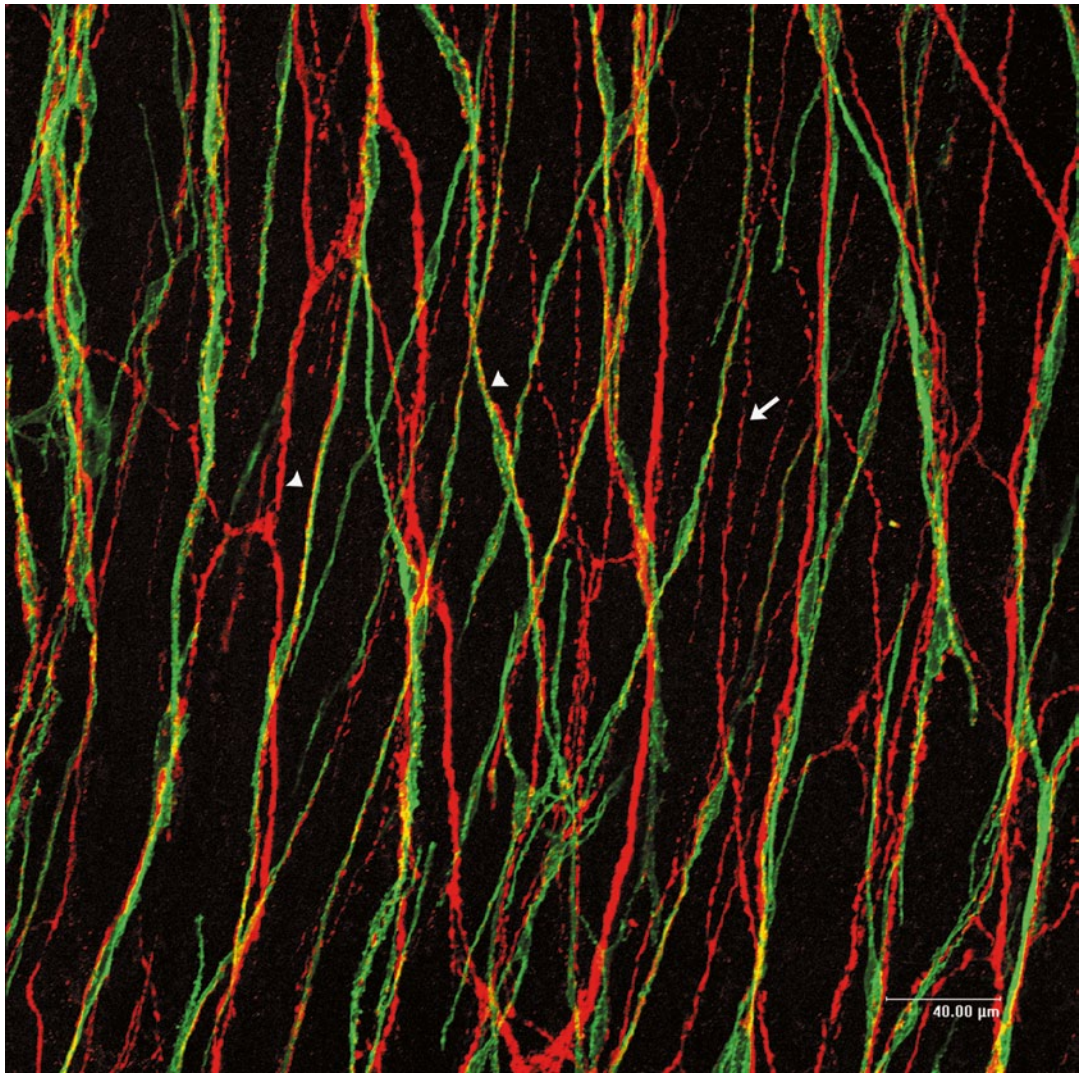

Fig. 2.10 ICC-LM in the guinea-pig antrum. Whole mount stretch preparation of the antrum showing the dense network of nerve fibres in the longitudinal muscle layer, where many nerve fibers show close association with ICC-LM (*arrowheads*) while some fine fibres are not associated with ICC-LM over long distance (*arrows*), suggesting the presence of direct and indirect innervations. *Bar* 40 µm. (Courtesy of Dr Kunisawa, Waseda University).

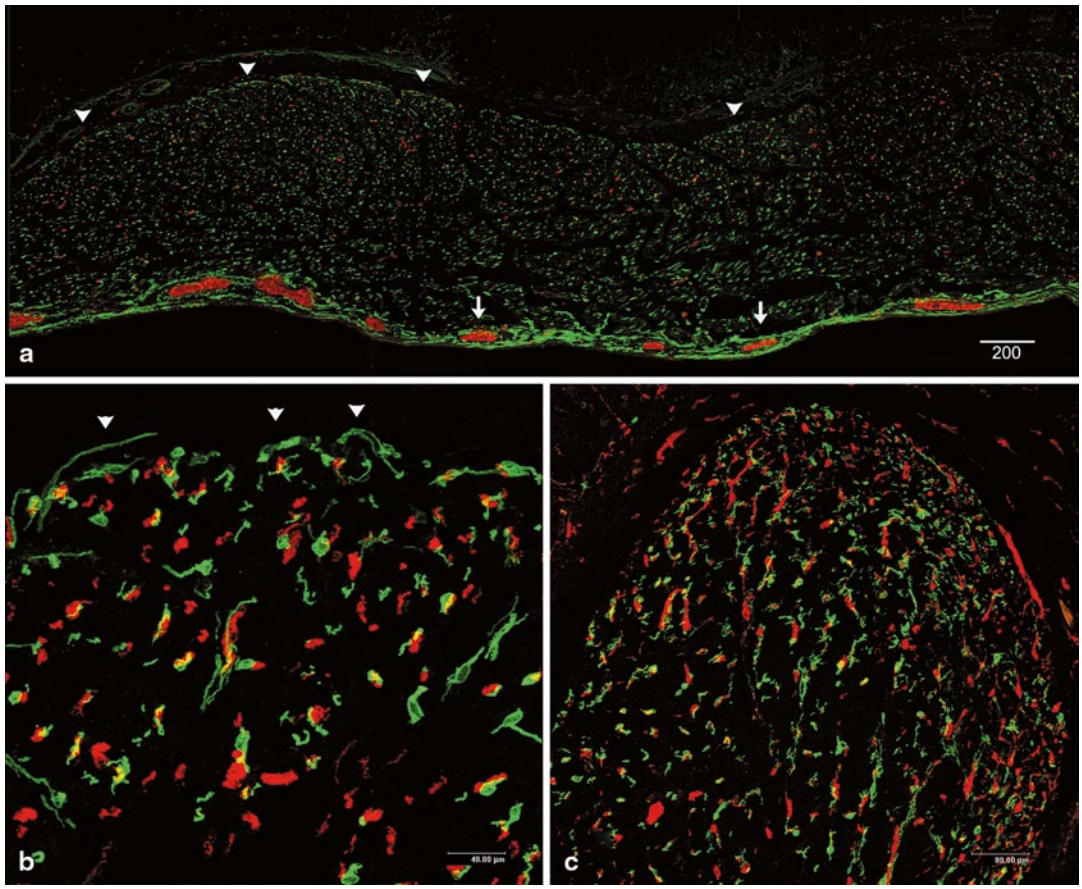

Fig. 2.11 Characteristic distribution of ICC around the guinea-pig pylorus. **a** A transverse section of the region near the pyloric sphincter, where ICC-SM are observed at the mucosal surface of the circular muscle layer (*arrowheads*) within a limited length. Strong c-Kit immunoreactive deposits representing ICC-MP are observed around the myenteric ganglia (*arrows*). *Bar* 200 μm. **b** Higher magnification of the region similar to the area indicated by arrowheads in **a**. c-Kit positive cells are observed on the submucosal surface of the circular muscle layer (*arrowheads*). *Bar* 40 μm. *ICC-SM are also observed in mice, rats and dogs. Therefore, ICC-SM probably have some particular significance related to their anatomical position adjacent to the gastro-duodenal junction or tubular structures which differs from the rest of the stomach.* **c** A transverse section of the pyloric sphincter containing numerous ICC-CM (*green*) in close association with nerves (*red*). *Bar* 80 μm. (Courtesy of Dr Kunisawa, Waseda University).

Small Intestine

3

The small intestine is comprised of the duodenum, the jejunum and the ileum. The duodenum shows peculiar features different from the former two in respect of its arrangement of ICC. Thus, the general features for the small intestine are described first and then the special features for the duodenum are described next.

ICC are mainly localized in two regions; the myenteric plexus and the deep muscular plexus that extends two-dimensionally in a plane between the inner thin (1–3 cells thick) and outer thick sublayers of the circular muscle in the mouse, rat and guinea-pig small int.estine. Few ICC-CM are found within the thick main sublayer of the circular muscle. c-Kit immunoreactivity is rarely observed in the longitudinal muscle layer in the small intestine.

T. Komuro, *Atlas of Interstitial Cells of Cajal in the Gastrointestinal Tract,*
DOI 10.1007/978-94-007-2917-9_3, © Springer Science+Business Media B.V. 2012

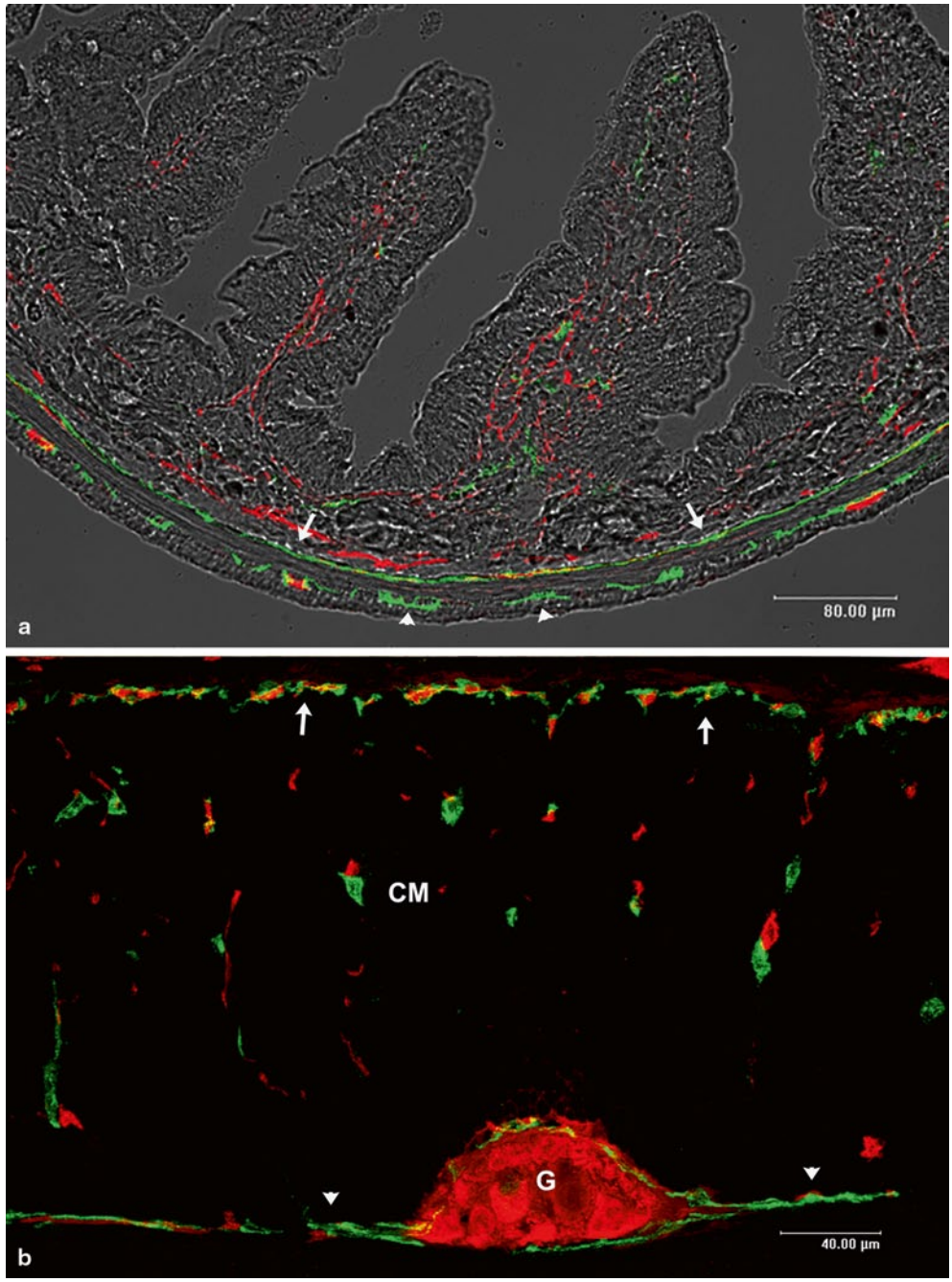

Fig. 3.1 Distribution of ICC in sections of the intestinal wall. **a** A transverse section of the guinea-pig small intestine observed with Nomarski optics merged with c-Kit positive ICC (*green*) and PGP9.5 positive nerves (*red*). ICC-DMP are clearly observed as a continuous line near the submucosal border of the circular muscle layer (*arrows*). ICC-MP are discontinuously observed as an elongated, thick mass located between the two muscle layer (*arrowheads*). ICC-CM and ICC-LM can not be detected at this magnification. *Bar* 80 µm (Courtesy of Dr. Tamada, Waseda University). **b** A longitudinal section of the guinea-pig jejunum stained by c-KIt/PGP9.5 immunohistochemistry. ICC-DMP (*green*) are observed in close association with nerves (*red*) at the innermost plane of the circular muscle layer (*arrows*). ICC-MP are seen around the myenteric ganglion (*G*) and in the space between the two muscle layer (*arrow heads*). A few ICC-CM are observed within the circular muscle layer (*CM*). *Bar* 40 µm (Courtesy of Ms Aoki, Waseda University).

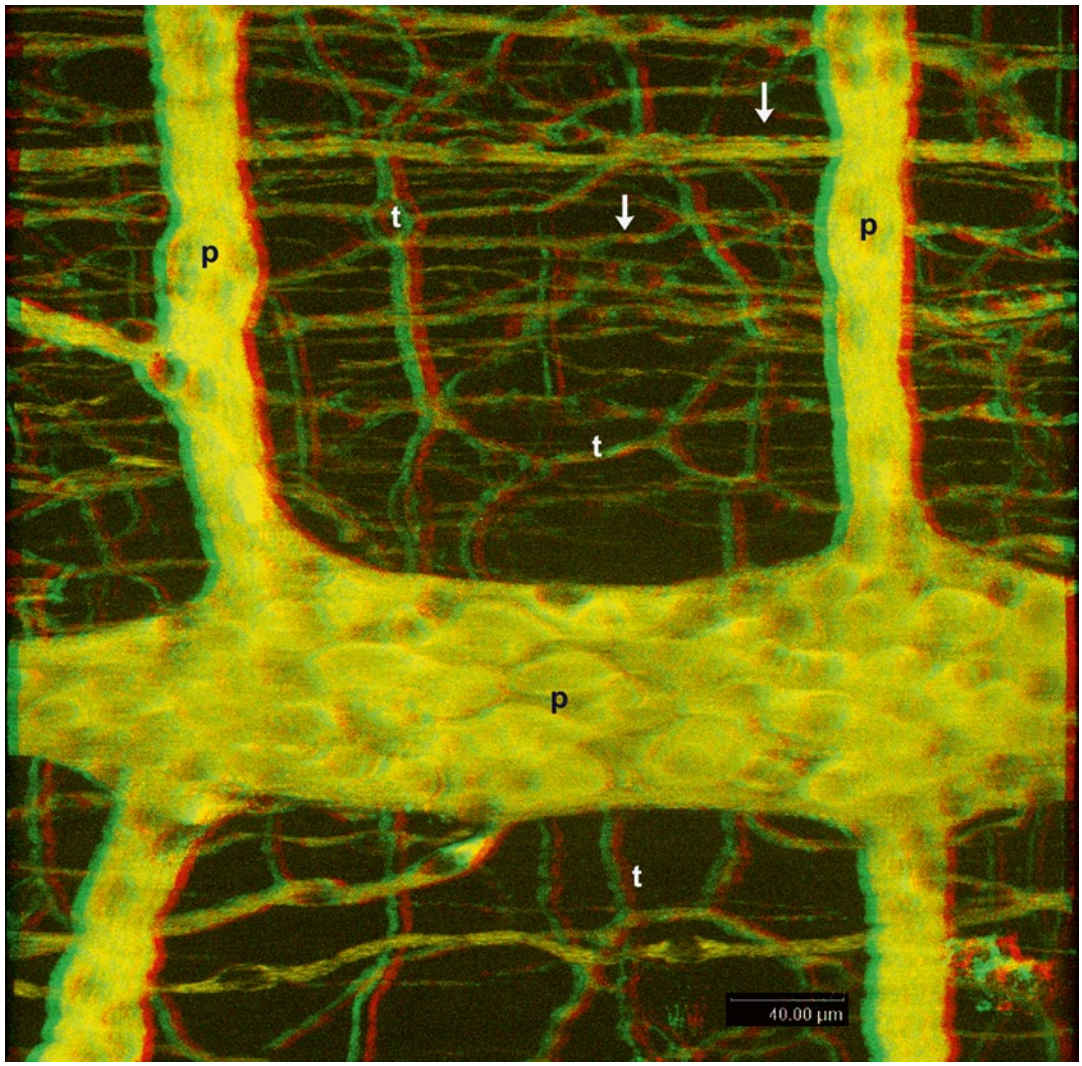

Fig. 3.2 3D organization of the nerve plexus in the guinea-pig jejunum. A fine tertiary network (*t*) of the myenteric plexus is observed other side of the primary plexus (*p*), while the nerve fibres in the circular muscle layer (*arrows*) are observed on this side. In the ganglion, individual ganglion cells are identified as oval cell bodies with a pale central area representing the nucleus. (View with *red/green* stereoscopic glasses). *Bar* 40 µm.

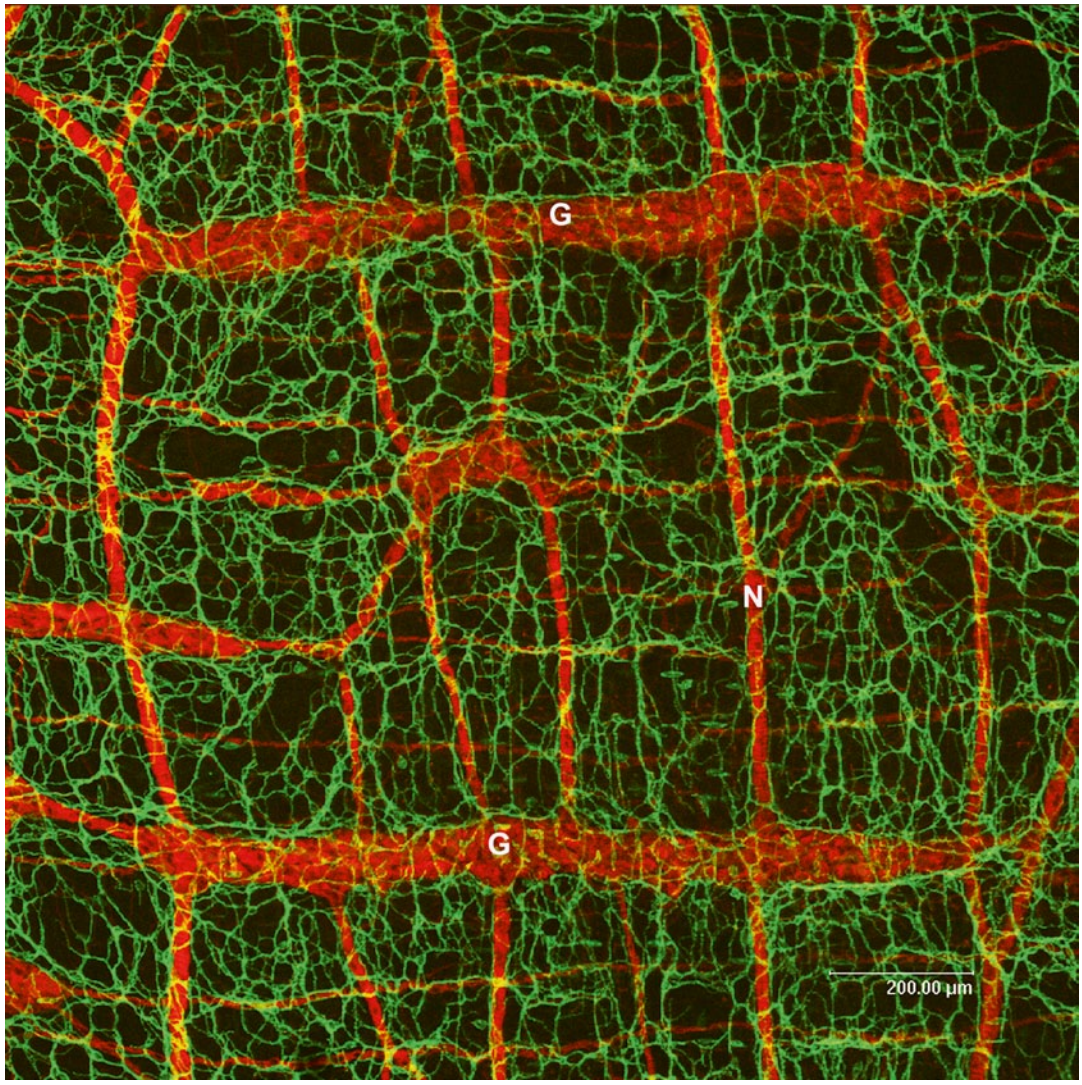

Fig. 3.3 Myenteric plexus and ICC-MP in the guinea-pig ileum. Multipolar shape of ICC-MP forms a dense cellular network (*green*) over the myenteric plexus (*red*) consisting of ganglion strands (*G*) and connecting nerve strands (*N*). These two networks appear to be independent of each other at first glance. *Bar* 200 µm. (Reproduced from Komuro [54] with permission of the publisher).

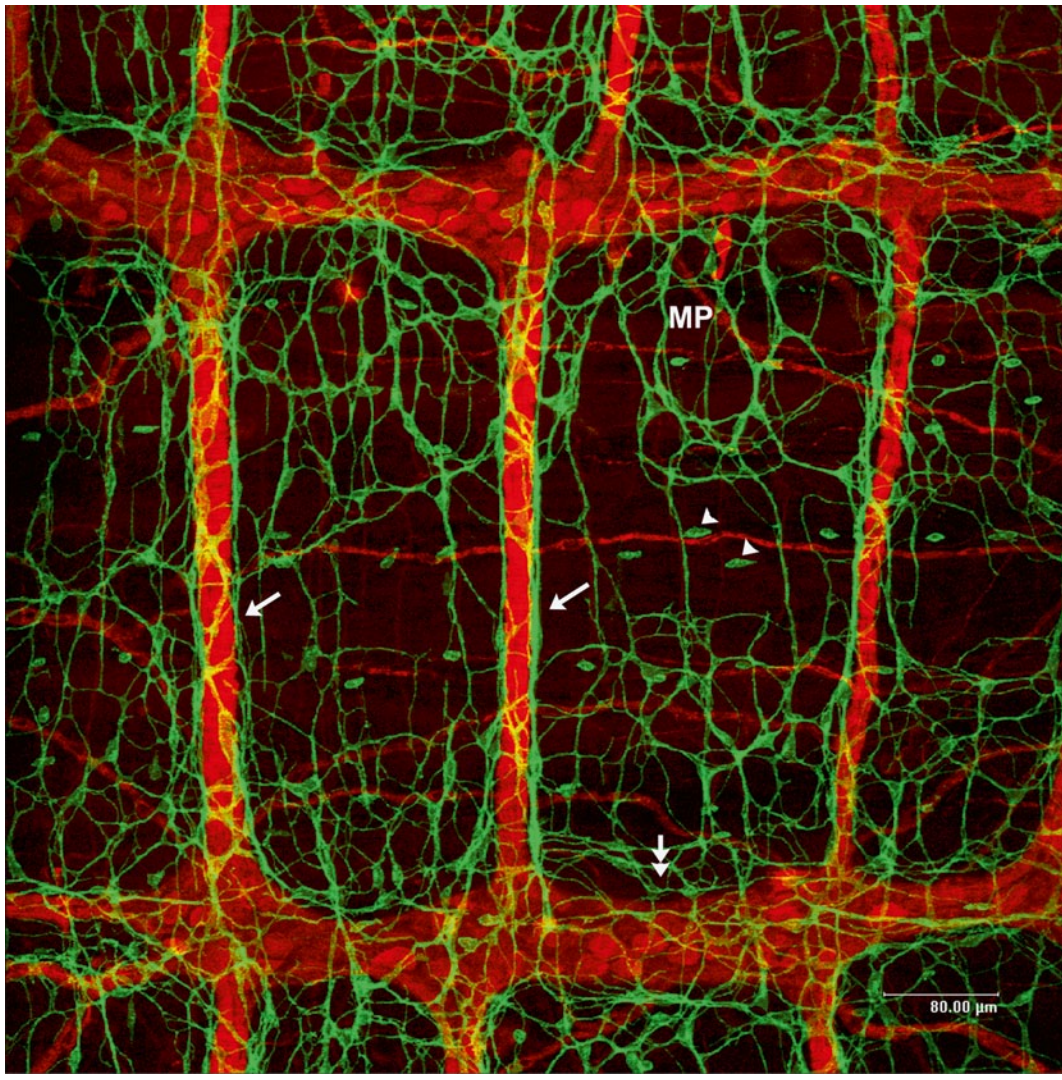

Fig. 3.4 Myenteric plexus (*red*) and ICC-MP (*green*) in the guinea-pig jejunum. Slightly higher magnification of the portion similar to Fig. 3.3 clearly shows the spatial relationship between ICC-MP and the myenteric plexus. ICC-MP form their own cellular network (*MP*) in the mesh of the primary plexus, while their cell processes appear to have a structural relationship with the ganglia (*double-headed arrows*) and connecting nerve strands (*arrows*). c-Kit positive elongated cell bodies along the secondary or tertiary plexus probably indicate immature stage of ICC (*arrowheads*). *Bar* 80 µm. *These cells appear to correspond to local progenitor cells, Kit^{low}CD44^{+}CD34^{+}Insr^{+}Igflr^{+} cells in the murine stomach* [38].

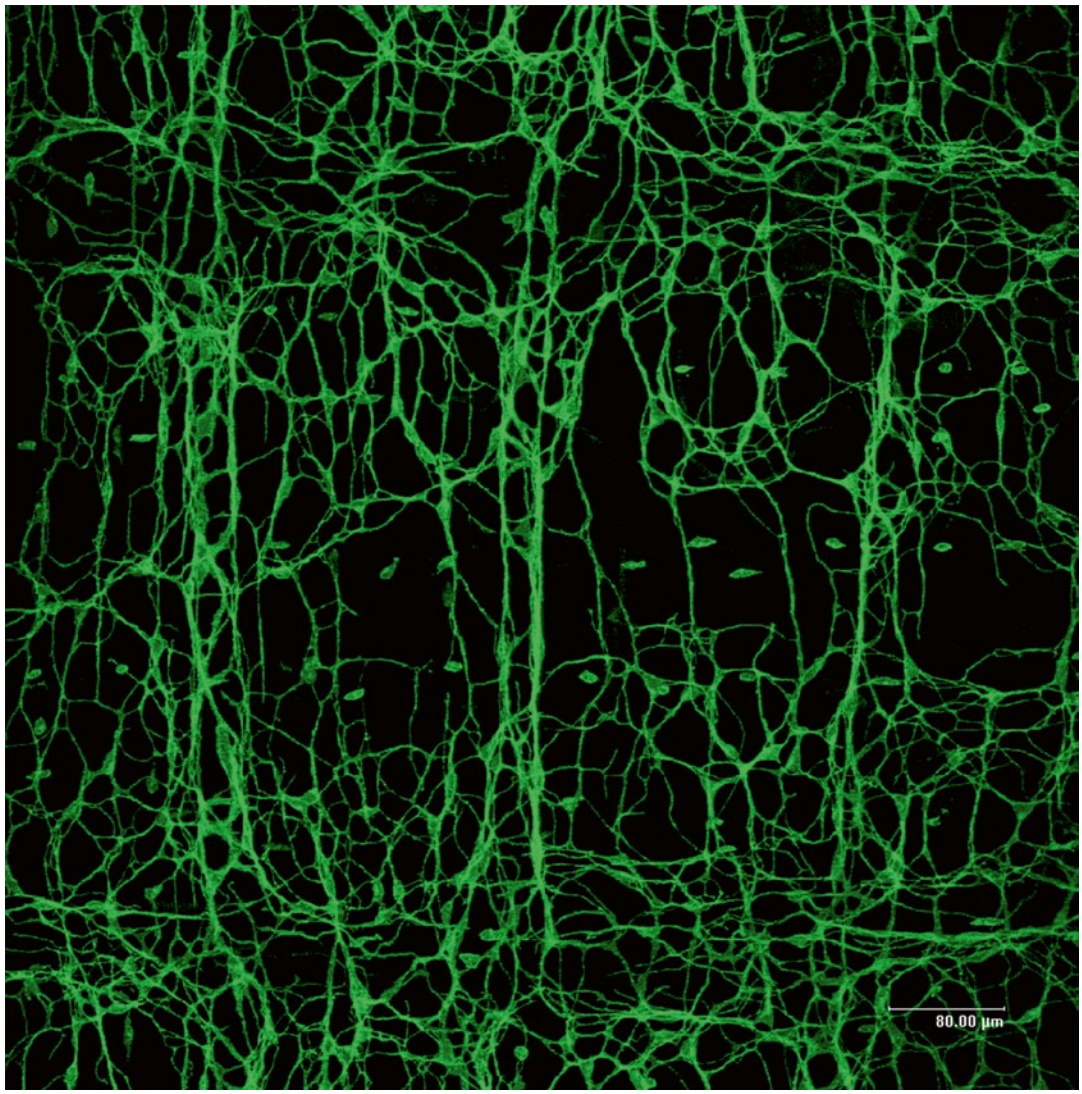

Fig. 3.5 The same network of ICC-MP as in Fig. 3.4. Without nerves, this picture clearly shows the continuity of the cellular reticulum of ICC-MP, throughout the portions of the ganglia, the connecting nerve strands and of the meshes of the primary plexus. *Bar* 80 µm.

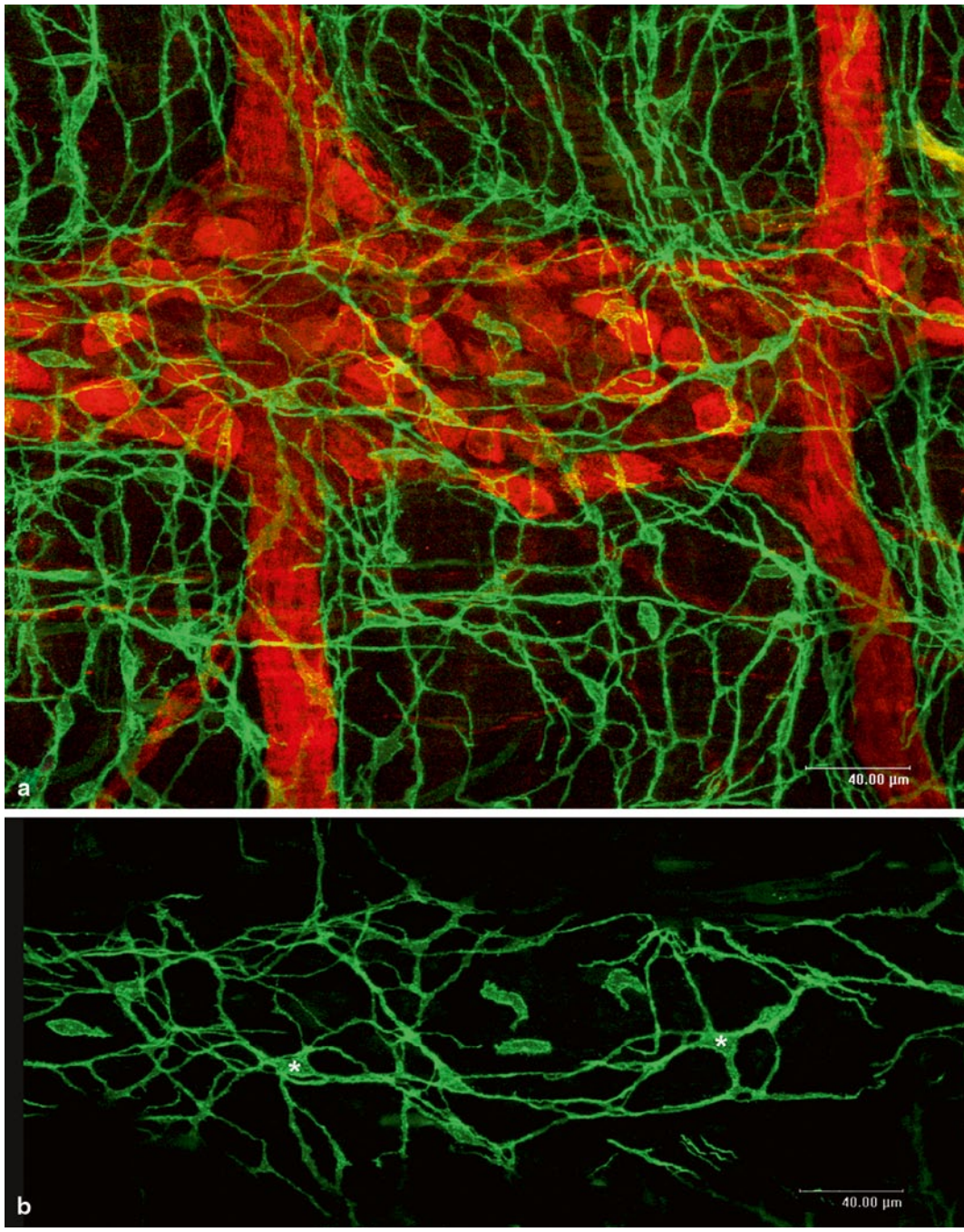

Fig. 3.6 ICC-MP (*green*) around the myentric ganglion (*red*) of the guinea-pig jejunum. **a** ICC-MP located around a ganglion. A single flat image made by the superimposition of the nerves and ICC shows their spatial relationships but obscures the structural detail of ICC-MP in this image. Individual ganglion cells are identified as strongly PGP9.5 immunoreactive, oval structures. *Bar* 40 µm. **b** Cellular network of ICC-MP around the same ganglion in **a** is clearly visible by removing the ganglion. (Note, processes projecting to multi-directions from the cell bodies (*)). *Bar* 40 µm.

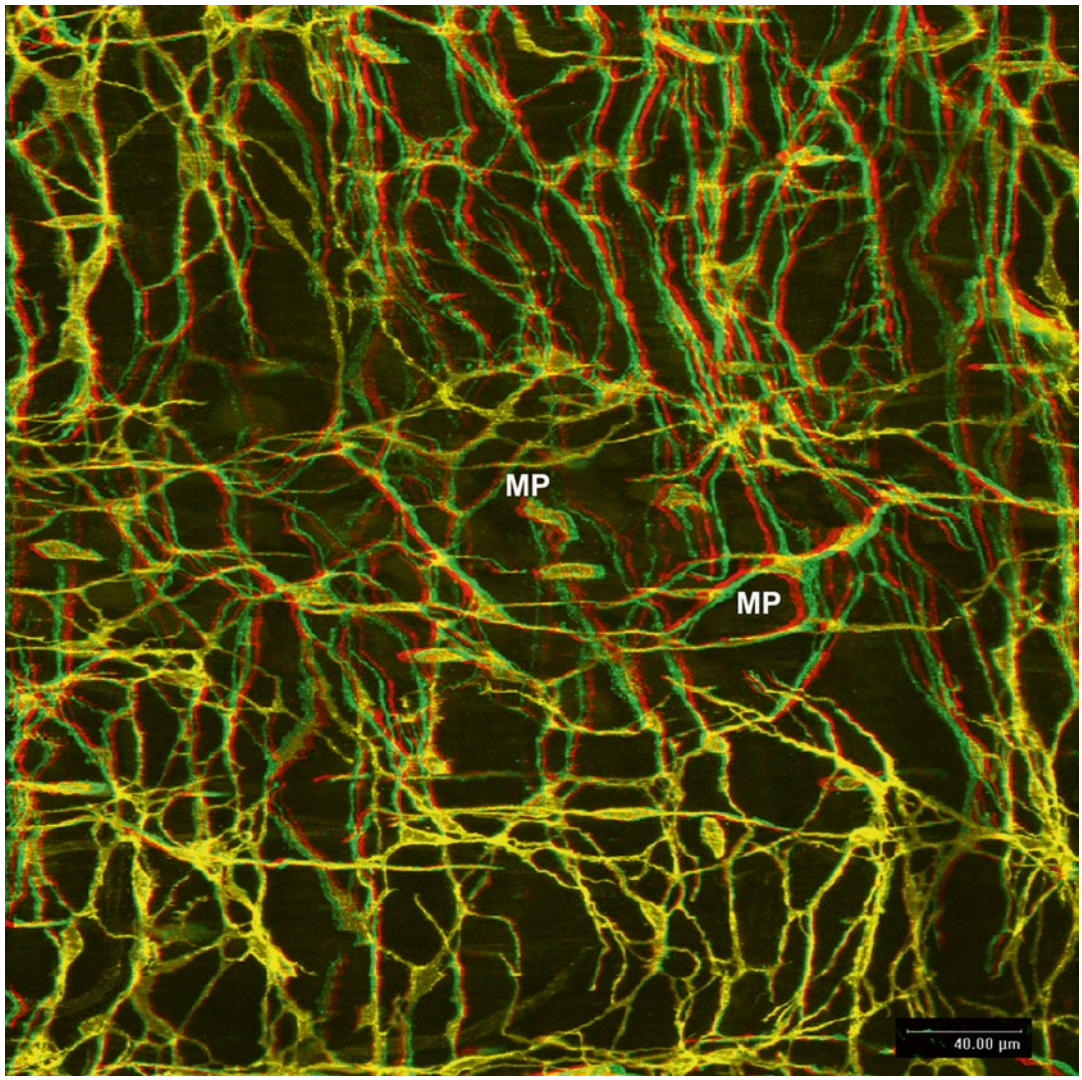

Fig. 3.7 Stereo-micrograph of ICC-MP as in Fig. 3.6. **a**. Multipolar cells of ICC-MP (*MP*) surround the ganglion by their processes to form a kind of basket (viewed with *red/green* stereoscopic glasses). *Bar* 40 µm.

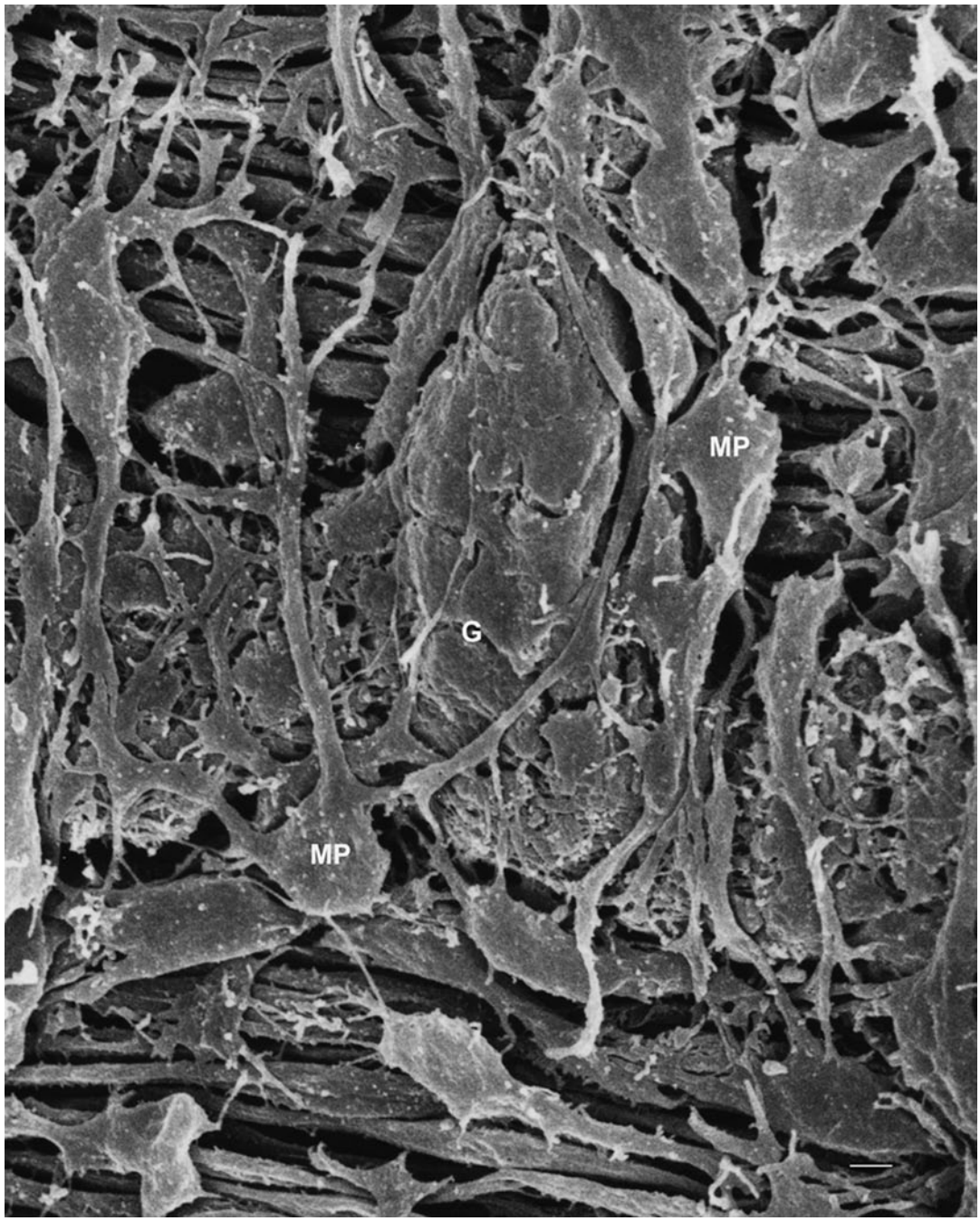

Fig. 3.8 A scanning electron micrograph showing ICC-MP (*MP*) of the rat small intestine, which surround the myenteric ganglion (*G*) with long slender processes. × 4300. *Bar* 2 μm. (Reproduced from Komuro [50] with permission of the publisher).

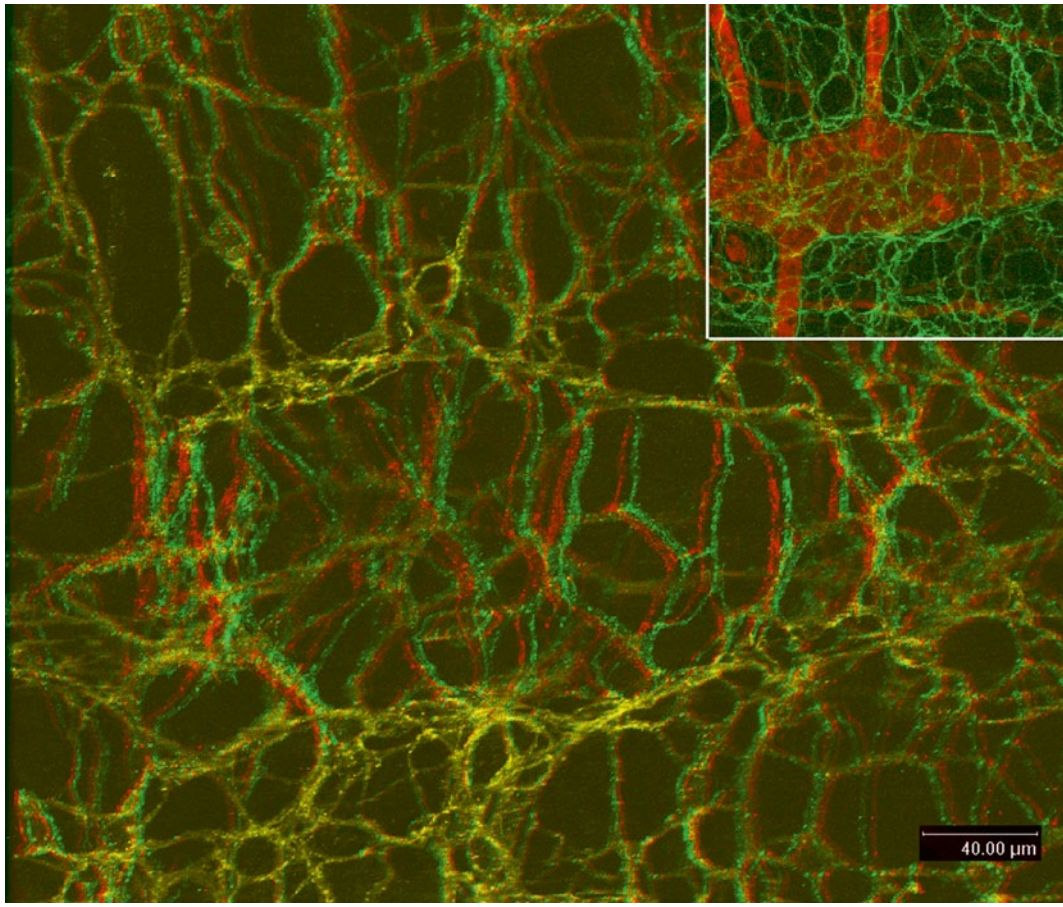

Fig. 3.9 Basket formation of ICC-MP of the guinea-pig small intestine. Stereo-micrograph of the basket structure formed by ICC-MP around the myenteric ganglion (view with *red/green* stereoscopic glasses). *Inset*; ICC-MP and the myenteric ganglion of the reconstructed portion. *Bar* 40 µm. (Reproduced from Hanani et al. [36] with permission of the publisher). *The significance of basket-like structures of ICC-MP in the small intestine and colon (see section of colon) in contrast to the irregular assembly of dense bundles of ICC-MP in the stomach, remains to be elucidated.*

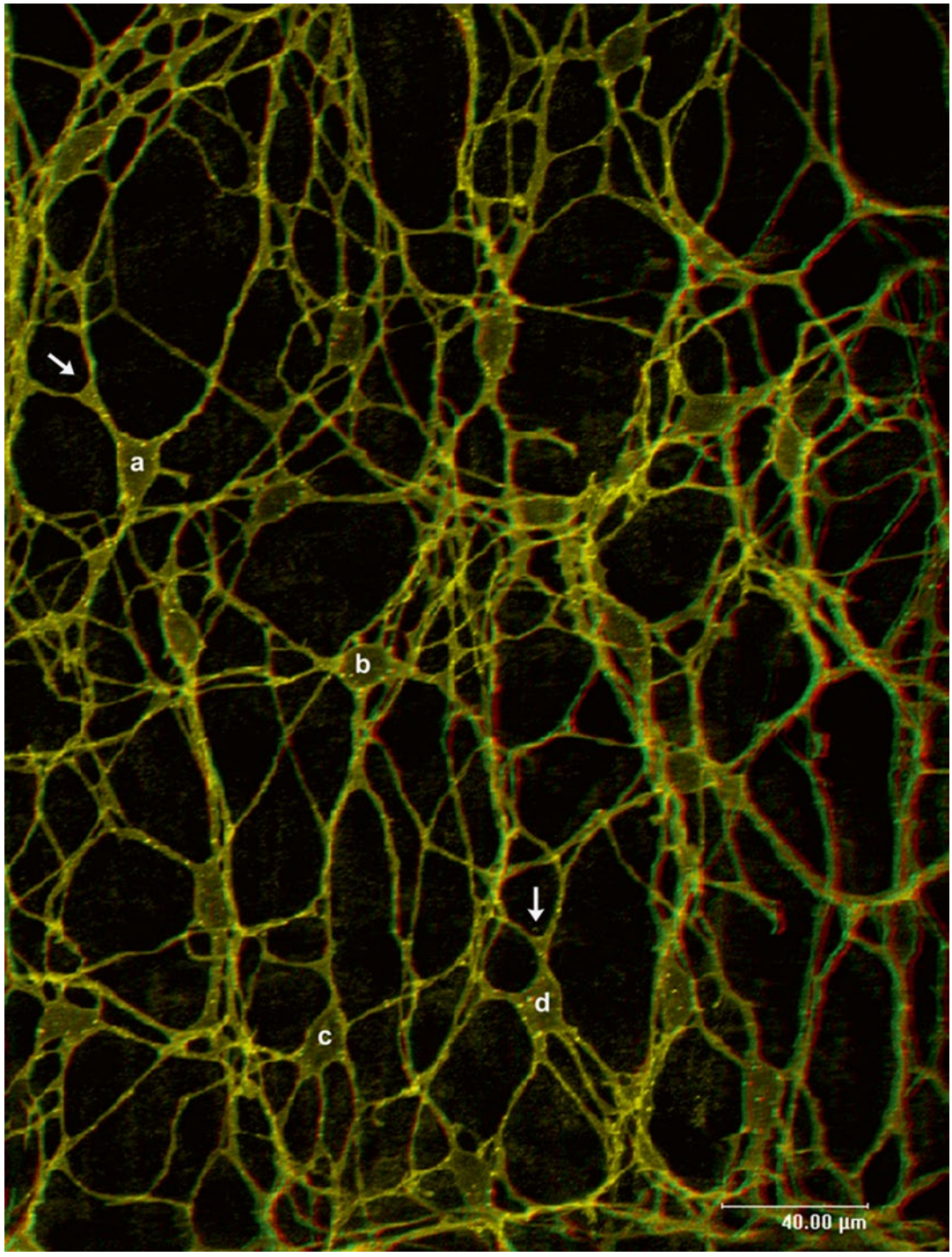

Fig. 3.10 Stereo-micrograph of ICC-MP network in the guinea-pig small intestine. ICC-MP located in the mesh of the primary plexus. *(a–d)* form a cellular reticulum in a very flat plane. They show a typical branching pattern of the processes i.e. dichotomy and connection with each other at the tips of the secondary or tertiary or further more branching processes. It is worth noting that triangular knots are observed at the branching point (*arrows*). (View with *red/green* stereoscopic glasses). *Bar* 40 µm.

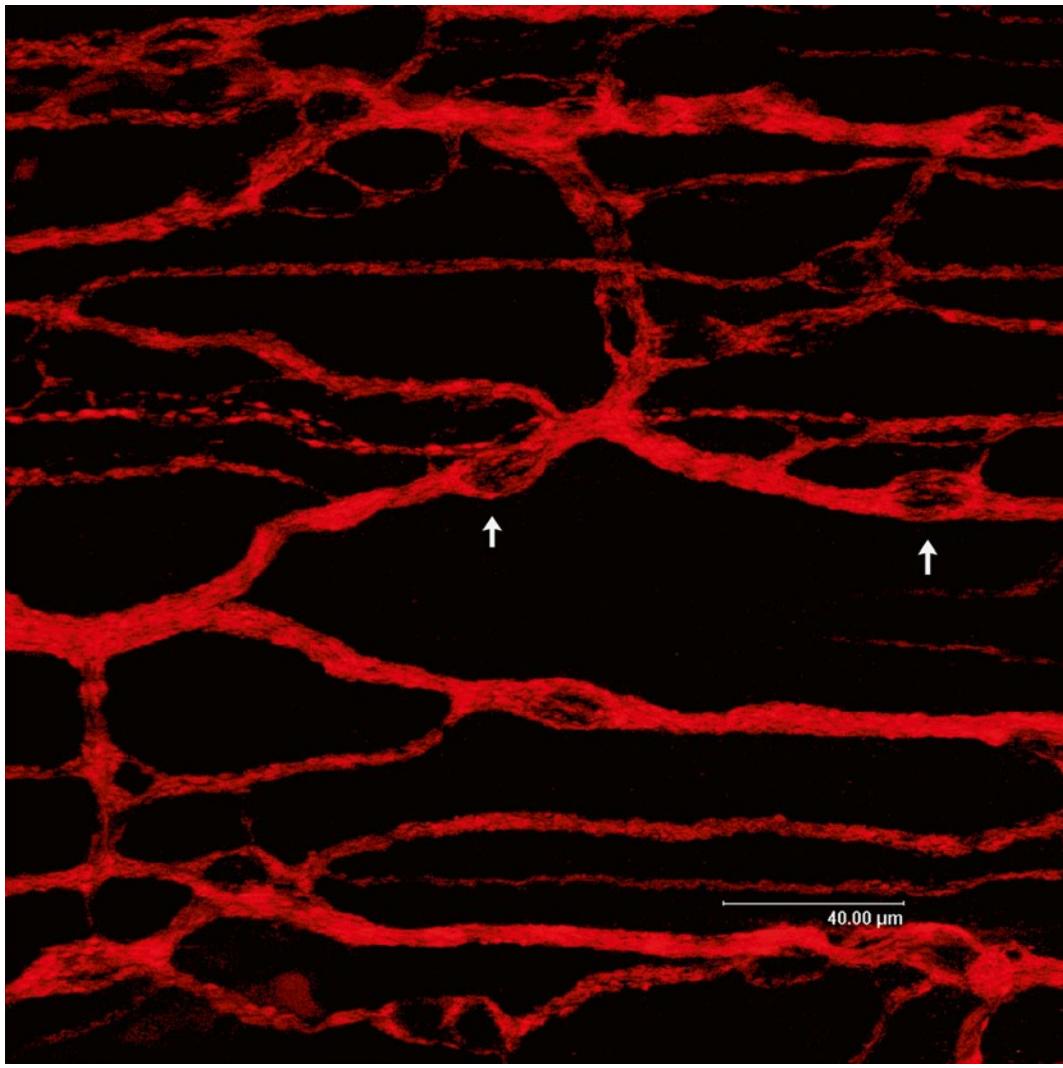

Fig. 3.11 Whole-mount stretch preparation of the guinea-pig small intestine stained with PGP9.5 immunohistochemistry showing the deep muscular plexus. Deep muscular plexus extends two-dimensionally in a plane between the inner thin and the outer thick circular muscle layers. The plexus consists of a dense network of nerve bundles which mainly run parallel with the axis of the circular muscle cells (*horizontal direction*) and interconnecting transverse or oblique nerve bundles. Hollow spaces within the thick nerve bundles (*arrows*) suggest the location of the glial cells, while the cell bodies of ICC-DMP are usually situated beside nerve bundles. *Bar* 40 µm.

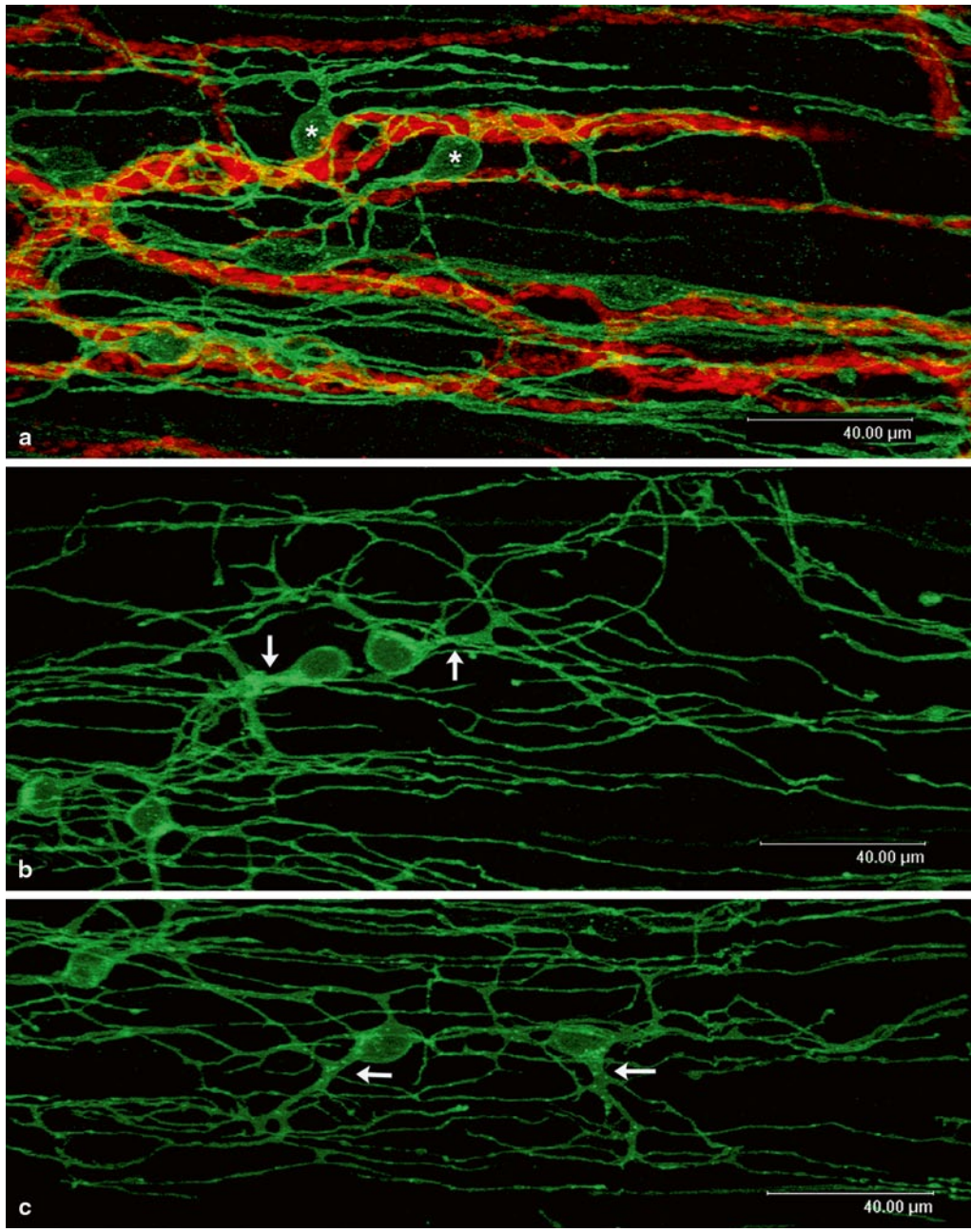

Fig. 3.12 ICC-DMP of the guinea-pig small intestine. **a** ICC-DMP (*green*) associated with the deep muscular plexus (*red*). Rounded cell bodies of ICC-DMP (*) are located beside thick nerve bundles and projects long slender processes along the nerve bundles that reflect the axis of the circular muscle cells. Cell bodies of ICC-DMP are often juxtaposed and send primary processes in opposite directions. This paired arrangement of ICC-DMP gives their network an unique appearance easily distinguishable from other networks. *Bar* 40 µm. **b** ICC-DMP and their processes. Their cell shape with extending processes can be clearly observed without nerves. Their rounded cell bodies are often juxtaposed and project 3–5 primary processes in opposite directions (*arrows*), from which further secondary and tertiary processes branch off along the axis of the circular muscle cells. The cell bodies measure 20–30 µm and the processes span more than 300 µm. *Bar* 40 µm (Modified from Hanani et al. [36]). **c** Another arrangement of ICC-DMP which also show juxtaposition of cell bodies. However, in this pair of cells, the primary processes (*arrows*) project from the cell bodies in the same direction and branch off secondary and tertiary processes in opposite directions. (Note, the continuity of the network formed by their processes). *Bar* 40 µm.

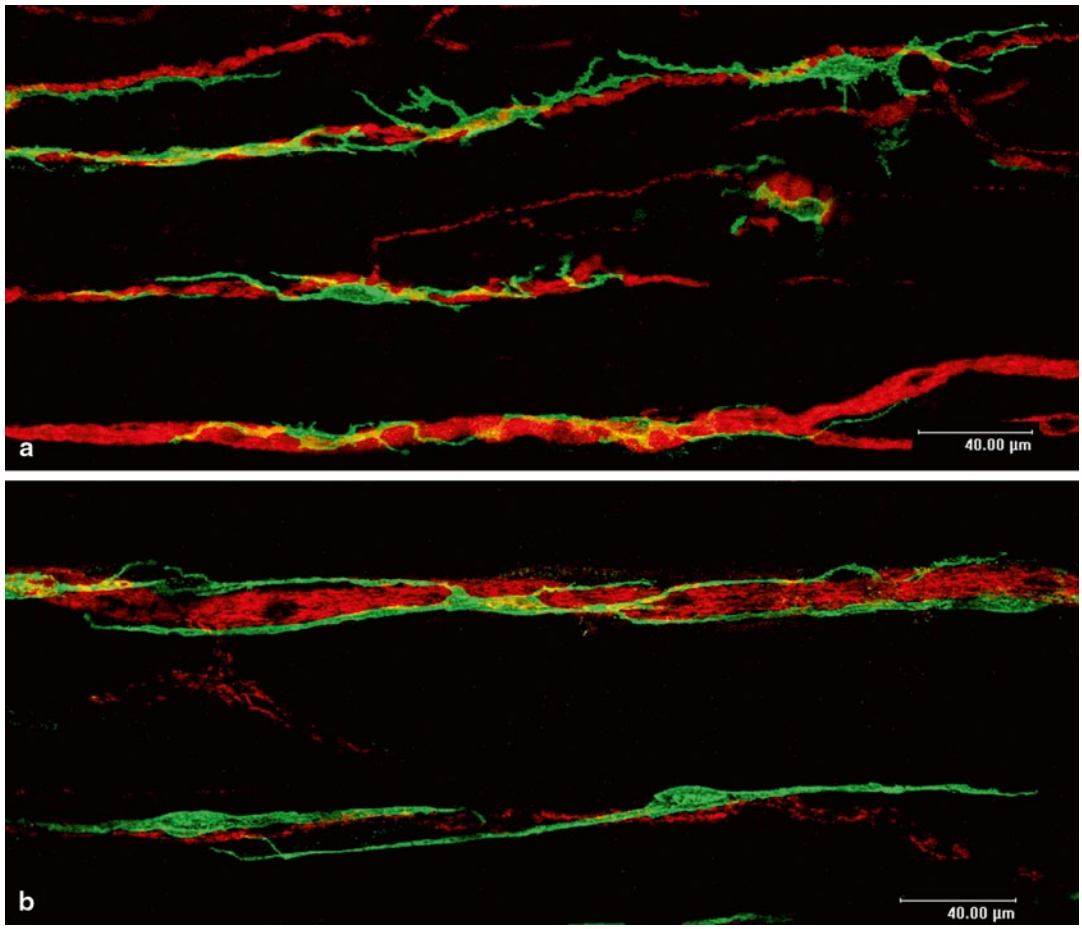

Fig. 3.13 ICC-CM in the main circular muscle layer of the guinea-pig small intestine. **a** ICC-CM (*green*) associated with the nerve bundles (*red*) within the main circular muscle layer. These cells are bipolar to multipolar in shape with secondary branches running along the axis of the circular muscle. They do not appear to form their own continuous network but are scattered along the nerve bundles rather independently. *Bar* 40 µm. **b** ICC-CM observed in a different specimen from **a**. ICC-CM in this observation field are much longer in length compared to those in **a**. *Bar* 40 µm.

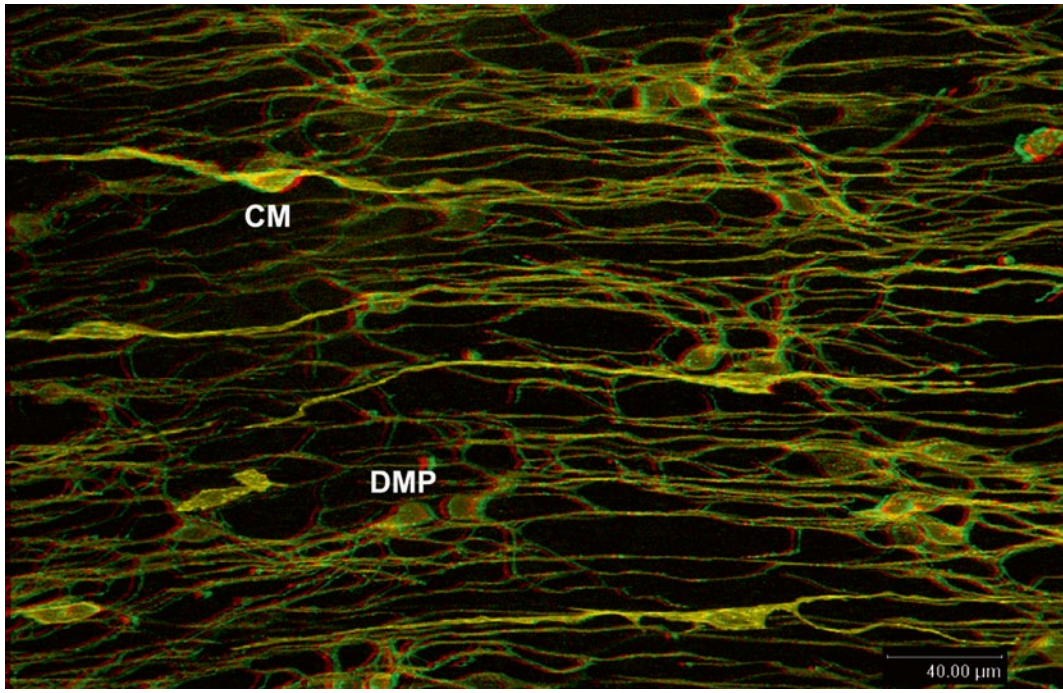

Fig. 3.14 Stereo-micrograph of ICC-DMP and ICC-CM in the guinea-pig small intestine. The cellular network of ICC-DMP (*DMP*) are clearly identified by the characteristic arrangement of the cell bodies in juxtaposition on the superficial plane. Long bipolar cells of ICC-CM (*CM*) are observed in the deeper region. (View with *red/green* stereoscopic glasses). *Bar* 40 µm.

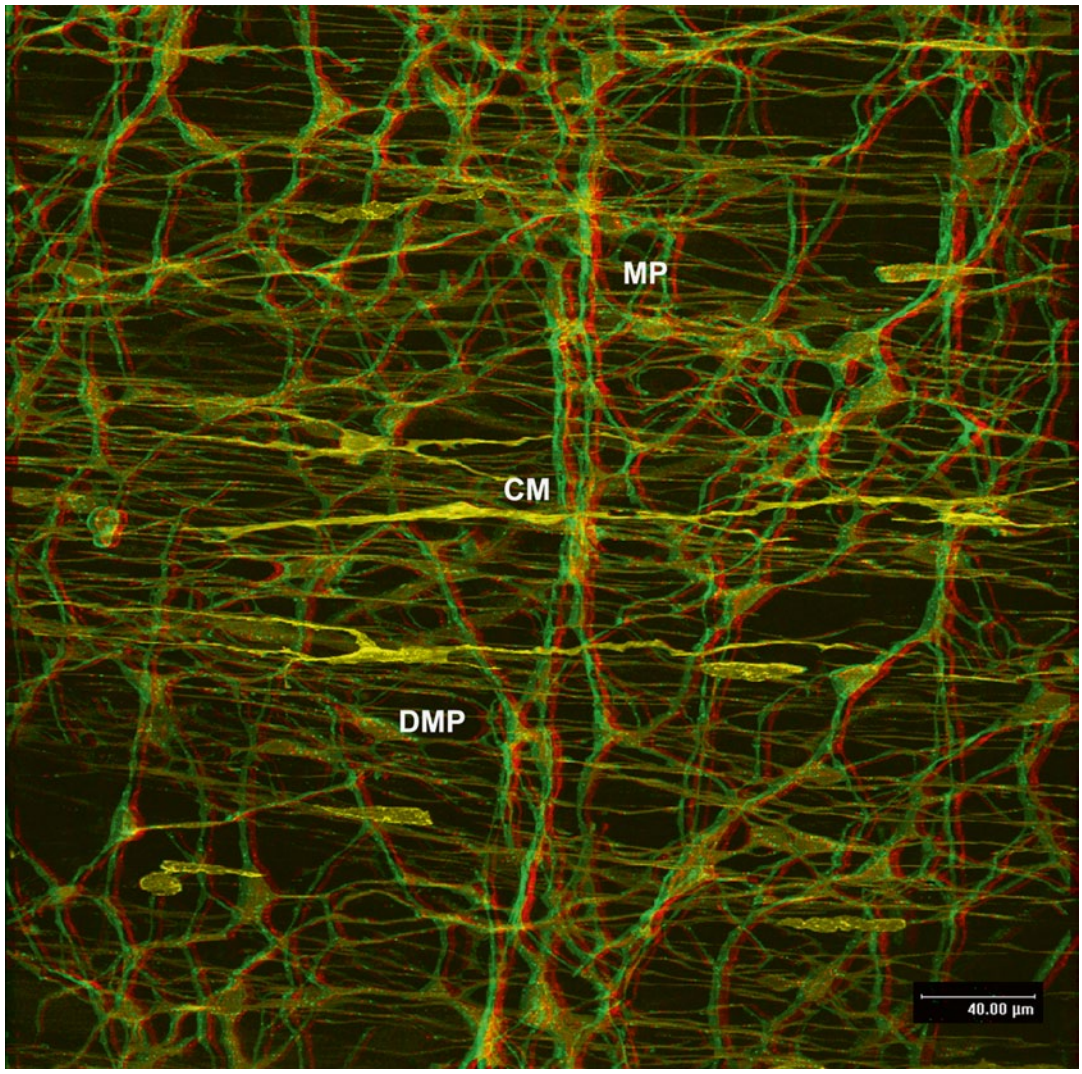

Fig. 3.15 Stereo-micrograph of ICC located in the muscle layer of the guinea-pig small intestine. Three subtypes of ICC including ICC-MP (*MP*), ICC-CM (*CM*) and ICC-DMP (*DMP*) are distinguished from the deeper region toward the superficial plane of the whole thickness of the intestine. This specimen containing the whole circular muscle layer confirms that ICC-CM are only sparsely scattered in the muscle layer and do not form their own network in the guinea-pig small intestine (view with *red/green* stereoscopic glasses). *Bar* 40 µm.

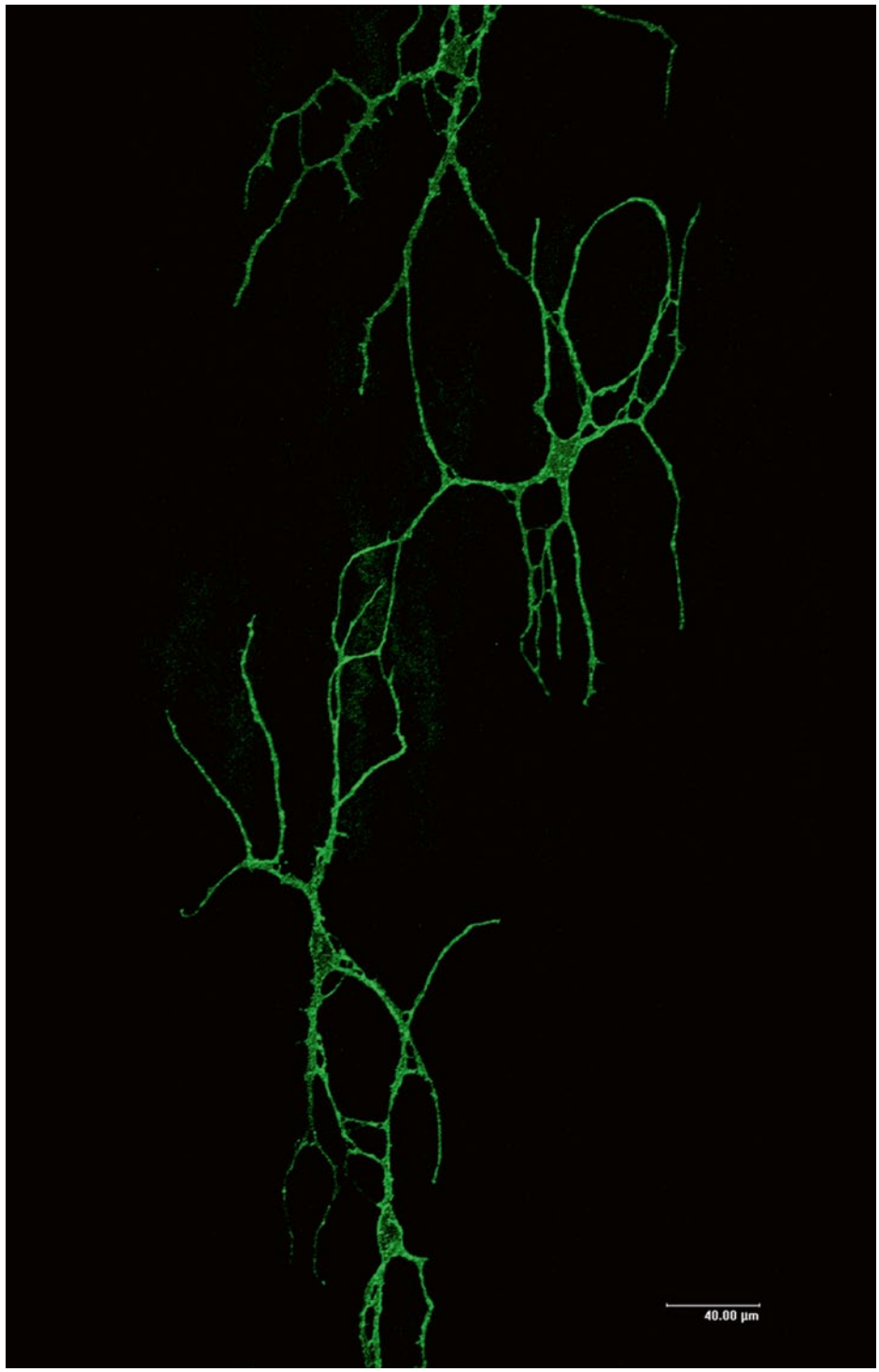

Fig. 3.16 ICC-SS in the subserosal layer of the guinea-pig small intestine. Peculiar shapes of multipolar cells are occasionally observed in the subserosal layer of the small intestine along the longitudinal direction of the intestinal wall. Their observation is rare and it is not certain whether ICC-SS of the small intestine are located at some points along the proximal to distal axis of the intestine or along the circumferential axis from the attachment of the mesentery. *Bar* 40 µm.

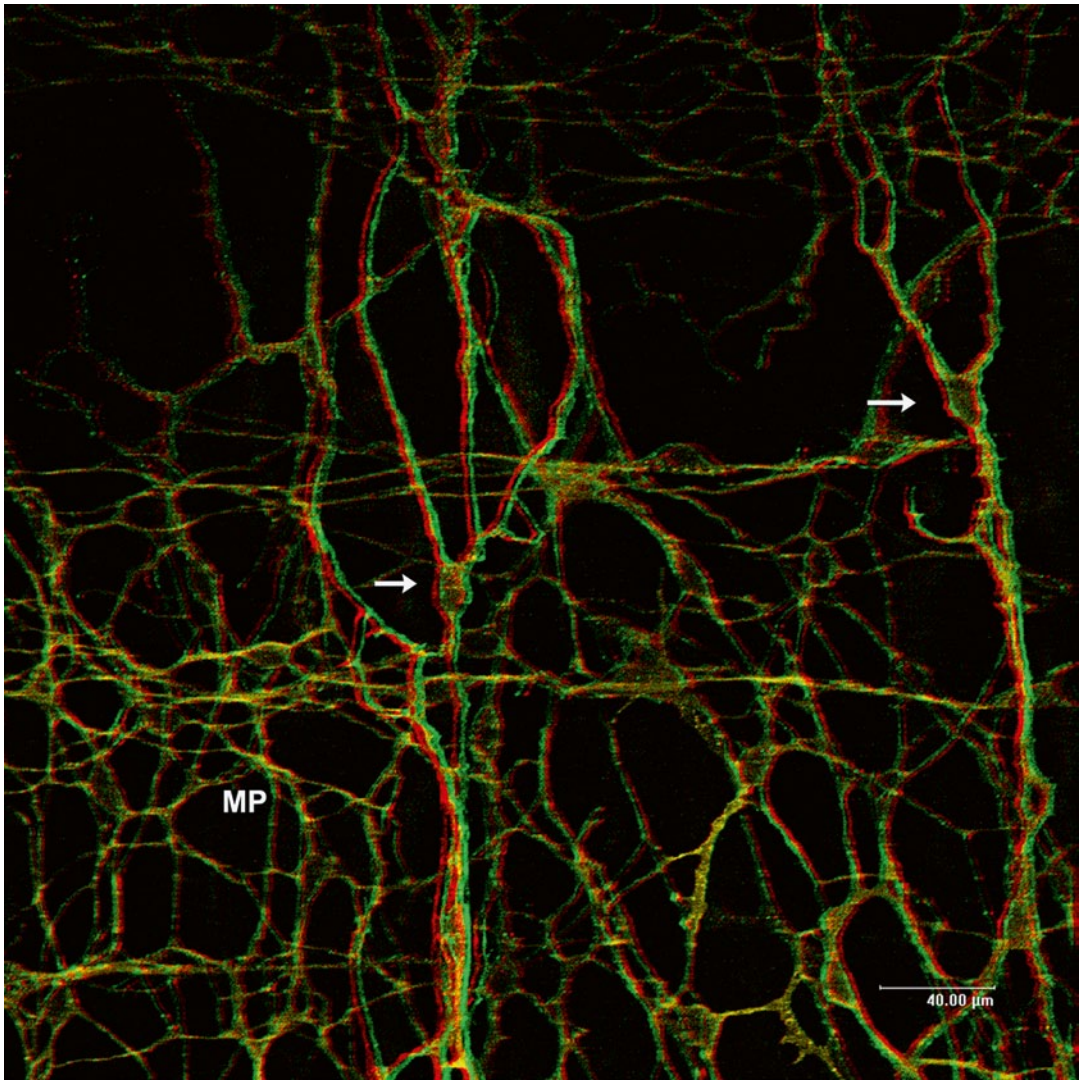

Fig. 3.17 Stereo-micrograph of ICC-SS and ICC-MP of the guinea-pig small intestine. Three-dimensional analysis clearly shows that the peculiar shapes of ICC-SS (*arrows*) are located in the superficial plane that is a different tissue layer from the deeper region that ICC-MP (*MP*) are located in (view with *red/green* stereoscopic glasses). *Bar* 40 µm.

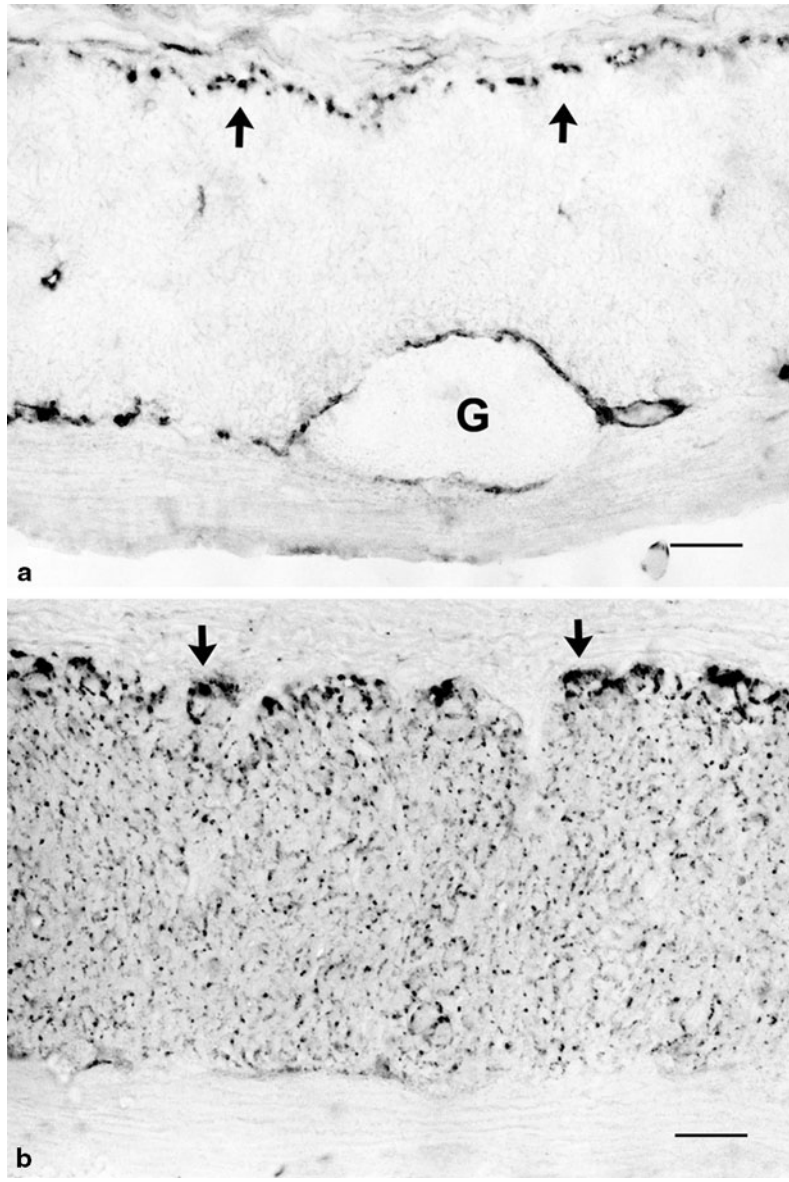

Fig. 3.18 Frozen sections stained by Immunohistochemistry for c-Kit and connexin 43 gap junction protein (C*x*43). **a** A longitudinal section of the guinea-pig small intestine showing that c-Kit immunoreactive deposits are located along the region of the deep muscular plexus (*arrows*) and around the myenteric ganglion (*G*). ×190. *Bar* 40 μm. **b** A longitudinal section of the guinea-pig small intestine showing that Cx43 immunoreactive deposits are densely distributed in the whole circular muscle layer. Large deposits are located along the deep muscular plexus (*arrows*). ×190. *Bar* 40μm. (Reproduced from Seki et al. [39] with permission of the publisher). *The dense distribution of Cx43 in the circular muscle layer indicates that the smooth muscle cells are coupled to each other by their own gap junctions, but are not intercalated by ICC-CM, since c-Kit immunoreactive cells are very few in the main circular muscle layer. On the other hand, strong immunoreactivity to both Cx43 and c-Kit in the DMP region suggests that ICC-DMP play a role as a mediator in neurotransmission, since ICC-DMP are known to be provided with rich innervation and abundant gap junctions connected with smooth muscle cells.*

This suggests that nerve signals from the myenteric neuron are first transmitted to ICC-DMP and then flow through the circular muscle cells in the guinea-pig small intestine.

The distribution density of Cx43 and c-Kit immunoreactive cells in the circular muscle layer appears to show some reciprocal relationships between them. In the guinea-pig colon, the distribution of Cx43 is less abundant but c-Kit immunoreactive cells are denser than those of the small intestine [39]. These observations seem to be compatible with the intercalated role of ICC in the neurotransmission.

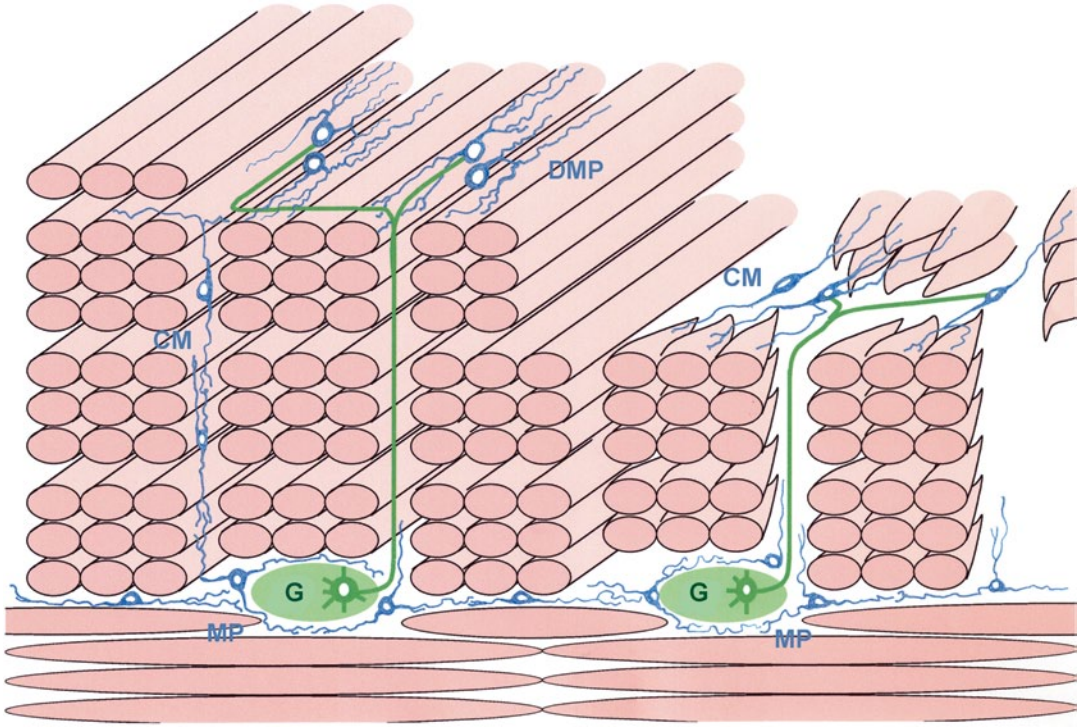

Fig. 3.19 Unanswered question about the pathway of nerve and pacemaker signals in the small intestine. Morphological and physiological evidence suggested that ICC-DMP (*DMP*) and ICC-CM (*CM*) act as intermediates in the transmission of nerve signals from the enteric nerves (*G*) to the smooth muscle cells that are connected with each other by gap junctions. However, it is not certain whether ICC-CM and ICC-DMP transmit pacemaker potentials generated by ICC-MP (*MP*) to the circular muscles and whether every ICC-CM and ICC-DMP play both functions of transmission of nerve signals and signals generated by ICC-MP. Other questions relate to the extent of the lateral gap junction-mediated connections between the circular muscle cells along the length of the intestinal tube (or how circular muscle cells are laterally separated by the connective tissue septum) and how muscle bundles are bound by ICC-CM or ICC-DMP with gap junctions.

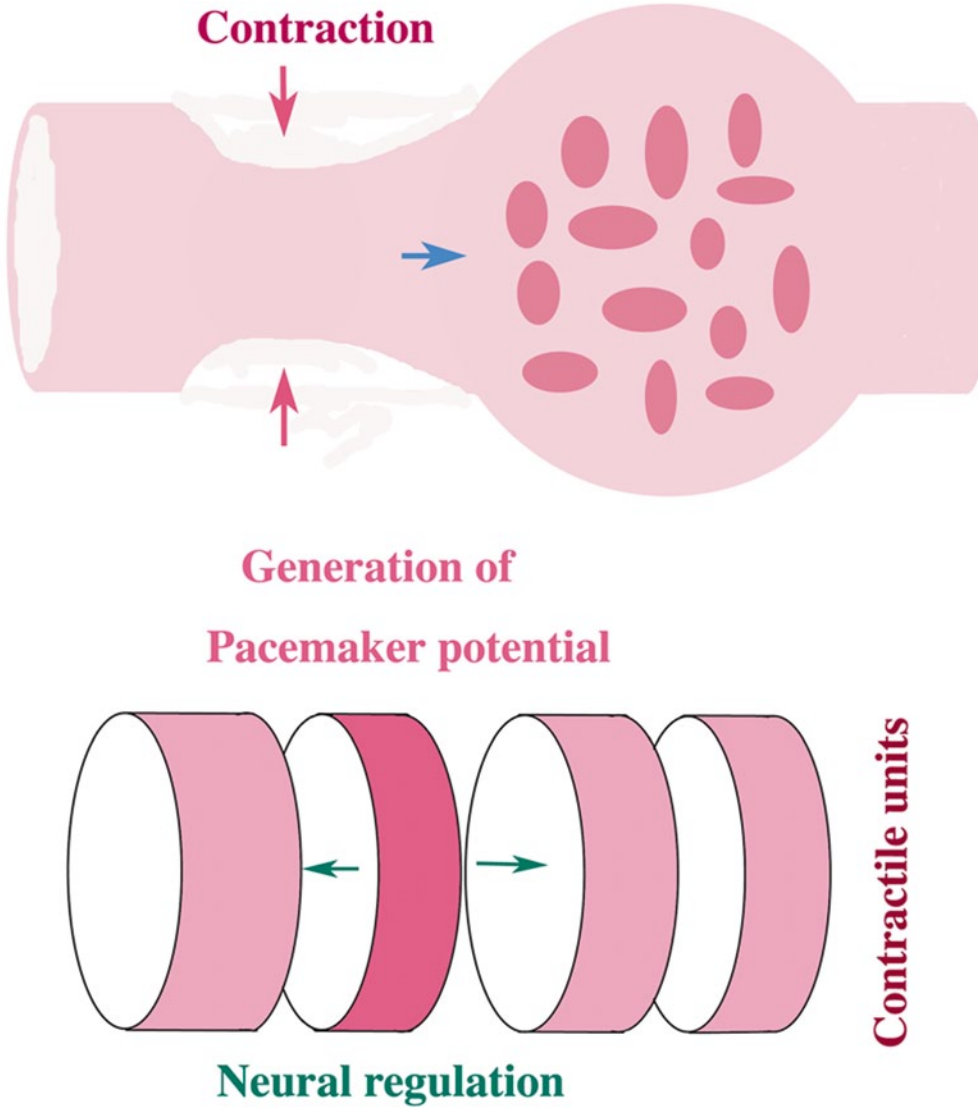

Fig. 3.20 Unanswered question about morphological units necessary for the peristalsis. Peristalsis is performed by a series of contractions and relaxations of short segments of the intestinal tube, where the neighbouring segments behave as different units. This process has been well interpreted by the precise studies about inhibitory and excitatory circuits of the enteric nerves. It has been demonstrated that ICC-MP of the stomach and the small intestine have pacemaker function. The cellular network of ICC-MP are connected with gap junctions (described below) and thus whole length of the intestinal tube would be electrically connected and regarded as a single functional syncytium. However, in reality, a kind of segmentation must exist to form functional units along the intestinal tube. It is not known how the cellular network of ICC-MP become disconnected along the length of intestine to constitute the segmental units in the peristalsis. Likewise, it is not known how the enteric nerves and the putative functional units of ICC-MP cooperate with each other. If there is no discernible structural basis, is this question simply explained by a different degree of decay or velocity of signals between the directions of their propagation? These are important issues for future studies.

A simple estimate of the size of the putative functional unit of ICC-MP can be made as follows: The jejunum from the guinea-pigs (weighing 300–400 g) fixed in a slightly distended condition measures about 2 cm in the circumference. A single cell of ICC-MP of the same materials spans about 150 μm along the circumference of the intestinal tube and thus at least, 130 ICC-MP or more are needed to cover the whole circumference. Therefore, if the circular muscle cells at a single section of the whole circumference need to contract simultaneously, at least 130 ICC-MP need to act synchronously to generate a pacemaker potential.

Duodenum

4

The proximal portion of the duodenum immediately adjacent to the gastric pylorus has a spherical shape and is called the duodenal bulb. This portion has peculiar features in the pattern of the myenteric plexus in it that quite different from that in the distal portion of the duodenum. However, these features gradually change towards the distal portion of the duodenum, which has regular pattern as in the rest of the small intestine (Fig. 4.1).

T. Komuro, *Atlas of Interstitial Cells of Cajal in the Gastrointestinal Tract,*
DOI 10.1007/978-94-007-2917-9_4, © Springer Science+Business Media B.V. 2012

Fig. 4.1 Comparison of the myenteric plexus between the duodenum and the jejunum. **a** Surface view of the proximal duodenum of the guinea-pig stained with NADH histochemistry showing the myenteric plexus consisting of a rather circular network with shorter and irregular shapes of the ganglia (*arrows*). (Courtesy of Ms Aoki Waseda University). ×10 *Bar* 500 μm. **b** Surface view of the guinea-pig small intestine (jejunum) stained with NADH histochemistry showing a regular rectangular pattern of the network of the myenteric plexus, in which the elongated ganglia (*arrows*) are mainly orientated along the axis of the circular muscle, and are connected by nerve strands (*arrow heads*) running perpendicularly. ×12 *Bar* 500 μm.

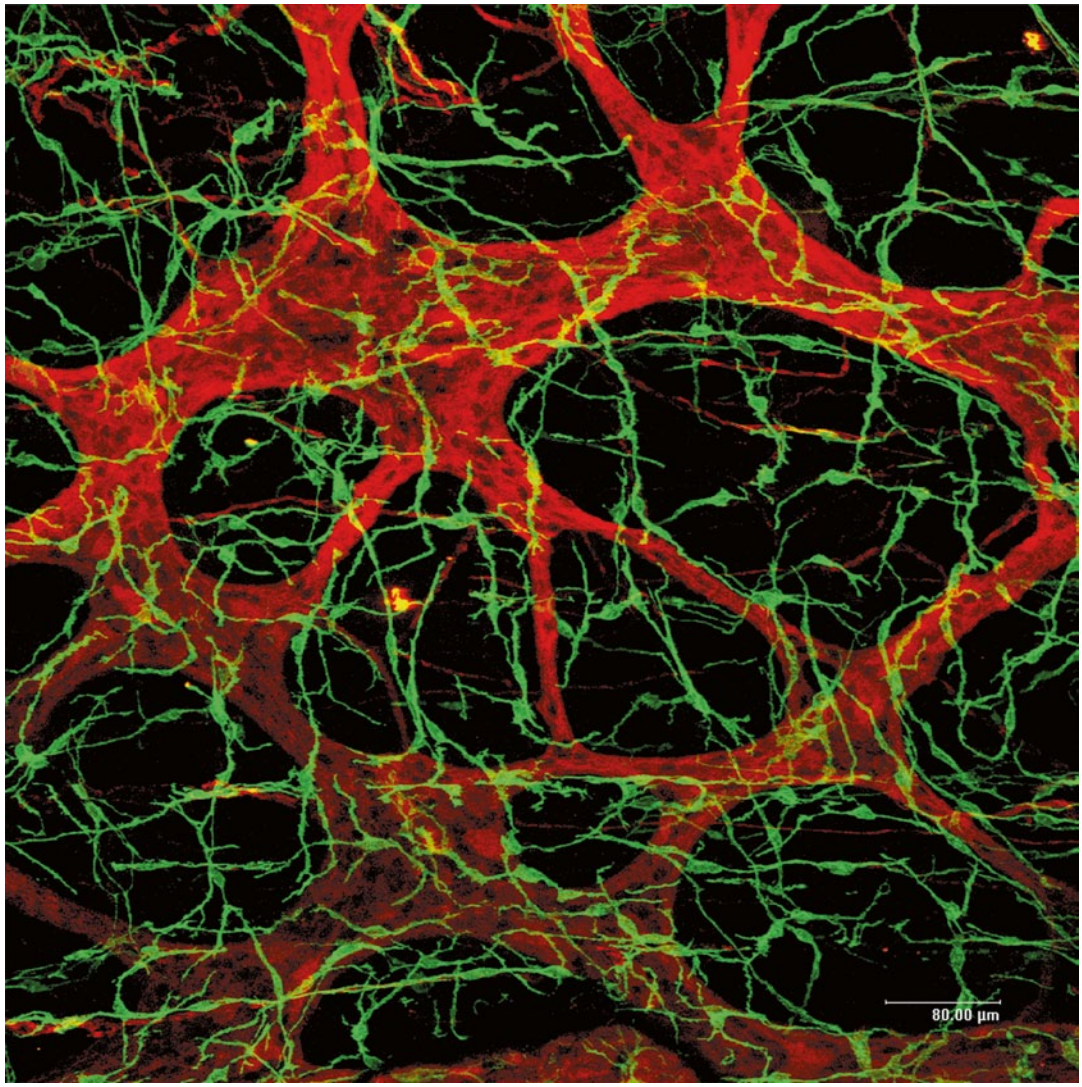

Fig. 4.2 Whole-mount stretch preparation showing ICC-MP in the proximal portion of the guinea-pig duodenum stained with c-Kit/PGP9.5 immunohistochemistry. Multipolar ICC-MP (*green*) are sparsely located over the irregular network of the myenteric plexus (*red*). Their network is discontinuous and less developed in comparison to other regions of the small intestine described above. *Bar* 80 µm. (Figures 4.2, 4.3: Courtesy of Dr Tamada, Waseda University).

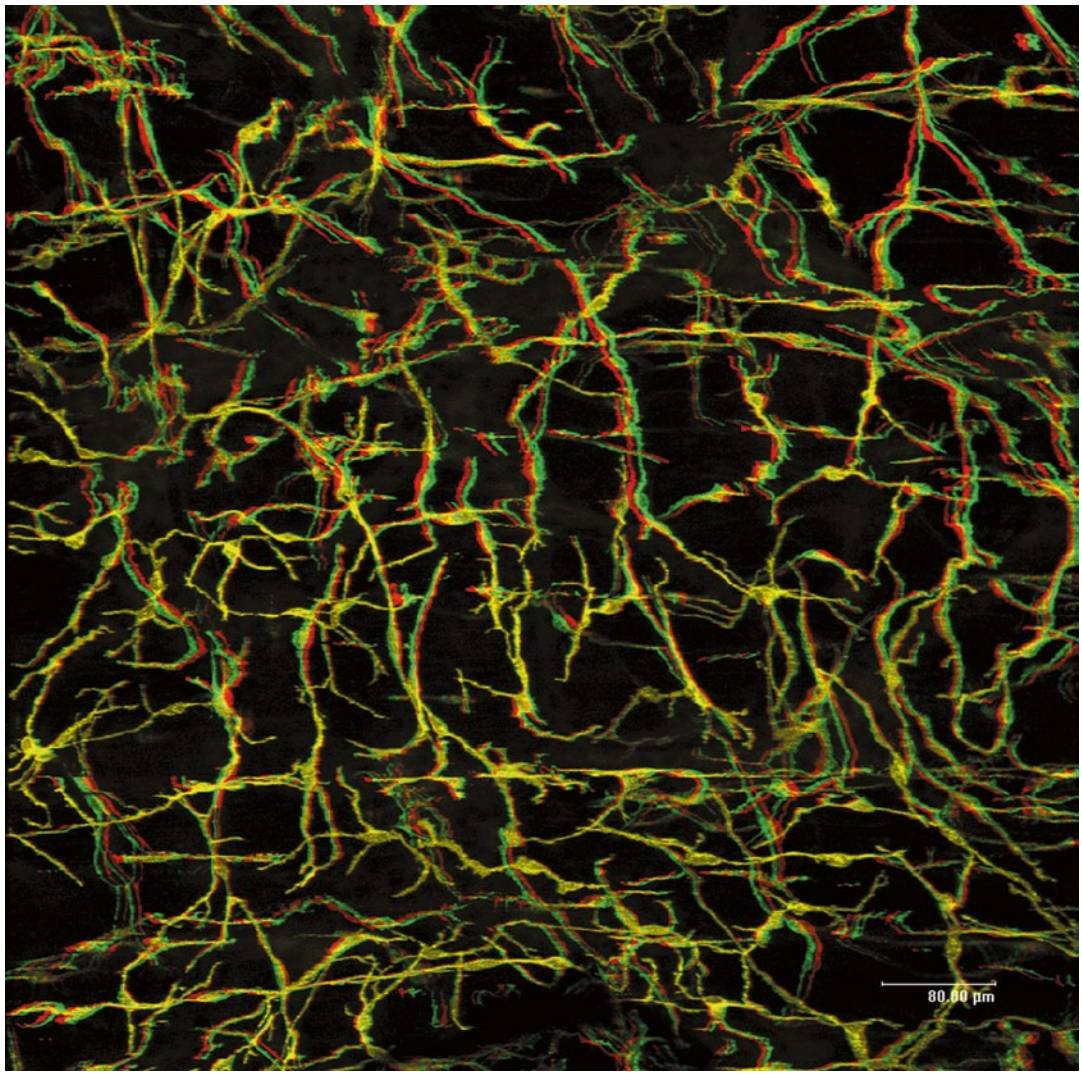

Fig. 4.3 Stereo-micrograph of ICC-MP reconstructed from the same portion as Fig. 4.2 3D observation makes it clear that ICC-MP in this portion do not form a tight network and also do not form basket structures around the ganglia unlike in the rest of the small intestine (jejunum and ileum) described above (view with *red/green* stereoscopic glasses). *Bar* 80 µm.

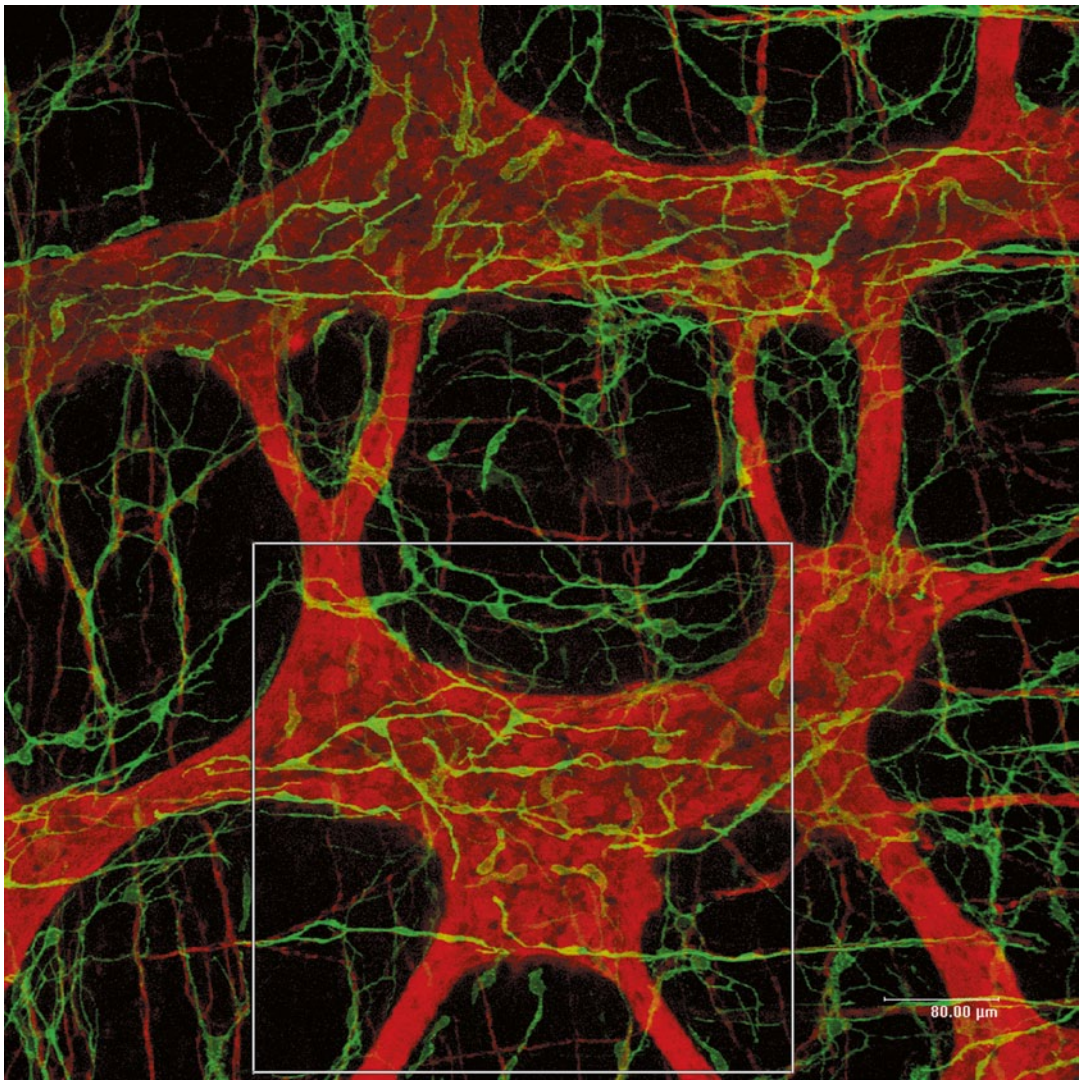

Fig. 4.4 Whole-mount stretch preparation showing ICC-MP of the guinea-pig proximal duodenum. In this specimen multipolar shaped ICC-MP (*green*) are clearly observed over the pentagonal framework of the myenteric plexus (*red*), but their cell density is low and the network is rather loose. *Bar* 80 µm. (Figures 4.4, 4.5, 4.6, 4.7, 4.8, 4.9: Courtesy of Ms Aoki, Waseda University).

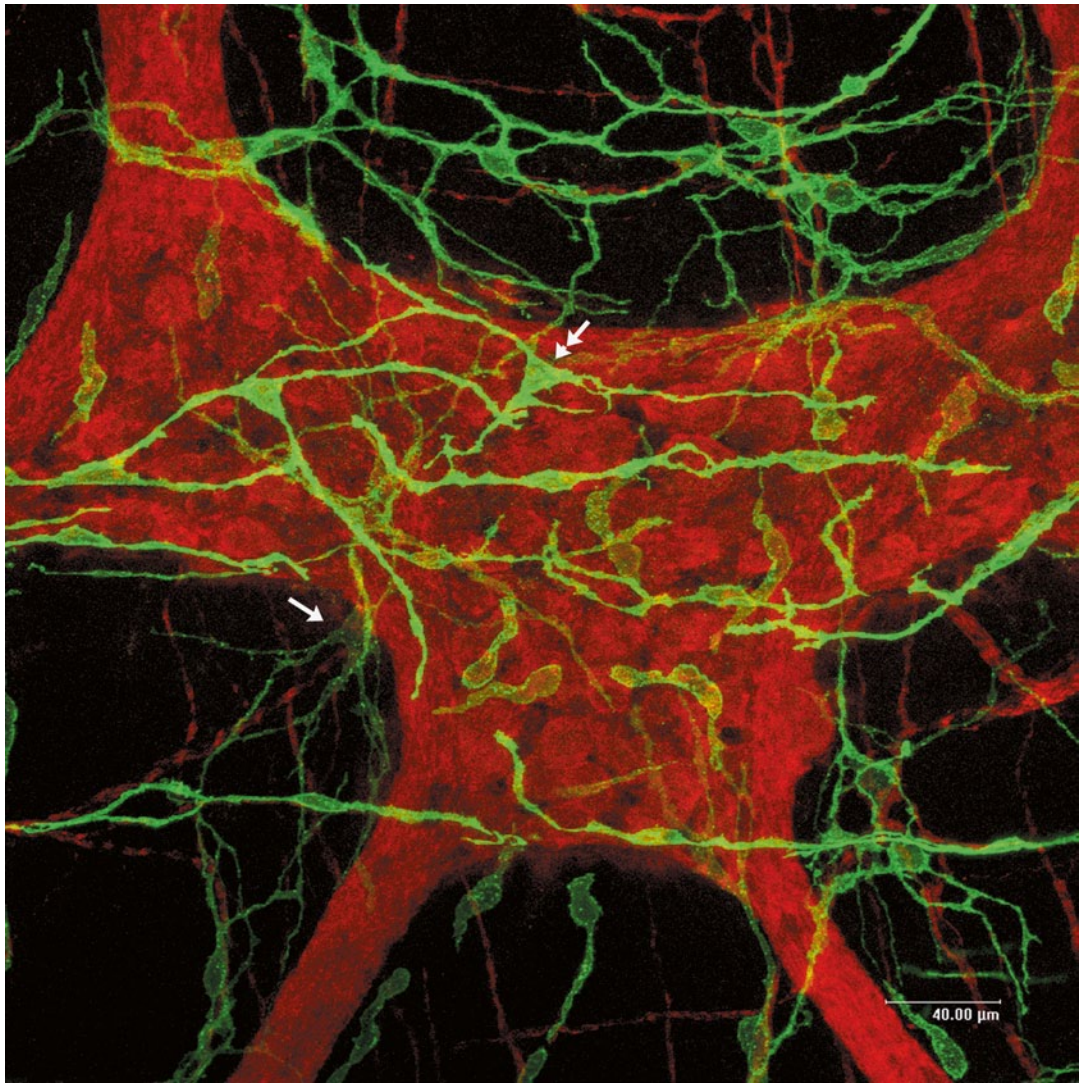

Fig. 4.5 Higher magnification of a part of the ganglion (*rectangle*) in Fig. 4.4. ICC-MP associated with both sides of the ganglia are superimposed with the ganglion and are observed in different staining intensity (*arrow* and *double-headed arrow*). However, their cell number and cell processes are so scarce that they do not form a proper cellular network. *Bar* 40 µm.

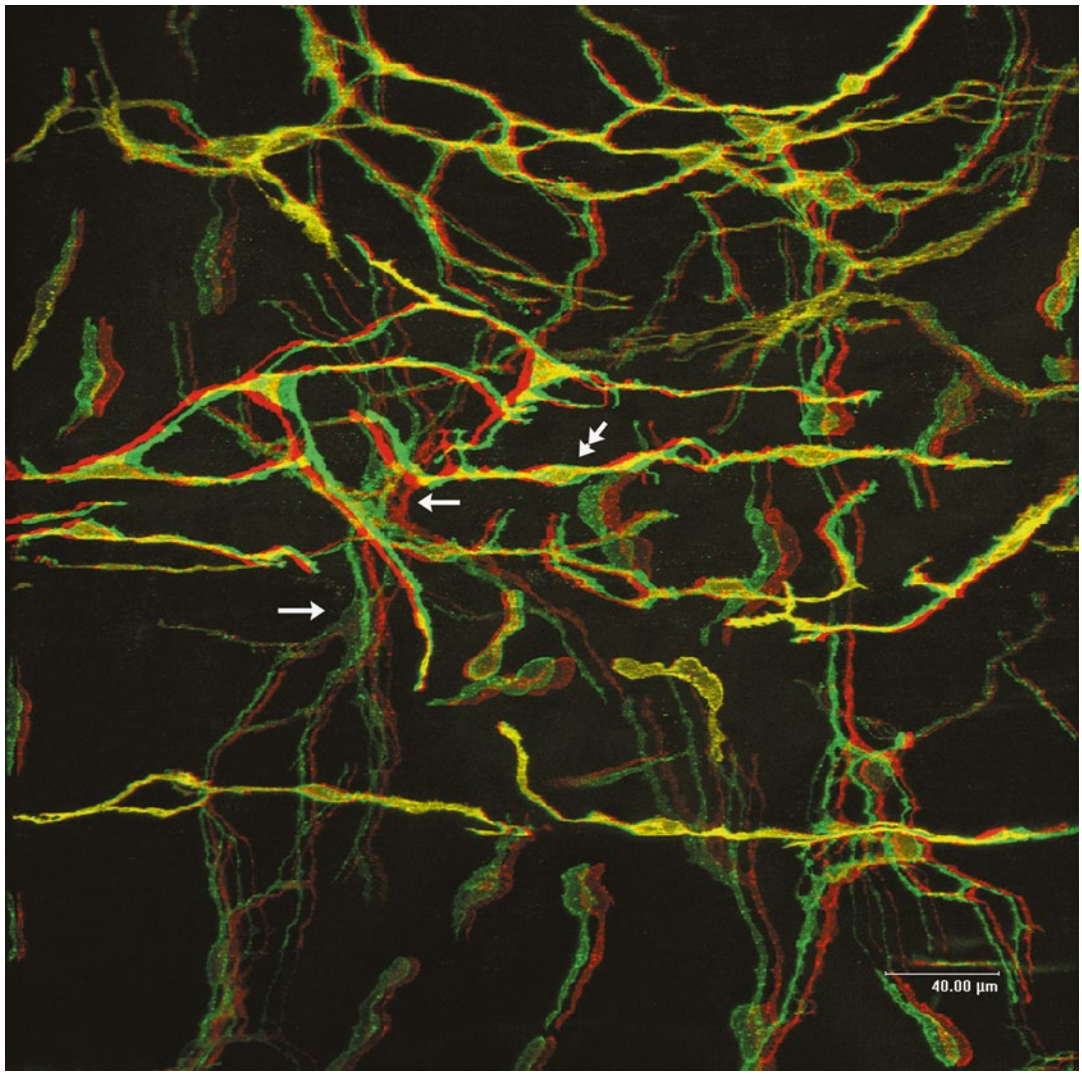

Fig. 4.6 Stereo-micrograph of ICC-MP in Fig. 4.5. ICC-MP on different sides of the ganglion with different staining intensities appear to surround the hollow space of ganglion, but do not form a clear basket structure around it, unlike in the jejunum and ileum. Note the presence of typical multipolar cells (*arrows*) intermingling with cells with only a few processes (*double-headed arrow*). *Bar* 40 µm.

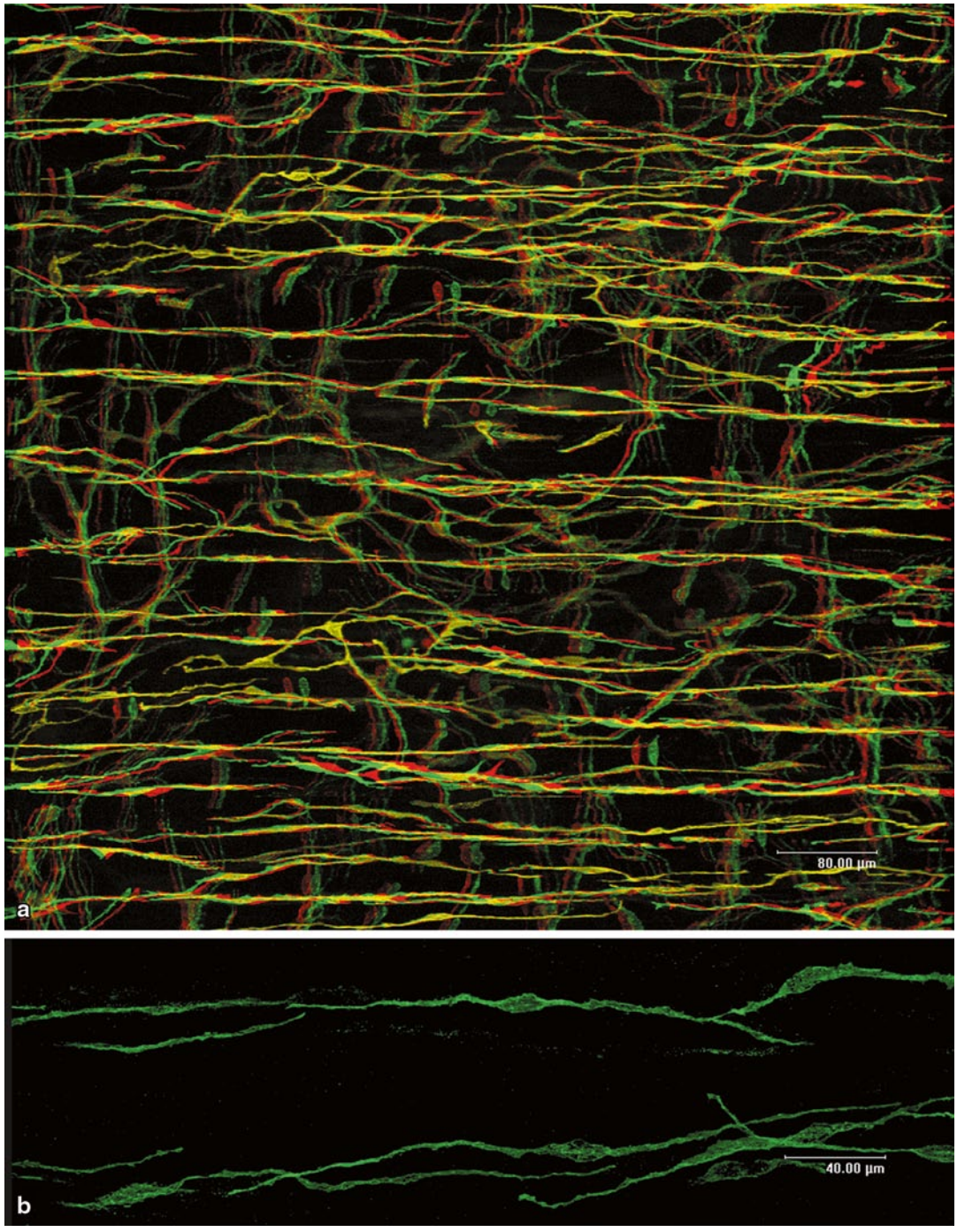

Fig. 4.7 ICC-CM in the guinea-pig duodenum. **a** Stereo-micrograph of the same area as in Fig. 4.4, including ICC-CM in the thickness of the confocal image. ICC-CM are densely distributed in the thickness of the muscle layer and form a cellular network by connecting with each other, unlike in the jejunum or ileum (view with *red/green* stereoscopic glasses). *Bar* 80 µm. **b** Higher magnification of ICC-CM of the guinea-pig duodenum, with a rather simple bipolar shape. *Bar* 40 µm.

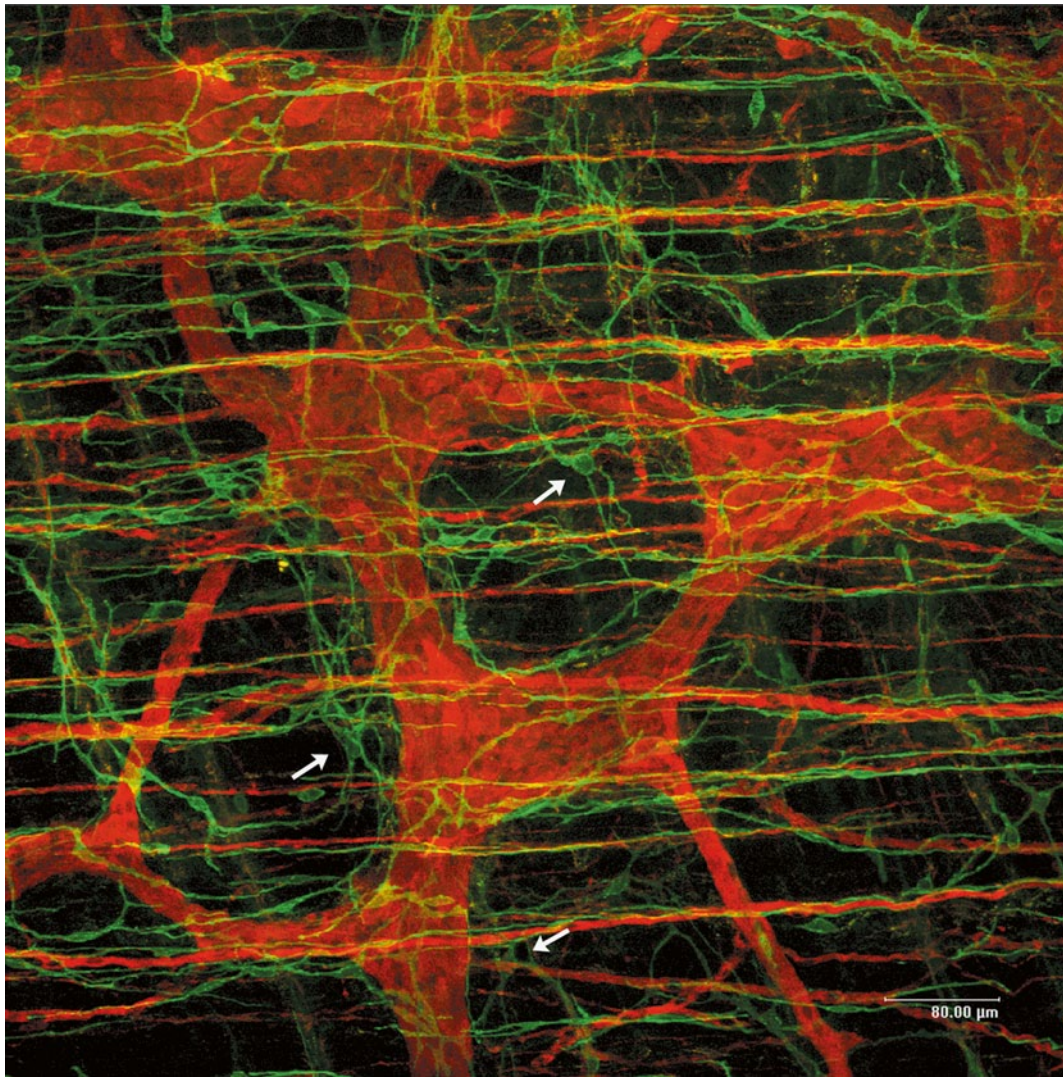

Fig. 4.8 Whole-mount stretch preparation showing the guinea-pig proximal duodenum. This micrograph reveals multipolar ICC (*arrows*) that have no relation to the nerve elements and which appear to surround certain structures that are not visible with c-Kit/PGP 9.5 immunohistochemistry. *Bar* 80 µm.

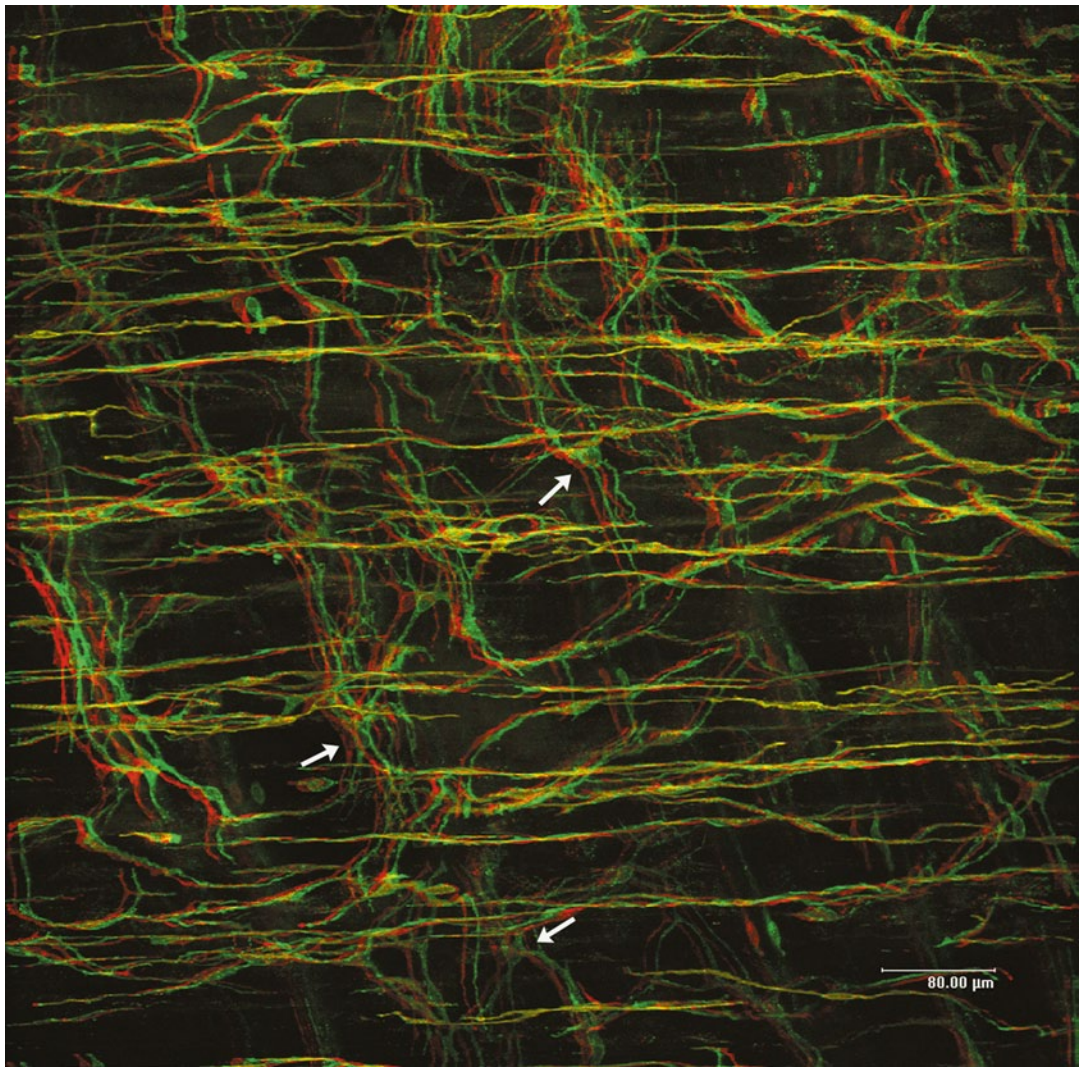

Fig. 4.9 Stereo-micrograph of ICC-MP reconstructed from the same portion of guinea-pig proximal duodenum as Fig. 4.8. Multipolar ICC (*arrows*) are observed in arranged as if they surround hollow structures. Possible candidates for the unknown structures are lymph vessels or blood vessels or secretory ducts of glands (view with *red/green* stereoscopic glasses). *Bar* 80 µm.

Colon

5

ICC are found in the myenteric region, as in the stomach and small intestine, and also at the interface between the submucosa and the circular muscle layer where the submuscular plexus is located. Fairly rich c-Kit immunoreactivity is observed in the circular muscle layer, often located in the connective tissue septa, apparently outlining muscle bundles. c-Kit positive cells are also found in the longitudinal muscle layer.

Taking account of the location and peculiar arrangement of the ICC-SS, and the main functions of the proximal colon, i.e. absorption and transport of fluids, it is tentatively proposed that the superficial network of ICC-SS acts as a stretch receptor to detect the circumferential expansion and swelling of the colon wall. The network of ICC-SS triggers the contraction of the longitudinal muscle to accelerate drainage of fluids from the colon. Active absorption of water and electrolytes in the mucosa followed by influx into the capillary network must cause expansion of venules passing through outer part of the wall and subsequently may cause inevitable leakage of fluid into the interstitial tissue matrix. This interstitial fluid should be drained through lymph vessels. Since venules and lymph vessels have only a poor coat of smooth muscle cells, movements of surrounding muscle layers of the colon wall probably facilitate and accelerate the transport of the vessel contents (Fig. 5.13).

T. Komuro, *Atlas of Interstitial Cells of Cajal in the Gastrointestinal Tract,*
DOI 10.1007/978-94-007-2917-9_5, © Springer Science+Business Media B.V. 2012

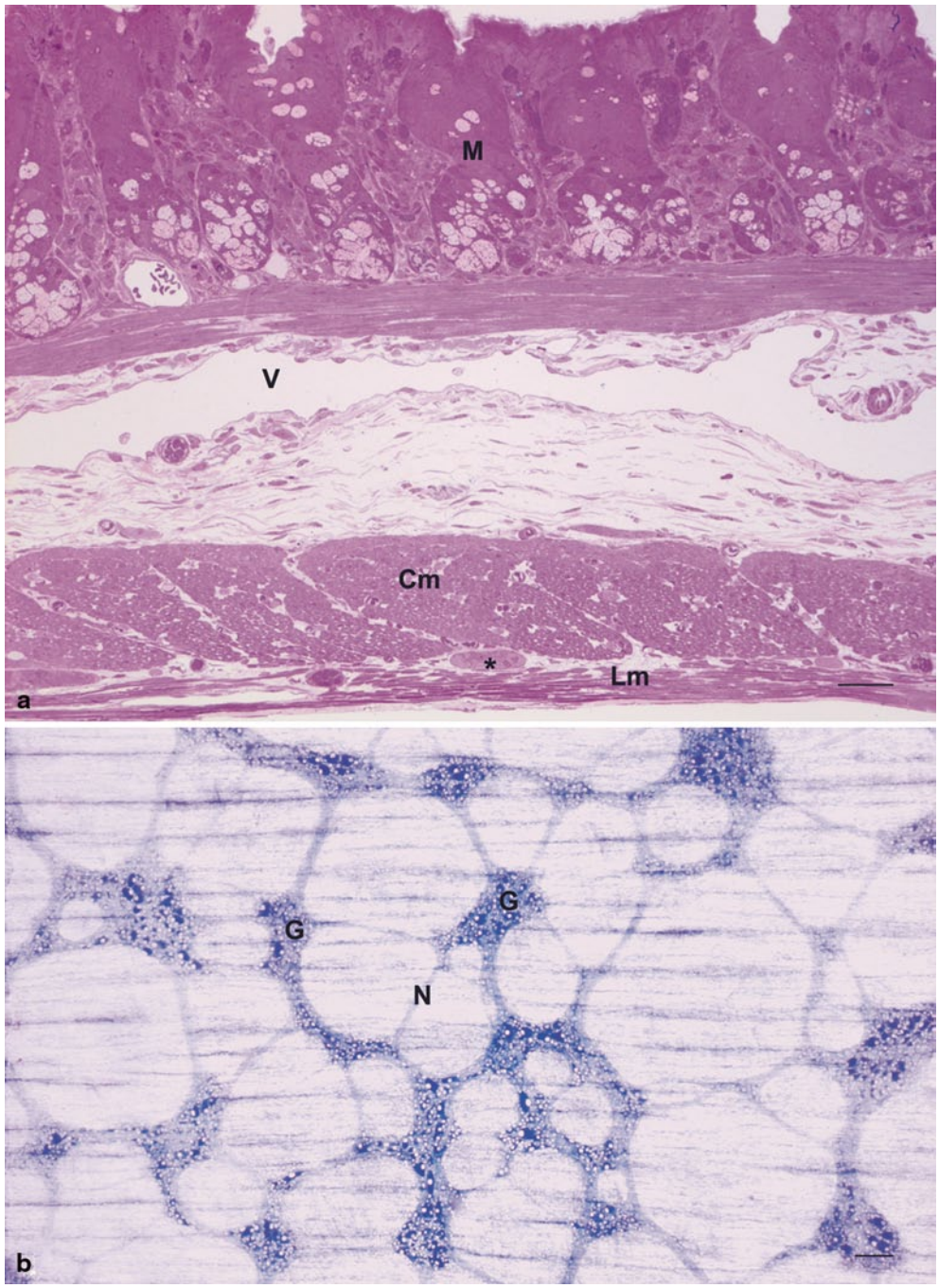

Fig. 5.1 Histological characteristics of the guinea-pig colon. **a** A longitudinal section of the proximal colon stained with toluidine blue. Underneath the darkly stained mucosa (*M*), a large lymph vessel (*V*) is conspicuous in the submucosal layer. The circular (*Cm*) and longitudinal (*Lm*) muscles are well developed, and the myenteric ganglion (*) is found between them. ×280. *Bar* 40 μm. (Courtesy of Dr Tamada, Waseda University). **b** Whole-mount stretch preparation of the guinea-pig proximal colon stained with NADH histochemistry, showing the myenteric plexus composed of thick and short ganglia (*G*) connected with rounded nerve strands (*N*). The major axes of the ganglia are irregular and are not always parallel with the axis of the circular muscles, unlike the case in the small intestine. ×80. *Bar* 100 μm. (Courtesy of Dr Mitsui, Nagoya City University).

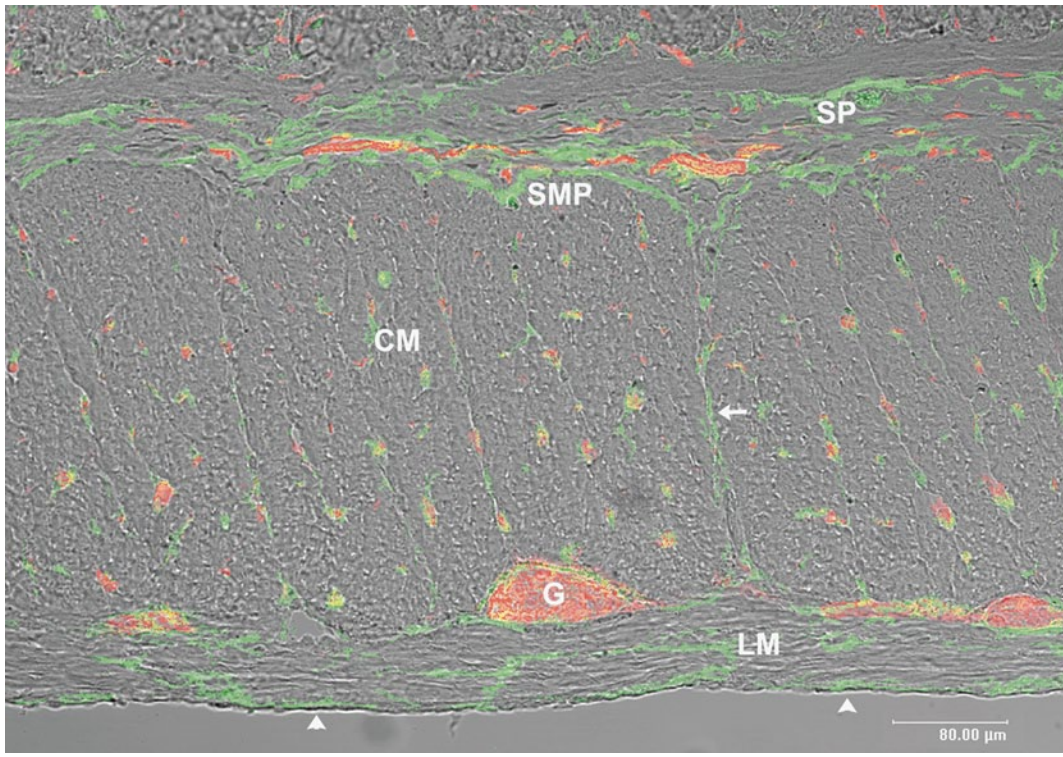

Fig. 5.2 A longitudinal section of the colon observed with Nomarski optics merged with c-Kit positive ICC (*green*) and PGP9.5 positive nerves (*red*). ICC-SMP are clearly observed in a way demarcating the submucosal border of the circular muscle layer (*SMP*). In the circular muscle layer ICC-CM are observed within the muscle bundles (*CM*) and in the septum between the bundles (*arrow*). ICC-MP are seen around the myenteric ganglia (*G*). ICC-LM are observed in the longitudinal muscle layer (*LM*). c-Kit immunoreative cells located at the outermost plane of the longitudinal muscle layer probably represent ICC-SS in the subserosal space (*arrowheads*). Further, ICC-SP (*SP*) associated with the submucosal plexus are observed in the connective tissue space of the submucosa. *Bar* 80 µm. (Courtesy of Dr Tamada, Waseda University).

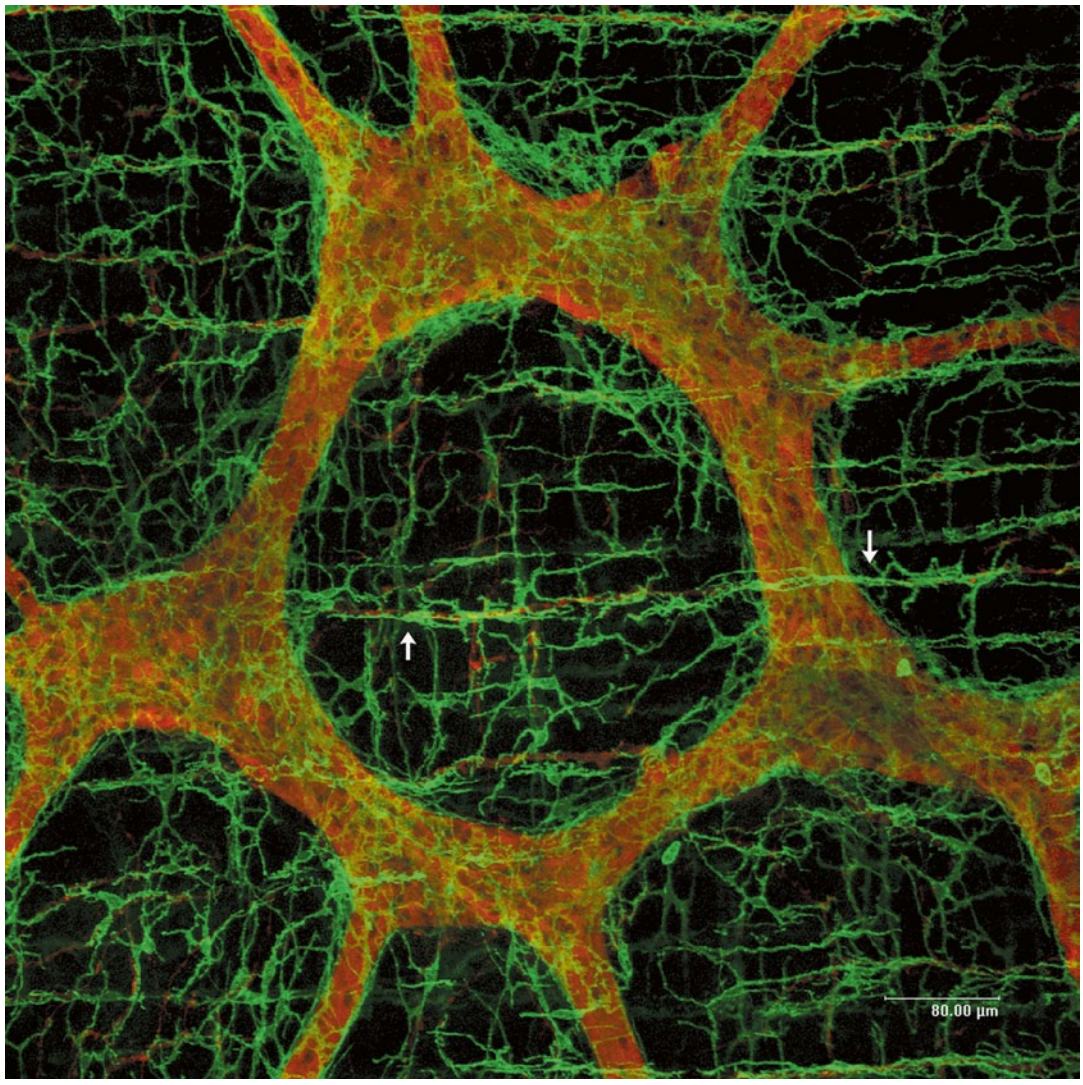

Fig. 5.3 ICC-MP in the guinea-pig proximal colon stained with c-Kit/PGP9.5 immunohistochemistry. Whole-mount stretch preparation of the colon showing ICC-MP (*green*) associated with the myenteric plexus (*red*). ICC-CM within the circular muscle layer are also seen as a horizontal array (*arrows*) in the superimposed image. *Bar* 80 µm.

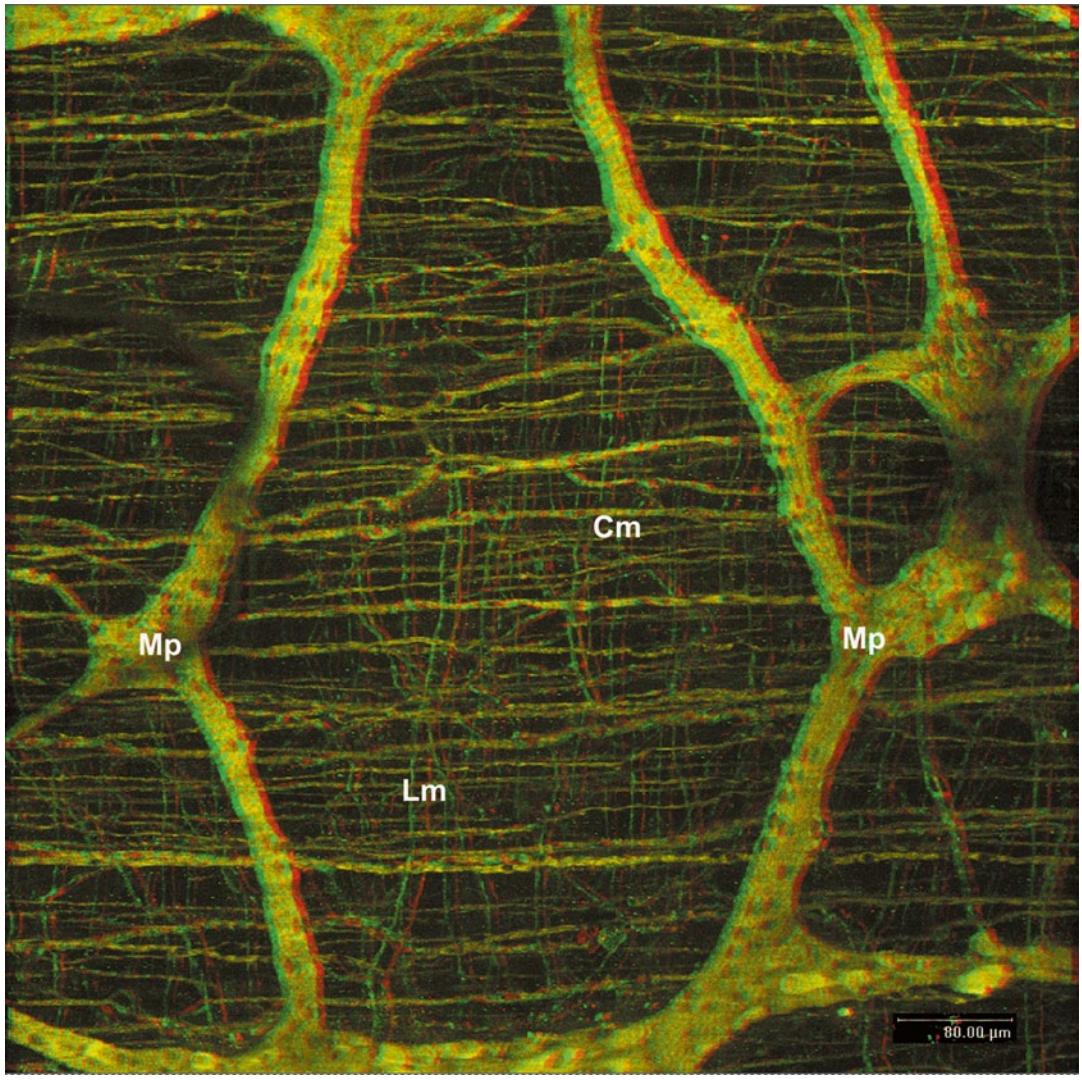

Fig. 5.4 Stereo-micrograph of the nerve plexus in the guinea-pig colon. A large mesh of the primary myenteric plexus (*Mp*) is sandwiched by the nerve fibers of both the circular (*Cm*) and the longitudinal muscle layers (*Lm*), oriented in horizontal and perpendicular directions, respectively (view with *red/green* stereoscopic glasses). *Bar* 80 µm.

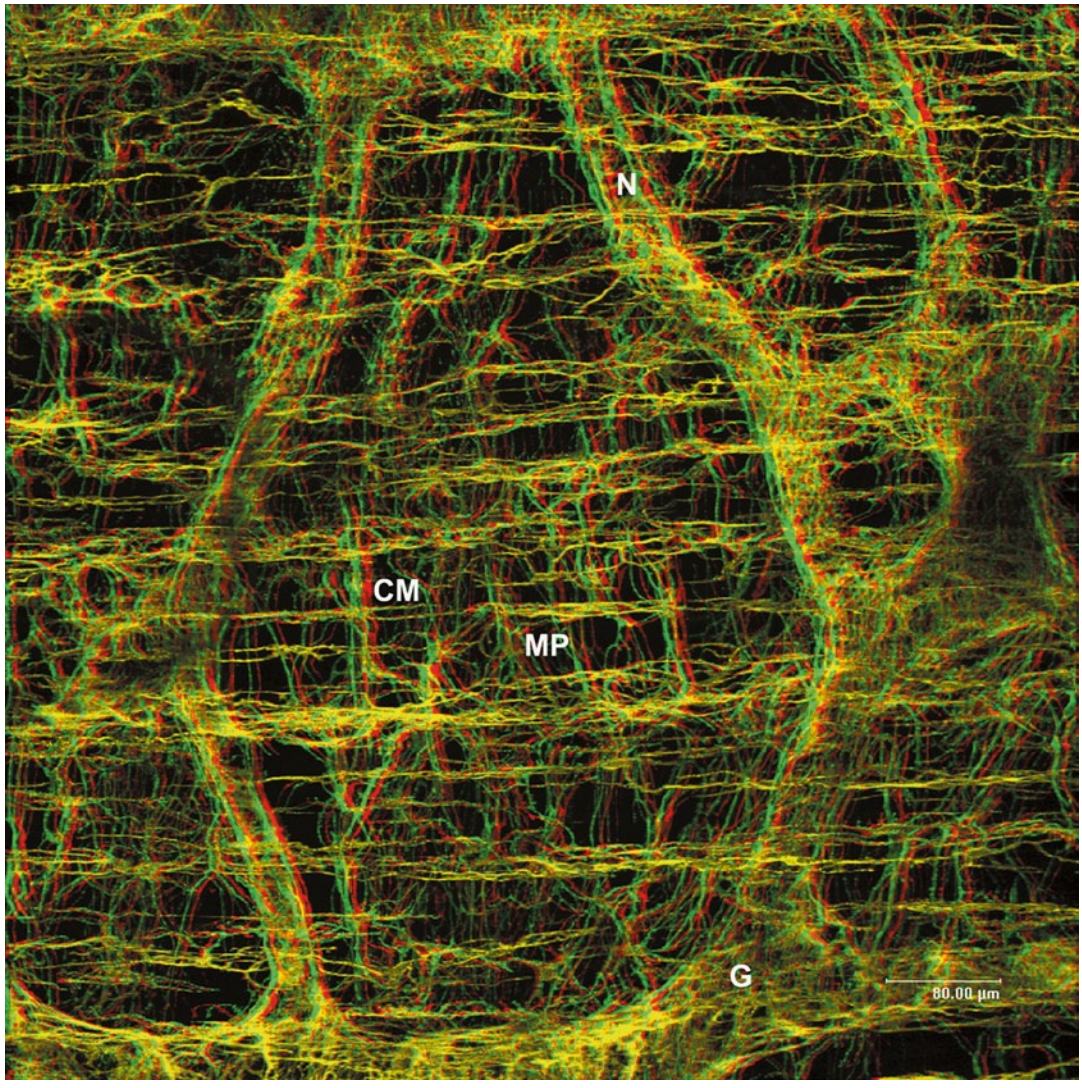

Fig. 5.5 Stereo-micrograph showing ICC associated with the nerves in Fig. 5.4. ICC-MP are observed along the contours of both ganglionic (*G*) and connecting nerve (*N*) strands to form basket structures around them. The cytoplasmic processes of ICC-CM (*CM*) communicate with each other at different depths in the tissue and with ICC-MP (*MP*) located in the meshes of the myenteric plexus (view with *red/green* stereoscopic glasses). *Bar* 80 µm.

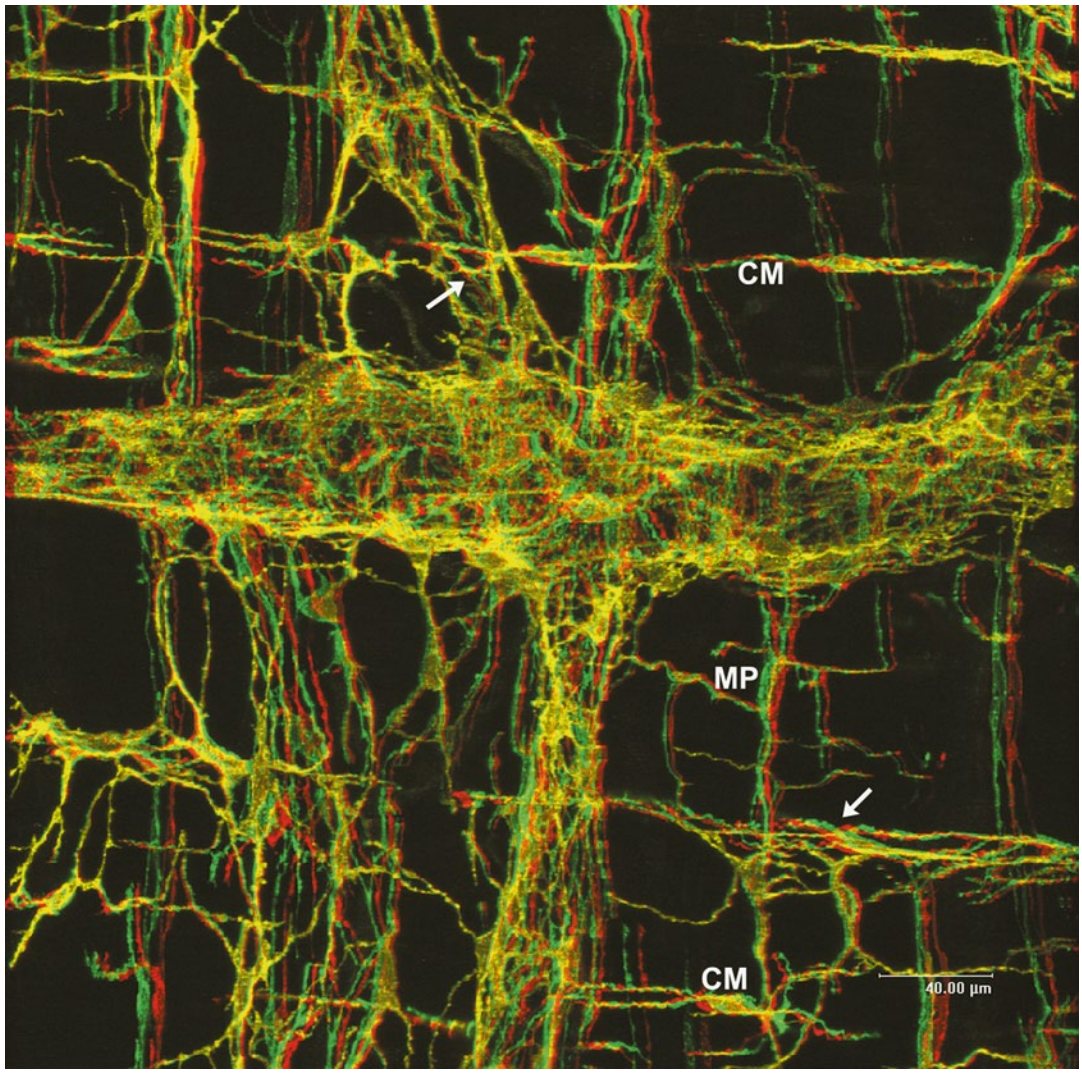

Fig. 5.6 3D arrangement of ICC-MP and ICC-CM in the guinea-pig colon. Higher magnification of stereomicrograph showing three-dimensional arrangement of the processes of ICC-CM (*CM*) and ICC-MP (*MP*). Connection between their processes can be seen (*arrows*). Basket formation of ICC-MP is clearly observed (view with *red/green* stereoscopic glasses). *Bar* 40 µm.

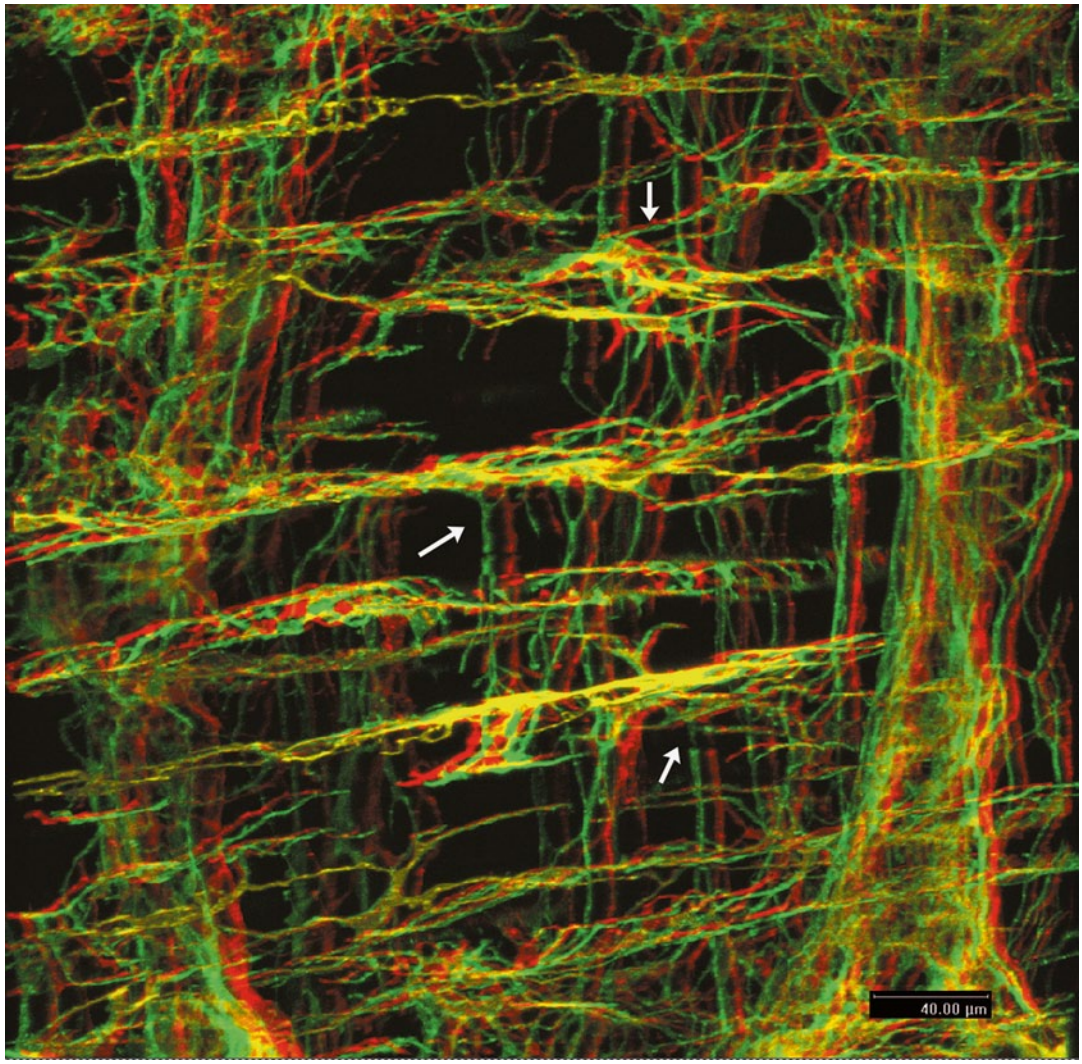

Fig. 5.7 Stereo-micrograph showing the connection between ICC-MP and ICC-CM in the guinea-pig colon. This micrograph shows connections (*arrows*) between the processes of ICC-MP and ICC-CM oriented vertically along the depth of tissue layer (view with *red/green* stereoscopic glasses). *Bar* 40 µm.

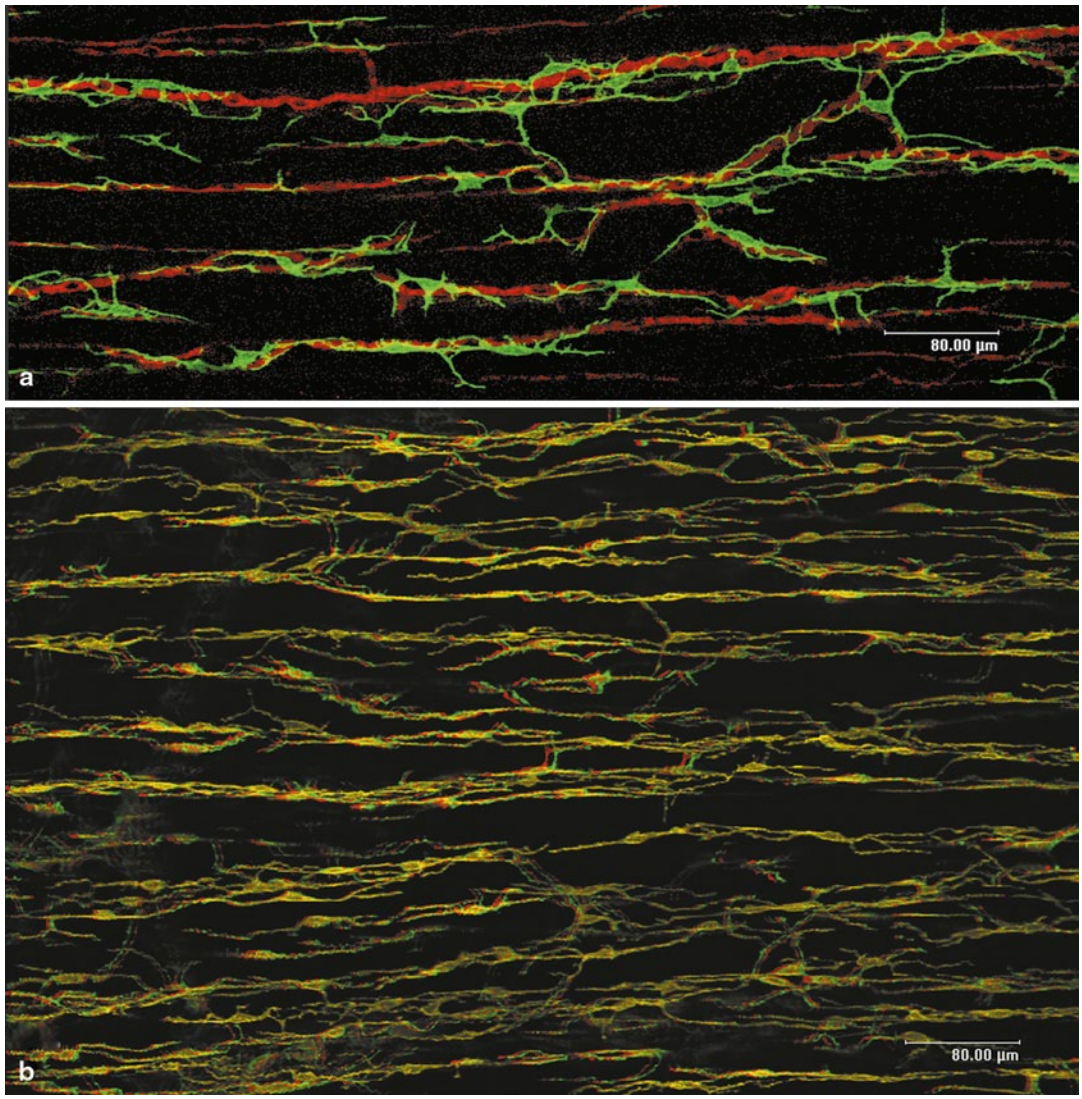

Fig. 5.8 ICC-CM in the guinea-pig colon. **a** ICC-CM are closely associated with the nerves within the circular muscle layer that are oriented mostly in parallel with the circular muscle cells. However, their cell shape is not simple bipolar, but they often have more than three branches, which differs from that in the stomach and small intestine in their cell shape, cell density and the degree of network continuity. *Bar* 80 µm. **b** Stereomicrograph of the ICC-CM of the guinea-pig colon which are observed as continuous cellular lines, unlike those in the small intestine. They appear to form a 3D network by the connections between ICC-CM at different depths in the tissue layers (view with *red/green* stereoscopic glasses). *Bar* 80 µm.

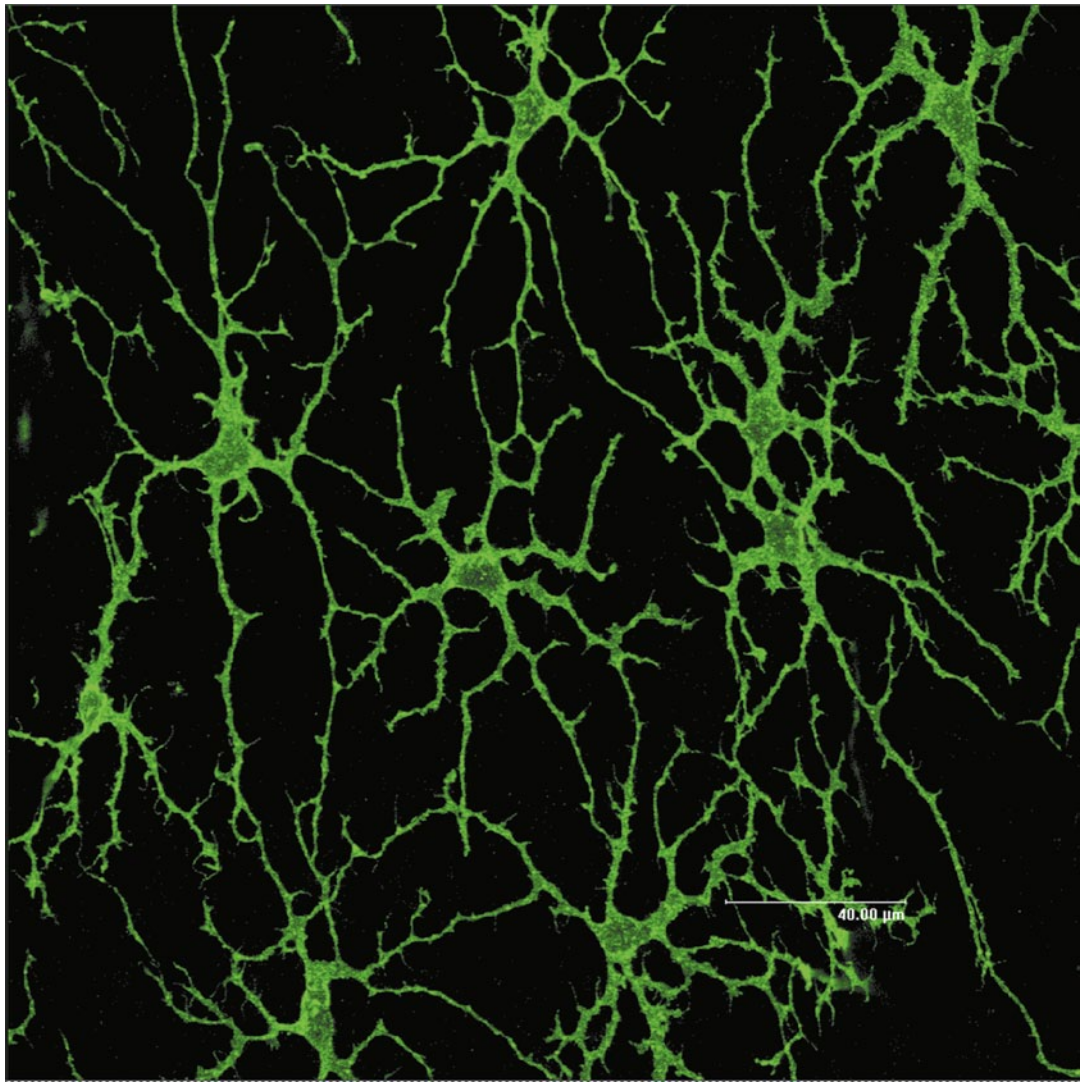

Fig. 5.9 ICC-SS in the subserosal layer of the guinea-pig proximal colon. ICC-SS in the subserosal layer are particularly well-developed in the proximal colon throughout the whole GI tract of the guinea-pigs. They are characterized by 3–7 primary processes that form secondary, tertiary and further branches. The processes often have tiny, spiny processes along their course. They usually branch by dichotomy, and triangular knots at the branching points are not obvious unlike in the ICC-MP. In this respect, ICC-SS are easily distinguished from ICC-MP that are also designated as the multipolar cells. *Bar* 40 µm. (Reproduced from Aranishi et al. [35] with permission of the publisher).

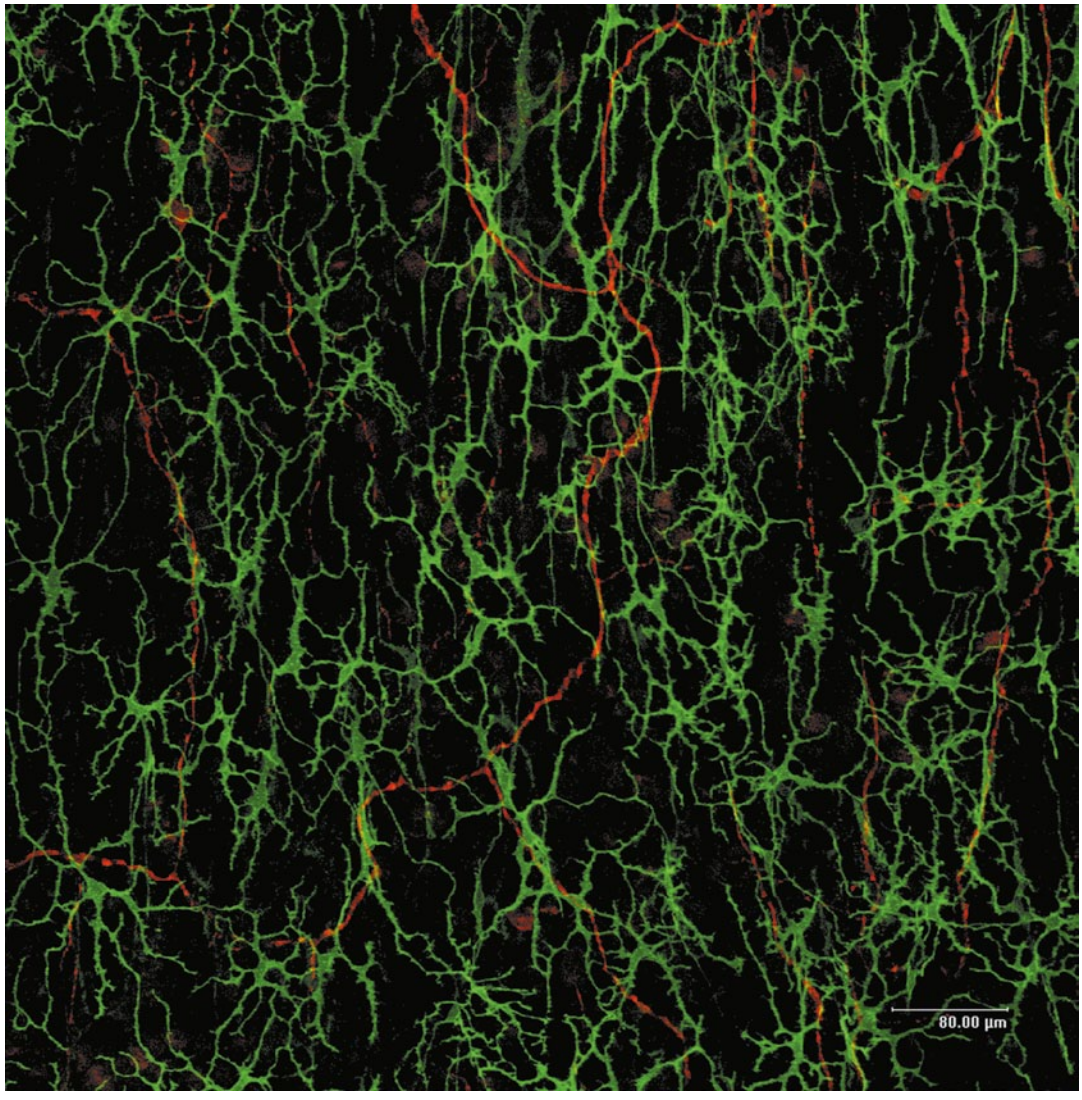

Fig. 5.10 ICC-SS and nerves in the guinea-pig proximal colon. Innervation of the subserosal layer appears to be poor and only a few nerve fibers (*red*) are observed. Close relationship between ICC-SS and nerves have not been elucidated. *Bar* 80 µm. (Figures 5.10, 5.11, 5.12, 5.13: Courtesy of Dr Tamada, Waseda University).

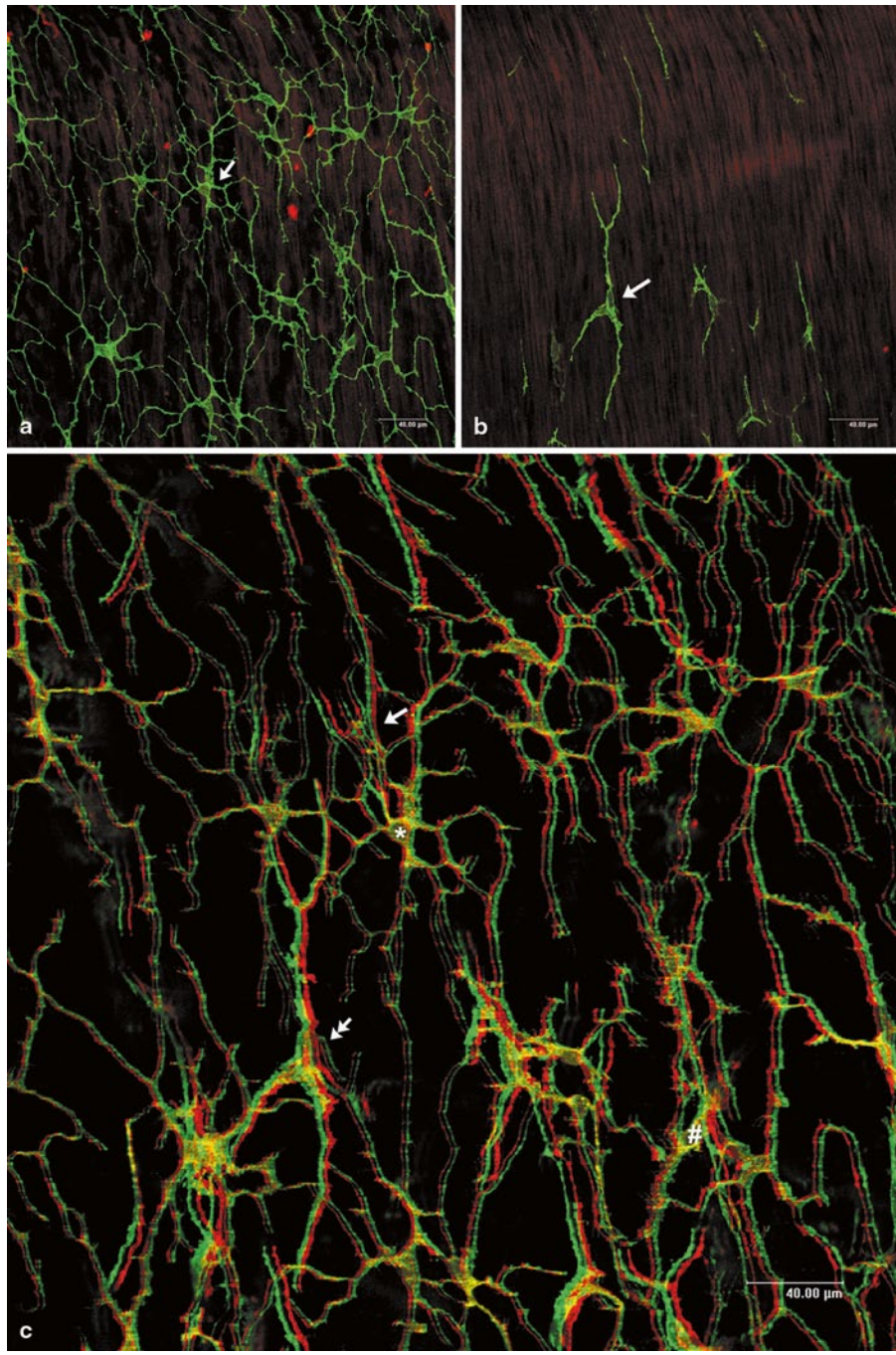

Fig. 5.11 Relationships between ICC-SS and ICC-LM. **a** ICC-SS (*green*) located in the subserosal layer immediately adjacent to the longitudinal muscle layer immunohistochemically stained for smooth muscle actin (*red*). The cell indicated by an arrow correspond to ICC-SS (*) in **c**. *Bar* 40 µm. **b** A few ICC-LM (*arrow*) located within the longitudinal muscle layer (*red*). The cell indicated by an arrow correspond to ICC-LM indicated by double-headed arrow in **c**. *Bar* 40 µm. **c** Three-dimensional reconstruction of confocal image of the same area in **a, b.** ICC-SS (*), which has a typical multipolar shape in the superficial plane, projects one primary process into the deeper layer of ICC-LM where its secondary branches has straight processes (*arrow*) being arranged along the axis of the longitudinal muscles. One cell body (#) located between the two layers has branching processes in the superficial plane in one hand, but on the other hand has straight processes in the deeper region of ICC-LM (view with *red/green* stereoscopic glasses). *Bar* 40 µm.

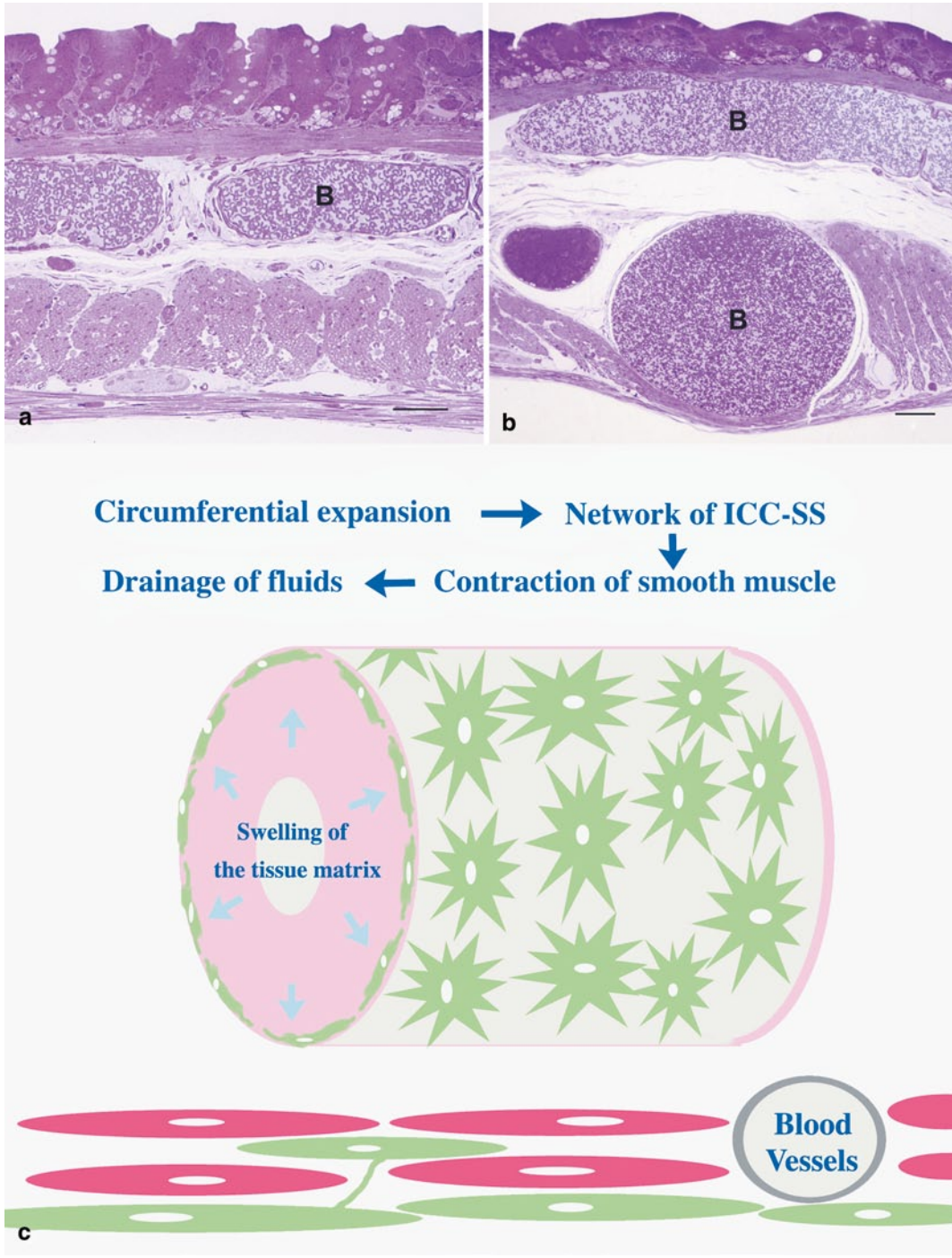

Fig. 5.12 Working hypothesis about the possible function of ICC-SS. **a** Longitudinal sections of the guinea-pig proximal colon stained with toluidine blue. Large blood vessels full of erythrocytes (*B*) are abundant in the submucosa. ×200 *Bar* 50 μm. (Reproduced from Aranishi et al. [35] with permission of the publisher). **b** Large blood vessels (*B*) bulge into the muscle layer, as well as in the submucosa. ×150 *Bar* 50 μm. (Courtesy of Dr Tamada, Waseda University). **c** Schematic illustration of a possible function of ICC-SS.

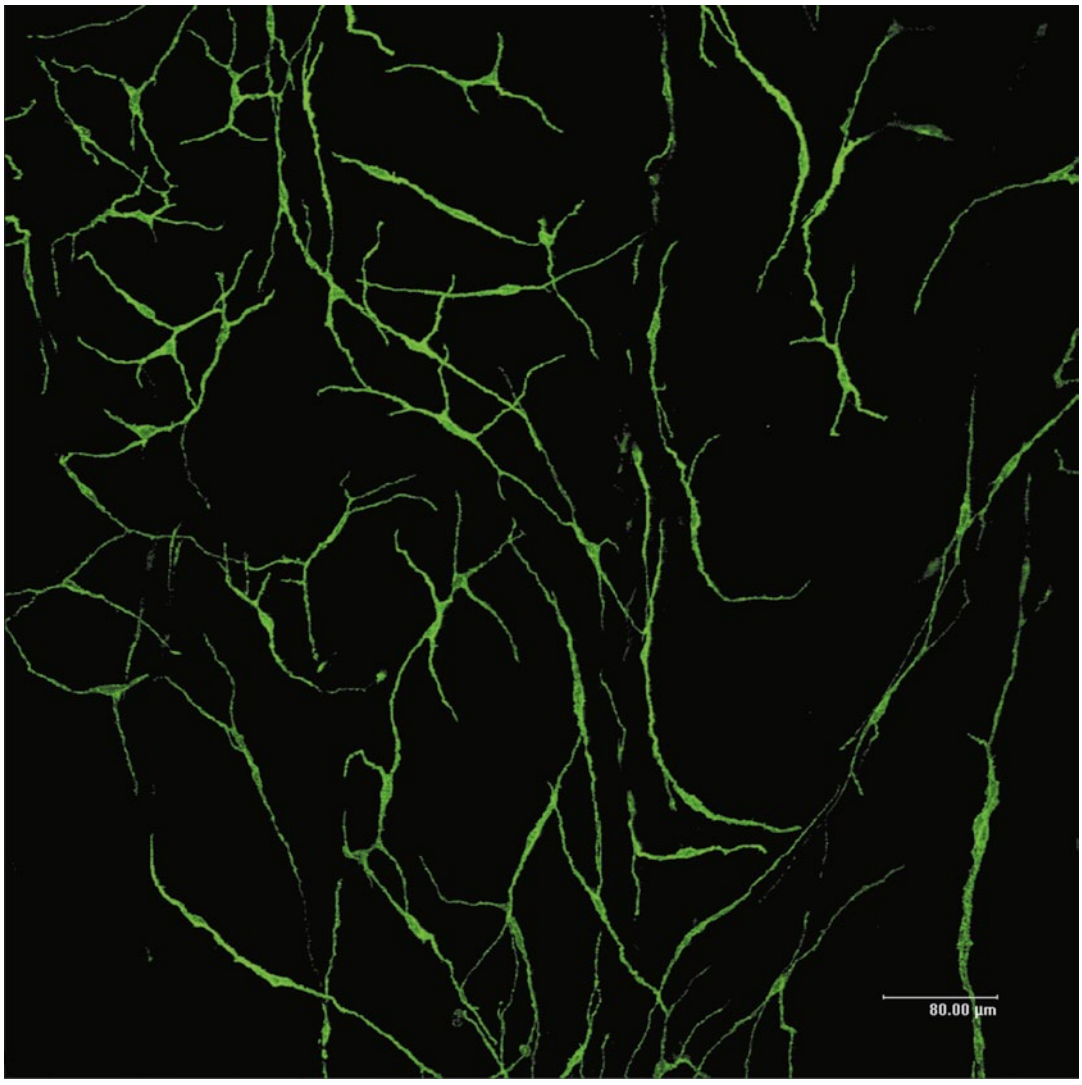

Fig. 5.13 ICC-SS in the guinea-pig distal colon. ICC-SS in the distal colon have a simpler cell shape than those in the proximal colon, and they have fewer and shorter cell processes. Their physiological significance has not yet been elucidated. *Bar* 80 µm.

Caecum

6

The structure and the significance of the caecum greatly differ among animals and the guinea-pig caecum described here has the taeniae, bundles of the longitudinal muscles, which have been frequently used for the smooth muscle research. ICC are rather densely distributed in the taeniae and within the circular muscle layer. ICC-MP are only sparsely distributed over the loose network of the myenteric plexus. ICC-SP are found in association with the submucosal plexus.

T. Komuro, *Atlas of Interstitial Cells of Cajal in the Gastrointestinal Tract,*
DOI 10.1007/978-94-007-2917-9_6, © Springer Science+Business Media B.V. 2012

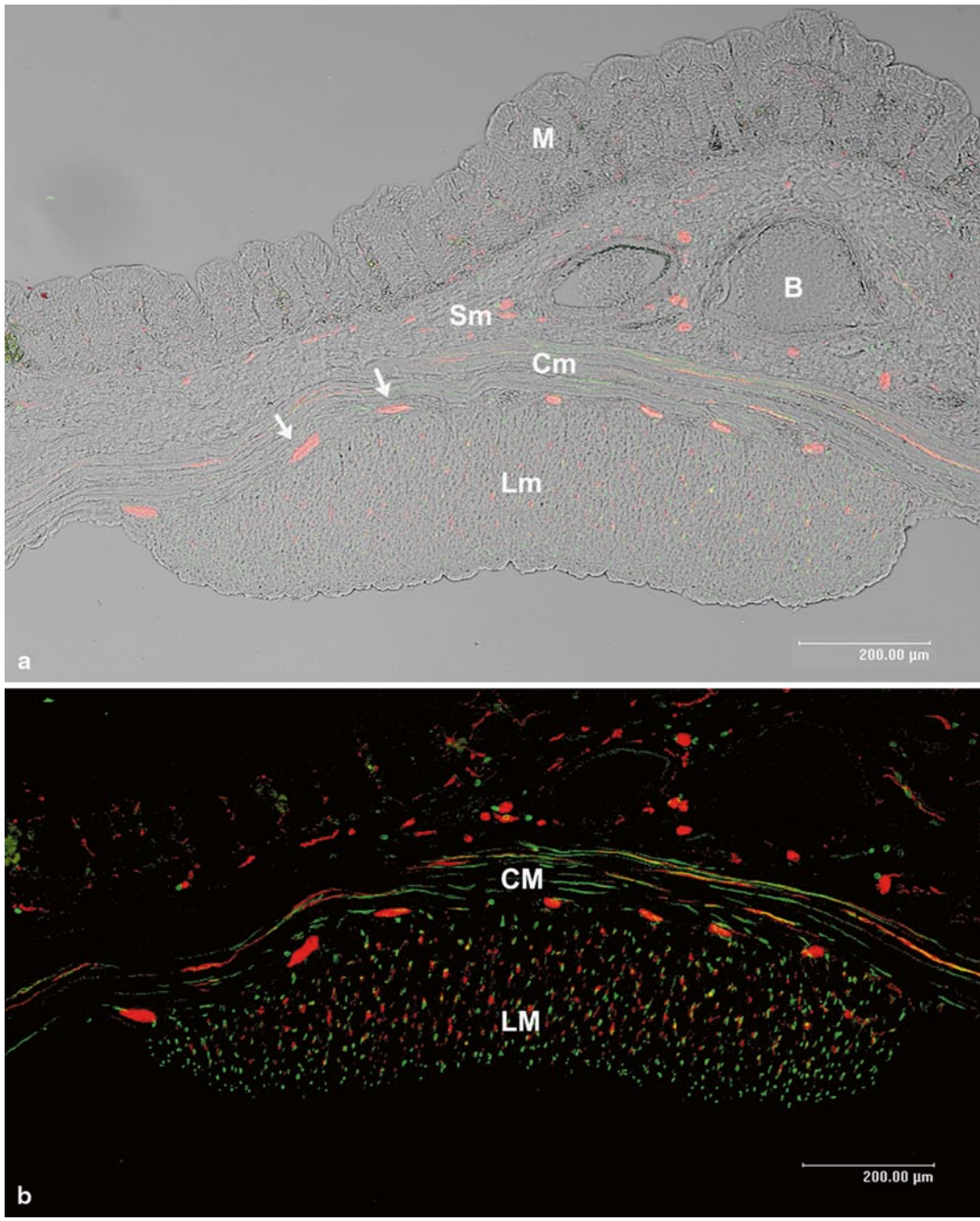

Fig. 6.1 A transverse section of the guinea-pig caecum containing a part of the taenia caeci. **a** Image observed with Nomarski optics merged with the image obtained by immunohistochemistry for c-Kit/PGP9.5 to make clear the contours of the specimen. The ganglia of the myenteric (*arrows*) are located between the circular muscle layer (*Cm*) and the longitudinal muscle of the taenia (*Lm*). The submucosa (*Sm*) underneath the mucosa (*M*) contains large blood vessels (*B*). *Bar* 200 µm. **b** The same area as in **a** showing clearer images of nerves (*red*) and ICC (*green*). Only a few ICC-CM (*CM*) are found in the circular muscle layer in a transverse section, while ICC-LM are densely distributed in the taenia (*LM*). *Bar* 200 µm. (Courtesy of Dr Tamada, Waseda University).

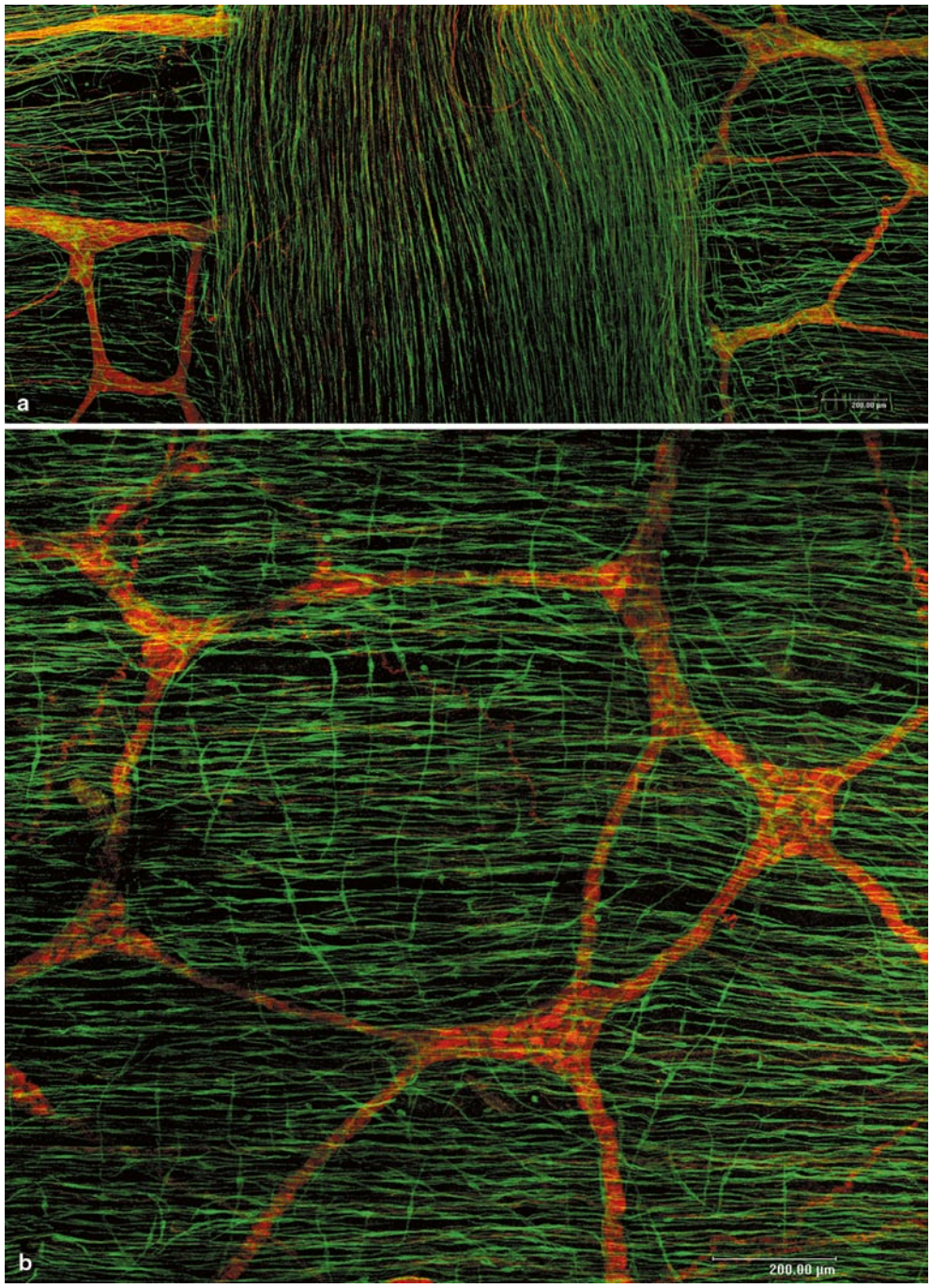

Fig. 6.2 ICC-CM and ICC-LM in the guinea-pig caecum. **a** A whole-mount stretch preparation of the guinea-pig caecum containing a part of taenia caeci. Perpendicularly oriented ICC-LM (*green*) within the taenia overlie the loose network of the myenteric plexus (*red*) and the underneath ICC-CM (*green*) oriented horizontally within the circular muscle layer. *Bar* 200 µm. **b** A whole-mount stretch preparation showing the muscle wall without the taenia, where numerous ICC-CM (*green*) are arranged horizontally along the axis of the circular muscle cells, while a few ICC-LM (*green*) are found along nearly perpendicular direction. The network of the myenteric plexus (*red*) is clearly observed because of minimal interference by only a few ICC-MP and ICC-LM. *Bar* 200 µm. (Courtesy of Dr Tamada, Waseda University).

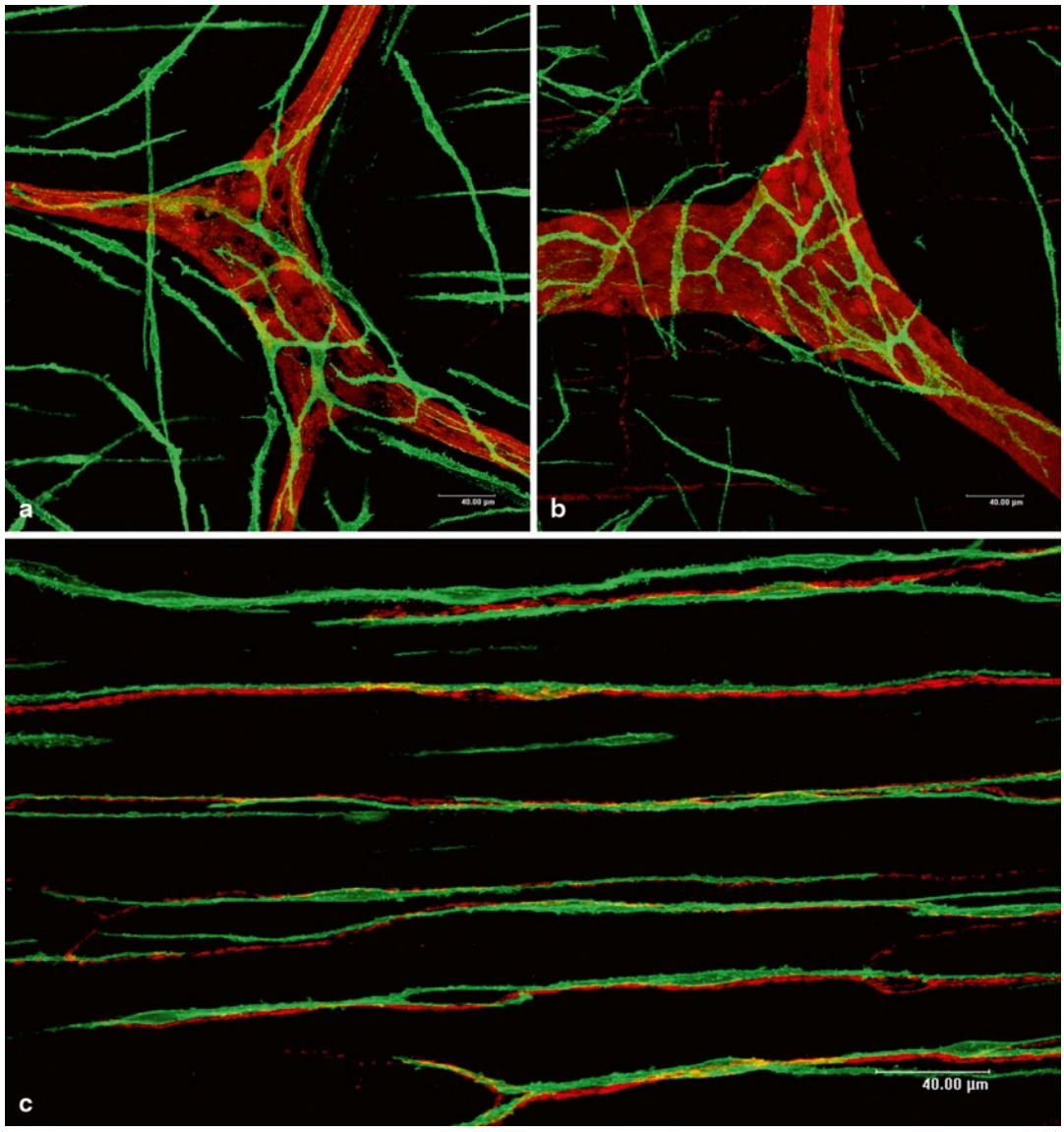

Fig. 6.3 ICC-MP and ICC-CM in the guinea-pig caecum. **a** Closer view of the myenteric ganglion (*red*) associated with a few multipolar shape of ICC-MP (*green*). *Bar* 40 µm. **b** Another myenteric ganglion (*red*) also shows a few ICC-MP around it. *Bar* 40 µm. **c** Closer observation of the bipolar ICC-CM (*green*) showing intimate association with the nerve bundles (*red*). *Bar* 40 µm. (Courtesy of Dr Tamada, Waseda University).

Ileocaecal Junction

7

The ileocaecal junction is believed to act as an anti-reflux barrier for colonic content into the terminal ileum. The ileocaecal junction including the valve shows characteristic features in the distribution patterns of ICC subtypes along the proximal to the distal area. The dense distribution of ICC in this area indicates the active involvement of ICC in the movement of the junctional area.

T. Komuro, *Atlas of Interstitial Cells of Cajal in the Gastrointestinal Tract,*
DOI 10.1007/978-94-007-2917-9_7, © Springer Science+Business Media B.V. 2012

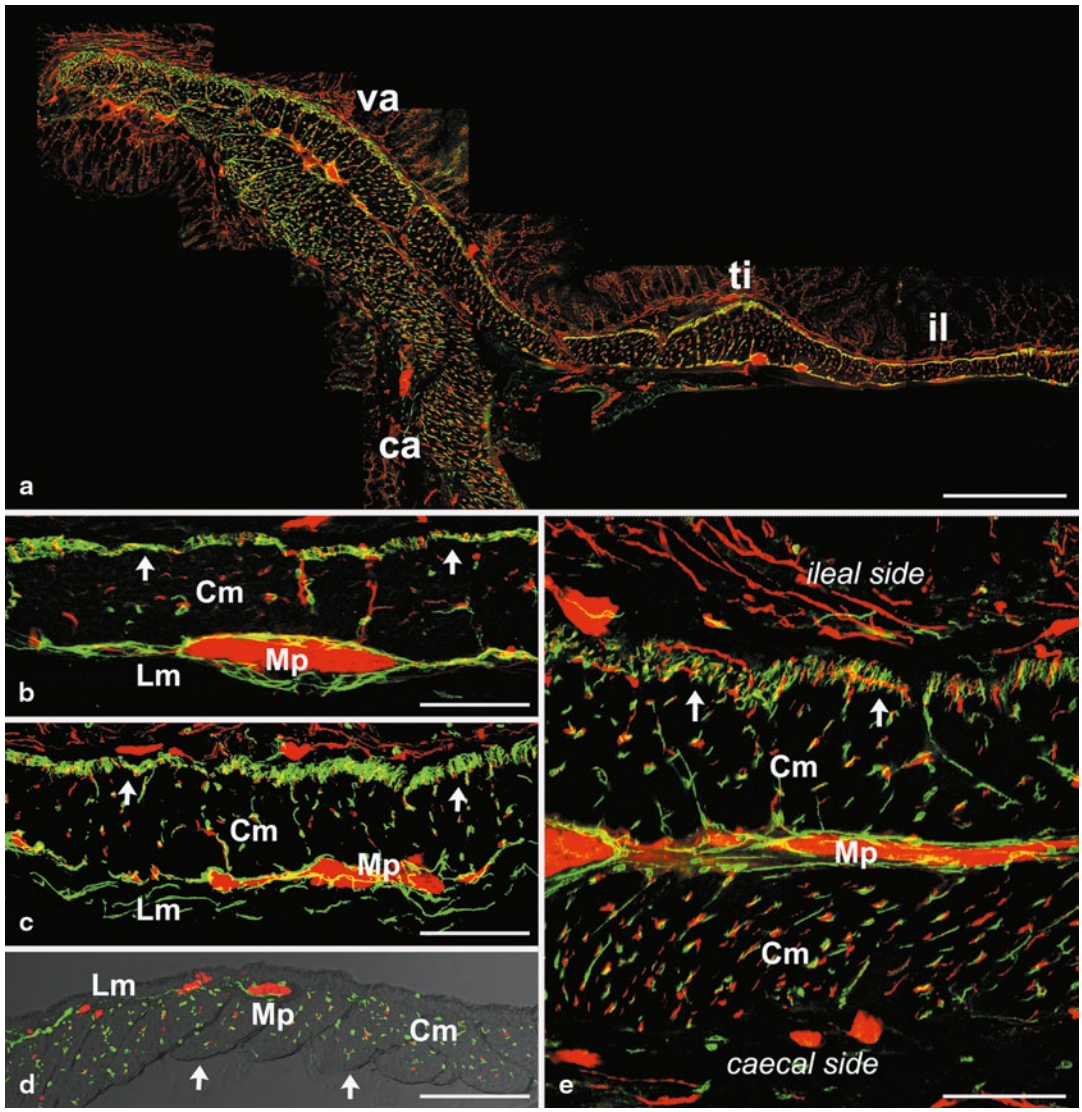

Fig. 7.1 Longitudinal sections of the guinea-pig ileocaecal junction showing ICC and nerves. **a** Overview of distribution of ICC and nerves in the ileocaecal junction. The ileocaecal junction as a dense distribution of ICC closely associated with the nerves. The terminal ileum immediately adjacent to the valve contains a thickened circular muscle layer (*il* ileum, *ti* terminal ileum, *va* valve, *ca* caecum). *Bar* 1 mm. (Figures 7.1, 7.2: Reproduced from Miyamoto-Kikuta et al. [79] with permission of the publisher). **b** Higher magnification of the ileum. ICC are found in the deep muscular plexus (*arrows*), around the myenteric plexus (*Mp*) and sparsely within the circular muscle layer (*Cm*). However, almost no ICC can be found within the longitudinal muscle layer (*Lm*). *Bar* 150 μm. **c** Higher magnification of the terminal ileum. Dense distributions of ICC are observed throughout the circular (*Cm*) and longitudinal (*Lm*) muscle layers and at the deep muscular (*arrows*) and the myenteric (*Mp*) plexus. *Bar* 150 μm. **d** Higher magnification of the caecum. The image obtained by immunohistochemistry has been merged with an image observed with Nomarski optics to make clear the contour of the specimen. ICC are observed throughout the circular (*Cm*) and longitudinal (*Lm*) muscle layers. Only a few ICC-MP can be detected around the myenteric plexus (*Mp*). ICC are not densely distributed near the submucosal border of the circular muscle layer (*arrows*), since deep muscular and submuscular plexus are both absent (different from ileum or colon). *Bar* 150 μm. **e** Higher magnification of the ileocaecal valve. ICC-MP are observed around the myenteric plexus (*Mp*) and ICC-CM are densely distributed within both the ileal and caecal sides of the circular muscle layers. ICC-DMP are only observed in the ileal side (*arrows*), but not in the caecal side. *Bar* 150 μm.

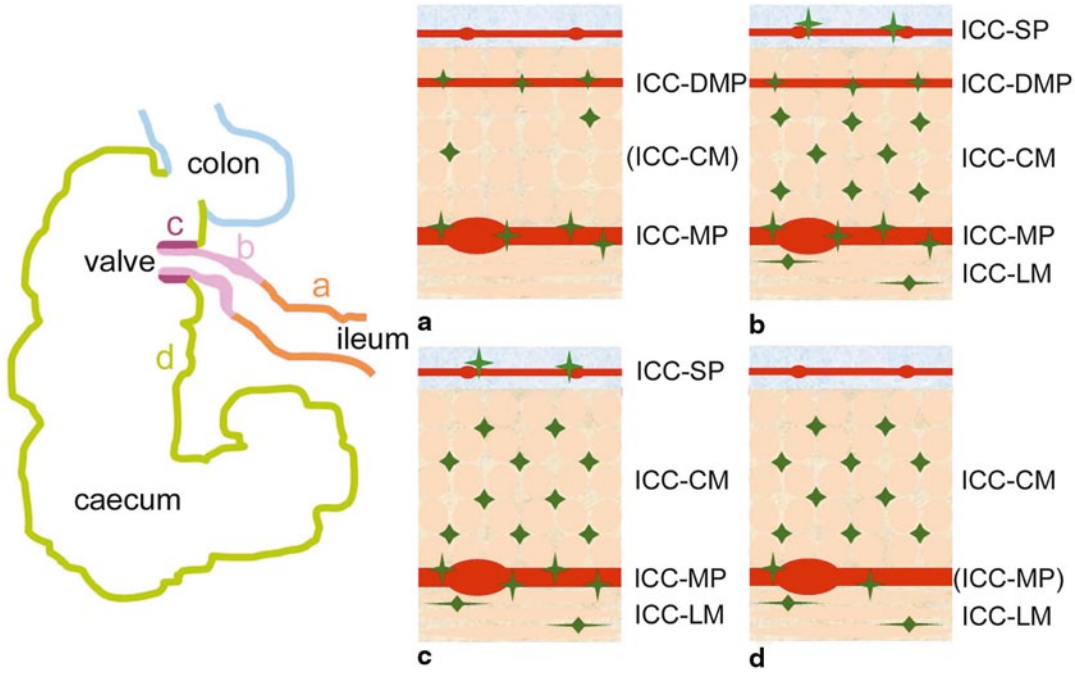

Fig. 7.2 Representation of the various distribution patterns of ICC (*green*) in the guinea-pig ileocaecal junction. *Left* Overview of the relevant anatomical region a (*a–d* indicated by side panels **a**–**d** on Right). **a** The main part of the ileum contains ICC-MP around the myenteric plexus, ICC-DMP and a few ICC-CM within the circular muscle layer but no ICC-LM within the longitudinal muscle layer. **b** Both the terminal ileum and the ileal side of the ileocaecal valve contain many ICC-CM and ICC-LM, in addition to ICC-DMP and ICC-MP. ICC-SP are also observed around the submucosal plexus. **c** The caecal side of the valve contains ICC-MP, ICC-CM and ICC-LM but no ICC-DMP. ICC-SP are also observed around the submucosal plexus. **d** The caecum contains many ICC-CM and ICC-LM but only a few ICC-MP. ICC are not observed in the vicinity of the submucosal border of the circular muscle layer because of the lack of both deep muscular and submuscular plexus (unlike the *ileum* or *colon*).

ICC Found in the Submucosal Layer

8

To date, ICC are found in close association with the submucosal plexus in the submucosa of the stomach, proximal colon and the caecum in the guinea-pig. However, the distribution and functional significance of ICC-SP throughout the GI tract remains to be elucidated.

T. Komuro, *Atlas of Interstitial Cells of Cajal in the Gastrointestinal Tract,*
DOI 10.1007/978-94-007-2917-9_8, © Springer Science+Business Media B.V. 2012

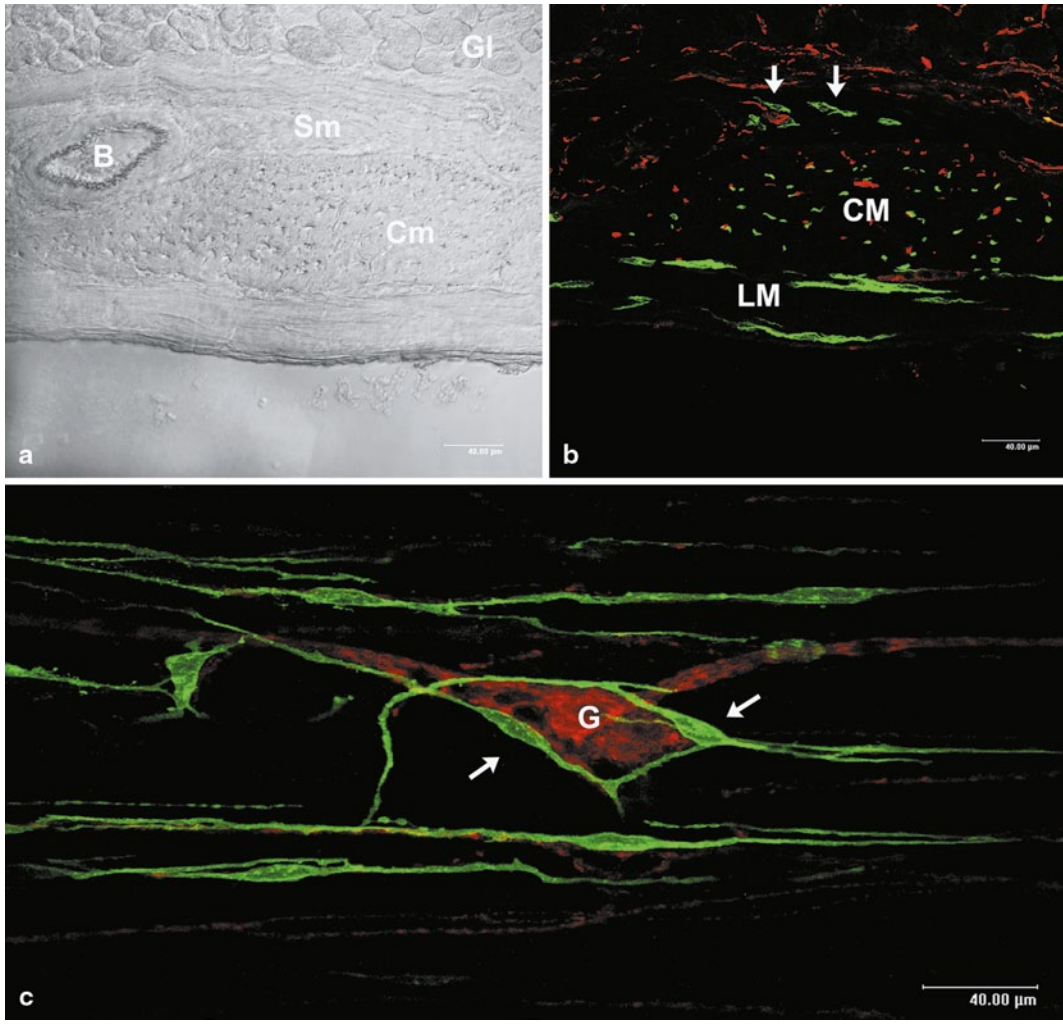

Fig. 8.1 ICC-SP in the guinea-pig stomach. **a** A longitudinal section of the gastric corpus observed with Nomarski optics showing the location of the submucosa (*Sm*) containing a large blood vessel (*B*) intervening between the bottom of the gastric glands (*Gl*) and the circular muscle layer (*Cm*). *Bar* 40 µm. **b** The same region as **a** showing immunoreactivity for c-Kit (*green*) and PGP 9.5 (*red*). Short spindle-shaped c-Kit immunoreactive ICC-SP are observed in the connective tissue space (*arrows*). ICC-CM (*CM*) and ICC-LM (*LM*) are also observed as green dots and long bipolar cells, respectively. *Bar* 40 µm. **c** Whole-mount stretch preparation of the corpus showing close association of ICC-SP (*arrows*) with the submucosal ganglion (*G*). *Bar* 40 µm. (Reproduced from Kunisawa and Komuro [80] with permission of the publisher).

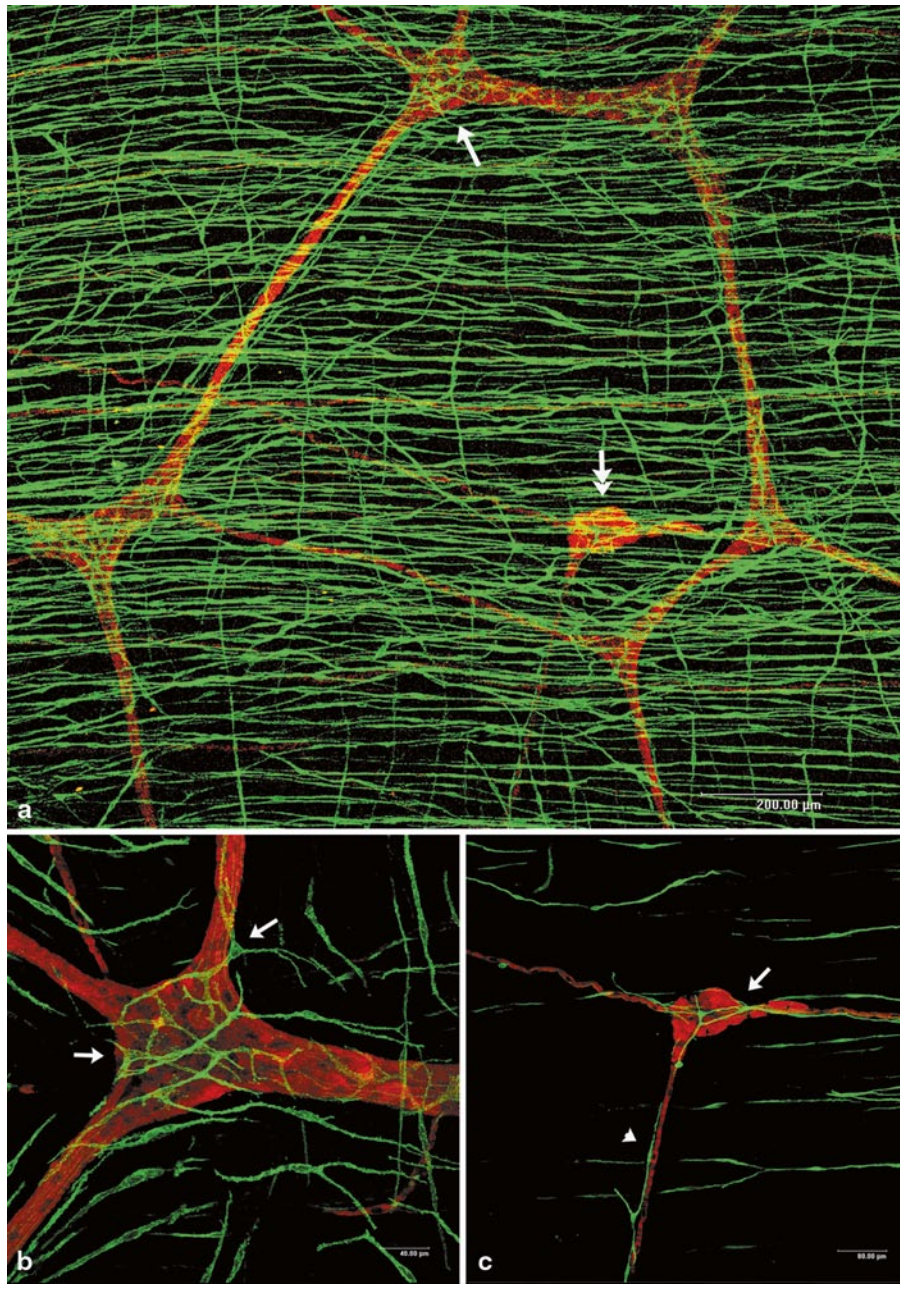

Fig. 8.2 ICC-SP in the guinea-pig caecum. **a** Whole-mount stretch preparation stained with c-Kit (*green*) and PGP9.5 (*red*) showing the area between the taenia of the guinea-pig caecum. The myenteric plexus is observed as a loose polygonal network consisting of the small ganglia (*arrow*) and long connecting nerve strands. Bipolar-shaped ICC-CM within the circular muscle layer run parallel to the circular muscle axis (*horizontal direction*) and a few ICC-LM within the longitudinal muscle layer also run in a nearly perpendicular direction to this axis. The submucosal ganglion (*double-headed arrow*) with thin nerve strands can be seen to be separate from the myenteric plexus (*arrow* ganglion shown in **b**, *double-headed arrow* ganglion shown in **c**). *Bar* 200 µm. **b** Closer view of the myenteric ganglion (*arrow* in **a**). Multipolar shaped ICC-MP associated with the myenteric plexus are observed around the ganglion (*arrows*). *Bar* 40 µm. **c** Closer observation of the submucosal ganglion (*double-headed arrow* in **a**) showing the multipolar ICC-SP associated with the submucosal plexus (*arrow*) on the ganglion and long bipolar ICC-SP (*arrow head*) along the nerve strands. *Bar* 80 µm. (Reproduced from Tamada and Komuro [81] with permission of the publisher).

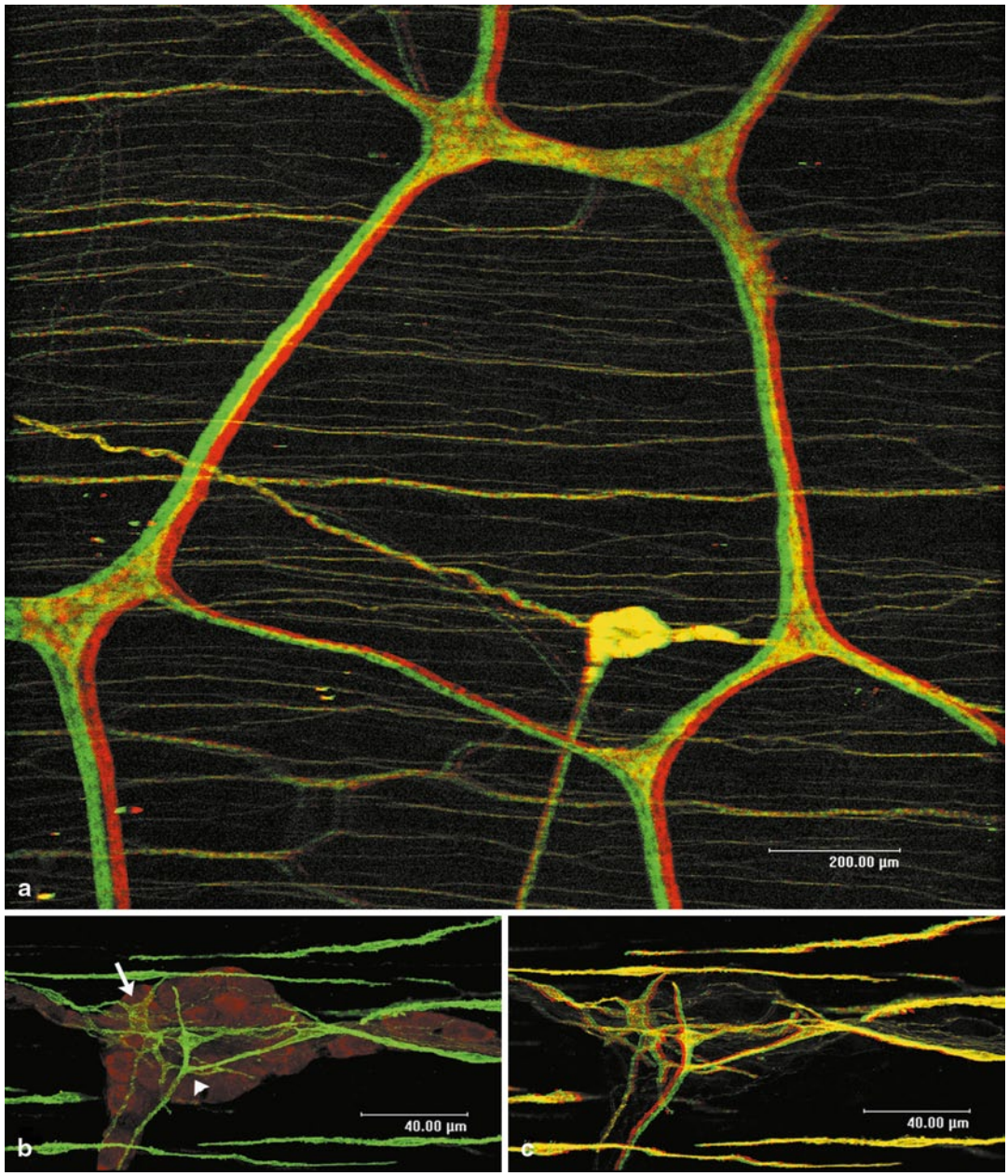

Fig. 8.3 3D demonstration of the myenteric and submucosal ganglia. **a** Stereo-micrograph of the same area as in Fig. 8.2a, showing the myenteric and submucosal plexus, which are located at different tissue layer depths (view with *red/green* stereoscopic glasses). Nerve fibers within the circular muscle layer (*running horizontally*) are also seen between the two plexuses. *Bar* 200 µm. **b** Higher magnification of the same ganglion as in Fig. 8.2c located within the thickness of the confocal image, including ICC-SP located on both sides of the ganglion and ICC-CM located nearby. Superimposed ICC-SP on the different sides of the ganglion differ in the staining intensity (*arrow, arrowhead*). *Bar* 40 µm. **c** Stereomicrograph reconstructed from serial confocal images included in **b** (viewed with *red/green* stereoscopic glasses). ICC-SP clearly surround the ganglion like a basket. *Bar* 40 µm. (Reproduced from Tamada and Komuro [81] with permission of the publisher).

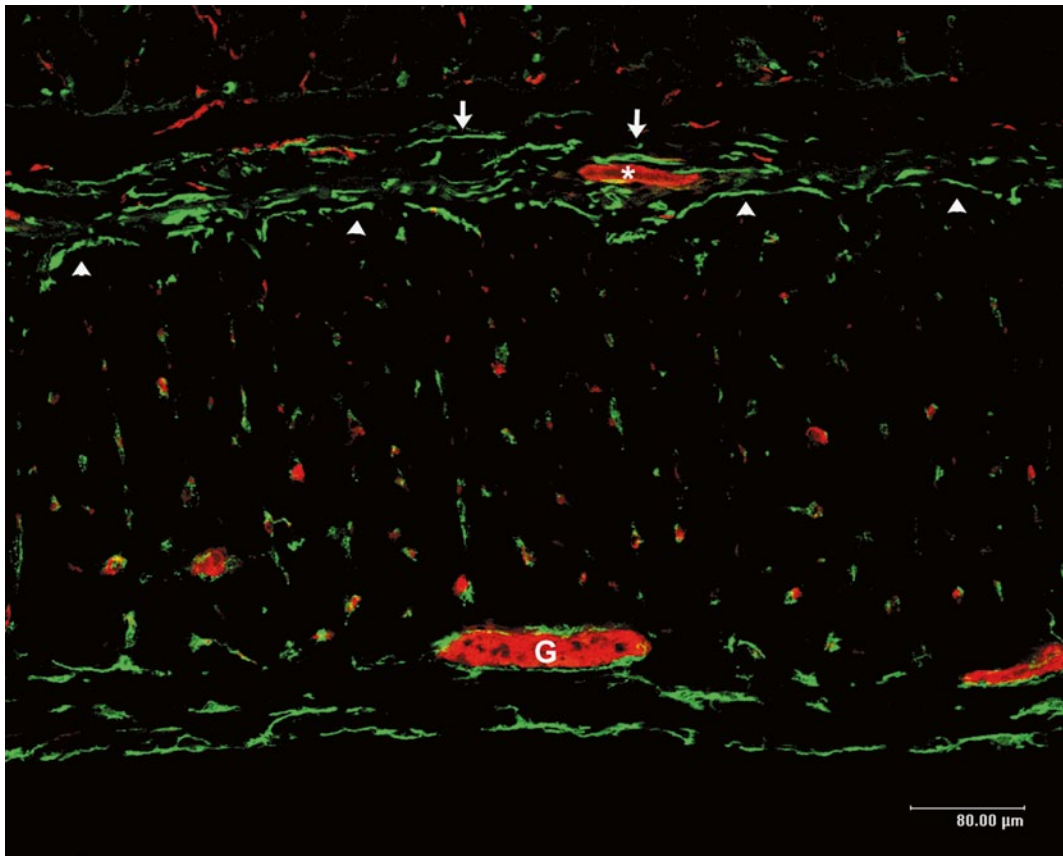

Fig. 8.4 ICC-SP in the guinea-pig proximal colon. A longitudinal section of the guinea-pig proximal colon showing many c-Kit immunoreactive ICC-SP (*arrows*) in the submucosal connective tissue space where a submucosal ganglion (*) is located. Submucosal border of the circular muscle layer is clearly demarcated by the c-Kit immunoreactivity of ICC-SMP (*arrowheads*). *G* indicates a myenteric ganglion. *Bar* 80 µm. (Courtesy of Dr Tamada, Waseda University).

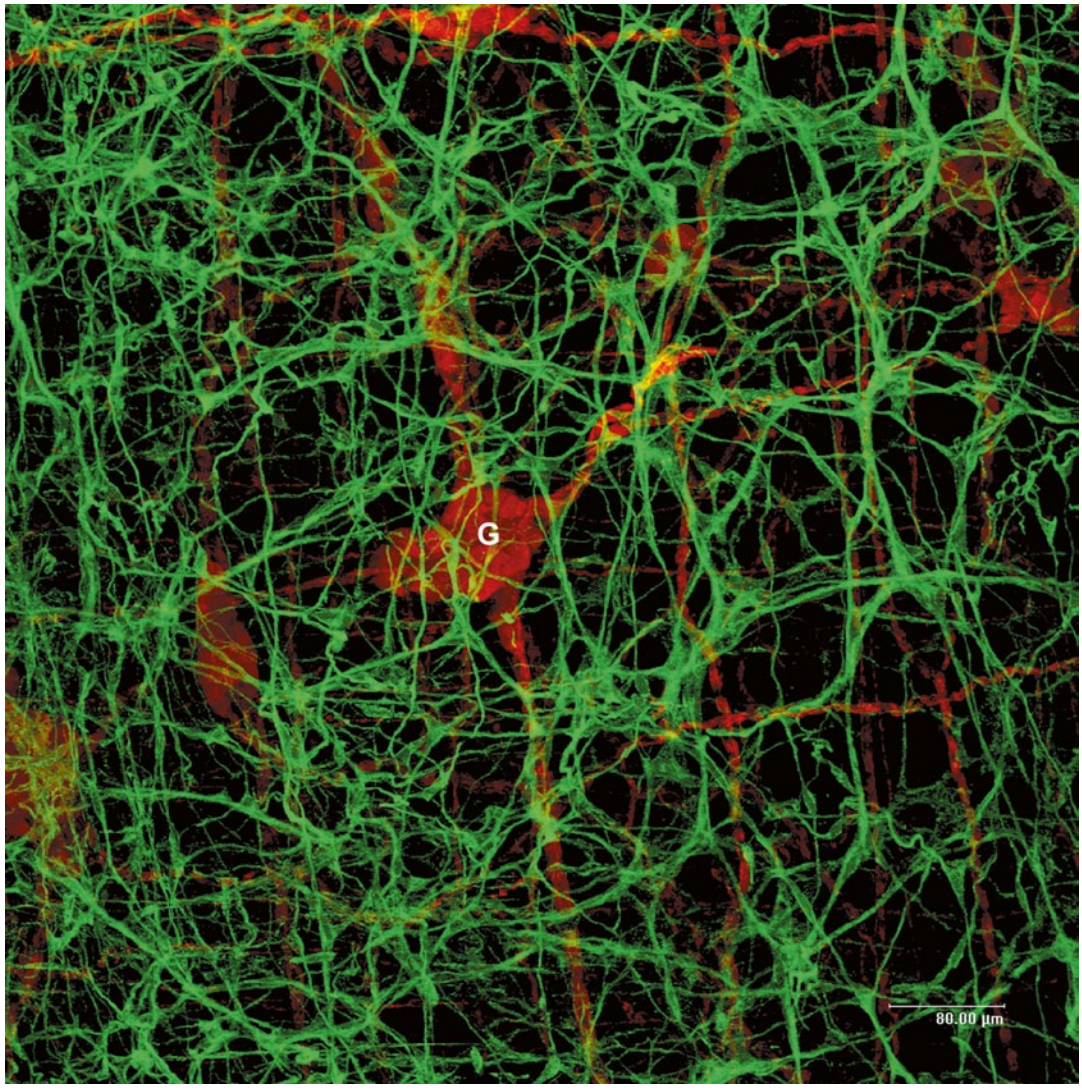

Fig. 8.5 ICC-SP observed in a stretch preparation of the guinea-pig proximal colon. Whole mount stretch preparation of the guinea-pig proximal colon showing a dense network of ICC-SP (*green*) over the submucosal ganglion (*red*) (*G*). *Bar* 80 µm. (Reproduced from Tamada and Komuro [84] with permission of the publisher).

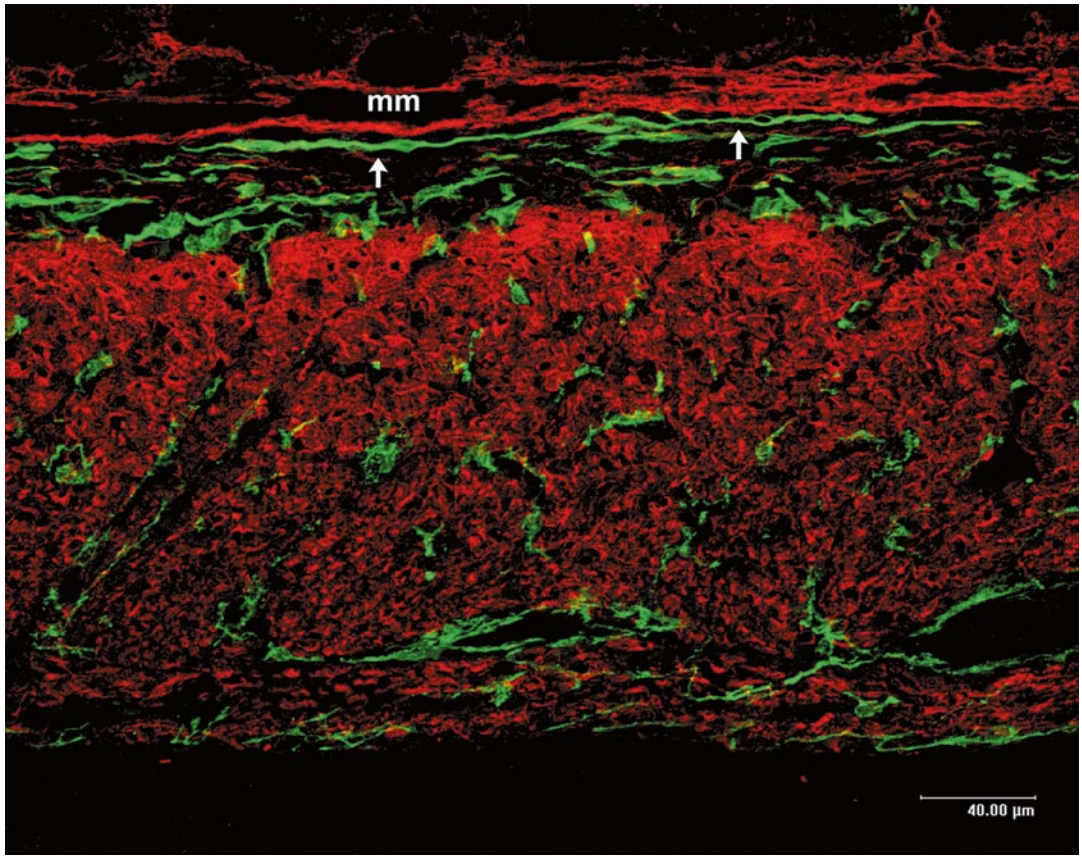

Fig. 8.6 ICC-SP located near the muscularis mucosae in the guinea-pig proximal colon. A longitudinal section of the guinea-pig proximal colon stained with c-Kit (*green*) and α-smooth muscle actin (*red*) immunohistochemistry. ICC-SP (*arrows*) are located in close vicinity to the muscularis mucosae (mm). *Bar* 40 µm. (Courtesy of Dr Tamada, Waseda University).

Part II

Ultrastructural Demonstration of ICC and Allied Cells

Ultrastructural Demonstration of ICC

9

ICC are characterized by such ultrastructural features as the presence of numerous mitochondria, abundant intermediate filaments, moderately developed Golgi apparatus, granular and smooth endoplasmic reticulum, close contacts with nerve varicosities and formation of gap junctions with each other and with smooth muscle cells. However, ICC show a certain range of morphological heterogeneity ranging from features similar to fibroblasts to those specific to smooth muscles cells such as caveolae, a basal lamina and subsurface cisterns, depending on their anatomical location and species. Indeed an early ultrastructural study described ICC-DMP of the dog small intestine as "hybrid cells" [40].

ICC are classified into three types. On one hand, Type 1 ICC are the least like muscle cells and the most like fibroblasts, while on the other hand, Type 3 are the most similar to smooth muscle cells. Type 2 ICC have an intermediate character (Table 9.1).

Table 9.1 Three types of ICC classified by their ultrastructural features. All types of ICC are positive for c-Kit immunoreactivity. (Modified from Komuro [37])

ICC type	Basal lamina	Caveolae	Gap junctions	Intermediate filaments	Mitochondria	Nerve contacts
Type 1 ICC (least like smooth muscle cells)	–	+–	++	++	++	++
Type 2 ICC (intermediate type)	+–	++	++	++	++	++
Type 3 ICC (most like smooth muscle cells)	++	++	++	++	++	++

Abundance: (++) present or numerous; (+/-) fuzzy or few; (-) absent.

T. Komuro, *Atlas of Interstitial Cells of Cajal in the Gastrointestinal Tract,*
DOI 10.1007/978-94-007-2917-9_9, © Springer Science+Business Media B.V. 2012

9.1 Ultrastructural Characteristics of ICC

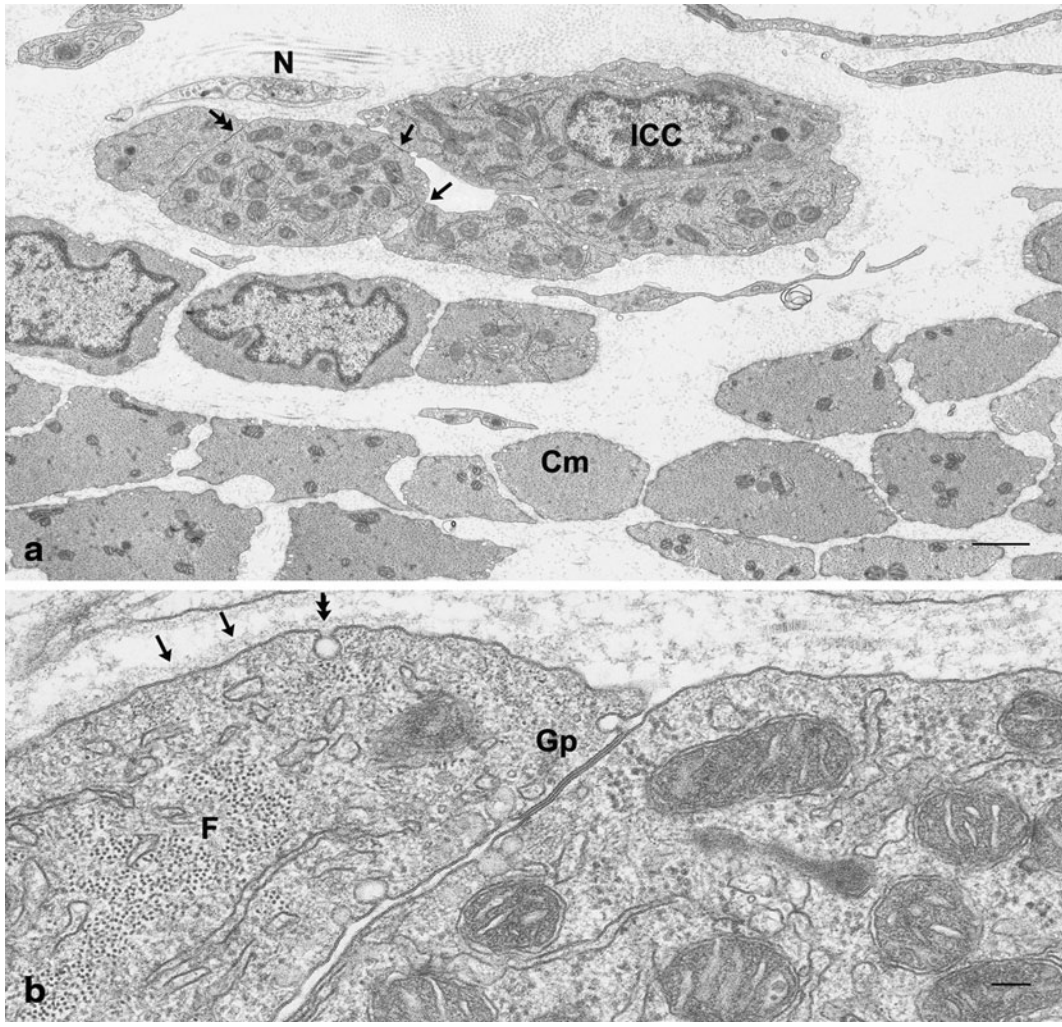

Fig. 9.1 **a** Cytoplasm and the cell membrane (I). **a** ICC-SM (*ICC*) located at the submucosal border of the circular muscle layer (*Cm*) of the guinea-pig gastric antrum. This type of cell has typical ultrastructural features of Type 3 ICC and is characterized by the presence of many mitochondria and large gap junctions (*arrow* and *double-headed arrow*). Cisterns of glandular endoplasmic reticulum are also observed in the perinuclear cytoplasm. Nerve fibres (*N*) are found in their close vicinity. ×9,600. *Bar* 1 μm. (Reproduced from Komuro [54] with permission of the publisher). **b** Higher magnification of a part of **a** (surrounding area of *double-headed arrow*) showing caveolae (*double-headed arrow*), basal lamina (*arrows*), cross section of the intermediate filaments (*F*) and a gap junction (*Gp*). ×62,000. *Bar* 0.1 μm.

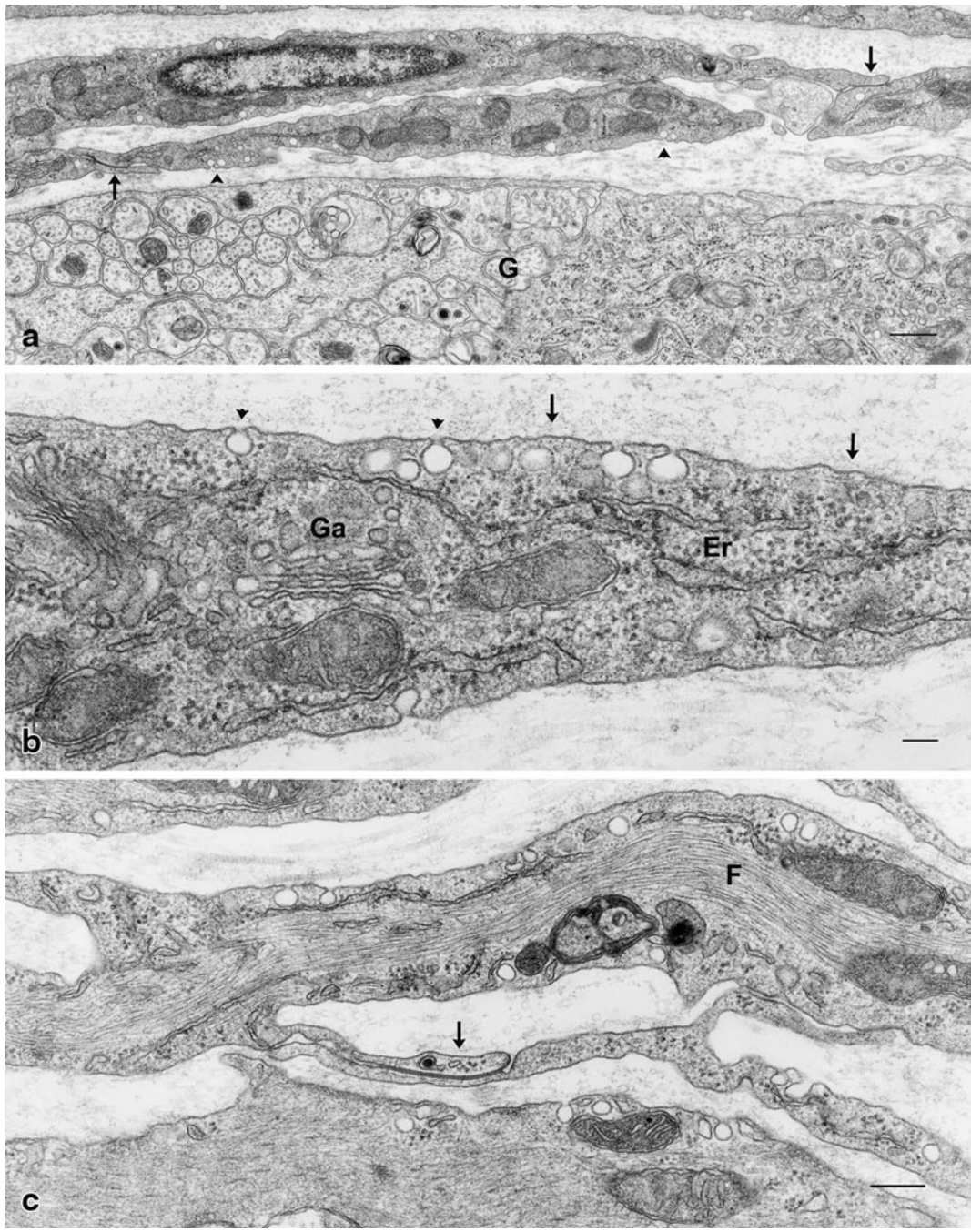

Fig. 9.2 Cytoplasm and the cell membrane (II). **a** ICC-MP located over the myenteric ganglion (*G*) of the mouse pylorus which form gap junctions (*arrows*) with the processes of the same type of cells even though the cytoplasm of those cells shows a close similarity to fibroblasts. Many caveolae are also observed along the cell membrane (*arrow heads*). ×8,600. *Bar* 1 μm (Figure 9.2a, c: Reproduced from Komuro et al. [74] with permission of the publisher). **b** A cell process of ICC-MP of the mouse stomach. The cytoplasm contains granular endoplasmic reticulum (*Er*) and Golgi apparatus (*Ga*), but also has caveolae (*arrow heads*) and basal lamina (*arrows*) along the cell membrane. Cisterns of the granular endoplasmic reticulum are not dilated unlike those often seen in the fibroblasts. ×63,000. *Bar* 0.1 μm (Reproduced from Komuro [54] with permission of the publisher). **c** A bundle of intermediate filaments (*F*) found in the cell process of ICC-MP in the mouse stomach. A gap junction is formed between thin processes (*arrow*). ×56,000. *Bar* 0.2 μm.

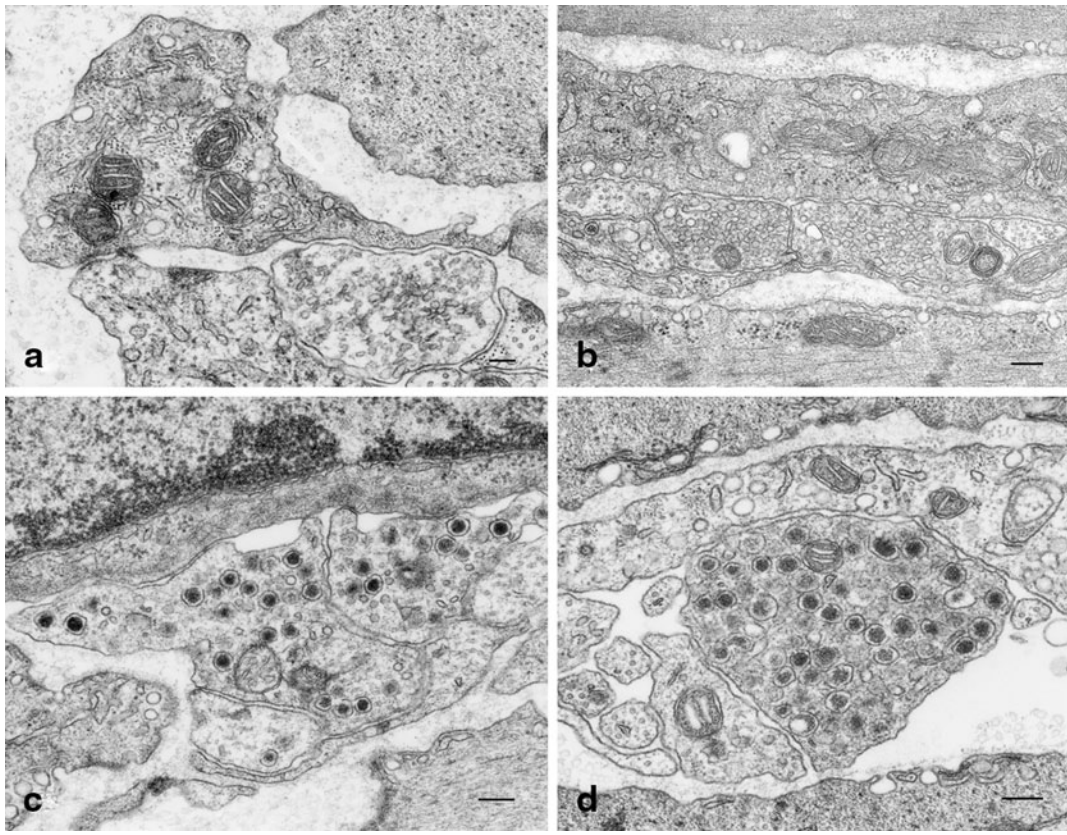

Fig. 9.3 Close contacts with nerve varicosities. **a** An axon varicosity containing clear flat vesicles closely adjacent to the process of ICC-SM in the rat stomach. ×40,000. *Bar* 1 μm (Reproduced from Mitsui and Komuro [68] with permission of the publisher). **b** An axon varicosity containing clear round vesicles closely adjacent to ICC-DMP in the rat small intestine. ×26,000. *Bar* 0.2 μm (Reproduced from Komuro and Seki [82] with permission of the publisher). **c** Close contact between an axon varicosity containing large cored vesicles and the cell body of ICC-MP in the mouse stomach. ×29,000. *Bar* 0.2 μm (Reproduced from Komuro et al. [74] with permission of the publisher). **d** Close contact between an axon varicosity containing large cored vesicles and ICC-DMP of the mouse small intestine. ×35,000. *Bar* 0.2 μm (Courtesy of Dr. Horiguchi, Fukui University).

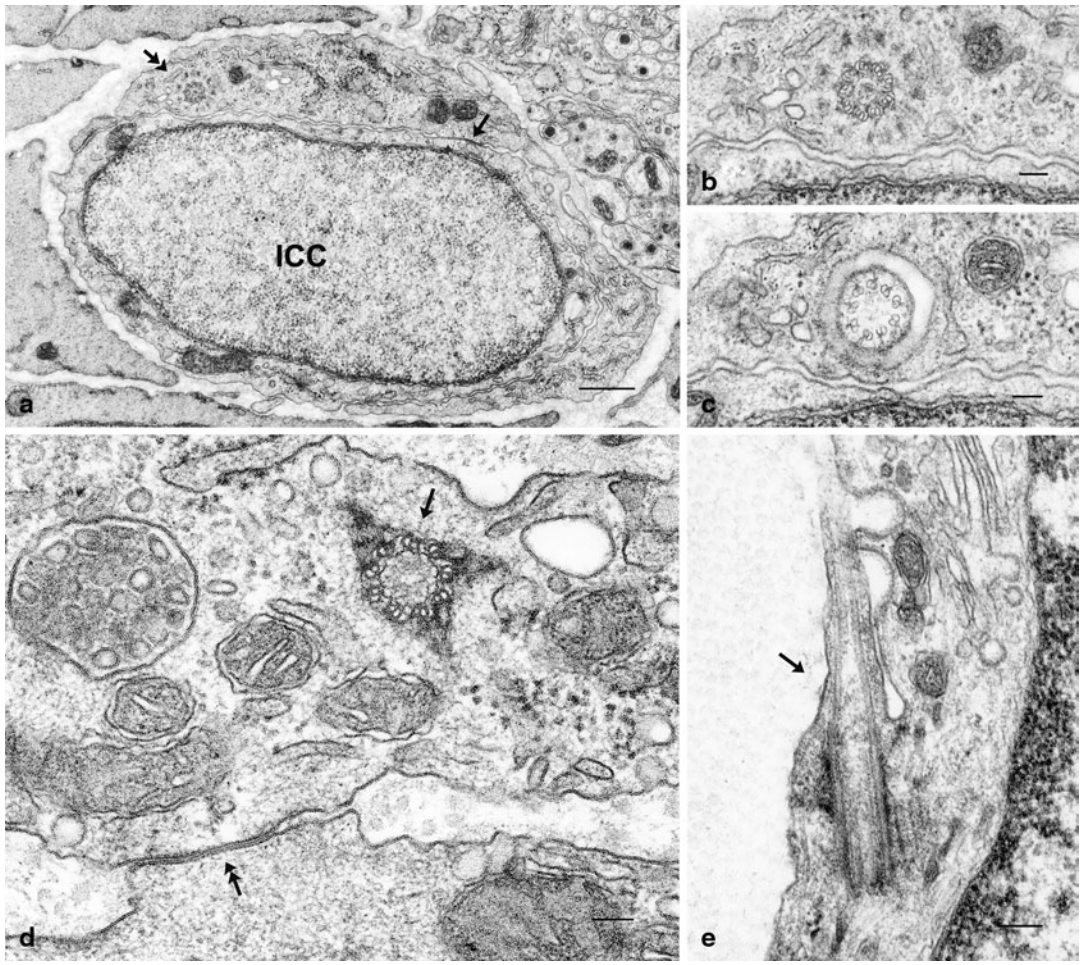

Fig. 9.4 Cilia and basal bodies. **a** ICC-CM (*ICC*) and a process of the same cell type in the guinea-pig colon are connected with each other with a gap junction (*arrow*). The process contains a basal body of cilium (*double-headed arrow*). Interestingly, ICC located in the connective tissue space often have cilia and the basal bodies. However, the frequent observations of cilia throughout every subtype of ICC suggest that cilia are one of the characteristic features of ICC. ×18,000. *Bar* 0.5 μm. **b** Higher magnification of the basal body indicated by double-headed arrow in **a**. ×50,000. *Bar* 0.1 μm. **c** A neighbouring section of **b** showing a cross section of the cilium. ×50,000. *Bar* 0.1 μm (Fig. 9.4a–c: Courtesy of Dr. Ishikawa, Waseda University). **d** A part of the cytoplasm of ICC-DMP in the rat small intestine containing a basal body (*arrow*). A gap junction is also observed between this cell and the neighboring cell (*double-headed arrow*). ×70,000. *Bar* 0.1 μm. **e** A longitudinal section of the cilium found in ICC-SS in the guinea-pig colon (*arrow*). ×75,000. *Bar* 0.1 μm (Courtesy of Dr. Tamada, Waseda University).

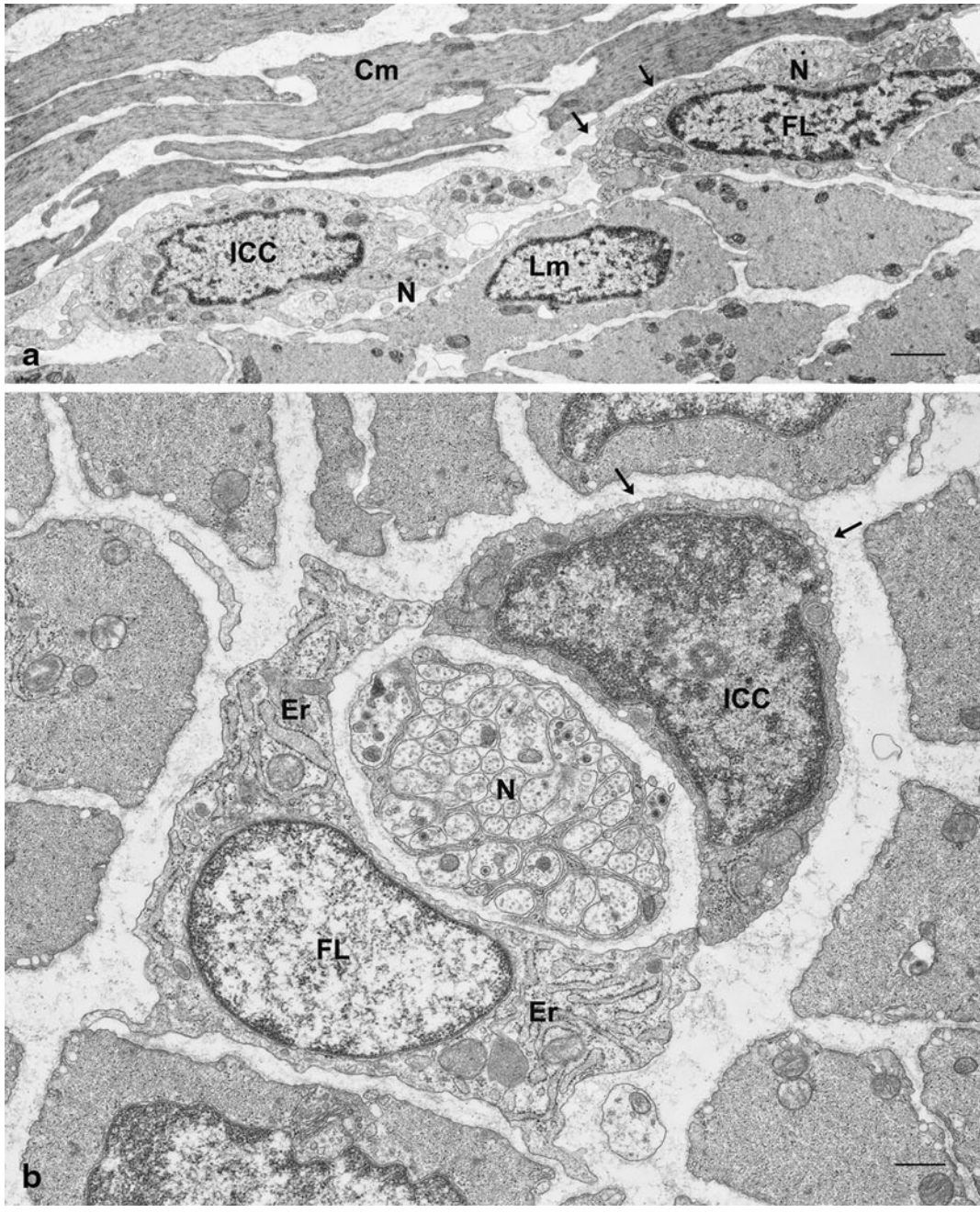

Fig. 9.5 Distinguishing ICC from other cell types (I). **a** ICC-MP (*ICC*) and fibroblast-like cell (*FL*) found in the region between the circular (*Cm*) and longitudinal (*Lm*) muscle layers of the rat small intestine. ICC is characterized by the presence of many mitochondria, while the fibroblast-like cell contains well-developed granular endoplasmic reticulum with dilated cisterns (*arrows*). Nerve fibers (*N*) are found in close vicinity to both types of cells. ×9,800. *Bar* 1 μm (Reproduced from Komuro et al. [15] with permission of the publisher). **b** ICC-CM (*CM*) and fibroblast-like cell (*FL*) associated with a nerve bundle in the circular muscle layer of the rat colon. The ICC is characterized by electron-dense cytoplasm and caveolae along the cell membrane (*arrows*), while the fibroblast-like cell shows well-developed granular endoplasmic reticulum (*Er*) in the cytoplasm and no caveolae along the cell membrane. ×18,000. *Bar* 0.5 μm (Reproduced from Komuro [30] with permission of the publisher).

The electron density of the cytoplasm is often discussed in relation to the identification of ICC, but it seems to be an unreliable criterion, as can be seen from the two types of cells in a and b.

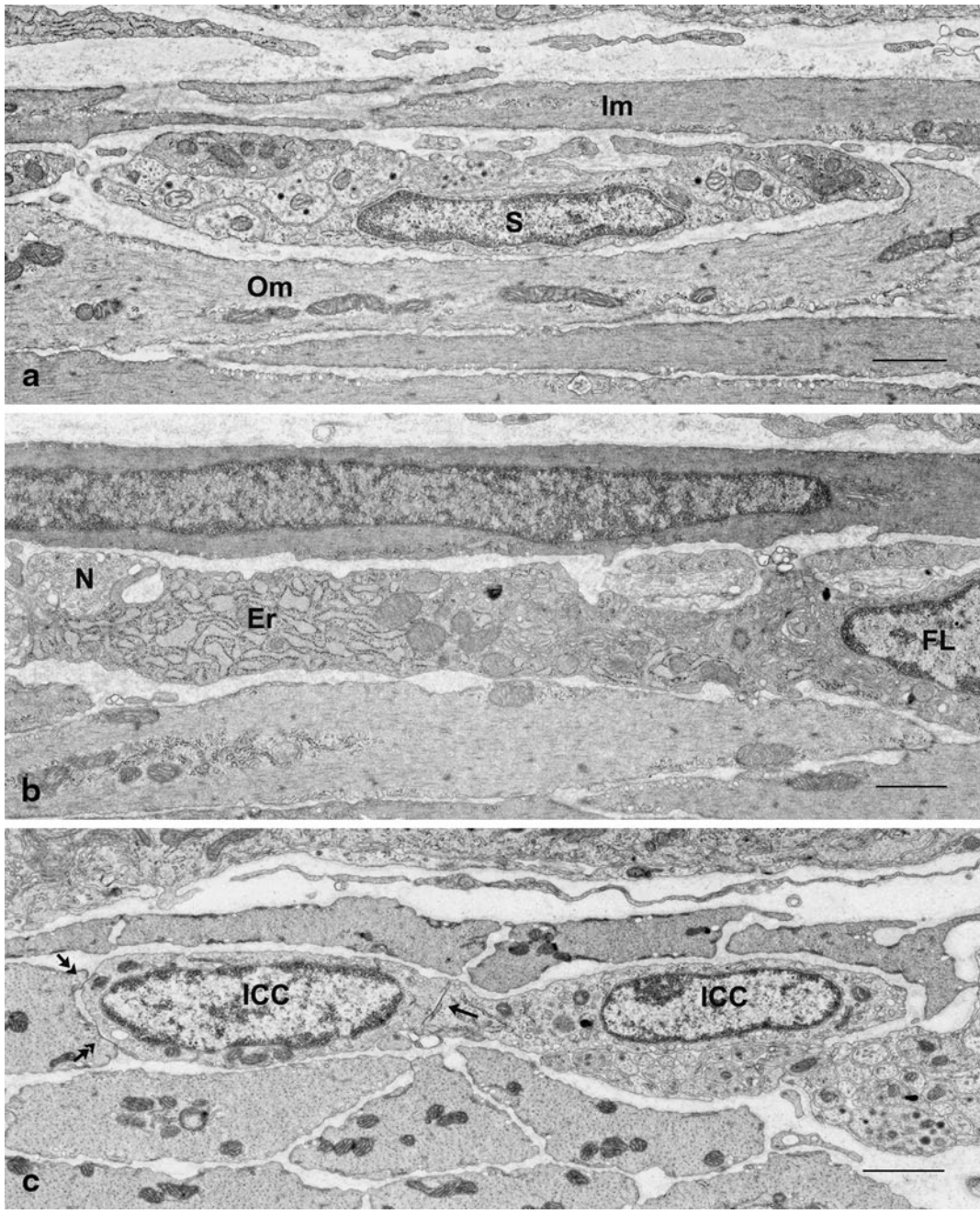

Fig. 9.6 Distinguishing ICC from other cell types (II). **a** Schwann cell (*S*) located in the region of the deep muscular plexus between the inner (*Im*) and outer (*Om*) sublayers of the circular muscle in the rat small intestine. It closely holds many nerve fibres by the thin processes. (Note, the poor cytoplasm in the perinuclear region). ×13,000. *Bar* 1 μm (Reproduced from Komuro and Seki [82] with permission of the publisher). **b** Fibroblast-like cell (*FL*) found in the region of the deep muscular plexus of the rat small intestine. Dilated cisterns of granular endoplasmic reticulum (*Er*) contain moderate electron dense materials. An axon varicosity containing many synaptic vesicles (*N*) is lodged in a surface indentation of the cell. ×13,000. *Bar* 1 μm (Reproduced from Komuro and Seki [82] with permission of the publisher). **c** ICC-DMP (*ICC*) of the mouse small intestine. These cells are connected by a gap junction with each other (*arrow*) and with the smooth muscle cell (*double-headed arrow*). Large gap junctions are the only reliable criteria in this profile of the cell that otherwise has few organelles. ×13,000. *Bar* 1 μm. (Reproduced from Komuro [54] with permission of the publisher).

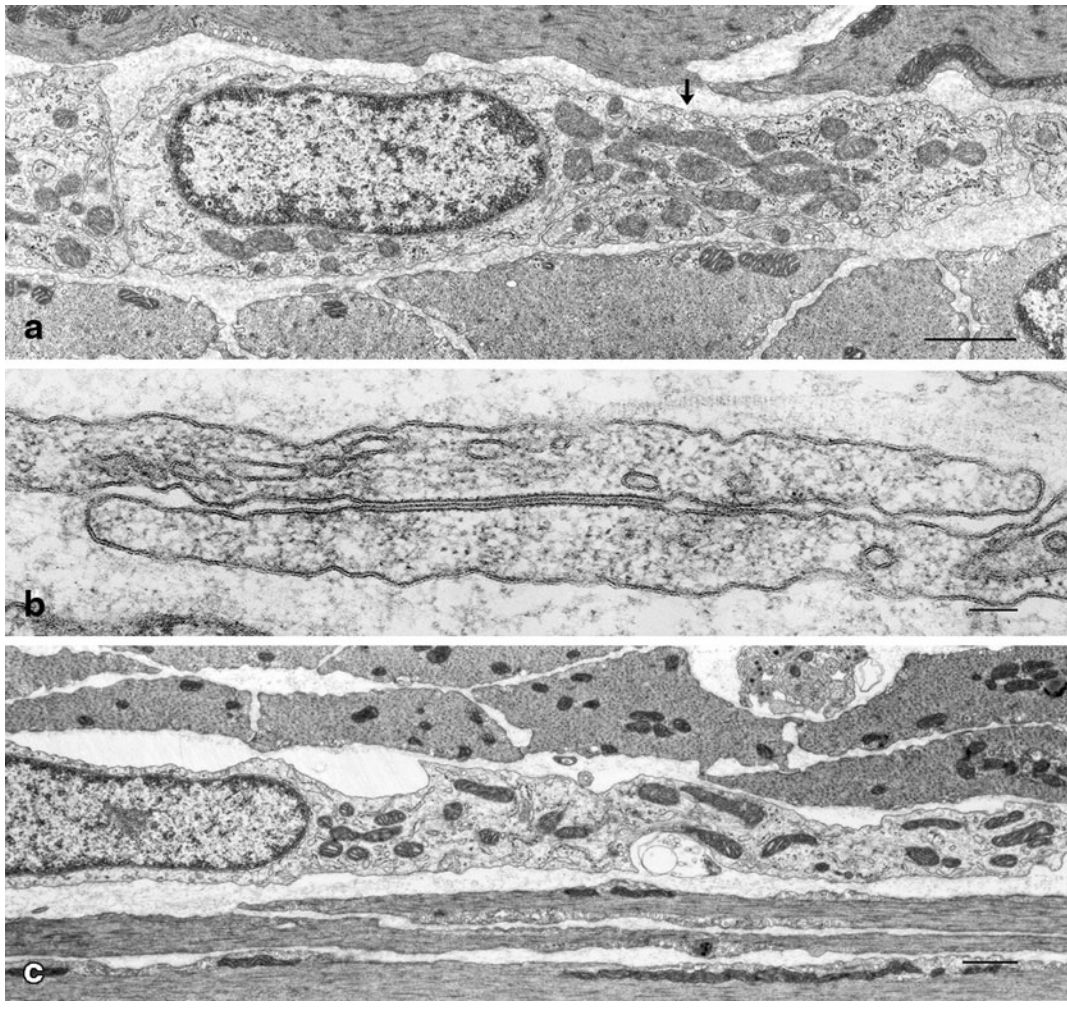

Fig. 9.7 ICC-MP of the small intestine. **a** ICC-MP of the rat small intestine belong to Type 1 ICC and are characterized by abundant mitochondria embedded in the electron-lucent cytoplasm. Caveolae are occasionally observed (*arrow*). ×16,000. *Bar* 1 μm (Reproduced from Komuro [50] with permission of the publisher). **b** A typical large gap junction between the slender processes of ICC-MP of the rat small intestine. ×1,65,000. *Bar* 0.05 μm (Reproduced from Horiguchi and Komuro [70] with permission of the publisher). **c** ICC-MP of the mouse small intestine which show very similar features to the rat small intestine described above. ×8,800. *Bar* 1 μm (Reproduced from Komuro et al. [74] with permission of the publisher).

9.2 Ultrastructural Features of ICC-MP

ICC-MP show some variations depending on the organ and the species in which they are found, and thus a specific set of ultrastructural features cannot be generalized. Important criteria of ICC distinguishing these cells from fibroblasts, such as the basal lamina and caveolae, are not always found in ICC-MP, though abundant mitochondria in the cytoplasm and large gap junctions are common. For example, ICC-MP of the mouse stomach described above (Fig. 9.2a–c) show Type 3 ultrastructural features (most muscle-like features), while ICC-MP of the mouse small intestine have the least muscle-like features described below (Fig. 9.7c). In this respect, ICC-MP require careful observation to correctly identify and interpret them.

9.3 Ultrastructural Features of ICC-CM and ICC-LM

ICC-CM and ICC-LM are prominent in the stomach and colon but not in the small intestine in the laboratory rodents including mice, rats and guinea-pigs, as already shown by immunohistochemical preparations. ICC-CM and ICC-LM of the stomach and colon have similar ultrastructural features, or Type 2 intermediate characteristics.

These cells connect with neighbouring smooth muscle cells via many large gap junctions and often show close contacts with nerve terminals containing many synaptic vesicles.

9.4 Ultrastructural Features of ICC-DMP

Ultrastructural features of ICC-DMP do not show major differences among the species and these cells belong to Type 3 most muscle-like ICC. A basal lamina and numerous caveolae are observed along the cell membrane. Subsurface cisterns of smooth endoplasmic reticulum can be found immediately beneath the cell membranes. Intermediate filaments are abundant in the cytoplasmic processes.

The most conspicuous feature of ICC-DMP is the frequent occurrence of large gap junctions that interconnect these cells with each other and also with smooth muscle cells. Their gap junctions with muscle cells are mainly formed with those of the outer subdivision, but some gap junctions with the muscle cells of inner sublayer are also observed. ICC-DMP have close contacts with nerve varicosities containing accumulations of synaptic vesicles. This means that ICC-DMP are intercalated between nerves and smooth muscle cells. Therefore, it is quite possible that ICC-DMP can act as an accessory route for neuromuscular transmission, as originally suggested by Cajal.

Two types of ICC-DMP have been described in the rat and guinea-pig below.

The functional significance of gap junctions in ICC-DMP can be evaluated from evidence that the percentage of the total cell area occupied by gap junctions is 1.3% in rats [42] and 4% in guinea-pigs [43]. These values are about 6 and 20 times greater respectively than the corresponding percentage area (0.2%) occupied by gap junctions on smooth muscle cells of the guinea-pig intestine [44]. The presence of these highly developed gap junctions also seem to be consistent with the notion that the well organized network of ICC-DMP acts as an impulse-conducting system analogous to that in the heart.

9.5 Ultrastructural Features of ICC-SMP

ICC-SMP of the colon are observed at the interface between the submucosa and the circular muscle layer. They have similar features to ICC-DMP and belong to Type 3 most muscle-like ICC. They are characterized by the presence of a basal lamina, caveolae and many mitochondria. They have gap junctions that interconnect with the same type of cells and connect with smooth muscle cells. Intermediate filaments are particularly abundant in the small processes. They often have close contacts with nerve varicosities containing many synaptic vesicles.

A specialized pacemaker function has been proposed in the colon, with ICC-SMP primarily responsible for generating the slow waves, and ICC-MP acting as secondary pacemaker cells described above. However, it remains to be elucidated as to the reason why ICC-SMP are the primary pacemaker cells in the colon.

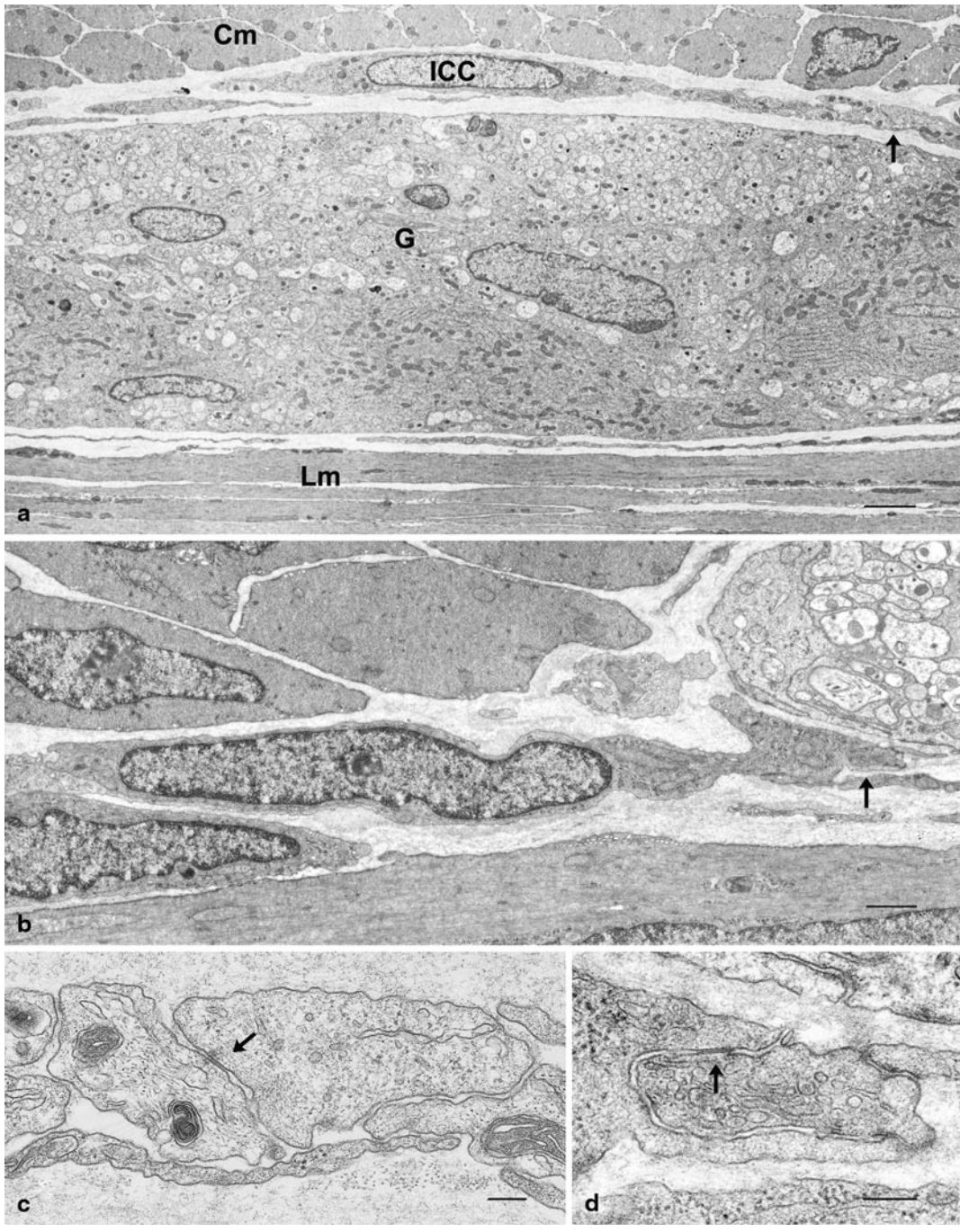

Fig. 9.8 ICC-MP of the small intestine and colon. **a** ICC-MP (*ICC*) of the guinea-pig small intestine located along the myenteric ganglion (*G*) between the inner circular (*Cm*) and outer longitudinal (*Lm*) muscle layers. ICC-MP of the guinea-pig small intestine belong to the least muscle-like cell type of ICC (Type 1) and at first glance resemble fibroblasts. But they contains bundle of intermediate filaments and form a gap junction at their tips (*arrow* and **c**). ×4,800. *Bar* 2 μm. **b** A ICC-MP of the rat colon that also shows similar cytoplasmic features to fibroblasts, but it forms a gap junction with the same type of cell (*arrow* and **d**). ×9,000. *Bar* 1 μm (Courtesy of Dr. Ishikawa, Waseda University). **c** Higher magnification of the region with arrow in **a**, showing the gap junction (*arrow*) observed between fine processes of ICC-MP. ×35,000. *Bar* 0.2 μm (Reproduced from Komuro et al. [15] with permission of the publisher). **d** Higher magnification of the gap junction (*arrow*) indicated by arrow in **b**. ×50,000. *Bar* 0.2 μm.

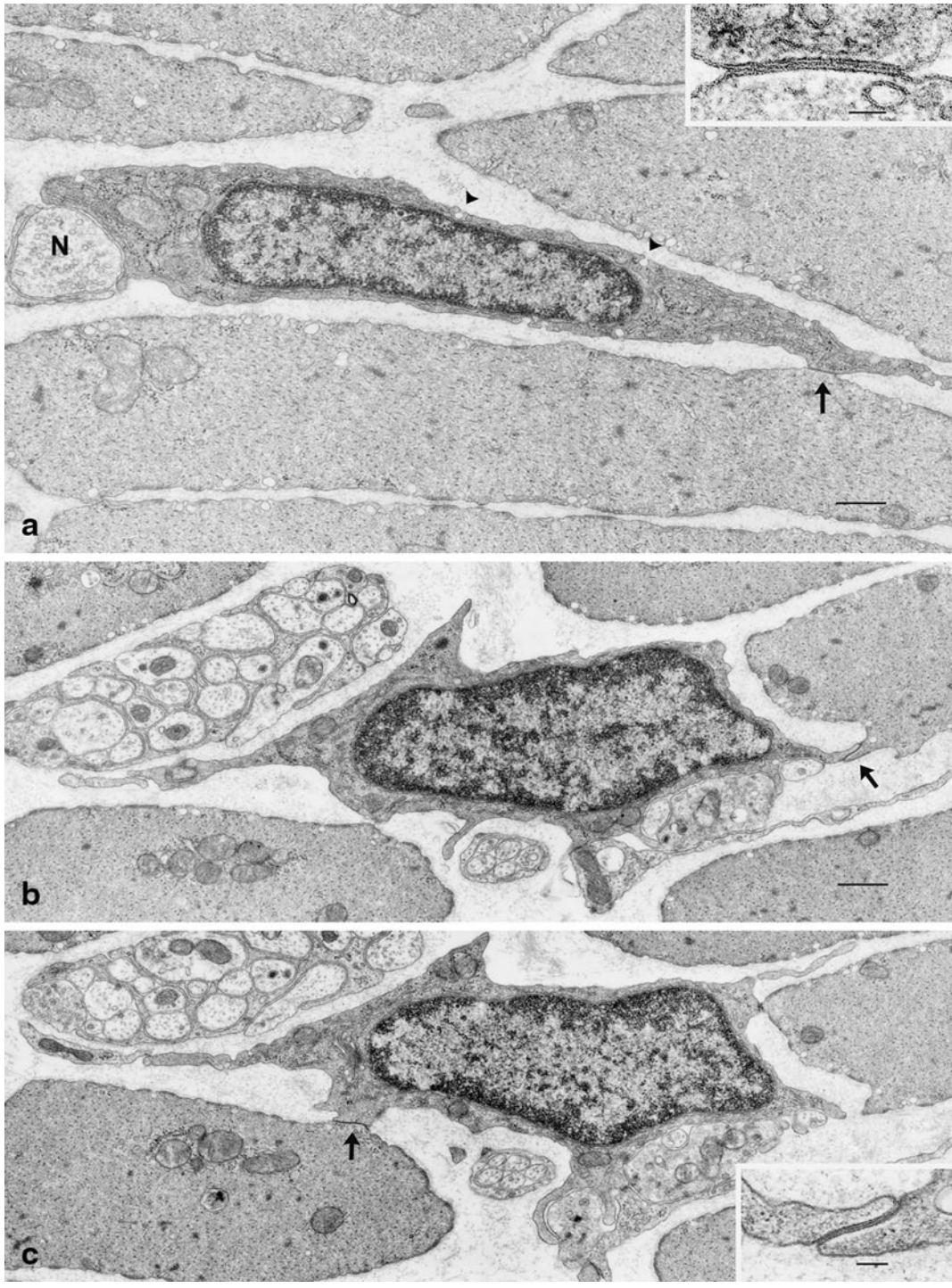

Fig. 9.9 ICC-CM intercalated between the nerve and muscles. **a** ICC-CM of the rat stomach, which show a close contact with a nerve terminal (*N*) on one hand and form a gap junction (*arrow*) with a smooth muscle cell on the other. Caveolae are indicated by *arrow-heads*. ×18,000. *Bar* 0.5 μm. *Inset* Higher magnification of the gap junction indicated by an *arrow*. ×66,000. *Bar* 0.1 μm (Reproduced from Ishikawa et al. [83] with permission of the publisher). **b**, **c** Serial sections of ICC-CM in the rat stomach showing frequent connections by gap junctions with neighboring smooth muscle cells (*arrows*). ×18,000. *Bar* 0.5 μm. *Inset* The gap junction indicated by the *arrow* in **b**. ×56,000. *Bar* 0.1 μm (Reproduced from Komuro [30] with permission of the publisher)

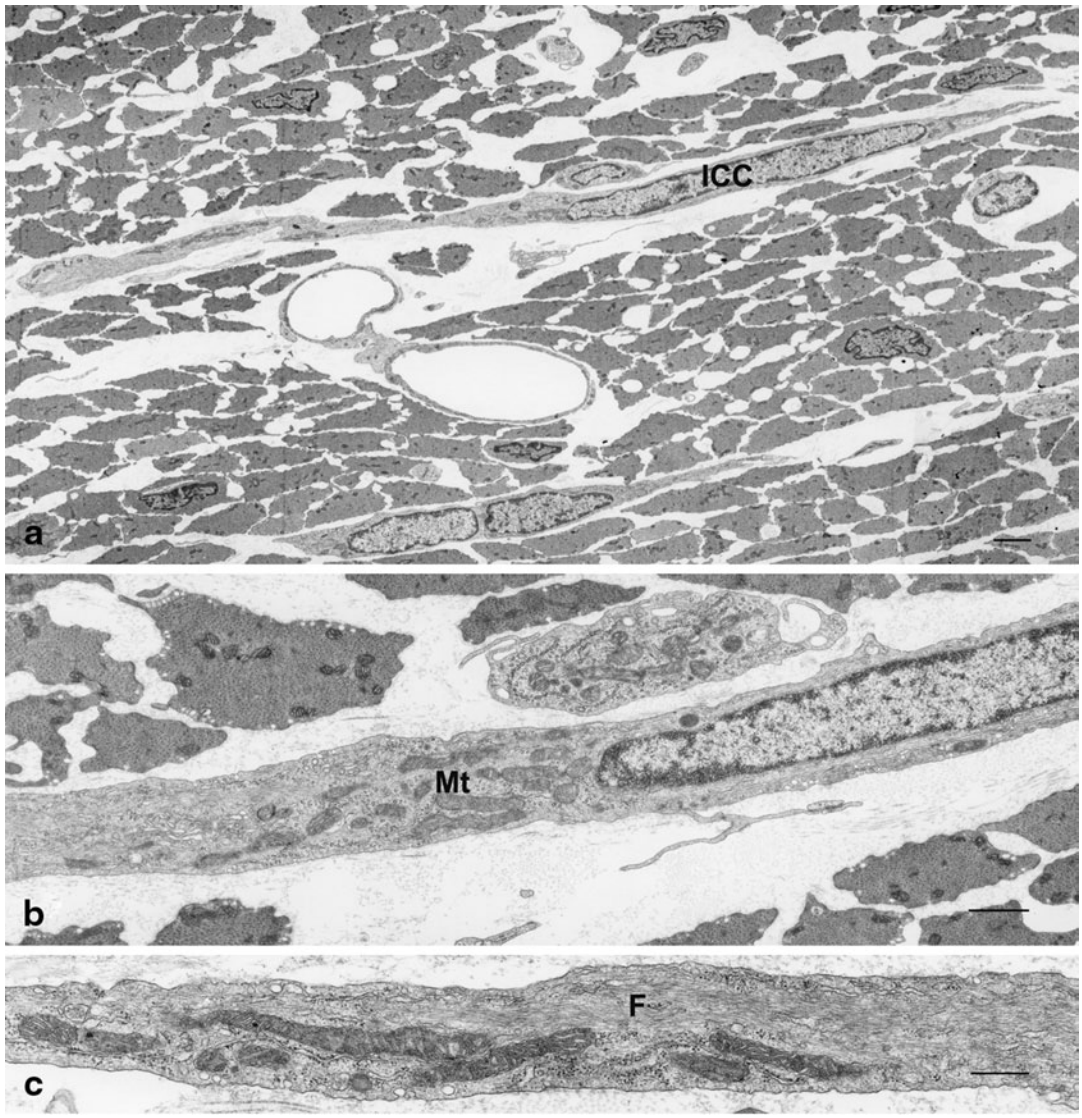

Fig. 9.10 ICC-CM in the rat stomach. **a** ICC found in the connective tissue septum in the circular muscle layer of the rat stomach. ×3,200. *Bar* 2 μm.

These cells are specially designated as ICC-SEP and are claimed to have different physiological significance, to transfer pacemaker depolarizations from ICC-MP to distant bundles of the circular muscle in the dog stomach [41]. **b** Higher magnification of the perinuclear cytoplasm of the same cell as **a** in a neighboring section characterized by many mitochondria (*Mt*). ×11,000. *Bar* 1 μm. **c** The further distal portion of the same cell as **a**, which is characterized by abundant intermediate filaments (*F*). ×19,000. *Bar* 0.5 μm (Reproduced from Mitsui and Komuro [68] with permission of the publisher).

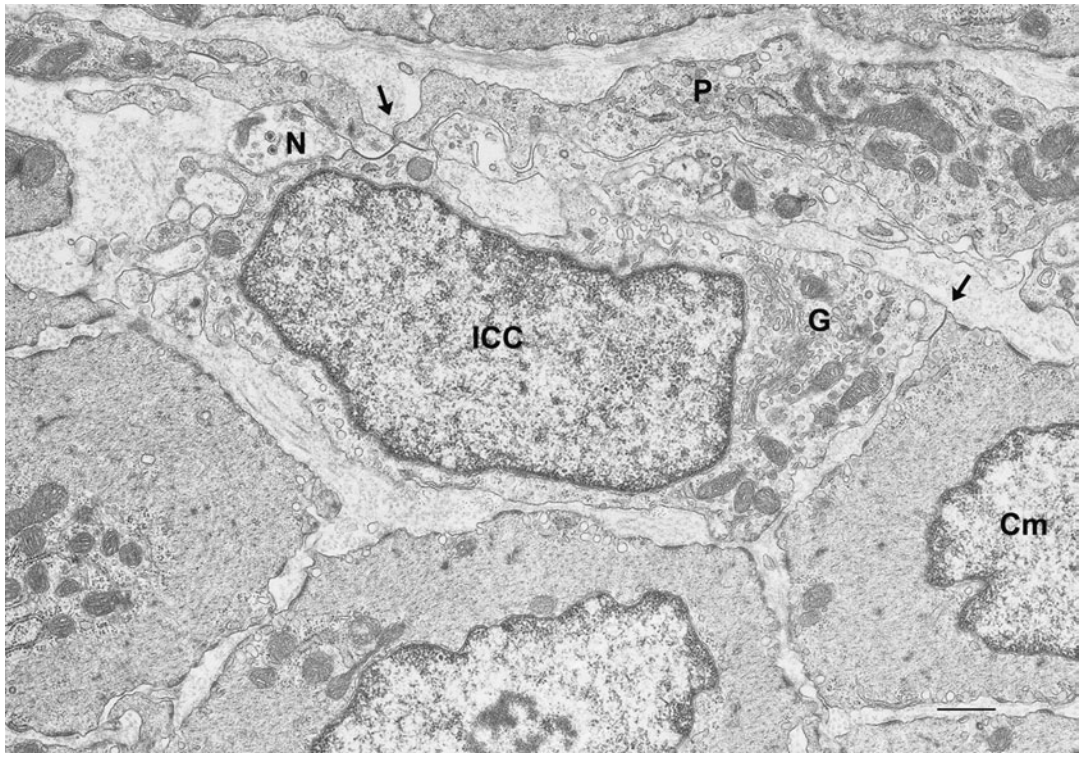

Fig. 9.11 Cross section of ICC-DMP of the rat small intestine. ICC-DMP (*ICC*) are characterized by electron-lucent cytoplasm and gap junctions (*arrows*) with processes of the same type of cell (*P*) containing many mitochondria and other gap junctions with the muscle cell of the circular layer (*Cm*). A nerve varicosity (*N*) is closely adjacent to the cell. Golgi apparatus (*G*) is located in the perinuclear region. ×18,000. *Bar* 0.5 μm (Reproduced from Komuro and Seki [82] with permission of the publisher).

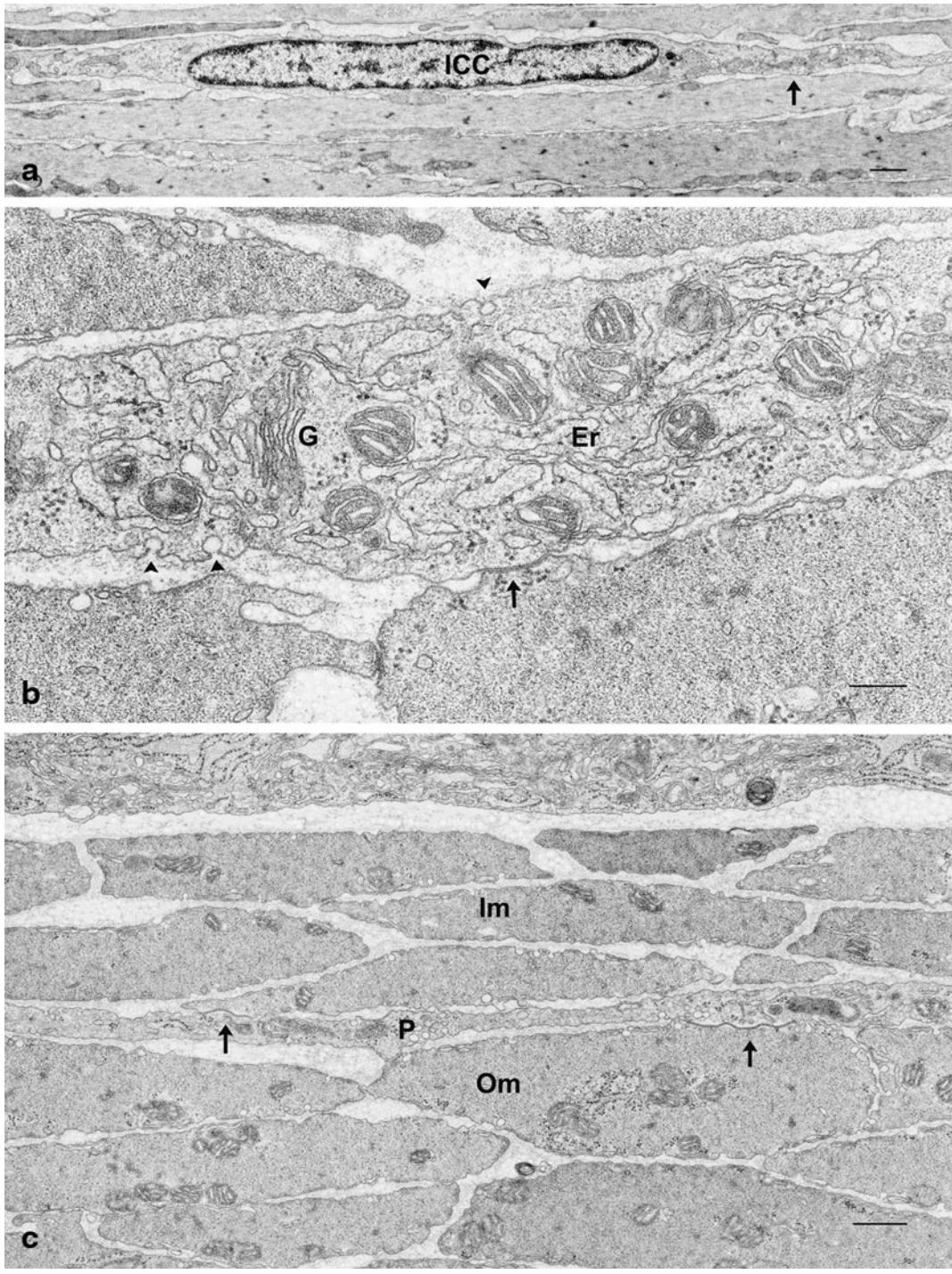

Fig. 9.12 Longitudinal section of ICC-DMP of the rat small intestine. **a** A slender cell body of an ICC-DMP (*ICC*) is located in the narrow space between the inner thin and outer thick circular muscle layers. It forms a gap junction with the adjacent muscle cell (*arrow*). ×7,000. *Bar* 1 μm. **b** The cytoplasm of an ICC-DMP of the rat small intestine, which is characterized by electron-lucent cytoplasm, caveolae (*arrowheads*), many mitochondria and formation of gap junction with the muscle cell (*arrow*). Golgi apparatus (*G*) and granular endoplasmic reticulum (*Er*) are also observed. ×46,000. *Bar* 0.2 μm. **c** A slender cell process (*P*) of an ICC-DMP forming gap junctions (*arrows*) with the muscle cells of inner (*Im*) and outer (*Om*) sublayers. ×19,000. *Bar* 0.5 μm (Reproduced from Komuro and Seki [82] with permission of the publisher).

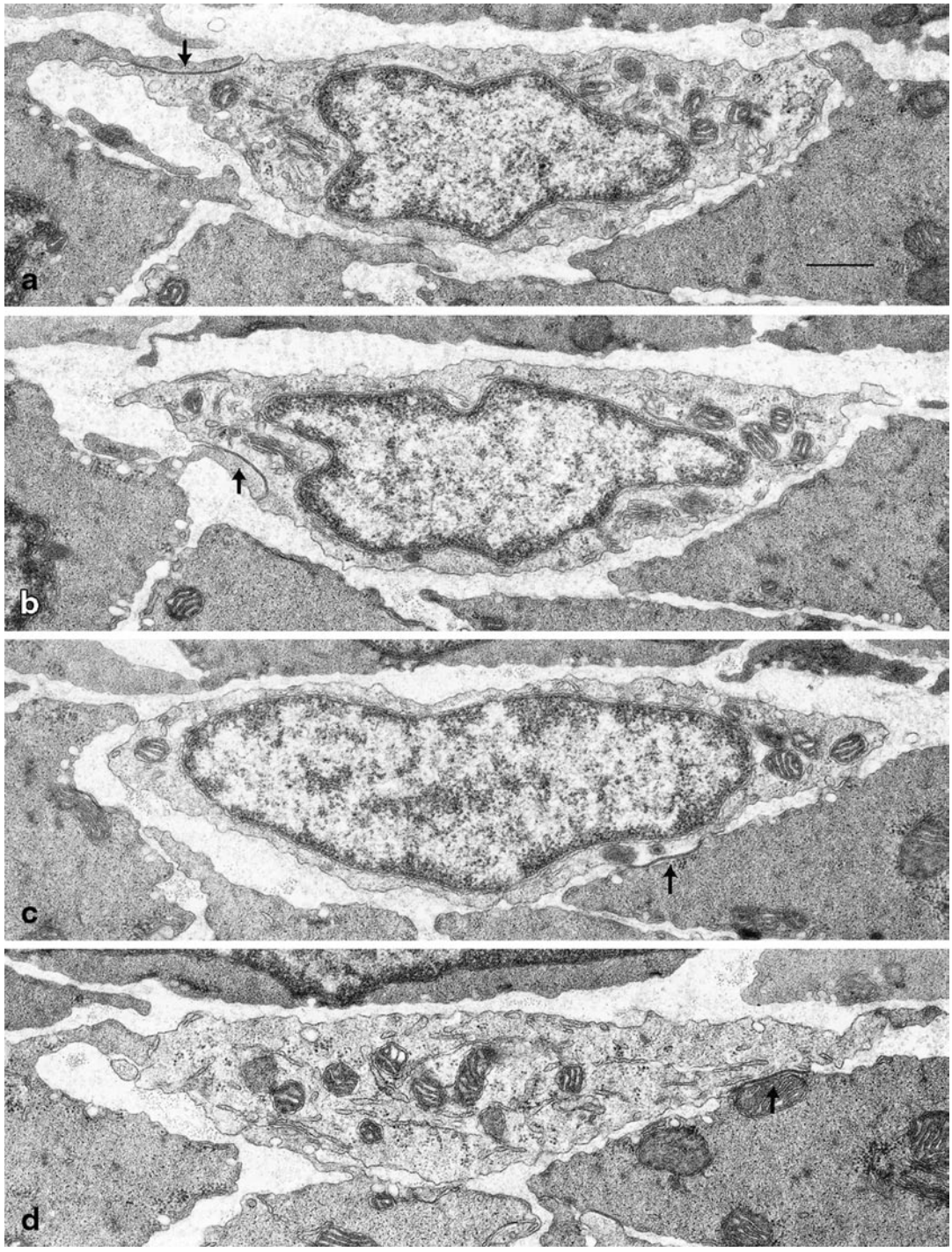

Fig. 9.13 Serial sections of ICC-DMP of the rat small intestine (**a–d**) showing how often a single cell of ICC-DMP forms gap junctions (*arrows*) with the adjacent smooth muscle cells. ×23,000. *Bar* 0.5 μm (Reproduced from Seki and Komuro [42] with permission of the publisher).

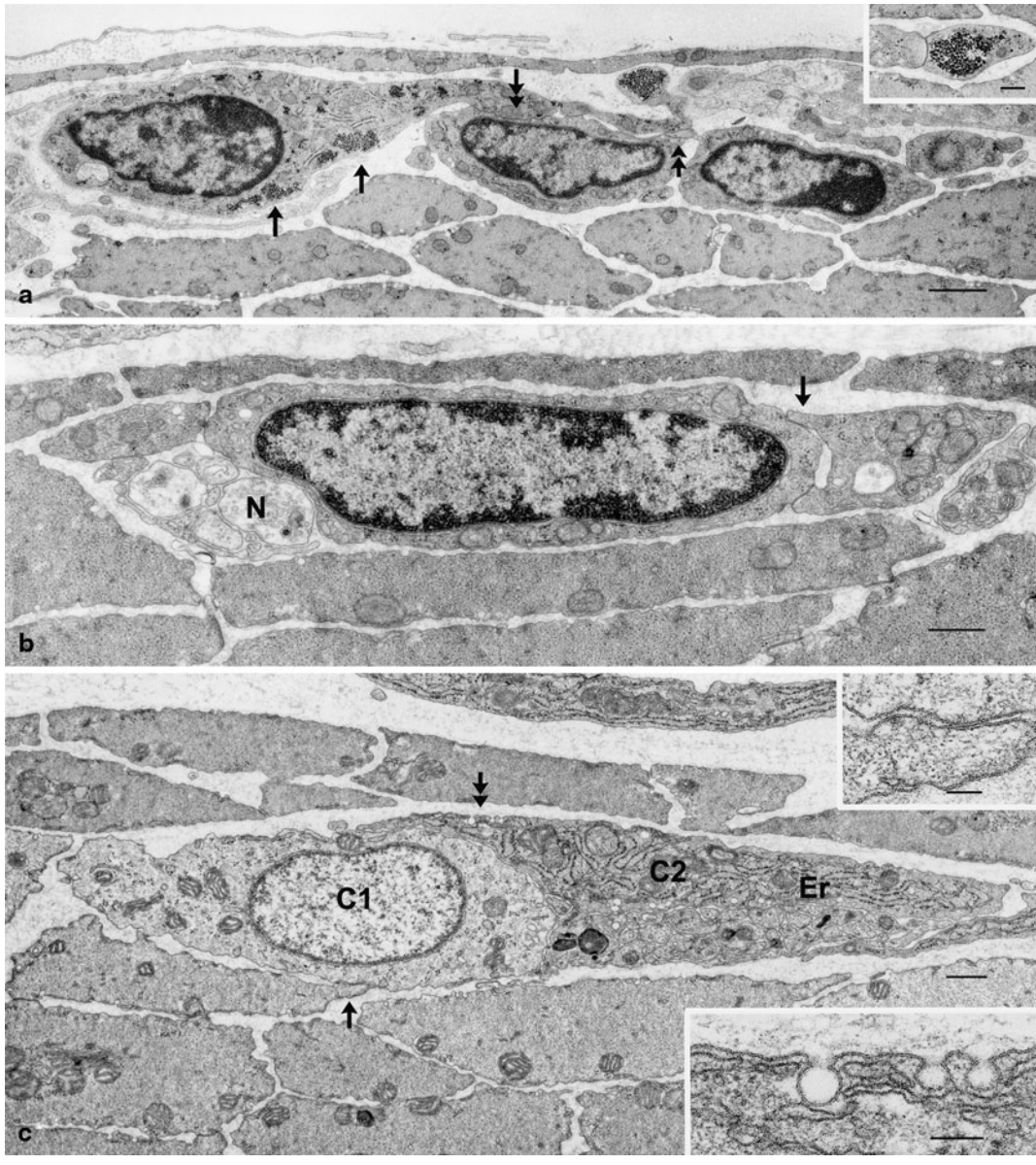

Fig. 9.14 Evidence potentially showing two subtypes of ICC-DMP. **a** A possible subtype of ICC-DMP in the guinea-pig small intestine, which is characterized by clusters of glycogen granules (*arrows*) and by forming gap junctions with the same type of cells (*double-headed arrow*). ×10,000. *Bar* 1 μm (Reproduced from Komuro et al. [15] with permission of the publisher). *Inset* Higher magnification of the small process containing glycogen granules and form a gap junction with the same type of the cell. *Bar* 0.5 μm. **b** Another subtype of ICC-DMP of the guinea-pig small intestine showing a gap junction with a process of the same type of cell containing many mitochondria (*arrow*) and close contact with a nerve varicosity containing many synaptic vesicles (*N*). ×18,000. *Bar* 0.5 μm (Reproduced from Komuro [30] with permission of the publisher). *These two types of cells are densely distributed in an alternate fashion in the space between the inner and outer sublayers of the circular muscle [43, 45]*. **c** Possible two types of ICC-DMP of the rat small intestine. One (*C1*) is characterized by electron-lucent cytoplasm and the other (*C2*) is characterized by electron-dense cytoplasm containing many cisterns of granular endoplasmic reticulum (*Er*). The arrow indicates a gap junction of the former cell and double-headed arrow indicate caveolae and basal lamina of the latter. ×15,000. *Bar* 0.5 μm. *Top inset* The gap junction indicated by the *arrow* ×60,000, *Bar* 0.1 μm; *Bottom inset* Caveolae and the basal lamina indicated by the double-headed arrow. ×90,000, *Bar* 0.1 μm (Reproduced from Seki and Komuro [48] with permission of the publisher).

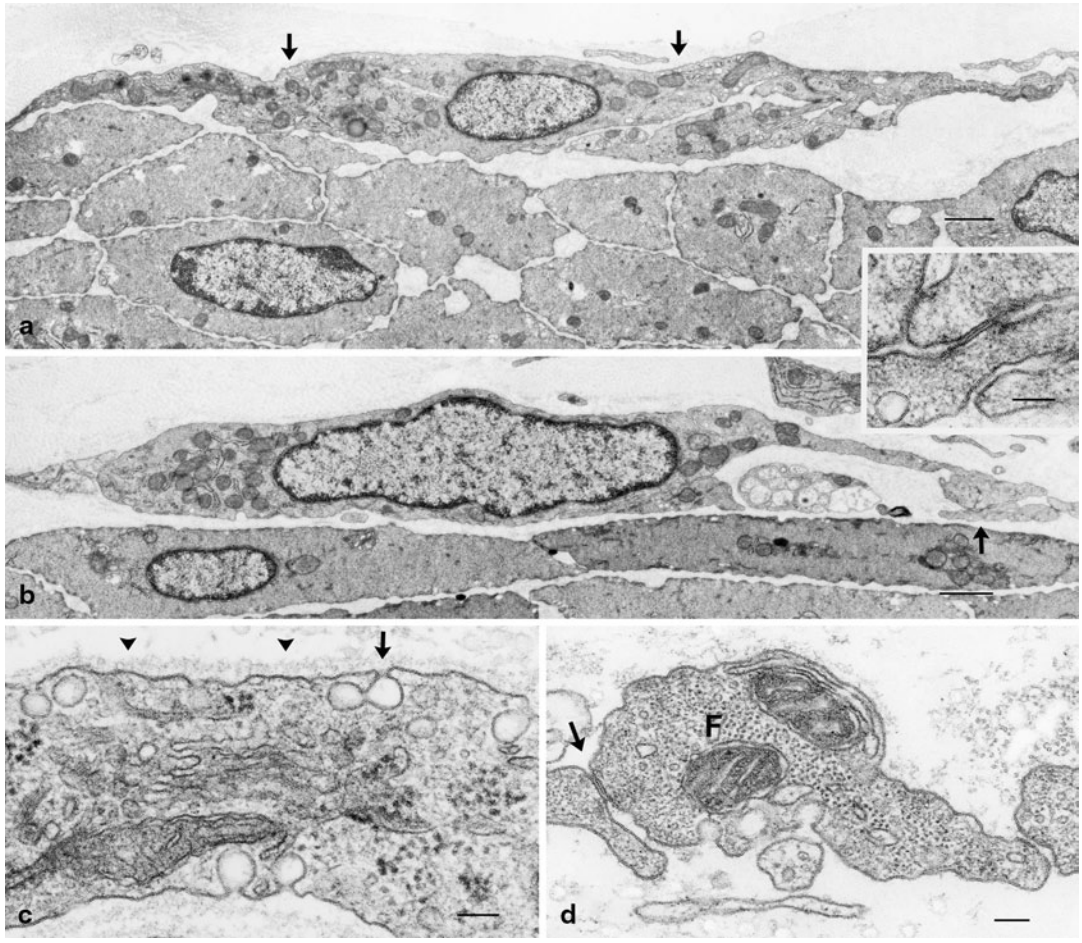

Fig. 9.15 ICC-SMP of the colon. **a** ICC-SMP at the submucosal border of the circular muscle layer of the guinea-pig colon. Many mitochondria and caveolae (*arrows*) are observed. ×8,200. *Bar* 1 μm (Reproduced from Komuro [30] with permission of the publisher). **b** ICC-SMP of the rat colon. This cell also contains many mitochondria and form gap junctions with the processes of the same type of cell (*arrow*) (Courtesy of Dr. Ishikawa, Waseda University). ×9,000. *Bar* 1 μm. *Inset* Higher magnification of the gap junction indicated by an *arrow* in **b**. ×70,000. *Bar* 0.1 μm. **c** Higher magnification of the process of the rat ICC-SMP showing the continuous basal lamina (*arrow heads*) and caveolae (*arrow*). ×68,000. *Bar* 0.1 μm. **d** Process of ICC-SMP of the guinea-pig colon showing abundant intermediate filaments (*F*) and gap junction (*arrow*). ×57,000. *Bar* 0.1 μm (Reproduced from Ishikawa and Komuro [73] with permission of the publisher).

9.6 Ultrastructural Features of ICC-SP

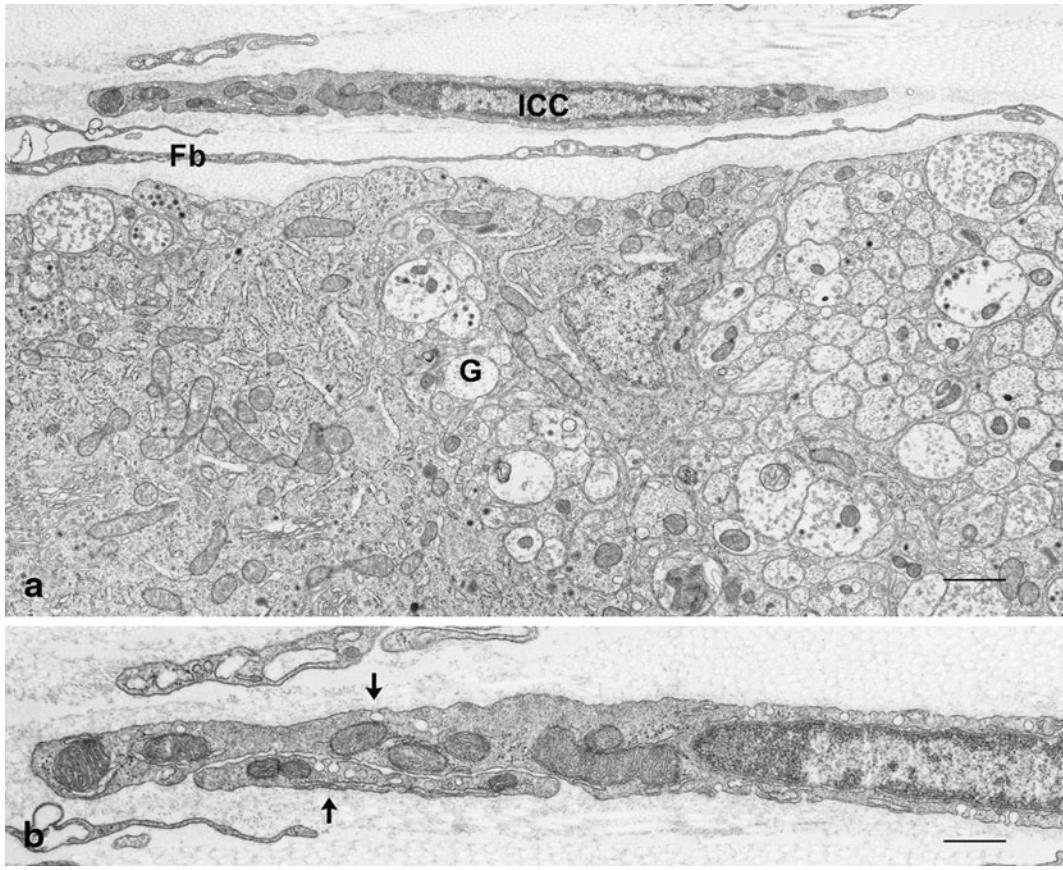

Fig. 9.16 ICC-SP in the guinea-pig proximal colon. **a** ICC-SP (*ICC*) located over the submucosal ganglion (*G*) in the guinea-pig proximal colon. Slender processes of the fibroblasts (*Fb*) are intervened between them. ×10,000. *Bar* 1 μm. **b** Higher magnification of the left half of the cell body of ICC-SP in **a**, showing caveolae (*arrows*) and many mitochondria in the cytoplasm. ×20,000. *Bar* 0.5 μm (Reproduced from Tamada and Komuro [84] with permission of the publisher).

Ultrastructural features of ICC-SP have only been observed in the guinea-pig colon so far, but ICC-SP, at least, in this material seems to have similar features to ICC found in/on the external muscle coat. They can be categorized as Type 3 cells or most muscle-like ICC.

Signal Pathways Between Nerves and Muscles Not Mediated by ICC

10

While an intercalated role of ICC in the neurotransmission to the smooth muscles has been demonstrated, there are morphological observations suggesting other possible forms of communication between nerves and smooth muscles.

Fibroblast-like cells (FL) were reported in the earlier studies of ICC in the tunica muscularis at different levels of the digestive tract of many species, including mouse small intestine, dog colon, and human small intestine and colon. These studies described the absence of specialized membrane contacts between FL and smooth muscle cells, and the absence of this feature was regarded as a discriminating characteristic from ICC.

However, the studies by Komuro and his group repeatedly revealed FL with small gap junctions in every tissue layer of every organ where ICC are located in the mice, rats, and guinea-pigs. It was assumed that their gap junctions act as routes for intercellular communication; conducting electrical or molecular signals for muscle contraction. Synapse-like close contacts between the FL and nerve varicosities containing many synaptic vesicles were observed in the guinea-pig small intestine.

Recent progress on the studies of fibroblast-like cells revealed that these cells are c-Kit negative, but are labeled with antibodies for platelet derived growth factor α (PDGFRα) and small conductance Ca^{2+}-activated K^{+}(SK3) channels [46, 47]. Physiological experiments using the mouse suggested that these cells mediate inhibitory responses to purines in the smooth muscles [48, 49].

10.1 Ultrastructural Features of Fibroblast-Like Cells

A remarkable feature of FL is that they all show very similar ultrastructural characteristics irrespective of the tissue layer, organ, or species in which they are found. The common features of FL suggest that they may have a more fundamental role than ICC regarding mediator function in the regulation of muscle contraction.

T. Komuro, *Atlas of Interstitial Cells of Cajal in the Gastrointestinal Tract,*
DOI 10.1007/978-94-007-2917-9_10, © Springer Science+Business Media B.V. 2012

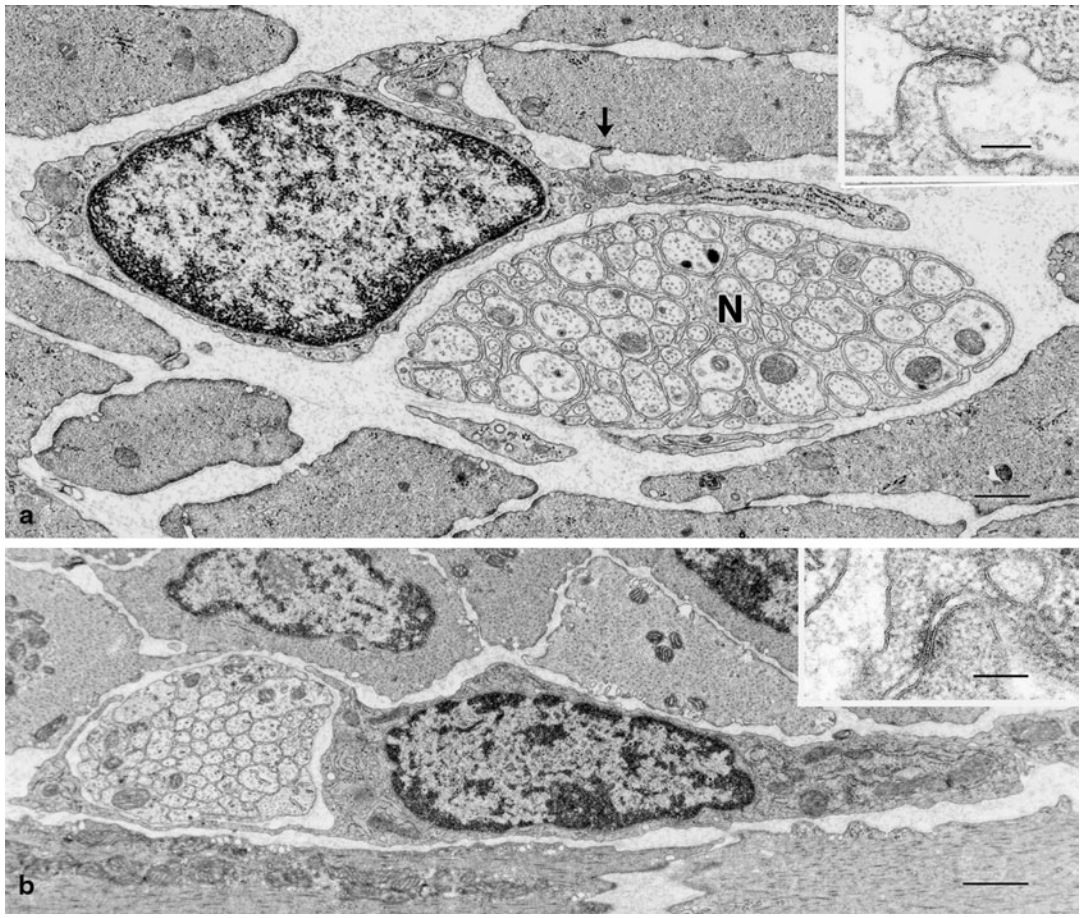

Fig. 10.1 Fibroblast-like cells found in the c-Kit mutant animals. **a** A fibroblast-like cell in the circular muscle layer of the stomach of *Ws/Ws* mutant rat which lacks c-Kit positive ICC-CM. Electron-lucent slender process located near a nerve bundle (*N*) contains a cistern of the granular endoplasmic reticulum and form a small gap junction with smooth muscle cell (*arrow*). × 18,000. *Bar* 0.5 μm. *Inset*; Higher magnification of the gap junction indicated by the arrow in **a**. × 80,000. *Bar* 0.1 μm. **b** A fibroblast-like cell in the region between the circular and longitudinal muscle layers of the small intestine of a *W/Wv* mutant mouse which is severely deficient of c-Kit-positive ICC-MP. × 11,000. *Bar* 1 μm. *Inset*; Higher magnification of the gap junction in the neighboring section of the same cell in **b**. × 86,000. *Bar* 0.1 μm. (Reproduced from Komuro [30] with permission of the publisher).

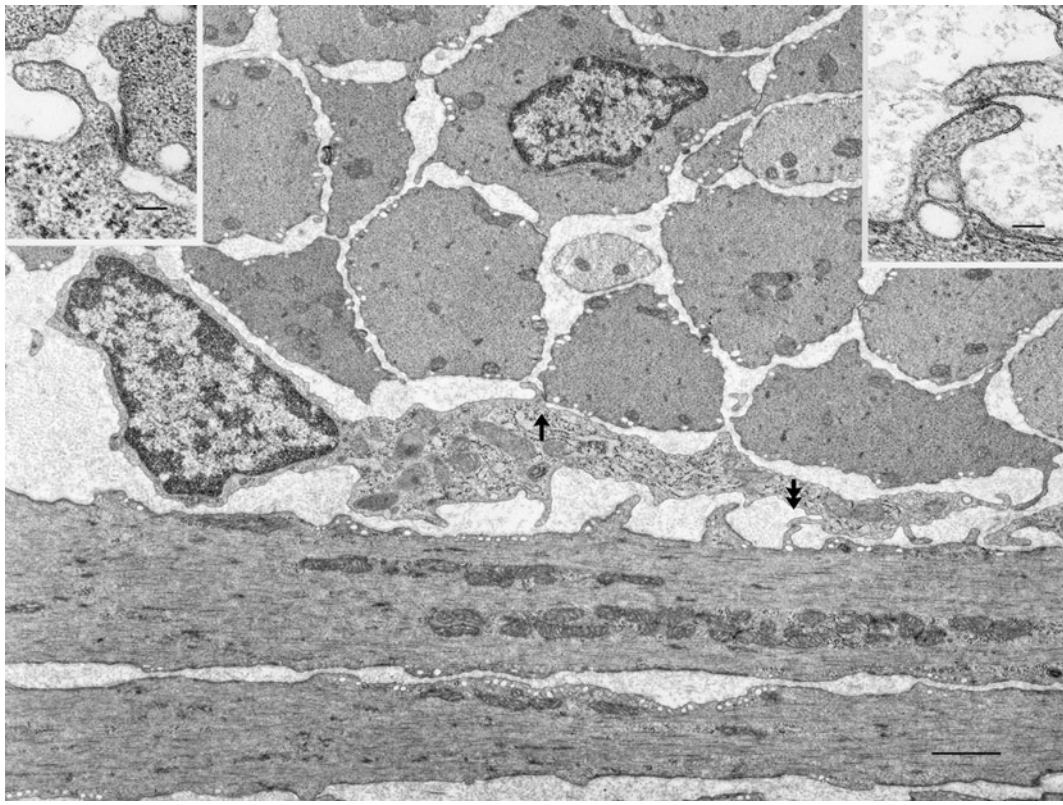

Fig. 10.2 A fibroblast-like cell in the myenteric region of the small intestine of *Ws/Ws* rat which lack c-Kit positive ICC-MP. It is characterized by well-developed cisterns of granular endoplasmic reticulum and forms small gap junction with muscle cells of both circular (*arrow*) and longitudinal (*double-headed arrow*) layers. ×11,000. *Bar* 1 μm. *Inset*; Higher magnification of the gap junctions indicated by an arrow and a double-headed arrow. ×52,000. *Bar* 0.1 μm. (Reproduced from Horiguchi and Komuro [70] with permission of the publisher).

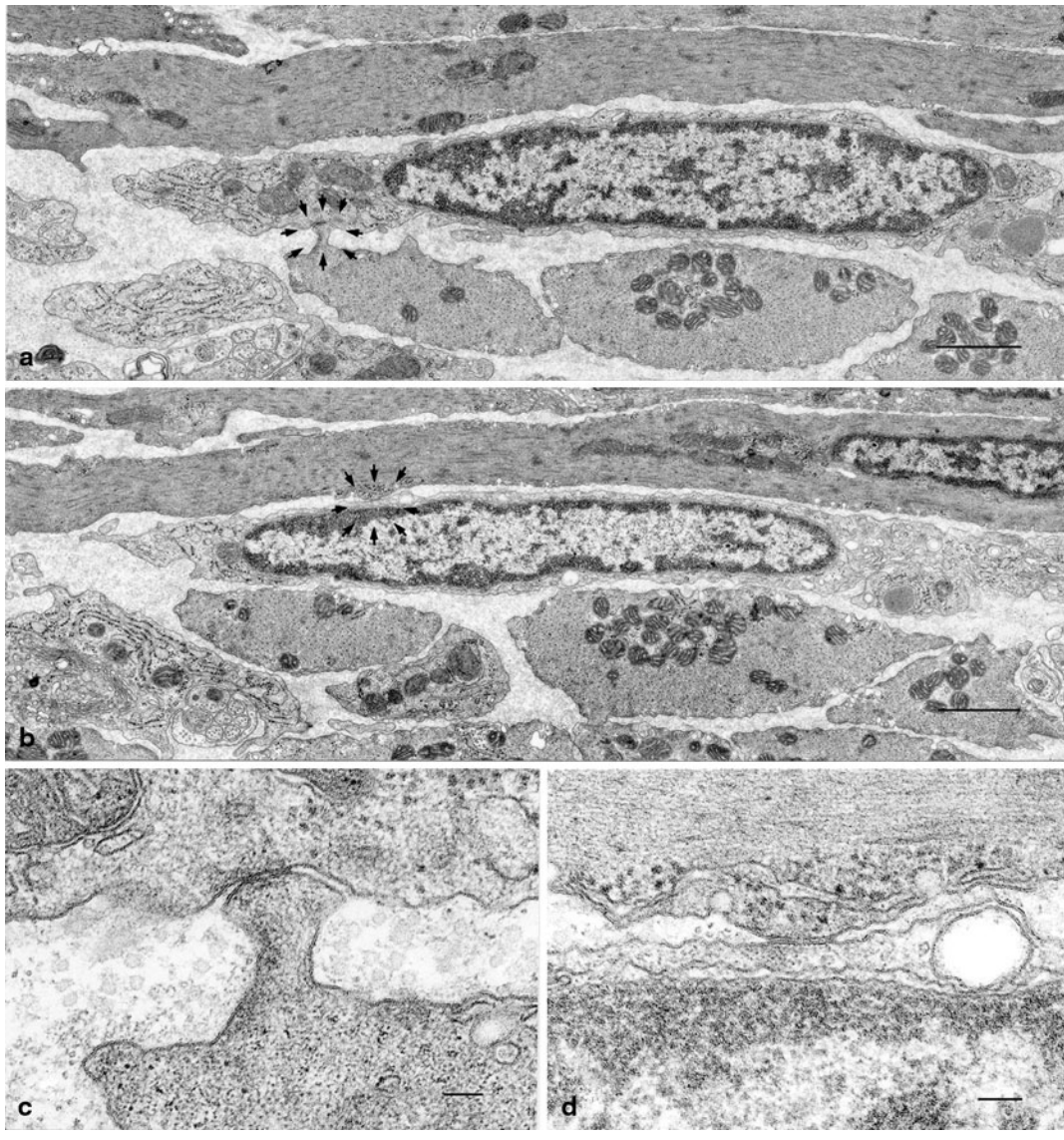

Fig. 10.3 Fibroblast-like cell in the myenteric region of the rat small intestine. **a** A fibroblast-like cell is located between the circular and longitudinal muscle layers and forms a small gap junction with the tip of a longitudinal muscle (encircled by *arrows*). ×14,000. *Bar* 1 μm. **b** A neighbouring section of the same cell in **a** showing a small gap junction between it and a circular muscle cell (encircled by *arrows*). × 14,000. *Bar* 1 μm. **c** Higher magnification of the gap junction indicated by the arrows in **a**. × 70,000. *Bar* 0.1 μm. **d** Higher magnification of the gap junction indicated by the arrows in **b**. × 70,000. *Bar* 0.1 μm. (Reproduced from Komuro [50] with permission of the publisher).

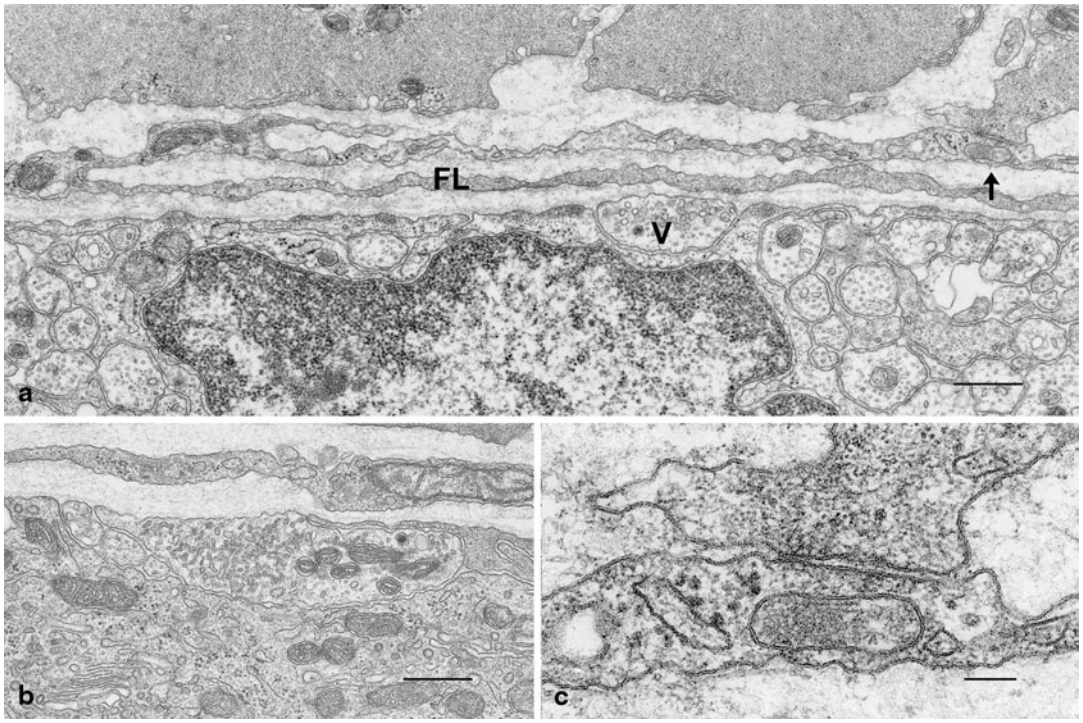

Fig. 10.4 Communication between fibroblast-like cells and nerves and/or muscles in the rat small intestine. **a** Close relationship between a surface varicosity of the myenteric ganglion (*V*) and a thin process of the fibroblast-like cell (*FL*). A parallel branching process with the cytoplasmic continuity with this cell forms a small gap junction with smooth muscle cell (*arrow*). × 23,000. *Bar* 0.5 μm.

This cell processes had been interpreted as ICC Komuro [50], but a series of observations in later studies incline to indicate that the cells showing only small gap junctions are identified as fibroblast-like cells and thus described here.

b Close relationship between a surface varicosity containing clear flat vesicles and a thin process of the fibroblast-like cell of the guinea-pig small intestine. × 25,000. *Bar* 0.5 μm. **c** Higher magnification of small gap junction indicated by arrow in **a**. × 87,000. *Bar* 0.1 μm. (Reproduced from Komuro [50] with permission of the publisher).

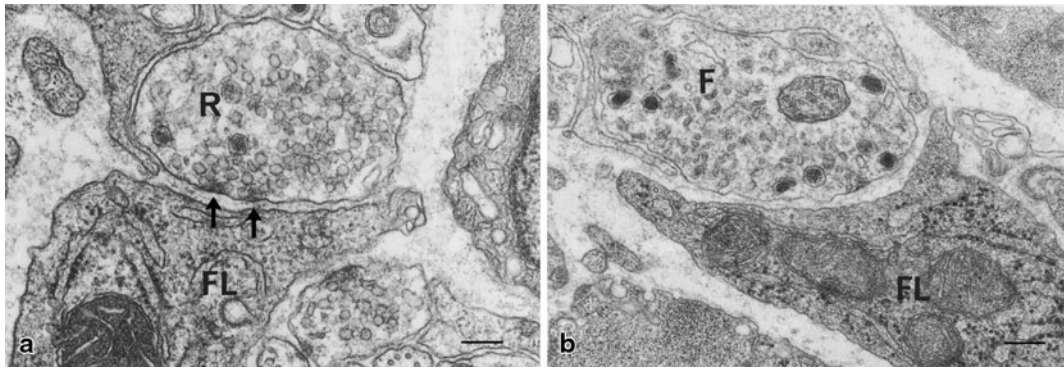

Fig. 10.5 Synaptic contact with fibroblast-like cells. **a** A nerve varicosity containing many clear round vesicles facing a fibroblast-like cell in the guinea-pig small intestine, which is characterized by well-developed granular endoplasmic reticulum. Electron-dense patches suggesting active sites are observed at the inner aspect of the axonal membrane (*arrows*). × 34,000. *Bar* 0.2 μm. **b** A nerve varicosity containing small flattened vesicles is also observed in a close distance of a fibroblast-like cell in the guinea-pig small intestine, which is characterized by cisterns of granular endoplasmic reticulum. × 33,000. *Bar* 0.2 μm. (Reproduced from Zhou and Komuro [43, 45] with permission of the publisher).

Those figures as a whole suggest that the fibroblast-like cells also play a role of intermediary of neurotransmission and communicate with both circular and longitudinal muscle cells.

10.2 PDGFRα Immunoreactive Cells

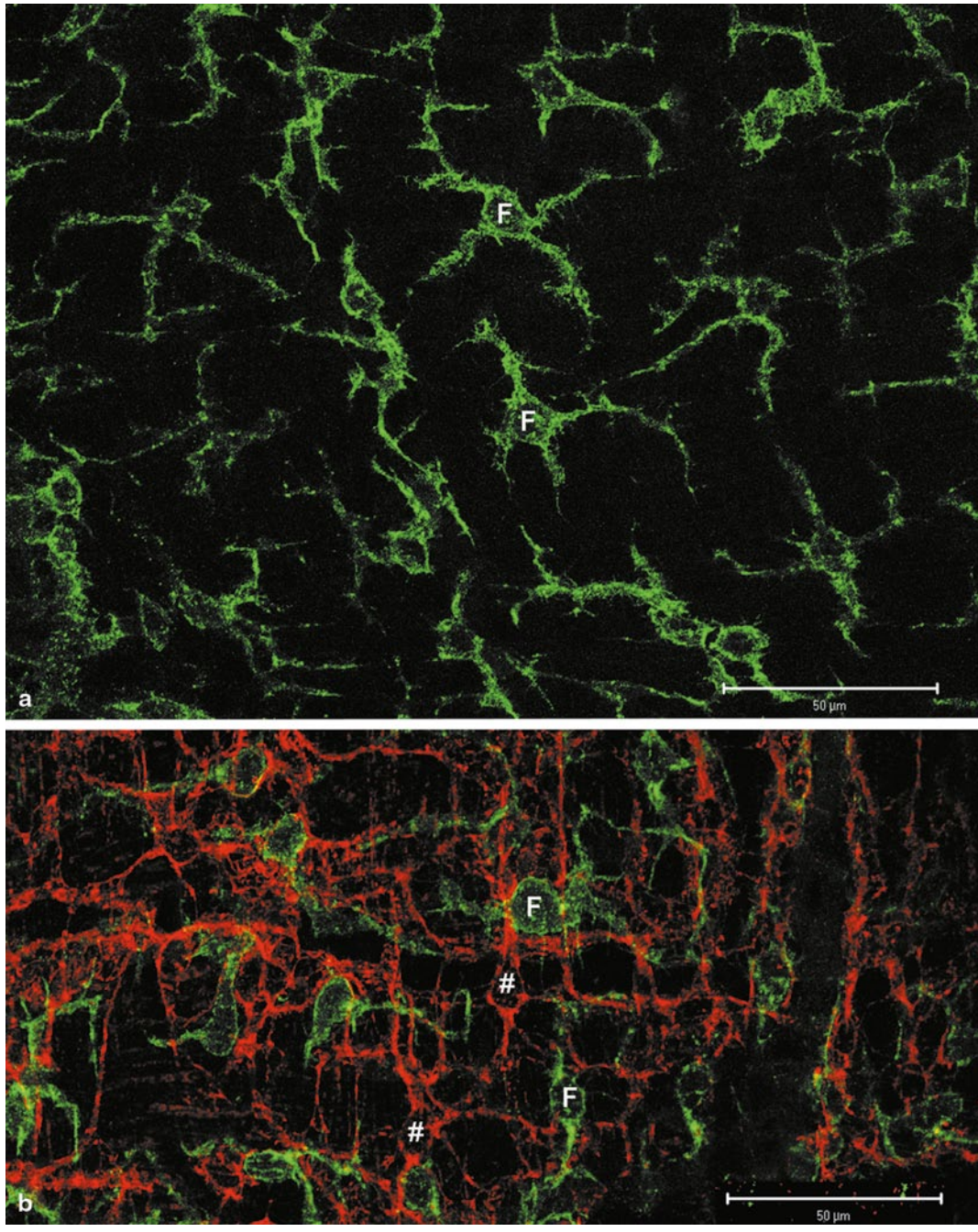

Fig. 10.6 PDGFRα immunoreactive cells. **a** PDGFRα immunoreactive cells (*F*) in the myenteric region of the mouse small intestine showing multipolar shape. **b** PDGFRα immunoreactive cells (*F*) and ICC-MP (*#*) of the mouse small intestine stained (*green*) for Ano1 (*red*) which has the same specificity as c-Kit Gomez-Pinilla et al. [51]. This picture makes clear that these two types of cells are similar in shape but are different types of cells located side by side in the same tissue layer. *Bar* 50 µm. (Courtesy of Dr Mitsui, Nagoya City University).

10.3 Direct Contacts Between Nerves and Muscles

While an intercalated role of ICC in the neurotransmission to the smooth muscles has been demonstrated, there are morphological evidence suggesting direct communication between nerves and muscles without intercalation of any types of cells.

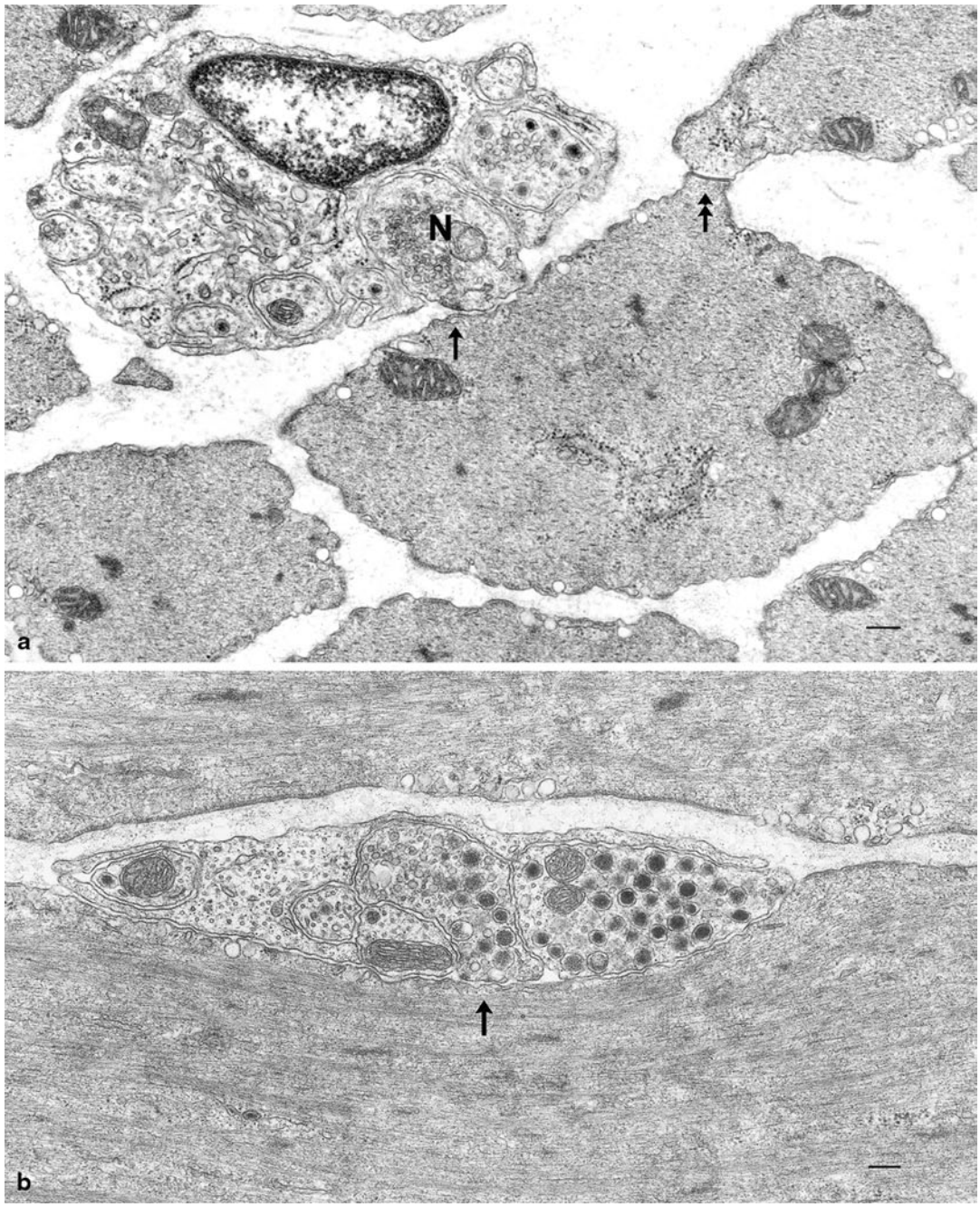

Fig. 10.7 Direct synaptic contact between the nerve varicosities and muscle cells. **a** An axon terminal containing small flattened vesicles (*N*) shows a close contact with a circular muscle cell of the rat antrum, which itself form a gap junction with a neighboring muscle cell (*double-headed arrow*). Note, another axon varicosity containing clear round vesicles. Electron-dense patch is observed at the inner aspect of the axonal membrane (*arrow*) suggesting an active site of the synaptic contact. ×30,000. *Bar* 0.2 μm. **b** Close contacts between a longitudinal muscle cell and axon terminals: one containing a mixture of small round agranular vesicles and large granular vesicles and the other containing only large granular vesicles. An electron-dense patch is observed at the inner aspect of one axonal membrane (*arrow*). ×28,000. *Bar* 0.2 μm. (Figures 10.6a, b, 10.7: Reproduced from Mitsui and Komuro [68] with permission of the publisher).

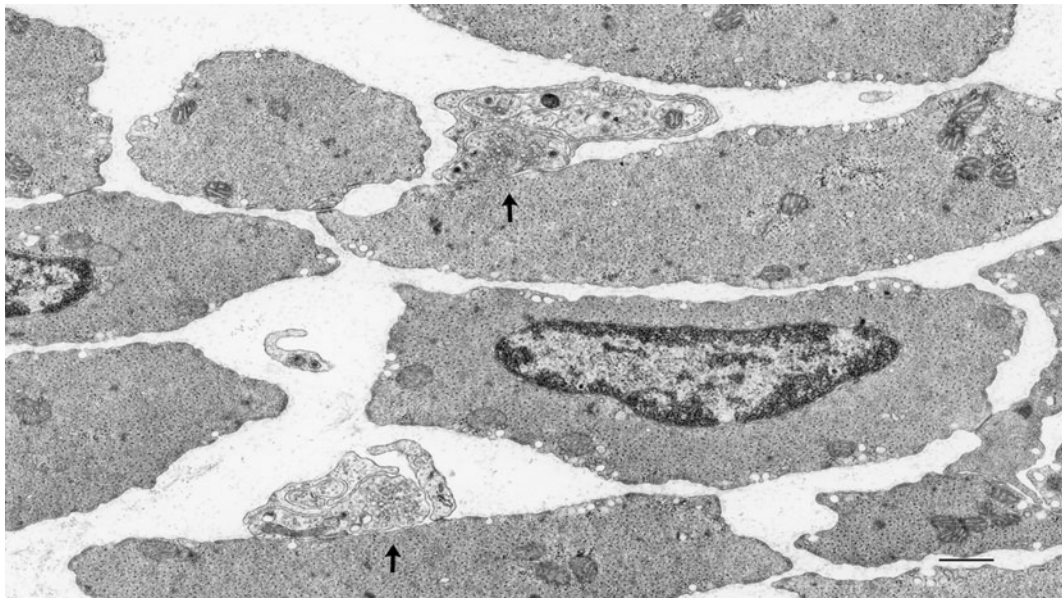

Fig. 10.8 Two neuromuscular junctions observed in a single section profile of the circular muscle of the rat antrum (*arrows*). × 18,000. *Bar* 0.5 μm.

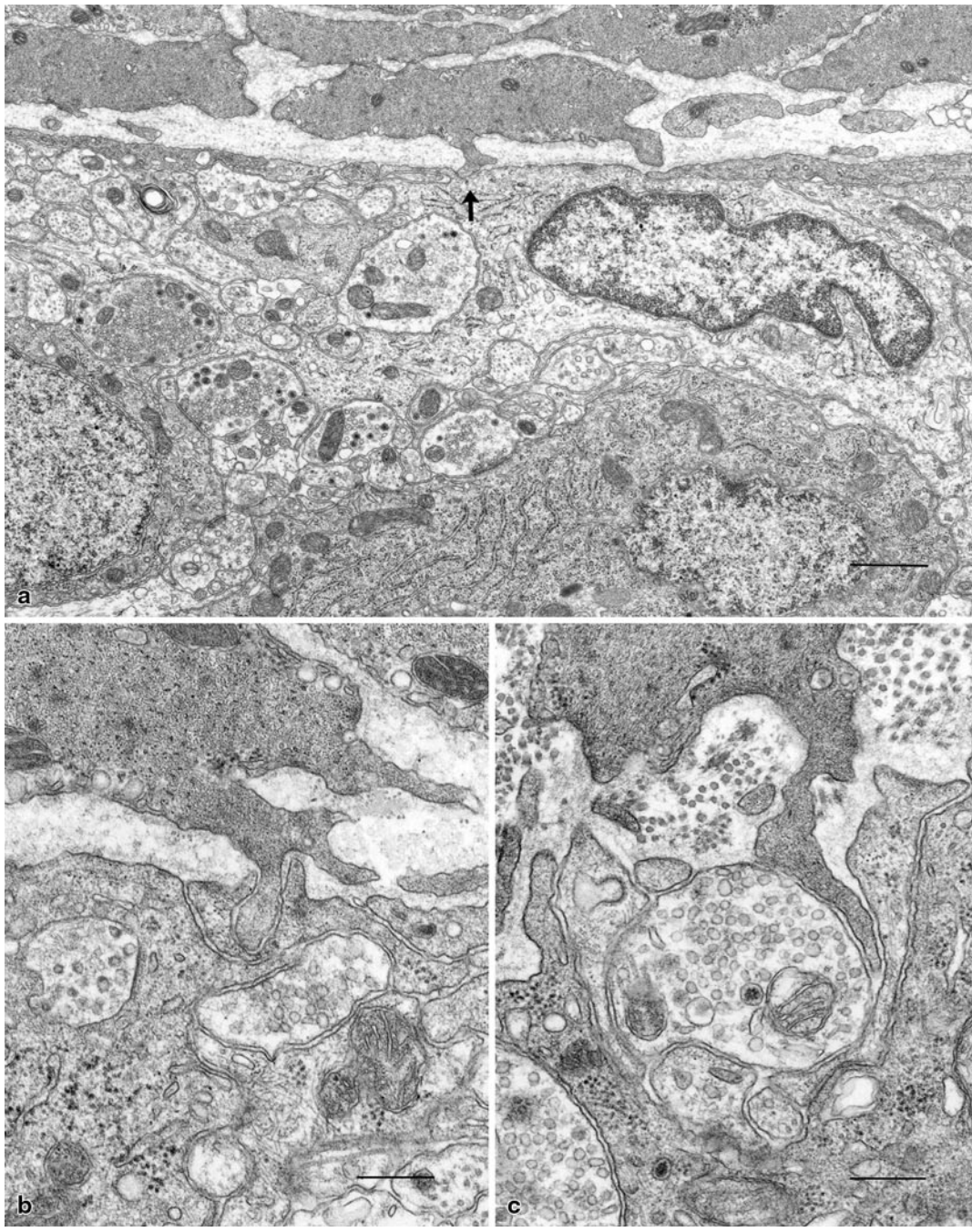

Fig. 10.9 Close contacts between the myenteric ganglia and the longitudinal muscle cells. **a** Membrane contact between a process of the longitudinal muscle cell and the glial cell of the myenteric ganglia of the rat small intestine (*arrow*). × 14,000. *Bar* 1 μm. **b** Peg-and-pocket junction between the longitudinal muscle cell and the glial cell within the myenteric ganglia of the rat small intestine. × 28,000. *Bar* 0.5 μm. **c** Close contact between a small process of the longitudinal muscle cell and a nerve varicosity containing many synaptic vesicles in the rat small intestine. × 28,000. *Bar* 0.5 μm. (Reproduced from Komuro [78] with permission of the publisher).

These direct contact observed in a–c are not found between the smooth muscle cells of the circular layer and the myenteric ganglia. Peg and socket structures with glial cells may function as anchoring devices that help maintaining the relative position between the ganglia and the longitudinal muscle during muscle contraction. These structures may also be involved in the regulation of muscle contraction or relaxation as a part of a multicellular apparatus that includes the ICC.

Issues for Future Studies

11

11.1 Skepticism About the Roles of ICC

As described above, modern progress in ICC studies has accumulated evidence supporting the pacemaker hypothesis [8] including the generation and propagation of electrical slow waves and transmission of the nerve signals to the smooth muscles in GI tract. [36, 52–55].

However, these functions of ICC were recently questioned by some researchers [56, 57]. As to the intercalated role of ICC in the transmission of nerve signals, Goyal and Chaundhury [57] criticized the hypothesis based on indirect evidence of the closer proximity and presence of synapses between the nerve varicosities and ICC, gap junctions between ICC and smooth muscles, and the presence of receptors and signaling pathways for neurotransmitters and ICC. They also claimed that some of the abnormalities in the models of c-Kit deficiency cannot be attributed to the loss of ICC but instead are due to effects of c-Kit deficiency on enteric nerves and smooth muscle cells. The c-Kit receptor pathway deficiency may cause smooth muscle dysfunction independent of the lack of the ICC. In particular, purinergic inhibitory neurotransmission and nitrergic inhibitory neurotransmission are controversial.

From the morphological point of view, there seems to be direct and indirect (via ICC) neurotransmission in the musculature of GI tract. However, so far, it is not clear whether these pathways show a particular distribution depending on the specific neuron type(s) or specific region of the organ or level of the GI tract. Careful functional experiments are required to directly prove the role of neurotransmission of ICC.

11.2 ICC Studies in the Human

With progress of ICC study demonstrating their regulatory functions in the gut motility, ICC have become an important clue to illuminate the etiology and symptoms of many diseases in the GI tract. Complete abolition or a reduction in the number of ICC or their degeneration is reported in Hirschsprung's disease, Crohn's disease, diabetes mellitus, infantile hypertrophic pyloric stenosis, chronic idiopathic intestinal pseudo-obstructions, chronic idiopathic constipation and ulcerative colitis [59, 60]. However, the significance of ICC in these diseases leaves plenty of controversies. Admitting the difficulty obtaining human material and the difficulty of comparison between the control and the patient, really cautious investigations are required to overcome the heterogeneity of the materials from different age, different gender and different level of the GI tract.

On the other hand, the study of gastrointestinal stromal tumors (GIST) may be one of the most successful cases in the application of explored new facts for medical therapy. GIST are common mesenchymal neoplasms of the GI tract, which occur anywhere in the GI tract from the lower oesophagus to the anus [60, 61]. Advances in ICC indicated that GIST share immunohistochemical, ultrastructural and histogenetic simi-

T. Komuro, *Atlas of Interstitial Cells of Cajal in the Gastrointestinal Tract,*
DOI 10.1007/978-94-007-2917-9_11, © Springer Science+Business Media B.V. 2012

larities with ICC. These facts allowed the test of signal transduction inhibition as cancer therapy that was successfully carried out with imanitib mesylate to block activity of Kit tyrosine kinase in patients with advanced GIST [62]. However, the presence of Kit resistant GIST has been recognized and cytogenetic study revealed that some Kit/Pdgfra inhibitor-resistant GIST are derived from common stem cells for normal and hyperplastic ICC that give rise to GIST [63]. Constant research works on the subject seem to be required for further advances in therapy to overcome these diseases.

With this in mind, the researchers dealing with human specimens are recognizing that ICC of human and of the large animal origin show some differences in both distribution and ultrastructure from ICC originating from the laboratory animals with a small body size [64, 65].

11.3 Questions About Determining Factor(s) of the Ultrastructural Subtype

In spite of the fact that in normal development ICC express c-Kit and their cell maturation depends on signaling between the c-Kit receptor and its ligand, stem cell factor (SCF), many reports indicate that a certain population of ICC can survive in the absence of proper Kit/SCF signaling. Such ICC were observed in both *c-kit* and stem cell factor mutant animals. They include ICC-MP in the pylorus of W/W^v mouse [66, 67], and ICC-MP and ICC-SM in the pylorus of *Ws/Ws* rat [68]. Other examples include the ICC-DMP of the *Ws/Ws* rat small intestine [69, 70], the ICC-DMP of the small intestine of the *Sl/Sld* mouse [71] and W/W^v mouse [72] and ICC-SMP of the *Ws/Ws* rat colon [73] (Fig. 11.1).

These ICC share common ultrastructural features and are classified into Type 3 ICC (Table 9.1). This type is most similar to smooth muscle cells, in respect of the presence of many caveolae and a distinct basal lamina [74], regardless of the organ or tissue layer concerned. The evidence suggests that the most muscle-like Type 3 ICC can develop and mature their characteristic cytological features independently of the Kit/SCF system, or that some other system can compensate in their cell maturation. These observations appear to raise important questions for future studies, such as why ICC show a fairly wide range of phenotypes and what factor(s) determine the ultrastructural features of particular type of ICC, despite the facts that ICC and smooth muscle cells are derived from the same mesechymal progenitor cells and that blockade of c-Kit signaling induces a smooth muscle cell phenotype.

11.4 Questions About the Involvement of More Cell Types for Regulation of the Smooth Muscle

The smooth musculature of GI tract is not simply composed of smooth muscle cells but contains a variety of cells including neurons and other cells. After many years of study of nerves, ICC are now accepted as an important component of the regulatory mechanism of smooth muscle movement. Involvement of macrophages and mast cells in muscle movement has been also demonstrated in many studies [75, 76]. Furthermore, recent studies revealed that so-called fibroblast-like cells have a special type of receptor (PDGFRα) and mediate inhibitory response to the musculature of the GI tract. These observations suggest that more cell types may be discovered as important components of the regulatory system of the smooth muscle in the near future (Fig. 11.2).

They may be cells that do not show peculiar morphological features and have been escaped the attention of researchers. The smooth musculature still seems to present a big frontier to be explored.

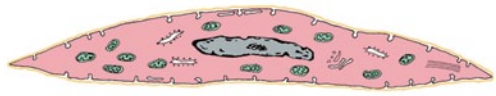

Most muscle-like ICC

Basal lamina ++
Caveolae ++
10nm Filaments ++
ICC-SM Ws/Ws, W/Wv
ICC-MP Ws/Ws
ICC-DMP Ws/Ws, W/Wv
ICC-SMP Ws/Ws

Intermediate Type

Basal lamina +-
Caveolae ++
10nm Filaments ++

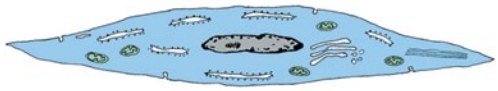

Least muscle-like ICC

Basal lamina -
Caveolae +-
10nm Filaments ++

All types of ICC are c-kit positive and are characterized by rich MITOCHONDRIA, formation of GAP JUNCTIONS and close contacts with NERVE TERMINALS.

Fig. 11.1 Schematic illustration showing the different dependency of ultrastructural subtypes on the c-Kit/SCF signaling system.

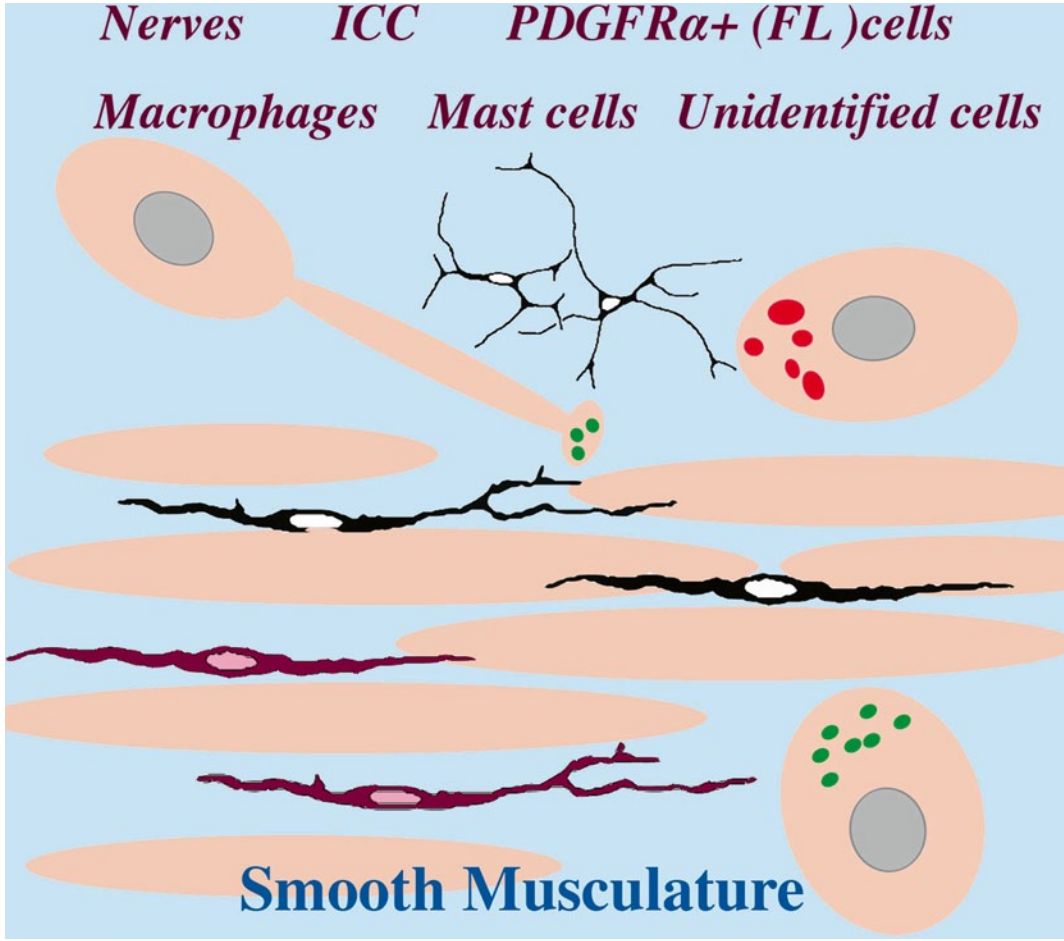

Fig. 11.2 Illustration of cell types involved in the movement of the smooth muscle.

References

1. Cajal SR (1893) Sur les ganglions et plexus nerveux de l'intestin. C R Soc Biol Paris 45:217–223
2. Cajal SR (1911) Histologie du systeme nerveux de l'homme et des vertebres, vol 2. Maloine, Tome 2 Paris, pp 891–942
3. Boeke J (1949) The sympathetic end formation, its synaptology, the interstitial cells, the periterminal network, and its bearing on the neurone theory. Discussion and critique. Acta Anat 8:18–61
4. Taxi J (1965) Contribution a l'etude des connexions des neurones moteurs du systeme nerveux autonome. Ann Sci Nat Zool Tome VII:413–474
5. Garcia-Lopez P, Garcia-Marin V, Martínez-Murillo R, Freire M (2009) Updating old ideas and recent advances regarding the interstitial cells of Cajal. Brain Res Rev 61:154–169
6. Richardson KC (1958) Electronmicroscopic observations on Auerbach's plexus in the rabbit, with special reference to the problem of smooth muscle innervation. Am J Anat 103:99–135
7. Imaizumi M, Hama K (1969) An electron microscopic study on the interstitial cells of the gizzard in the love-bird (Uroloncha domestica). Z Zellforsch 97:351–357
8. Thuneberg L (1982) Interstitial cells of Cajal: intestinal pacemaker cells? Adv Anat Embryol Cell Biol 71:1–130
9. Thuneberg L (1989) Interstitial cells of Cajal. In: Wood JD (ed) Handbook of physiology. The gastrointestinal system, vol 1. Am Physiol Soc, Bethesda
10. Thuneberg L (1999) One hundred years of interstitial cells of Cajal. Microsc Res Tech 47:223–238
11. Faussone-Pellegrini MS, Thuneberg L (1999) Guide to the identification of interstitial cells of Cajal. Microsc Res Tech 47:248–266
12. Maeda H, Yamagata A, Nishikawa S, Yoshinaga K, Kobayashi S, Nishi K, Nishikawa S (1992) Requirement of c-*kit* for development of intestinal pacemaker system. Development 116:369–375
13. Torihashi S, Ward SM, Nishikawa S, Nishi K, Kobayashi S, Sanders K (1995) c-kit-dependent development of interstitial cells and electrical activity in the murine gastrointestinal tract. Cell Tissue Res 280:97–111
14. Komuro T, Zhou DS (1996) Anti-c-kit protein immunoreactive cells corresponding to the interstitial cells of Cajal in the guinea-pig small intestine. J Auton Nerv Syst 61:169–174
15. Komuro T, Tokui K, Zhou DS (1996) Identification of the interstitial cells of Cajal. Histol Histopathol 11:769–786
16. Lecoin L, Gabella G, Douarin NL (1996) Origin of the c-*kit*-positive interstitial cells in the avian bowel. Development 122:725–733
17. Young HM, Ciampoli D, Southwell BR, Newgreen DF (1996) Origin of interstitial cells of Cajal in the mouse intestine. Dev Biol 180:97–107
18. Torihashi S, Ward SM, Sanders KM (1997) Development of c-kit-positive cells and the onset of electrical rhythmicity in murine small intestine. Gastroenterology 112:144–155
19. Kluppel MJ, Huizinga JD, Malysz J, Bernstein A (1998) Developmental origin and kit-dependent development of the interstitial cells of Cajal in the mammalian small intestine. Dev Dyn 211:60–71
20. Hara Y, Kubota M, Szurszewski JH (1986) Electrophysiology of smooth muscle of the small intestine of some mammals. J Physiol 372:501–520
21. Suzuki N, Prosser CL, Dahms V (1986) Boundary cells between longitudinal and circular layers essential for electrical slow waves in cat intestine. Am J Physiol 250:G287–G294
22. Huizinga JD, Thuneberg L, Kluppel M, Malysz J, Mikkelsen HB, Bernstein A (1995) W/kit gene required for interstitial cells of Cajal and for intestinal pacemaker activity. Nature 373:341–349
23. Ward SM, Burns AJ, Torihashi S, Sanders KM (1994) Mutation of the proto-oncogene c-*kit* blocks development of interstitial cells and electrical rhythmicity in murine intestine. J Physiol (Lond) 480:91–97
24. Dickens EJ, Hirst GD, Tomita T (1999) Identification of rhythmically active cells in guinea-pig stomach. J Physiol 514:515–531
25. Smith TK, Reed JB, Sanders KM (1987) Interaction of two electrical pacemakers in muscularis of canine proximal colon. Am J Physiol 252:C290–C299
26. Conklin JL, Du C (1990) Pathways of slow-wave propagation in proximal colon of cats. Am J Physiol 258:G894–G903
27. Serio R, Barajas-Lopez C, Daniel EE, Berezin I, Huizinga JD (1991) Slow-wave activity in colon: role of network of submucosal interstitial cells of Cajal. Am J Physiol 260:G636–G645
28. Rae MG, Fleming N, McGregor DB, Sanders KM, Keef KD (1998) Control of motility patterns in the human colonic circular muscle layer by pacemaker activity. J Physiol 510:309–320

29. Pluja L, Alberti E, Fernandez E, Mikkelsen HB, Thuneberg L, Jimenez, M (2001) Evidence supporting presence of two pacemakers in rat colon. Am J Physiol 281:G255–G266
30. Komuro T (1999) Comparative morphology of interstitial cells of Cajal: ultrastructural characterization. Microsc Res Tech 47:267–285
31. Ward SM, Sanders KM (2001) Interstitial cells of Cajal: primary target of enteric motor innervation. Anat Rec 262:125–135
32. Beckett EAH, Takeda Y, Yanase H, Sanders KM, Ward SM (2005) Synaptic specializations exist between enteric motor nerves and interstitial cells of Cajal in the murine stomach. J Comp Neurol 493:193–206
34. Fox EA, Phillips RJ, Martinson FA, Baronowsky EA, Powley TL (2000) Vagal afferent innervation of smooth muscle in the stomach and duodenum of the mouse Morphology and topography. J Comp Neurol 428:558–576
35. Aranishi H, Kunisawa Y, Komuro T (2009) Characterization of interstitial cells of Cajal in the subserosal layer of the guinea-pig colon. Cell Tissue Res 335:323–329
35. Fox EA, Phillips RJ, Byerly S, Baronowsky EA, Chi MM, Powley TL (2002) Selective loss of vagal intramuscular mechanoreceptors in mice mutant for steel factor, the c-Kit receptor ligand. Anat Embryol 205:325–342
36. Hanani M, Farrugia G, Komuro T (2005) Intercellular coupling of interstitial cells of Cajal in the digestive tract. Int Rev Cytol 242:249–282
37. Komuro T (2006) Structure and organization of interstitial cells of Cajal in the gastrointestinal tract. J Physiol 576:653–658
38. Lorincz A, Redelman D, Horváth VJ, Bardsley MR, Chen H, Ordög T (2008) Progenitors of interstitial cells of cajal in the postnatal murine stomach. Gastroenterology 134:1083–1093
39. Seki K, Zhou DS, Komuro T (1998) Immunohistochemical study of the c-*kit* expressing cells and connexin 43 in the guinea-pig digestive tract. J Auton Nerv Syst 68:182–187
40. Duchon G, Henderson R, Daniel EE (1974) Circular muscle layers in the small intestine. In: Daniel EE (ed) Proceedings of the 4th international symposium on gastrointestinal motility. Mitchell Press Banff, Alberta, pp 635–646
41. Horiguchi K, Semple GS, Sanders KM, Ward SM (2001) Distribution of pacemaker function through the tunica muscularis of the canine gastric antrum. J Physiol (Lond) 537:237–250
42. Seki K, Komuro T (1998) Further observation of the gap junction-rich cells in the deep muscular plexus of the rat small intestine. Anat Embryol 197:135–141
43. Zhou DS, Komuro T (1992a) Interstitial cells associated with the deep muscular plexus of the guinea-pig small intestine, with special reference to the interstitial cells of Cajal. Cell Tissue Res 268:205–216
44. Gabella G, Blundell D (1979) Nexuses between the smooth muscle cells of the guinea-pig ileum. J Cell Biol 82:239–247
45. Zhou DS, Komuro T (1992b) The cellular network of interstitial cells associated with the deep muscular plexus of the guinea pig small intestine. Anat Embryol 186:519–527
46. Vanderwinden JM, Rumessen JJ, de Kerchove d'Exaerde A Jr, Gillard K, Panthier JJ, de Laet MH, Schiffmann SN (2002) Kit-negative fibroblast-like cells expressing SK3, a $Ca2^{+}$-activated K^{+} channel, in the gut musculature in health and disease. Cell Tissue Res 310:349–358
47. Iino S, Horiguchi K, Horiguchi S, Nojyo Y (2009) c-Kit-negative fibroblast-like cells express platelet-derived growth factor receptor α in the murine gastrointestinal musculature. Histochem Cell Biol 131:691–702
48. Fujita A, Takeuchi T, Jun H, Hata F (2003) Localization of $Ca2^{+}$-activated K^{+} channel, SK3, in fibroblast-like cells forming gap junctions with smooth muscle cells in the mouse small intestine. J Pharmacol Sci 92:35–42
49. Kurahashi M, Zheng H, Dwyer L, Ward SM, Don Koh S, Sanders KM (2010) A functional role for the 'fibroblast-like cells' in gastrointestinal smooth muscles. J Physiol 589:697–710
50. Komuro T (1989) Three-dimensional observation of the fibroblast-like cells associated with the rat myenteric plexus, with special reference to the interstitial cells of Cajal. Cell Tissue Res 255:343–351
51. Gomez-Pinilla PJ, Gibbons SJ, Bardsley MR, Lorincz A, Pozo MJ, Pasricha PJ, Van de Rijn M, West RB, Sarr MG, Kendrick ML, Cima RR, Dozois EJ, Larson DW, Ordog T, Farrugia G (2009) Ano1 is a selective marker of interstitial cells of Cajal in the human and mouse gastrointestinal tract. Am J Physiol Gastrointest Liver Physiol 296:G1370–G1381
52. Huizinga JD, Thuneberg L, Vanderwinden JM, Rumessen JJ (1997) Interstitial cells of Cajal as targets for pharmacological intervention in gastrointestinal motor disorders. TIPS 18:393–403
52. Sanders KM (1996) A case for interstitial cells of Cajal as pacemakers and mediators of neurotransmission in the gastrointestinal tract. Gastroenterology 111:492–515
54. Komuro T (2004) Morphological features of interstitial cells of Cajal. In: Kitamura Y, Miettinenn M, Hirota S, Kanakura Y (eds) Gastrointestinal stromal tumor(GIST): from pathology to molecular target therapy. Monograph on cancer research, vol 53. Japan Scientific Societies Press & Karger, Tokyo, pp 109–134
55. Sanders KM, Hwang SJ, Ward SM (2010) Neuroeffector apparatus in gastrointestinal smooth muscle organs. J Physiol 588:4621–4639
56. Sarna SK (2008) Are interstitial cells of Cajal pluri-function cells in the gut? Am J Physiol Gastrointest Liver Physiol 294:G372–G390
57. Goyal RK, Chaudhury (2010) Mounting evidence against the role of ICC in neurotransmission to smooth muscle in the gut. Am J Physiol Gastrointest Liver Physiol 298:G10–G13

58. Vanderwinden JM, Rumessen JJ (1999) Interstitial cells of Cajal in human gut and gastrointestinal disease. Microsc Res Tech 47:344–360
59. Rolle U, Piaseczna-Piotrowska A, Puri P (2007) Interstitial cells of Cajal in the normal gut and in intestinal motility disorders of childhood. Pediatr Surg Int 23:1139–1152
60. Hirota S, Isozaki K, Moriyama Y, Hashimoto K, Nishida T, Ishiguro S, Kawano K, Hanada M, Kurata A, Takeda M, Muhammad Tunio G, Matsuzawa Y, Kanakura Y, Shinomura Y, Kitamura Y (1998) Gain-of-function mutations of c-kit in human gastrointestinal stromal tumors. Science 279:577–580
61. Miettinen M, Lasota J (2001) Gastrointestinal stromal tumors–definition, clinical, histological, immunohistochemical, and molecular genetic features and differential diagnosis. Virchows Arch 438:1–12
62. Demetri GD (2002) Identification and treatment of chemoresistant inoperable or metastatic GIST: experience with the selective tyrosine kinase inhibitor imatinib mesylate (STI571). Eur J Cancer 38:S52–S59
63. Bardsley MR, Horváth VJ, Asuzu DT, Lorincz A, Redelman D, Hayashi Y, Popko LN, Young DL, Lomberk GA, Urrutia RA, Farrugia G, Rubin BP, Ordog T (2010) Kit^{low} stem cells cause resistance to Kit/platelet-derived growth factor alpha inhibitors in murine gastrointestinal stromal tumors. Gastroenterology 139:942–952
64. Rumessen JJ, Vanderwinden JM (2003) Interstitial cells in the musculature of the gastrointestinal tract: Cajal and beyond. Int Rev Cytol 229:115–208
65. Rumessen JJ, Vanderwinden JM, Rasmussen H, Hansen A, Horn T (2009) Ultrastructure of interstitial cells of Cajal in myenteric plexus of human colon. Cell Tissue Res 337:197–212
66. Ward SM, Morris G, Reese L, Wang XY, Sanders KM (1998) Interstitial cells of Cajal mediate enteric inhibitory neurotransmission in the lower esophageal and pyloric sphincters. Gastroenterology 115:314–329
67. Seki K, Komuro T (2002) Distribution of interstitial cells of Cajal and gap junction protein, Cx 43 in the stomach of wild-type and W/Wv mutant mice. Anat Embryol 206:57–65
68. Mitsui R, Komuro T (2002) Direct and indirect innervation of smooth muscle cells of rat stomach, with special reference to the interstitial cells of Cajal. Cell Tissue Res 309:219–227
69. Horiguchi K, Zhou DS, Seki K, Komuro T, Hirota S, Kitamura Y (1995) Morphological analysis of c-kit expressing cells, with reference to interstitial cells of Cajal. J Smooth Muscle Res 31:303–305
70. Horiguchi K, Komuro T (1998) Ultrastructural characterization of interstitial cells of Cajal in the rat small intestine using control and Ws/Ws mutant rats. Cell Tissue Res 293:277–284
71. Ward SM, Burns AJ, Torihashi S, Harney SC, Sanders KM (1995) Impaired development of interstitial cells and intestinal electrical rhythmicity in steel mutants. Am J Physiol 269:C1577–C1585
72. Malysz J, Thuneberg L, Mikkelsen HB, Huizinga JD (1996) Action potential generation in the small intestine of W mutant mice that lack interstitial cells of Cajal. Am J Physiol 271:G387–G399
73. Ishikawa K, Komuro T (1996) Characterization of the interstitial cells associated with the submuscular plexus of the guinea-pig colon. Anat Embryol 194:49–55
74. Komuro T, Seki K, Horiguchi K (1999) Ultrastructural characterization of the interstitial cells of Cajal. Arch Histol Cytol 62:295–316
75. Sato K, Torihashi S, Hori M, Nasu T, Ozaki H (2007) Phagocytotic activation of muscularis resident macrophages inhibits smooth muscle contraction in rat ileum. J Vet Med Sci 69:1053–1060
76. Mikkelsen HB (2010) Interstitial cells of Cajal, macrophages and mast cells in the gut musculature: morphology, distribution, spatial and possible functional interactions. J Cell Mol Med 14:818–832
77. Komuro T, Hashimoto Y (1990) Three-dimensional structure of the rat intestinal wall (mucosa and submucosa). Arch Histol Cytol 53:1–21
78. Komuro T (1988) The lattice arrangement of the collagen fibres in the submucosa of the rat small intestine: scanning electron microscopy. Cell Tissue Res 251:117–121
79. Miyamoto-Kikuta S, Ezaki T, Komuro T (2009) Distribution and morphological characteristics of the interstitial cells of Cajal in the ileocaecal junction of the guinea-pig. Cell Tissue Res 338:29–35
80. Kunisawa Y, Komuro T (2008) Interstitial cells of Cajal associated with the submucosal plexus of the Guinea-pig stomach. Neurosci Lett 434:273–276
81. Tamada H, Komuro T (2011) Three-dimensional demonstration of the interstitial cells of Cajal associated with the submucosal plexus in guinea-pig caecum. Cell Tissue Res 344:183–188
82. Komuro T, Seki K (1995) Fine structural study of interstitial cells associated with the deep muscular plexus of the rat small intestine, with special reference to the intestinal pacemaker cells. Cell Tissue Res 282:129–134
83. Ishikawa K, Komuro T, Hirota S, Kitamura Y (1997) Ultrastructural identification of the c-kit-expressing interstitial cells in the rat stomach: a comparison of control and Ws/Ws mutant rats. Cell Tissue Res 289:137–143
84. Tamada H, Komuro T (2012) Ultrastructural characterization of interstitial cells of Cajal associated with the submucosal plexus in the proximal colon of the guinea pig. Cell Tissue Res (in press, Accepted: 20 Dec 2011)

Index

T. Komuro, *Atlas of Interstitial Cells of Cajal in the Gastrointestinal Tract,*
DOI 10.1007/978-94-007-2917-9, © Springer Science+Business Media B.V. 2012